
Lab Medicine

Novel *PKD1* Mutations in Patients with Autosomal Dominant Polycystic Kidney Disease

Hyerin Kim, MD,[1,2] *Hyung-Hoi Kim, MD, PhD,*[1,2] *Chulhun L. Chang, MD, PhD,*[3] *Sang Heon Song, MD, PhD,*[2,4] *Namhee Kim, MD,*[2,5*]

Laboratory Medicine 2021;52:174-180

DOI: 10.1093/labmed/lmaa047

ABSTRACT

Objective: Autosomal dominant polycystic kidney disease (ADPKD) is the most common genetic kidney disease. Identifying mutated causative genes can provide diagnostic and prognostic information. In this study, we describe the clinical application of a next generation sequencing (NGS)-based, targeted multi-gene panel test for the genetic diagnosis of patients with ADPKD.

Methods: We applied genetic analysis on 26 unrelated known or suspected patients with ADPKD. A total of 10 genes related to cystic change of kidney were targeted. Detected variants were classified according to standard guidelines.

Results: We identified 19 variants (detection rate: 73.1%), including *PKD1* (n = 18) and *PKD2* (n = 1). Of the 18 *PKD1* variants, 8 were novel.

Conclusion: Multigene panel test can be a comprehensive tool in a clinical setting for genetic diagnosis of ADPKD. It allows us to identify clinically significant novel variants and confirm the diagnosis, and these objectives are difficult to achieve using conventional diagnostic tools.

Keywords: Polycystic kidney disease; Sequence analysis; PKD1; PKD2

Autosomal dominant polycystic kidney disease (ADPKD) is the most commonly inherited kidney disease, with an estimated incidence in the general population of 1 in 1000.[1] It is characterized by the progressive development of renal and/or extrarenal cysts and accounts for approximately 5% of patients who need dialysis or kidney transplantation.[2] Mutations in polycystic kidney disease 1 (*PKD1*; 16p13.3), encoding polycystin-1 (PC-1), and polycystic kidney disease 2 (*PKD2*; 4q22.1), encoding polycystin-2 (PC-2), are responsible for approximately 85% and 15% of ADPKD cases, respectively.[3] The disorder is inherited with a varied clinical expression, despite nearly 100% penetrance for mutated *PKD1* or *PKD2*.[4]

[1]Department of Laboratory Medicine, Pusan National University Hospital, Busan, Korea, [2]Biomedical Research Institute, Pusan National University Hospital, Busan, Korea, [3]Department of Laboratory Medicine, Pusan National University Yangsan Hospital, Yangsan, Korea, [4]Division of Nephrology, Department of Internal Medicine, Pusan National University Hospital, Busan, Korea, [5]Department of Laboratory Medicine, Dong-A University College of Medicine, Busan, Korea

*To whom correspondence should be addressed. nkim@dau.ac.kr

A simple diagnosis of ADPKD can be made if the affected patient has enlarged kidneys with multiple bilateral cysts and a positive family history. Renal imaging by ultrasonography, computed tomography (CT), or magnetic resonance imaging (MRI) can detect renal cysts sensitively. Age-dependent criteria, based on the number of cysts, have been developed for individuals who have a 50% risk of developing ADPKD.[5–9] However, imaging-based diagnosis may be insufficient in some situations; for such cases, genetic testing can be valuable to obtain a definite diagnosis. These situations include young, high-risk patients with insufficient renal imaging findings, patients with unknown family history and clear findings of multiple renal cysts, and young family members being considered as donors for kidney transplantation.[10] Genetic testing is age-independent, and therefore is useful as a confirmatory test.

In addition, ADPKD can be confused with several other polycystic kidney diseases with different causative genes but clinical similarity. Identifying whether a patient harbors mutations on *PKD1* or *PKD2* can provide prognostic

information for assessing the risk of early-onset disease and allow preimplantation genetic diagnostics to be performed.[2] However, to date, most cases of ADPKD have been diagnosed through imaging techniques and clinical symptoms, and limited information regarding the genetic spectrum of Korean patients with ADPKD is available.[11–14]

The emergence of next-generation sequencing (NGS)-based targeted multi-gene panel test has revolutionized genetic diagnostics, enabling differential diagnosis with a single test. In this study, we describe the clinical application of NGS-based targeted multi-gene panel test for genetic diagnosis of patients diagnosed with or suspected to have ADPKD.

Materials and Methods

Patient Selection

We performed mutational analysis using peripheral blood on 26 unrelated known or suspected patients with ADPKD, who had previously been diagnosed using imaging techniques such as ultrasonography or CT, from September 2017 to June 2018, at Pusan National UniversityHospital. The biospecimens and data used in this study were provided by the Biobank of Pusan National University Hospital, a member of the Korea Biobank Network. The study protocol was reviewed and approved by the Institutional Review Board of Pusan National University Hospital, and informed consent was waived after committee approval (1704-005-006).

Genetic Analysis and Interpretation

Genomic DNA was extracted from peripheral blood leukocytes using the QuickGene DNA whole blood kit (Fujifilm, Tokyo, Japan). Considering the opinion of clinicians, medical management guidelines from professional societies, known detection frequency, the patient samples were tested with a custom multi-gene panel, targeting 10 genes (*PKD1, PKD2, PKHD1, TSC1, TSC2, VHL, HNF1B, NPHP1, NPHP3,* and *NPHP4*) which are known to play a role in polycystic kidney disease. The analytical performance of the custom panel showed an estimated NGS analytical sensitivity of > 99.96% (lower limit of the 95% CI) and an estimated analytical specificity of > 99.99% (lower limit of the 95% CI) for single nucleotide variant detection and insertion/deletion variant detection (range 1–15 nucleotides in length) cDNA libraries were generated using a solution-based Agilent SureSelect target enrichment system (Agilent Technologies, Santa Clara, CA) according to the manufacturer's instructions. Paired-end sequencing was performed on a MiSeq (Illumina Inc, San Diego, CA) platform. Obtained sequences were analyzed using an in-house bioinformatics pipeline. All candidate variants detected by NGS were confirmed by long-range, nested polymerase chain reaction. Variants were subjected to clinical interpretation using 2015 ACMG/AMP guidelines for sequence variants classification.[15] To confirm the pathogenicity of the variants, analysis of available family members in the pedigree was carried out by direct sequencing. Multiplexed ligation-dependent probe amplification (MLPA) was also performed for all patients to detect large genomic rearrangements such as deletions and duplications.

Results

Among 26 patients with known or suspected ADPKD, we identified 19 variants (detection rate: 73.1%), including 18 *PKD1* variants and one *PKD2* variant. We did not detect any aberrant variants in other target genes. Five patients (19.2%) were found not to harbor any clinically significant variants, and 2 patients (7.7%) harbored mutations in genes other than target genes (*LAMB2* c.3644C > G and *PLCE1* c.6290G > A). These variants were detected in incidentally captured off-target reads due to sequence variation at the probe binding site, and are classified as "incidental findings" because they associated with diseases unrelated to the patient's present condition. Of the 19 patients with identified *PKD1* or *PKD2* variants, 12 were males, 7 were females, with a mean age of 48.9 (22–67) years (**Table 1**). "Pathogenic" or "likely pathogenic" variants were found in 15 patients; 14 *PKD1* variants and 1 *PKD2* variant. Among the 14 *PKD1* variants, 5 mutations were novel, including 4 frameshift, 1 missense, and 1 splice donor site variants. Two known and 2 novel *PKD1* variants of uncertain significance (VUS) was also identified. All variants detected in the present investigation were heterozygous. (**Table 2**).

Each candidate mutation was assessed for its co-segregation with disease in the relevant available family members (at least 1 normal and 1 available affected

DOI: 10.1093/labmed/lmaa047

Table 1. Demographic, Phenotypic Information and Detected Variants in 26 Study Participants

Patient ID	Sex	Age (years)	Mutated gene	Clinical significance of variant	Family history (Y/N)	Phenotype	Extrarenal involvement
P01	F	35	*PKD1*	Pathogenic	NA	HT	-
P02	F	57	*PKD1*	Pathogenic	Y	ESRD	Liver
P03	M	47	*PKD1*	Pathogenic	Y	CKD G3	Liver
P04	M	37	*PKD1*	Pathogenic	Y	CKD G3	Liver, seminal vesicle
P05	M	62	*PKD1*	Pathogenic	Y	CKD G3, HT	Liver
P06	F	56	*PKD1*	Pathogenic	N	Normal	Liver, pancreas
P07	M	37	*PKD1*	Pathogenic	Y	HT	Liver, seminal vesicle
P08	M	56	*PKD1*	Pathogenic	Y	HU, HT	Liver
P09	M	67	*PKD1*	Pathogenic	Y	ESRD	Liver
P10	F	59	*PKD1*	Pathogenic	NA	ESRD	Liver
P11	F	61	*PKD1*	LP	NA	HU, HT	Liver
P12	M	43	*PKD1*	LP	NA	CKD G3	Liver
P13	M	45	*PKD1*	LP	NA	HT	-
P14	M	32	*PKD1*	LP	N	Normal	Liver
P15	F	60	*PKD2*	LP	Y	CKD G3	Liver
P16	M	63	*PKD1*	VUS	Y	Normal	-
P17	M	22	*PKD1*	VUS	Y	HU	Liver
P18	M	26	*PKD1*	VUS	Y	HT	-
P19	F	64	*PKD1*	VUS	Y	Normal	Liver, pancreas
P20	F	39	*LAMB2*	VUS	Y	Normal	-
P21	F	29	*PLCE1*	VUS	N	Normal	Liver, ovary
P22	M	45	-	-	N	HU	-
P23	F	53	-	-	Y	Normal	Liver
P24	F	59	-	-	Y	PU	-
P25	M	36	-	-	NA	Normal	Liver
P26	M	24	-	-	Y	Normal	-

LP, likely pathogenic; VUS, variant of uncertain significance; NA, not available; HT, hypertension; ESRD, end-stage renal disease; CKD, chronic kidney disease; HU, hematuria.

member). However, available family members in pedigree are limited and we could not obtain sufficient evidence for the segregation analysis.

Discussion

In this study, we performed a comprehensive search for mutations in a set of cystic change of kidney related genes, including *PKD1* and *PKD2* in 26 unrelated, known, or suspected patients with ADPKD. We identified 19 variants (detection rate: 73.1%), including 18 *PKD1* variants and one *PKD2* variant. Previous studies have shown that the variant detection rates varied depending on the race of study participants or the combination of test methods (**Table 3**).[11,16–18] In particular, in 2 studies conducted based on NGS in Japan, the detection rate was increased when MLPA was additionally performed. The fact that our study included not only patients diagnosed with ADPKD but also those with suspected ADPKD, could be a possible reason for our relatively low detection rate. We performed long-range PCR to confirm the sequencing results and MLPA to detect large genomic rearrangement, but no additional abnormal findings were detected.

We identified 4 variants of uncertain significance (VUS). According to clinical interpretation using 2015 ACMG/AMP guidelines for sequence variants classification,[15] PS2 (de novo—both maternity and paternity confirmed—in a patient with the disease and no family history) and PP1 (co-segregation with disease in multiple affected family members with a gene definitively known to cause the disease) provide evidence for causative pathogenic mutations. To clarify the clinical significance of the detected VUS using PS2 and PP1, each candidate variants was assessed for its co-segregation with the disease in the relevant available family members. However, due to the limitation of available family members in pedigree, parents test and segregation

Table 2. Details of Variants Identified in Korean ADPKD Patients by NGS

Patient ID	Gene	Exon	cDNA change	Amino acid change	Variant effect	Novelty	Classification evidence	SIFT/MutationTaster/ PolyPhen2/CADD
Pathogenic								
P01	*PKD1*(NM_001009944.2)	4	c.418_424 delGCGGAGG	p.Ala140fs	Frameshift	Novel	PVS1, PM2, PP4	NA
P02	*PKD1*	5	c.690C > A	p.Cys230*	Nonsense	Known	PVS1, PM2, PP4, PP5	NA/disease causing/NA/9.798
P03	*PKD1*	6	c.1295C > T	p.Ala432Val	Missense	Known	PVS1, PP3, PM2, PP4	Damaging/disease causing/probably damaging/13.44
P04	*PKD1*	11	c.2784_2796del	p.Glu929Valfs*18	Frameshift	Novel	PVS1, PM2, PP4	NA
P05	*PKD1*	13	c.2992dupG	p.Ala998fs	Frameshift	Novel	PVS1, PM2, PP4	NA
P06	*PKD1*	28	c.9584G > A	p.Trp3195*	Nonsense	Known	PVS1, PM2, PM6, PP4	NA/disease causing/NA/15.95
P07	*PKD1*	36	c.10745dupC	p.Val3584Argfs*43	Frameshift	Known	PVS1, PM2, PP4, PP5	NA
P08	*PKD1*	40	c.11381delC	p.Thr3794Serfs*32	Frameshift	Novel	PVS1, PM2, PP4	NA
P09	*PKD1*	46	c.12445-5_12451 delCCCAGTTCCGCC	p.Phe4149Thrfs*47	Frameshift	Known	PVS1, PM2, PP5	NA
P10	*PKD1*		c.2853 + 1G > T		Splicing site mutation	Novel	PVS1, PM2, PP4	NA/disease causing/NA/15.54
Likely pathogenic								
P11	*PKD1*	5	c.664G > C	p.Ala222Pro	Missense	Novel	PM1, PM2, PM6, PP4	Damaging/polymorphism/probably damaging/7.803
P12	*PKD1*	6	c.1261C > T	p.Arg421Cys	Missense	Known	PM1, PM2, PM6, PP3, PP4, PP5	Damaging/disease causing/probably damaging/22.2
P13	*PKD1*	15	c.5983C > T	p.Arg1995Cys	Missense	Known	PM1, PM2, PM6, PP4, PP5	Damaging/polymorphism/probably damaging/9.647
P14	*PKD1*	15	c.6868G > T	p.Asp2290Tyr	Missense	Known	PM1, PM2, PM6, PP4, PP5	Damaging/polymorphism/probably damaging/20.7
P15	*PKD2* (NM_000297.3)	4	c.964C > T	p.Arg322Trp	Missense	Known	PM1, PM2, PP3, PP4, PP5	Damaging/disease causing/probably damaging/27.3
VUS								
P16	*PKD1*	11	c.2102C > A	p.Thr701Asn	Missense	Known	PM1, PM2, PP4	Tolerated/polymorphism/possibly damaging/1.938
P17	*PKD1*	15	c.4810G > A	p.Val1604Met	Missense	Known	PM1, PP3, PP4, BS1	Damaging/disease causing/probably damaging/21.8
P18	*PKD1*	30	c.10034G > C	p.Arg3345Pro	Missense	Novel	PM2, PP3, PP4	Damaging/disease causing/probably damaging/17.53
P19	*PKD1*	46	c.12665T > A	p.Leu4222Gln	Missense	Novel	PM2, PP4	Damaging/disease causing/benign/18.09

Table 3. Different Variant Detection Rates Depending on the Races and Methods in Previous Studies

Study	Country	Method	Variant detection rate
Studies in which NGS was not used			
Kim et al. (2000)[13]	Korea	PCR, SSCP	6.59% (6/91)
Rossetti et al. (2007)[19]	U.S.A.	DHPLC, LR-PCR, DS	89.1% (180/202)
Hoefele et al. (2011)[20]	Germany	LR-PCR, DS	64.5% (60/93)
Audrezet et al. (2012)[21]	France	LR-PCR, DS, QFM PCR or Array-CGH	89.9% (629/700)
Yu et al. (2011)[16]	China	DHPLC, LR-PCR, DS	52.3% (34/65)
Choi et al. (2014)[11]	Korea	LR-PCR, DS, MLPA	90.0% (18/20)
Kurashige et al. (2015)[18]	Japan	LR-PCR, DS, q-PCR or MLPA	83.9% (135/161)
NGS-based methods			
Rossetti et al. (2012)[22]	U.S.A.	LR-PCR, NGS	62.8% (115/183)
Tan et al. (2014)[23]	U.S.A.	LR-PCR, NGS	64.0% (16/25)
Trujillano et al. (2014)[24]	Spain	NGS	83.3% (10/12)
Eisenberger et al. (2015)[25]	Germany	NGS	63.6% (35/55)
Mallawaarachchi et al. (2016)[26]	Australia	WGS, LR-PCR, DS	85.7% (24/28)
Kinoshita et al. (2016)[27]	Japan	LR-PCR, NGS, MLPA	89.1% (90/101, NGS only) 93.1% (94/101, NGS + MLPA)
Mochizuki et al. (2019)[28]	Japan	NGS, DS, MLPA	86.5% (96/111, NGS only) 91.9% (102/111, NGS + DS + MLPA)
Wang et al. (2019)[29]	China	NGS, DS	89.4%
This study	Korea	NGS, LR-PCR, DS, MLPA	73.1% (19/26)

SSCP, single-strand conformation polymorphism; DHPLC, denaturing high performance liquid chromatography; LR-PCR, long range-PCR; DS, direct sequencing; NGS, next-generation sequencing; QFM PCR, quantitative fluorescent multiplex PCR; Array-CGH, array-comparative genomic hybridization; q-PCR, quantitative PCR; MLPA, multiplex ligation-dependent probe amplification; WGS, whole genome sequencing

analysis were insufficient for PS2 and PP1, and it is the limitation of this study.

The mutation detection rate in this study was relatively lower than those of most previous studies; we have found that panel-based tests involving relevant genes in clinically diagnosed or suspected cases are useful for differential diagnosis and genetic confirmation. In suspected patients with ADPKD, the possibility of a disease other than ADPKD should be considered. The diseases to be considered include the following: benign-appearing multiple benign simple cysts, medullary cystic kidney disease and tuberous sclerosis showing autosomal dominant inheritance, and autosomal recessive polycystic kidney disease (ARPKD).[30,31] In many inherited polycystic kidney diseases, the causative genes have been already identified. As NGS becomes cost-effective and clinically applicable, multi-gene panel analysis can be used to diagnose confounding diseases that are not easily distinguished from ADPKD based on conventional imaging techniques or family history.

Understanding the genetic background of patients is also useful for medical management and predicting prognosis. Some early-onset ADPKD can be caused by the co-inheritance of a mutation in another gene.[32,33] Tuberous sclerosis complex gene 2 (*TSC2)* is located adjacent to *PKD1,* and contiguous deletions of both genes induce severe polycystic kidney disease in infancy or early childhood with end-stage renal disease (ESRD).[5,32,34] In addition, genetic analysis of ADPKD genes provides a reliable diagnostic tool for young high-risk individuals under 40 years with equivocal imaging results, who can be evaluated as potential living kidney donors.[8]

Patients with *PKD2* mutations, compared to patients with *PKD1* mutations, present a milder clinical course consisting of late onset of symptoms, longer life span, lower risk of renal failure, and lower risk of adverse events.[35] Although we could not compare the phenotype and prognosis between patients with *PKD1* and *PKD2* mutations in this study, due to an insufficient number of patients with *PKD2* mutations, hypertension and hematuria occur more commonly in patients with *PKD1* mutations than in those with *PKD2*, which is thought to be associated with a poor prognosis in patients with *PKD1* mutations. In addition, recent studies have shown that truncated mutations (frameshifting, nonsense, and splicing) rather than noncutting mutations (miss sense and in-frame changes) in the *PKD1* gene are associated with adverse outcomes.[9] In this study, no significant phenotypic differences were found between truncating and nontruncating mutations. However, it was difficult to

make an accurate comparison because the medical records of some patients did not indicate the time of onset, duration, and degree of renal dysfunction. In future studies, it is necessary to compare the prognosis of patients with various classifications of ADPKD through more consistent and structured evaluation and regular follow-up.

In conclusion, NGS-based multigene analysis can serve as a comprehensive and cost-effective tool in a clinical setting for genetic diagnosis of inherited renal diseases, including ADPKD. The use of this technique will facilitate the identification of many clinically significant novel variants and help differentiate between several ADPKD-like diseases. These objectives are difficult to achieve with conventional diagnostic protocols. **LM**

Acknowledgements

We thank our colleagues from the Department of Laboratory Medicine, Pusan National University Hospital who provided expertise that greatly assisted the research.

Author Contributions

All authors confirmed they have contributed to the intellectual content of this paper and have met the following 4 requirements: (A) significant contributions to the conception and design, acquisition of data, or analysis and interpretation of data; (B) drafting or revising the article for intellectual content; (C) final approval of the published article; and (D) agreement to be accountable for all aspects of the article thus ensuring that questions related to the accuracy or integrity of any part of the article are appropriately investigated and resolved.

Conceptualization

N Kim, SH Song. Methodology: Chulhun L. Chang, Hyung-Hoi Kim. Data curation: H Kim. Writing—original draft preparation: H Kim. Writing—review and editing: N Kim.

Funding

This study was supported by Biomedical Research Institute Grant (2018B034), Pusan National University Hospital

Study Institution

Pusan National University Hospital

Ethics Statement

The study protocol was reviewed and approved by the Institutional Review Board of Pusan National University Hospital, and informed consent was waived after committee approval (1704-005-006).

References

1. Wilson PD. Polycystic kidney disease. *N Engl J Med.* 2004;36(10):1868–1873.
2. Harris PC, Rossetti S. Molecular diagnostics for autosomal dominant polycystic kidney disease. *Nat Rev Nephrol.* 2010;6(4):197–206.
3. Audrézet MP, Corbiere C, Lebbah S, et al. Comprehensive PKD1 and PKD2 mutation analysis in prenatal autosomal dominant polycystic kidney disease. *J Am Soc Nephrol.* 2016;27(3):722–729.
4. Gradzik M, Niemczyk M, Gołębiowski M, Pączek L. Diagnostic imaging of autosomal dominant polycystic kidney disease. *Pol J Radiol.* 2016;81:441–453.
5. Pei Y. Diagnostic approach in autosomal dominant polycystic kidney disease. *Clin J Am Soc Nephrol.* 2006;1(5):1108–1114.
6. Pei Y, Obaji J, Dupuis A, et al. Unified criteria for ultrasonographic diagnosis of ADPKD. *J Am Soc Nephrol.* 2009;20(1):205–212.
7. Ravine D, Gibson RN, Walker RG, Sheffield LJ, Kincaid-Smith P, Danks DM. Evaluation of ultrasonographic diagnostic criteria for autosomal dominant polycystic kidney disease 1. *Lancet.* 1994;343(8901):824–827.
8. Zhao X, Paterson AD, Zahirieh A, He N, Wang K, Pei Y. Molecular diagnostics in autosomal dominant polycystic kidney disease: utility and limitations. *Clin J Am Soc Nephrol.* 2008;3(1):146–152.
9. Pei Y, Hwang YH, Conklin J, et al. Imaging-based diagnosis of autosomal dominant polycystic kidney disease. *J Am Soc Nephrol.* 2015;26(3):746–753.
10. Torres VE, Harris PC, Pirson Y. Autosomal dominant polycystic kidney disease. *Lancet.* 2007;369(9569):1287–1301.
11. Choi R, Park HC, Lee K, et al. Identification of novel PKD1 and PKD2 mutations in Korean patients with autosomal dominant polycystic kidney disease. *BMC Med Genet.* 2014;15:129.
12. Eo HS, Lee JG, Ahn C, et al. Three novel mutations of the PKD1 gene in Korean patients with autosomal dominant polycystic kidney disease. *Clin Genet.* 2002;62(2):169–174.
13. Kim UK, Jin DK, Ahn C, et al. Novel mutations of the PKD1 gene in Korean patients with autosomal dominant polycystic kidney disease. *Mutat Res.* 2000;432(1-2):39–45.
14. Lee JG, Lee KB, Kim UK, et al. Genetic heterogeneity in Korean families with autosomal-dominant polycystic kidney disease (ADPKD): the first Asian report. *Clin Genet.* 2001;60(2):138–144.
15. Richards S, Aziz N, Bale S, et al. Standards and guidelines for the interpretation of sequence variants: a joint consensus recommendation of the American College of Medical Genetics and Genomics and the Association for Molecular Pathology. *Genet Med*. 2015;17(5):405–424.
16. Yu C, Yang Y, Zou L, et al. Identification of novel mutations in Chinese Hans with autosomal dominant polycystic kidney disease. *BMC Med Genet.* 2011;12:164.

17. Chang MY, Chen HM, Jenq CC, et al. Novel PKD1 and PKD2 mutations in Taiwanese patients with autosomal dominant polycystic kidney disease. *J Hum Genet.* 2013;58(11):720–727.
18. Kurashige M, Hanaoka K, Imamura M, et al. A comprehensive search for mutations in the PKD1 and PKD2 in Japanese subjects with autosomal dominant polycystic kidney disease. *Clin Genet*. 2015;87(3):266–272.
19. Rossetti S, Consugar MB, Chapman AB, et al. Comprehensive molecular diagnostics in autosomal dominant polycystic kidney disease. *J Am Soc Nephrol.* 2007;18(7):2143–2160.
20. Hoefele J, Mayer K, Scholz M, Klein HG. Novel PKD1 and PKD2 mutations in autosomal dominant polycystic kidney disease (ADPKD). *Nephrol Dial Transplant.* 2011;26(7):2181–2188.
21. Audrezet MP, Cornec-Le Gall E, Chen JM, et al. Autosomal dominant polycystic kidney disease: comprehensive mutation analysis of PKD1 and PKD2 in 700 unrelated patients. *Hum Mutat.* 2012;33(8):1239–1250.
22. Rossetti S, Hopp K, Sikkink RA, et al. Identification of gene mutations in autosomal dominant polycystic kidney disease through targeted resequencing. *J Am Soc Nephrol*. 2012;23(5):915–933.
23. Tan AY, Michaeel A, Liu G, et al. Molecular diagnosis of autosomal dominant polycystic kidney disease using next-generation sequencing. *J Mol Diagn*. 2014;16(2):216–228.
24. Trujillano D, Bullich G, Ossowski S, et al. Diagnosis of autosomal dominant polycystic kidney disease using efficient PKD1 and PKD2 targeted next-generation sequencing. *Mol Genet Genomic Med*. 2014;2(5):412–421.
25. Eisenberger T, Decker C, Hiersche M, et al. An efficient and comprehensive strategy for genetic diagnostics of polycystic kidney disease. *PLoS One*. 2015;10(2):e0116680.
26. Mallawaarachchi AC, Hort Y, Cowley MJ, Whole-genome sequencing overcomes pseudogene homology to diagnose autosomal dominant polycystic kidney disease. *Eur J Hum Genet.* 2016;24(11):1584–1590.
27. Kinoshita M, Higashihara E, Kawano H, et al. Technical evaluation: Identification of pathogenic mutations in PKD1 and PKD2 in patients with autosomal dominant polycystic kidney disease by next-generation sequencing and use of a comprehensive new classification system. *PLoS One.* 2016;11(11):e0166288.
28. Mochizuki T, Teraoka A, Akagawa H, et al. Mutation analyses by next-generation sequencing and multiplex ligation-dependent probe amplification in Japanese autosomal dominant polycystic kidney disease patients. *Clin Exp Nephrol*. 2019;23(8):1022–1030.
29. Wang T, Li Q, Shang S, et al. Identifying gene mutations of Chinese patients with polycystic kidney disease through targeted next-generation sequencing technology. *Mol Genet Genomic Med*. 2019;7(6):e720.
30. Alves M, Fonseca T, de Almeida EAF. Differential diagnosis of autosomal dominant polycystic kidney disease. In: Li X, editor. *Polycystic Kidney Disease [Internet]*. Brisbane (AU): Codon Publications; 2015 Nov. Chapter 1. Available from: https://www.ncbi.nlm.nih.gov/books/NBK373390/ doi: 10.15586/codon.pkd.2015.ch1.
31. Chapman AB, Devuyst O, Eckardt KU, et al. Autosomal-dominant polycystic kidney disease (ADPKD): executive summary from a Kidney Disease: Improving Global Outcomes (KDIGO) Controversies Conference. *Kidney Int*. 2015;88(1):17–27.
32. Cornec-Le Gall E, Alam A, Perrone RD. Autosomal dominant polycystic kidney disease. *Lancet*. 2019;393(10174):919–935.
33. Bergmann C, von Bothmer J, Ortiz Bruchle N, et al. Mutations in multiple PKD genes may explain early and severe polycystic kidney disease. *J Am Soc Nephrol*. 2011;22(11):2047–2056.
34. Consugar MB, Wong WC, Lundquist PA, et al. Characterization of large rearrangements in autosomal dominant polycystic kidney disease and the PKD1/TSC2 contiguous gene syndrome. *Kidney Int*. 2008;74(11):1468–1479.
35. Hateboer N, v Dijk MA, Bogdanova N, et al. Comparison of phenotypes of polycystic kidney disease types 1 and 2. *The Lancet.* 1999;353(9147):103–107.
36. Neumann HP, Jilg C, Bacher J, et al. Epidemiology of autosomal-dominant polycystic kidney disease: an in-depth clinical study for south-western Germany. *Nephrol Dial Transplant.* 2013;28(6):1472–1487
37. Obeidova L, Elisakova V, Stekrova J, et al. Novel mutations of PKD genes in the Czech population with autosomal dominant polycystic kidney disease. *BMC Med Genet.* 2014;15:41.

CRISPR-Based Approaches for Efficient and Accurate Detection of SARS-CoV-2

Wancun Zhang, PhD,[1,2] Kangbo Liu, MD,[3] Pin Zhang, MD,[1] Weyland Cheng, PhD,[1] Linfei Li, MD,[1] Fan Zhang, MD,[4] Zhidan Yu, PhD,[1] Lifeng Li, PhD,[1] Xianwei Zhang, PhD[2]*

Laboratory Medicine 2021;52:116-121

DOI: 10.1093/labmed/lmaa101

ABSTRACT

An outbreak of COVID-19, caused by infection with SARS-CoV-2 in Wuhan, China in December 2019, spread throughout the country and around the world, quickly. The primary detection technique for SARS-CoV-2, the reverse-transcription polymerase chain reaction (RT-PCR)–based approach, requires expensive reagents and equipment and skilled personnel. In addition, for SARS-CoV-2 detection, specimens are usually shipped to a designated laboratory for testing, which may extend the diagnosis and treatment time of patients with COVID-19. The latest research shows that clustered regularly interspaced short palindromic repeats (CRISPR)–based approaches can quickly provide visual, rapid, ultrasensitive, and specific detection of SARS-CoV-2 at isothermal conditions. Therefore, CRISPR-based approaches are expected to be developed as attractive alternatives to conventional RT-PCR methods for the efficient and accurate detection of SARS-CoV-2. Recent advances in the field of CRISPR-based biosensing technologies for SARS-CoV-2 detection and insights into their potential use in many applications are reviewed in this article.

Keywords: SARS-CoV-2, 2019-nCoV, COVID-19, CRISPR, diagnosis

Coronaviruses (CoVs), with 4 major structural proteins including spike, membrane, envelope, and nucleoprotein, are positive-sense, single-strand RNA viruses.[1,2] Before SARS-CoV-2, there were 6 CoVs that were known to be pathogenic to humans: HCoV-OC43, HCoV-NL63, HCoV-HKU1, HCoV-229E, SARS-CoV, and MERS-CoV,[3-5] with the latter 2 being highly transmissible and pathogenic. SARS-CoV-2 (previously named 2019-nCoV) is a new coronavirus causing COVID-19, which was first observed in December 2019 in Wuhan, China.[6,7] As of August 17, 2020, based on the data provided by the World Health Organization, 7,716,255 people were confirmed to be infected globally, with 774,413 deaths. According to a response plan recently shared by the US government with the *New York Times,* the SARS-CoV-2 pandemic may continue for more than 18 months. According to this document, a "multi-wave disease" may occur in the next year and a half. Therefore, there is an urgent need for a point-of-care diagnosis method that can be used for SARS-CoV-2 screening.

Abbreviations:

RT-PCR, reverse-transcription polymerase chain reaction; CRISPR, clustered regularly interspaced short palindromic repeats; CoVs, coronaviruses; mNGS, metagenomic next-generation sequencing; Cas, CRISPR-associated; crRNA, CRISPR RNA; SHERLOCK, Specific High Sensitivity Enzymatic Reporter Unlocking; aM, attomolar; LAMP, loop-mediated isothermal amplification; AIOD-CRISPR, All-In-One Dual CRISPR-Cas12a; STOP, SHERLOCK Testing in One Pot; LOD, limit of detection.

[1]Henan Key Laboratory of Children's Genetics and Metabolic Diseases, Children's Hospital Affiliated to Zhengzhou University, Henan Children's Hospital, Zhengzhou, China, [2]Zhengzhou Key Laboratory of Precise Diagnosis and Treatment of Children's Malignant Tumors, Department of Pediatric Oncology Surgery, Children's Hospital Affiliated to Zhengzhou University, Zhengzhou, China, [3]Biological Testing Room, Henan Medical Equipment Inspection Institute, Henan Medical Equipment Inspection and Testing Engineering Technology Research Center, Henan Medical Equipment Biotechnology and Application Engineering Research Center, Zhengzhou, China, [4]Department of Orthopedics, Fengqiu County People's Hospital, Xinxiang, China

*To whom correspondence should be addressed.
zhangxw956658@126.com

Currently, nucleic-acid-based tests have been widely used as the standard method for the detection of SARS-CoV-2. Metagenomic next-generation sequencing (mNGS) and reverse-transcription polymerase chain reaction (RT-PCR) are 2 molecular methods that are frequently used for the diagnosis of SARS-CoV-2.[8-11] Originally used for the identification of this new viral species, mNGS is considered one of the most important methods of detection. However, its wider application is limited by its cost and longer detection time of nearly a day. Therefore, mNGS is not suitable for large-scale screening for SARS-CoV-2.[11,12] In addition,

RT-PCR assay for the detection of SARS-CoV-2 is faster and more affordable in comparison than mNGS-based approaches. Nevertheless, the need for a thermocycler for RT-PCR-based diagnostics hinders its use in low-resource settings and curbs the assay throughput. In addition, currently available RT-PCR kits are variable, offering sensitivities ranging between 45% and 60%. Thus, in the early course of an infection, repeat testing may be required to reach a diagnosis.[13] Consequently, RT-PCR and mNGS-based approaches are not suitable for the point-of-care diagnosis of SARS-CoV-2.

Aside from a lower demand for sophisticated temperature controlling instruments, isothermal molecular methods are advantageous beause of faster nucleic acid amplification.[14,15] Clustered regularly interspaced short palindromic repeats (CRISPR) is a biotechnologic technique well-known for its use in gene editing. In addition, CRISPR has been recently used for the in vitro detection of nucleic acids. The latest research shows that CRISPR-based approaches can rapidly and efficiently detect SARS-CoV-2 with high sensitivity and specificity at isothermal conditions.[16,17] Therefore, CRISPR-based approaches, emerging as a powerful and precise tool for SARS-CoV-2 diagnosis, are expected to be used for SARS-CoV-2 screening in homes and primary hospitals.

Efficient and Accurate Detection of SARS-CoV-2

Rapid, effcient, and accurate identification of infectious diseases is essential to optimize clinical care and guide infection control and public health interventions to limit disease spread in both highly specialized medical centers and remote health care settings. Many methods exist for detecting nucleic acids, and each technology has different advantages and limitations.[14,18-22] The ideal diagnostic test would be inexpensive and accurate and would provide a result rapidly, allowing for point-of-care use on multiple specimen types without the need for technical personnel or sophisticated equipment. Highly pathogenic viruses can emerge in remote settings but can also spread globally (eg, Ebola virus and Middle East respiratory syndrome coronavirus), requiring a method that provides early rapid and accurate detection, limiting the spread of infectious diseases and promoting timely care.[23]

The CRISPR and CRISPR-associated (Cas) adaptive immune systems contain programmable endonucleases that can be used for CRISPR-based diagnostics. Although some Cas enzymes target DNA, single-effector RNA-guided RNases, such as Cas13a, can be reprogrammed with CRISPR RNAs (crRNAs) to provide a platform for specific RNA sensing. Upon recognition of its RNA target, activated Cas13a engages in "collateral" cleavage of nearby nontargeted RNAs, which allows Cas13a to detect the presence of a specific RNA in vivo by triggering programmed cell death or in vitro by nonspecific degradation of labeled RNA. The Specific High Sensitivity Enzymatic Reporter Unlocking (SHERLOCK), based on nucleic acid amplification and Cas13a-mediated collateral cleavage of a reporter RNA, allows for real-time, rapid, and specific detection of the target with attomolar (aM) sensitivity.[17,24]

Compared with the RT-PCR-based approach, CRISPR-based approaches have the following advantages: isothermal signal amplification obviating the need for thermocycling, rapid turnaround time, single nucleotide target specificity, integration with accessible and easy-to-use reporting formats such as lateral flow strips, and no requirements for complex laboratory infrastructure.[16] Therefore, CRISPR-based approaches are expected to be used for the rapid, sensitive, and visual detection of SARS-CoV-2.

Visualization and Portable Onsite Detection of SARS-CoV-2

Reducing the global infectivity of SARS-CoV-2 requires efficient and accurate nucleic acid diagnostic tools. However, the typical detection time for screening and diagnosing patients with suspected SARS-CoV-2 has been >24 hours, given the need to ship specimens overnight to designated laboratories. In addition, testing typically relies on expensive equipment and well-trained personnel, all of which is not conducive to the rapid

Lab Medicine 2021;52;116–121 117
DOI: 10.1093/labmed/lmaa101

control of the epidemic.[25-27] In such a backdrop, any development toward ultrasensitive, cheaper, and portable diagnostic tests for the assessment of suspected infection, regardless of the presence of qualified personnel or sophisticated equipment for virus detection, could help advance the diagnosis of COVID-19.

Isothermal amplification methods, such as recombinase polymerase amplification[28] and loop-mediated isothermal amplification (LAMP),[29] have been developed as attractive alternatives to the conventional PCR method because of their simplicity, rapidity, and low cost. However, there is still a challenge to develop these methods into a reliable point-of-care diagnostic for clinical applications because of nonspecific signals.[30,31] Notably, whereas CRISPR is a biotechnological technique well-known for its use in gene editing, it has been recently used for the in vitro detection of nucleic acids, thereby emerging as a powerful and precise tool for molecular diagnosis.[32-34]

Lucia et al[26] developed a Cas12-based diagnostic tool to detect synthetic SARS-CoV-2 RNA sequences in a proof-of-principle evaluation. The test proved to be sensitive, rapid, and potentially portable. More important, the Cas12-based diagnostic tool can provide visualization of the results. Ding et al[35] developed the All-In-One Dual Cas12a (AIOD-CRISPR) assay for simple, rapid, ultrasensitive, one-step approach for visual detection of SARS-CoV-2. In the AIOD-CRISPR assay, a crRNA pair is introduced to initiate dual Cas12a detection, improving the detection of SARS-CoV-2 nucleic acids (DNA and RNA) with a sensitivity of few copies. Therefore, the AIOD-CRISPR assay has potential for the development of next-generation point-of-care molecular diagnostics.

Joung et al developed a simple chemical test that is suitable for point-of-care use in detecting SARS-CoV-2 in 1 hour, called STOPCovid (SHERLOCK Testing in One Pot). This simplified test, STOPCovid, provides a sensitivity comparable to RT-PCR-based SARS-CoV-2 tests and has a limit of detection of 100 copies of viral genome input in saliva or nasopharyngeal swabs per reaction. Using lateral flow readout, the test returns results in 70 minutes. Using fluorescence readout, the test returns results in 40 minutes. Moreover, in their study, 12 positive and 5 negative results from nasopharyngeal swabs were detected by STOPCovid and by RT-PCR, meaning that STOPCovid and RT-PCR test results were consistent with each other. Thus, STOPCovid can significantly aid "test-trace-isolate" efforts, especially in low-resource settings, which is critical for long-term public health safety and for effectively reopening society.[27] Therefore, the CRISPR-based approach is critical for virus detection in regions that lack resources to use the currently available methods.

Ultra-Sensitive Detection of SARS-CoV-2

Clinical studies have shown that the viral titers of hospitalized patients can fluctuate day-to-day with no correlation with the severity of the disease.[8,36,37] In 24 various specimens from patients in the recovery period, RNA was detected as negative for both the *N* gene and the *ORF1b* gene at several days after their readmission to the hospital using a commercial kit whose lower limit of detection (LOD) was relatively high (500 copies/mL). However, using a higher-sensitivity SHERLOCK kit with an LOD of 100 copies/mL, 75% of specimens were positive for the *S* gene and 41.6% for *ORF* genes, suggesting that the carrier status of the virus may exist in patients who have recovered from COVID-19.[38-42] Therefore, more sensitive RNA detection methods are required to detect and monitor these patients.

The CRISPR-nCoV approach developed by Hou et al[11] showed near single-copy sensitivity for SARS-CoV-2 detection and great clinical sensitivity with a shorter turnaround time than RT-PCR. Broughton et al[16] developed the SARS-CoV-2 DETECTR lateral flow assay, which performs simultaneous reverse transcription and isothermal amplification using LAMP followed by Cas12 detection, where it can be visualized on a lateral flow strip with a limit of detection of 10 copies/μL within 30 minutes. The CRISPR-based SHERLOCK technique for the detection of COVID-19 developed by F. Zhang et al[25] can detect COVID-19 target sequences in a range between 20 and 200 aM (10–100 copies per μL of input) within 60 minutes using synthetic COVID-19 virus RNA fragments. These ultrasensitive CRISPR-based approaches, along with STOPCovid,[27] the AIOD-CRISPR assay,[35] and the Cas12a-based detection system,[26] can accurately and effectively monitor and manage patients with COVID-19 during their recovery period.

Highly Specific Detection of SARS-CoV-2

Highly specific detection of SARS-CoV-2 is essential for the control of the pandemic. Hou et al[11] tested their CRISPR-nCoV technique with DNA from human cells and a panel of microbes including bacteria commonly found in respiratory infections, human coronaviruses, other viruses commonly found in respiratory infections, and other bacteria. None of these interference specimens triggered a false positive reaction. Their CRISPR-nCoV approach showed a sensitivity of 100% by detecting all 52 SARS-CoV-2 positive results. No false positives were found in any of the 62 negative results, including all the patients infected with human coronavirus, suggesting CRISPR-nCoV as a promising molecular assay for SARS-CoV-2 detection with great sensitivity and specificity.[11]

The CRISPR-based DETECTR lateral flow assay (SARS-CoV-2 DETECTR) developed by Broughton et al[16] provides a visual and faster alternative to the Centers for Disease Control and Prevention SARS-CoV-2 real-time RT-PCR assay. In their study, 11 respiratory swab specimens collected from 6 patients who were PCR-positive COVID-19 and 12 nasopharyngeal swab specimens from patients with influenza and common human seasonal coronavirus infections and healthy donors were assessed by the SARS-CoV-2 DETECTR. Relative to the RT-PCR results, the SARS-CoV-2 DETECTR was 90% sensitive and 100% specific for detection of the coronavirus in the respiratory swab specimens, corresponding to positive and negative predictive values of 100% and 91.7%, respectively.[16] A recent study by Patchsung et al[43] showed that the SHERLOCK assay has 100% specificity and 97% sensitivity in detecting SARS-CoV-2. Therefore, the CRISPR-based approach is expected to be used for specific point-of-care diagnosis of SARS-CoV-2.

Rapid Detection of SARS-CoV-2

The establishment of the SARS-CoV-2 rapid method is essential for responding to the outbreak of SARS-CoV-2. The IgG/IgM test kit has a short turnaround time with no specific requirements for additional equipment or skilled technicians, and it can be used as a point-of-care diagnosis method. However, the IgG/IgM test kit has a high rate of false positives and is not suitable for clinical use alone. It has been recommended that the IgG/IgM test kit could likely remedy false negatives inherent in respiratory swab specimens and could be administered as a complementary option to RT-PCR.[44,45] The CRISPR-based approach requires only 40 minutes for the entire detection process. However, the RT-PCR-based approach requires approximately 1.5 hours for a completion run of the PCR program. The mNGS method takes approximately 20 hours, which includes 8 hours of library preparation, 10 hours of sequencing, and 2 hours of bioinformatic analysis. Therefore, CRISPR-nCoV presents a significant advantage in effective turnaround time over RT-PCR and mNGS.[11] The Cas12-based lateral flow assay reported by Broughton et al[16] can be completed within 1 hour, as can the CRISPR-based SHERLOCK technique for the detection of SARS-CoV-2.[25] As previously mentioned, the STOP approach developed by Joung et al[27] returns results in 70 minutes using lateral flow readout and in 40 minutes using fluorescence readout. Therefore, a CRISPR-based approach can be used for the rapid detection of SARS-CoV-2.

Conclusion

The rapid spread of SARS-CoV-2 is clearly a major concern for countries across the world. Infection with COVID-19 can be diagnosed using an RT-PCR-based approach, but inadequate access to reagents and equipment has slowed disease detection. The CRISPR-based approaches, such as STOP, SHERLOCK, and DETECTR, can provide highly sensitive, efficient, and specific detection of SARS-CoV-2 using multiple types of specimens (saliva, nasopharyngeal swab, respiratory swab, oropharyngeal swab, and bronchoalveolar lavage fluid). In addition, CRISPR-based lateral flow assay for the detection of SARS-CoV-2 is rapid, low-cost, and portable. Aside from the lower demand for sophisticated temperature controlling instruments, isothermal molecular methods are advantageous because of their faster nucleic acid amplification. These key traits of the CRISPR-based method are critical for viral detection in regions that may lack resources for currently available methods.

Lab Medicine 2021;52;116–121
DOI: 10.1093/labmed/lmaa101

On May 8, 2020, the first CRISPR test for SARS-CoV-2 was approved in the United States. This new diagnostic kit was based on an approach codeveloped by CRISPR pioneer Feng Zhang at the Broad Institute of the Massachusetts Institute of Technology and Harvard University in Cambridge, Massachusetts. The diagnostic kit will be used to test for the novel coronavirus in laboratories that are certified to provide clinical test results. We believe that more CRISPR-based approaches will be approved for clinical testing of SARS-CoV-2 in the future. **LM**

Acknowledgments

This work was funded by the China Postdoctoral Science Foundation (No. 2020M672301), Scientific and Technological Projects of Henan Province (202102310068), the Henan Medical Science and Technology Program (LHGJ20190937), the Henan Provincial Key Laboratory of Children's Genetics and Metabolic Diseases Foundation (SS201902 and SS201906), and the Henan Neural Development Engineering Research Center for Children Foundation (SG201904 and SG201906). Thanks to Mengmeng Chen for great efforts in checking the English of this manuscript.

References

1. Ren LL, Wang YM, Wu ZQ, et al. Identification of a novel coronavirus causing severe pneumonia in human: a descriptive study. *Chin Med J (Engl).* 2020;133(9):1015–1024.
2. Lu R, Zhao X, Li J, et al. Genomic characterisation and epidemiology of 2019 novel coronavirus: implications for virus origins and receptor binding. *Lancet.* 2020;395(10224):565–574.
3. Su S, Wong G, Shi W, et al. Epidemiology, genetic recombination, and pathogenesis of coronaviruses. *Trends Microbiol.* 2016;24(6):490–502.
4. de Groot RJ, Baker SC, Baric RS, et al. Middle East respiratory syndrome coronavirus (MERS-CoV): announcement of the Coronavirus Study Group. *J Virol.* 2013;87(14):7790–7792.
5. Weiss SR, Navas-Martin S. Coronavirus pathogenesis and the emerging pathogen severe acute respiratory syndrome coronavirus. *Microbiol Mol Biol Rev.* 2005;69(4):635–664.
6. Coronaviridae Study Group of the International Committee on Taxonomy of Viruses. The species severe acute respiratory syndrome-related coronavirus: classifying 2019-nCoV and naming it SARS-CoV-2. *Nat Microbiol* 2020; 5:536–544.
7. Zhang W, Zhang P, Wang G, Cheng W, Chen J, Zhang X. Recent advances of therapeutic targets and potential drugs of COVID-19. *Pharmazie.* 2020;75(5):161–163.
8. Wang W, Xu Y, Gao R, et al. Detection of SARS-CoV-2 in different types of clinical specimens. *JAMA.* 2020;323(18):1843–1844.
9. Liu R, Han H, Liu F, et al. Positive rate of RT-PCR detection of SARS-CoV-2 infection in 4880 cases from one hospital in Wuhan, China, from Jan to Feb 2020. *Clin Chim Acta.* 2020;505:172–175.
10. Liu R, Fu A, Deng Z, Li Y, Liu T. Promising methods for detection of novel coronavirus SARS-CoV-2. *View* 2020;1(1):e4.
11. Hou T, Zeng W, Yang M, et al. Development and evaluation of a CRISPR-based diagnostic for 2019-novel coronavirus. *PLoS Pathog* 2020;16(8):e1008705.
12. Ai JW, Zhang HC, Xu T, et al. Optimizing diagnostic strategy for novel coronavirus pneumonia, a multi-center study in Eastern China. Preprint. Posted online February 16, 2020. *medRxiv* 113325. doi: 10.1101/2020.02.13.20022673.
13. Al-Tawfiq JA, Memish ZA. Diagnosis of SARS-CoV-2 infection based on CT scan vs. RT-PCR: reflecting on experience from MERS-CoV. *J Hosp Infect* 2020; 105:154–155.
14. Zhang W, Zhang P, Zhang F, et al. Real-time and rapid quantification of microRNAs in cells and tissues using target-recycled enzyme-free amplification strategy. *Talanta.* 2020;217:121016.
15. Zhao Y, Chen F, Li Q, Wang L, Fan C. Isothermal amplification of nucleic acids. *Chem Rev.* 2015;115(22):12491–12545.
16. Broughton JP, Deng X, Yu G, et al. CRISPR-Cas12-based detection of SARS-CoV-2. *Nat Biotechnol* 2020;38(7):870–874.
17. Kellner MJ, Koob JG, Gootenberg JS, Abudayyeh OO, Zhang F. SHERLOCK: nucleic acid detection with CRISPR nucleases. *Nat Protoc.* 2019;14(10):2986–3012.
18. Du Y, Pothukuchy A, Gollihar JD, Nourani A, Li B, Ellington AD. Coupling sensitive nucleic acid amplification with commercial pregnancy test strips. *Angew Chem Int Ed Engl.* 2017;56(4):992–996.
19. Green AA, Silver PA, Collins JJ, Yin P. Toehold switches: de-novo-designed regulators of gene expression. *Cell.* 2014;159(4):925–939.
20. Pardee K, Green AA, Ferrante T, et al. Paper-based synthetic gene networks. *Cell.* 2014;159(4):940–954.
21. Kumar RM, Cahan P, Shalek AK, et al. Deconstructing transcriptional heterogeneity in pluripotent stem cells. *Nature.* 2014;516(7529):56–61.
22. Zhang W, Hu F, Zhang X, et al. Ligase chain reaction-based electrochemical biosensor for the ultrasensitive and specific detection of single nucleotide polymorphisms. *New J Chem* 2019;43:14327–14335.
23. Chertow DS. Next-generation diagnostics with CRISPR. *Science* 2018;360:381–382.
24. Gootenberg JS, Abudayyeh OO, Lee JW, et al. Nucleic acid detection with CRISPR-Cas13a/C2c2. *Science.* 2017;356(6336):438–442.
25. Zhang F, Abudayyeh OO, Gootenberg JS. A protocol for detection of COVID-19 using CRISPR diagnostics (v.20200321). https://www.broadinstitute.org/files/publications/special/COVID-19%20detection%20(updated).pdf. Accessed November 9, 2020.
26. Lucia C, Federico P-B, Alejandra GC. An ultrasensitive, rapid, and portable coronavirus SARS-CoV-2 sequence detection method based on CRISPR-Cas12. Preprint. Posted online March 2, 2020. *bioRxiv*. doi: 10.1101/2020.02.29.97/1127.
27. Joung J, Ladha A, Saito M, et al. Point-of-care testing for COVID-19 using SHERLOCK diagnostics (v.20200505). Preprint. Posted online May 8, 2020. *medRxiv.* doi: 10.1101/2020.05.04.20091231.
28. Piepenburg O, Williams CH, Stemple DL, Armes NA. DNA detection using recombination proteins. *PLoS Biol.* 2006;4(7):e204.
29. Chen G, Chen R, Ding S, et al. Recombinase assisted loop-mediated isothermal DNA amplification. *Analyst.* 2020;145(2):440–444.
30. Rolando JC, Jue E, Barlow JT, Ismagilov RF. Real-time kinetics and high-resolution melt curves in single-molecule digital LAMP to differentiate and study specific and non-specific amplification. *Nucleic Acids Res.* 2020;48(7):e42.
31. Tian B, Minero GAS, Fock J, Dufva M, Hansen MF. CRISPR-Cas12a based internal negative control for nonspecific products of exponential rolling circle amplification. *Nucleic Acids Res.* 2020;48(5):e30.
32. Manguso RT, Pope HW, Zimmer MD, et al. In vivo CRISPR screening identifies Ptpn2 as a cancer immunotherapy target. *Nature.* 2017;547(7664):413–418.

33. Breslow DK, Hoogendoorn S, Kopp AR, et al. A CRISPR-based screen for Hedgehog signaling provides insights into ciliary function and ciliopathies. *Nat Genet.* 2018;50(3):460–471.
34. Tsai SQ, Nguyen NT, Malagon-Lopez J, Topkar VV, Aryee MJ, Joung JK. CIRCLE-seq: a highly sensitive in vitro screen for genome-wide CRISPR-Cas9 nuclease off-targets. *Nat Methods.* 2017;14(6):607–614.
35. Ding X, Yin K, Li Z, Liu C. All-in-One Dual CRISPR-Cas12a (AIOD-CRISPR) assay: a case for rapid, ultrasensitive and visual detection of novel coronavirus SARS-CoV-2 and HIV virus. Preprint. Posted online March 21, 2020. *bioRxiv*. doi: 10.1101/2020.03.19.998724.
36. Zou L, Ruan F, Huang M, et al. SARS-CoV-2 viral load in upper respiratory specimens of infected patients. *N Engl J Med.* 2020;382(12):1177–1179.
37. Holshue ML, DeBolt C, Lindquist S, et al. First case of 2019 novel coronavirus in the United States. *N Engl J Med* 2020;382:929–936.
38. An J, Liao X, Xiao T, et al. Clinical characteristics of recovered COVID-19 patients with re-detectable positive RNA test. *Ann Transl Med*. 2020;8(19):1084.
39. Lan L, Xu D, Ye G, et al. Positive RT-PCR test results in patients recovered from COVID-19. *JAMA* 2020;323:1502–1503.
40. Ling Y, Xu SB, Lin YX, et al. Persistence and clearance of viral RNA in 2019 novel coronavirus disease rehabilitation patients. *Chin Med J* 2020;133:1039–1043.
41. Qu YM, Kang EM, Cong HY. Positive result of Sars-Cov-2 in sputum from a cured patient with COVID-19. *Travel Med Infect Dis.* 2020;34:101619.
42. Xing Y, Ni W, Wu Q, et al. Prolonged presence of SARS-CoV-2 in feces of pediatric patients during the convalescent phase. Preprint. Posted online March 13, 2020. *medRxiv*. doi: 10.1101/2020.03.11.20033159.
43. Patchsung M, Jantarug K, Pattama A, et al. Clinical validation of a Cas13-based assay for the detection of SARS-CoV-2 RNA. *Nat Biomed Eng.* Published online August 26, 2020. doi: 10.1038/s41551-020-00603-x.
44. Zhou Q, Zhu D, Yan H, et al. A preliminary study on analytical performance of serological assay for SARS-CoV-2 IgM/IgG and application in clinical practice. Preprint. Posted online May 9, 2020. *medRxiv*. doi: 10.1101/2020.05.05.20092551.
45. Liu Y, Liu Y, Diao B, et al. Diagnostic indexes of a rapid IgG/IgM combined antibody test for SARS-CoV-2. Preprint. Posted online March 30, 2020. *medRxiv*. doi: 10.1101/2020.03.26.20044883.

Review

Effects of Cell-Derived Microparticles on Immune Cells and Potential Implications in Clinical Medicine

*Egarit Noulsri, PhD**

Laboratory Medicine 2021;52:122-135

DOI: 10.1093/labmed/lmaa043

ABSTRACT

In the past few years, interest has increased in cell-derived microparticles (MPs), which are defined by their size of from 0.1 to 1 μm, and can be derived from various cell types, including endothelial cells, leukocytes, red blood cells (RBCs), and platelets. These MPs carry negatively charged phosphatidylserine (PS) on their surfaces and proteins packaged from numerous cellular components. MPs that have been shed by the body can play important roles in the pathophysiology of diseases and can affect various biological systems. Among these systems, the immune components have been shown to be modulated by MPs. Therefore, understanding the roles of MPs in the immune system is crucial to developing alternative therapeutic treatments for diseases. This review describes the effects of MPs on various immune cells and provides plausible potential applications of the immune-modulating properties of MPs in clinical medicine.

Keywords: laboratory, microparticle, quantitation, flow cytometry, immune cell, immune modulation

Abbreviations:

MPs, microparticle; DCs, dendritic cell; RBCs, red blood cells; PS, phosphatidylserine; PE, phosphatidylethanolamine; PC, phosphatidylcholine; SP, sphingomyelin; EM, electron microscope; DLS, dynamic light scattering; NTA, nanoparticle tracking analysis; FSC, forward scatter; SSC, side scatter; FL, fluorescent; TF, tissue factor; PPP, platelet-poor plasma; PFP, platelet-free plasma; WBC, white blood cell; PMPs, phosphatidylserine-exposing microparticles; sCD40L, soluble CD40 ligand; fMLP, N-formyl-met-leu-phe; PMN, polymorphonuclear; STAT, signal transducer and activator of transcription; ICAM-1, intercellular adhesion molecule 1;TNF, tumor necrosis factor; IL, interleukin; LPS, lipopolysaccharide; TGF, transforming growth factor; TGF-α, transforming growth factor type alpha; NK, natural killer; IFN, interferon; APCs, antigen-presenting cells; NOD, nucleotide oligomerization domain; EMPs, endothelial microparticles; GM-CSF, granulocyte-macrophage colony-stimulating factor; HLA-DP, human leukocyte antigen DP; HLA-DQ, human leukocyte antigen-DQ; HLA-DR, human leukocyte antigen-DR; aGVHD, acute graft-vs-host disease; MSCs, mesenchymal stromal cells; PHA, phytohemaggutinin; Tregs, regulatory T cells; ANCA, antineutrophil cytoplasmic antibody; mRNA, messenger RNA; PMA, phorbol myristate acetate; CVD, cardiovascular disease; BMI, body mass index; LXRs, liver X receptors; FRS, Framingham risk score; HDL-C, high-density lipoprotein cholesterol; TRALI, transfusion-related acute lung injury; IVIG, intravenous immunoglobulin; Ig, immunoglobulin; CD40L, CD40 ligand; sCD40L, soluble CD40L; CCR5, chemokine receptor 5; gp120, glycoprotein 120; IBS, inhibitory budding signal; Gag, group-specific antigen; EMV, exosome and microvesicle

Research Division, Faculty of Medicine Siriraj Hospital, Mahidol University, Bangkok, Thailand

*To whom correspondence should be addressed.
egarit.nou@mahidol.ac.th

The immune system is composed of heterogeneous cell populations. These immune cells are relatively quiescent in the steady state but share the ability to respond to infection, inflammation, and other perturbations. The responses mounted by immune cells typically involve changes in the expression of large numbers of genes and result in the acquisition of new functions, including high-output production of cytokines, lipid mediators, tissue-remodeling enzymes, and toxic gases, as well as the ability to migrate through tissues and undergo cellular division.

In addition to responding to pathogens, accumulated evidence[1–4] has shown that these immune cells can be modulated by other agents or drugs. Cell-derived microparticles (MPs) are cytoplasmic fragments originating from various cell types upon activation or apoptosis induction. Recent findings have demonstrated that MPs can alter various immune cells by triggering biochemical and molecular factors, as well as transcription ones, resulting in activation and repression of immune functions. Understanding these complex interactions between MPs and immune cells is important to developing alternative therapeutic interventions and to treating diseases.

This review article first provides a brief overview of MP characterizations and their biological functions. Next, the effects of MPs on various immune cells, including granulocytes, monocytes, dendritic cells (DCs), and lymphocytes, are addressed. Finally, this review will discuss the potential application in clinical medicine of the immune-modulating abilities of MPs.

Characterizations and Biological Functions of MPs

MPs are submicron-sized (average, <1 μm) membrane fragments. MPs are released from various cells, including red blood cells (RBCs), platelets, endothelial cells, and leukocytes, on activation or apoptosis induction. The results of in vitro studies[5–8] have demonstrated that MPs release can also be induced by inflammation cytokines, transcription inhibitors, and cellular stress inducers.

In the past few years, several studies have examined the mechanism of MP formation, leading to improved understanding of the roles of various biological molecules in the MP-release process. These molecular processes have been previously reviewed.[9,10] In normal physiological circumstances, phospholipids are asymmetrically distributed in the inner and outer plasma membranes. Phosphatidylserine (PS) and phosphatidylethanolamine (PE) are predominately expressed in the inner leaflet of the plasma membrane, whereas phosphatidylcholine (PC) and sphingomyelin (SP) are enriched in the outer surface of the plasma membrane. This asymmetrical distribution is regulated by an active process that involves several enzymes. The expression of PS and PE on the outer surface of the membrane is controlled by the flippase enzyme, which transports PS and PE back to the inner leaflet.[11] When the cells are activated, the asymmetrical distribution is disrupted by an enzyme called floppase, an ATP-dependent transporter of PS from the inner leaflet to the outer leaflet of the plasma membrane.

Also, the scramblase enzyme is a bidirectional nonspecific lipid transporter. This enzyme is activated by the accumulation of Ca2+ in the intracellular compartment, leading to the gradient-dependent distribution of phospholipids in the plasma membrane.[11] The increase of intracellular Ca^{2+} influx is also associated with changes in the permeability of mitochondria and the activation of protease enzymes, including caspase and calpains, for example. The activation of these enzymes results in cytoskeleton reorganization, cellular contraction and, finally, membrane *blebbing* (bulging) in the form of vesicles or MPs. The existence of these cytoskeletal changes has been supported by the findings of a study[12] that show the cleavage of the cytoskeleton during apoptosis and MP release due to ROCK-1 activation and the Rho/GTP pathway. Knowing this molecular mechanism might increase pharmacological control of MP release in pathological circumstances.

Given the importance of MPs in clinical medicine and the interest in MP research, various methods have been developed to quantitate and characterize MPs.[13,14] In summary, these approaches can be classified as physical or biochemical analysis. Biochemical analysis can be used to determine the protein composition of the MPs—an example of this approach is immunoblotting.[15] In contrast, physical analysis can be used to determine the size distribution and concentration of MPs in clinical specimens. Examples of tools used in this method of physically characterizing MPs include the electron microscope (EM),[16,17] dynamic light scattering (DLS),[18] nanoparticle tracking analysis (NTA),[19] and capture-based assay.[20,21]

Of the current approaches to MP analysis, flow cytometry is the most commonly used in routine clinical laboratories. This approach is based on the principle of intercepting a cell in a hydrodynamic focusing chamber with a laser. This interception creates 3 signals: forward scatter (FSC), side scatter (SSC), and fluorescent (FL). The FSC and SSC relate to the size and internal complexity of a cell, respectively. The FL relates to the binding of antibody-conjugated fluorescent dye and its specific target on the cell. To identify the origin of MPs, a specimen might be diluted and then incubated with the antibody of interest. An MP gate is established using size-standard beads. Then, to eliminate the noise signal and debris from the instrument and the specimen, a threshold is applied. Further, the concentration of MPs can be obtained relative to reference microbeads that have a known concentration.

Although flow cytometry can analyze at a rate of 1000 particles per minute, the flow cytometry analysis of MPs has several limitations. First, the low expression of the antigen of interest on the MPs might decrease its sensitivity, and the detection of MPs is based on the availability of commercial antibodies in the market.

Second, the cost of reference microbeads is relatively high, especially in resource-scarce settings, which limits their application in routine laboratories. Given this issue, previous

DOI: 10.1093/labmed/lmaa043

study reports[22,23] have proposed an affordable approach to quantitating MPs using flow cytometry.

Third, MPs with a size less than 1 μm might be below the sensitivity of the analysis. This suggestion is supported by the findings of a study[24] that show the limitations of conventional flow cytometry when detecting MPs that had sizes larger than 500 nm. Also, such small particles might be detected as a single particle when they are close together, a phenomenon known as the *swarm effect*,[25] which results in underestimation of the concentration of MPs in a clinical specimen. Finally, flow cytometry detects MPs based on the binding between PS and annexin V. Due to heterogeneity of MPs, the expression of PS on the surface of MPs can vary from high to low, or even negative.[26]

Considering this heterogeneity, authors such as McEntire et al[27]have proposed alternative reagents for identifying MPs. These coauthors detected MPs in blood products using 3 different principles. Their results showed that MP quantitation using annexin V was similar to that using bio-maleimide. However, higher MP concentrations were detected using lactadherin than using conventional annexin V. More studies are needed to confirm the appropriateness of the use of these reagents for MP quantitation in clinical specimens.

In addition to physical characteristics and biochemical and protein composition, MP function can also be assessed using an assay based on the analysis of the tissue factor (TF) expressed on the surface membrane. The MPs are captured using an anti–tissue factor antibody coated on a plate. In the presence of Ca^{2+} and phospholipids, FVIIa and TF complexes are formed, leading to the transformation of FX into FXa. Then, a chromogenic substrate is added to measure the activity, which is directly proportional to that of the TF on the surface of the MPs. Several investigations[28,29] have reported applying this approach in clinical laboratories.

Although there are many approaches to determining the concentration of MPs, several issues must be considered. Many types of anticoagulants are used in routine laboratories. Shah et al[30] found that blood specimens collected in heparin showed increased MP concentrations, compared with those collected in sodium citrate. Connor et al[31] demonstrated that MP concentrations were higher in blood collected in sodium citrate than in that collected in EDTA. Collectively, these reports suggest the effects of anticoagulants on MP quantitation.

In MP analysis, platelets and plasma must be separated to avoid activating the platelets, which might lead to higher MP concentrations. For this purpose, centrifugation must be applied. Examining PMP using flow cytometry showed that the MP concentrations were higher in platelet-poor plasma (PPP) than in platelet-free plasma (PFP),[32] suggesting that the use of different centrifugation speeds during preparation might affect the concentration of MPs. To increase the accuracy and reliability of the results, it is recommended that MPs be analyzed in fresh specimens,[33] which helps to avoid changes in the concentrations and physical characteristics of the released MPs. However, in some circumstances, MP analysis must be performed with stored specimens, which might have been prepared using various processes. One study report[34] stated that MP concentrations were increased 10-fold in frozen-thawed PPP. The effect of storage on MP quantitation is also supported by study results[35] that found that storing PFP at 80°C for 4 weeks markedly affected the concentration of MPs and their size distribution. Other factors that contribute to preanalytical and analytical analysis of MPs have previously been reviewed.[14,36]

In recent years, an increasing amount of literature[37–39] has been published on the roles of MPs on disease pathophysiology. Due to highly expressing annexin-V binding sites and tissue factors, the procoagulant ability of MPs is well documented. Also, MPs are capable of interacting with other cells to participate in thrombosis, inflammation, and angiogenesis.[40–42] In neuroscience, Geiser et al[43] reported a potential pathophysiological link between elevated concentrations of platelet-derived MPs and cerebrovascular infarction in patients with prosthetic heart valves. In addition to these studies, during the past few years, many more data have become available on the ability of MPs to modulate the immune cells. **Figure 1** summarizes these potential effects of MPs on various leukocytes.

Effects of MPs on Various Cell Types in the Immune System

Granulocytes

Neutrophils are the most abundant type of white blood cell (WBC) in the peripheral-blood circulation. They play an essential role in first-line protection against bacterial infections. Neutrophils are also phagocytic cells, which contain a vast array of microbicidal molecules. Accumulated evidence suggests various roles of MPs in the functions of granulocytes. Martin et al[44,45] showed

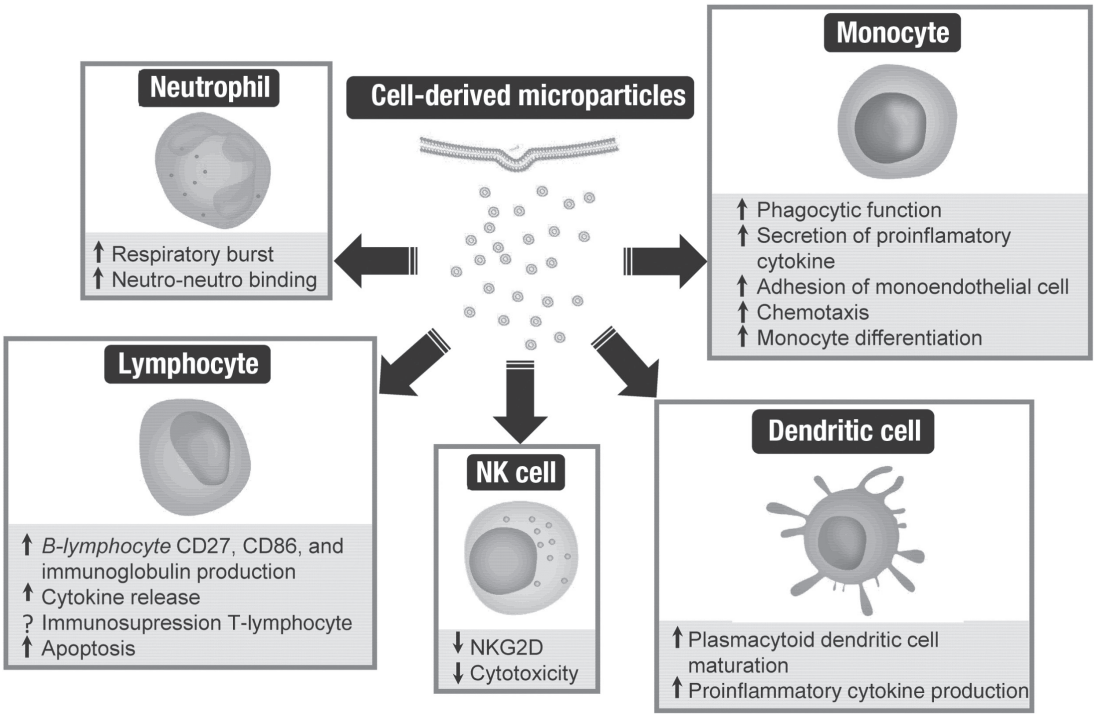

Figure 1

Schematic overview of the influence of microparticles (MPs) on immune cells.

that PS-exposing MPs (PMPs) could bind to PR3 protein, which is a family of neutrophil-derived proteases, resulting in an increased respiratory burst in neutrophils. Xie et al[46] also found increased soluble CD40 Ligand (sCD40L) in PMPs isolated from platelet concentrate—these PMPs could prime the N-formyl-met-leu-phe (fMLP)–activated polymorphonuclear (PMN) respiratory burst.

A study report by Forlow et al[47] states that PMPs can enhance the binding of neutrophils to other neutrophils that are already bound to the surface of the flow chamber. The molecular mechanism has been thought to be mediated by the interaction between the P-selectin on the platelet and the P-selectin-glycoprotein ligand 1 on the neutrophil, suggesting that PMPs can promote cell interaction by inducing adhesion molecules. Apart from these modulation activities, Xie et al[46] demonstrated that PMPs obtained from PFP primed the PMN respiratory burst activated by fMLP. Also, the role of MPs in neutrophil activation has been mentioned in connection with decompression sickness,[48] a systemic disorder due to gas bubbles in the blood.

Monocytes

Monocytes and macrophages serve 3 important functions in the immune response: phagocytosis, antigen presentation, and cytokine production. The results of a study by Niessen et al[49] have shown that MPs can induce the phagocytic function of monocytes and the secretion of proinflammatory cytokines thought the signal transducer and activator of transcription (STAT) pathway.

Barry et al[50] demonstrated that PMPs can increase adhesion between monocytes and endothelial cells through the interaction of intercellular adhesion molecule 1 (ICAM-1) and macrophage antigen 1. Further, MPs derived from platelets and the arachidonic acid isolated from these MPs can increase the chemotaxis of U937 monocytic cells. Both effects can be inhibited by GF 109203X, which blocks the protein kinase C signaling agents, suggesting that this interaction is mediated by the protein kinase C pathway.[50] Further investigation revealed that the MPs reduced the release of the proinflammatory cytokines tumor necrosis factor (TNF)–α, interleukin (IL)–8, and IL-10 induced by zymosan A and lipopolysaccharide (LPS) in a

DOI: 10.1093/labmed/lmaa043

dose-dependent manner. Blocking the binding of the PS exposed on the surface of the MPs to its receptors on macrophages inhibited the release of TNF-α but not that of the other cytokines. In contrast, neutralizing the antibodies to transforming growth factor (TGF)–β blocked the release of TNF-α, IL-8, and IL-10, suggesting that the anti-inflammatory effects of MPs were mediated by a second mediator, namely, TGF-α.[51]

Ismail et al[52] examined the roles of MPs in differentiating naïve monocytes, demonstrating that macrophage-derived MPs transferred microRNA to monocytes and induced differentiation of the macrophages. This role of MPs has been confirmed by Saha et al,[53] who found that MPs derived from alcohol-treated monocytes increased the surface expression of CD68 (a macrophage marker) and the M2 markers CD206 (a mannose receptor) and CD163 (a scavenger receptor), the secretion of IL-10 and TGF-β, and phagocytic activity, all of which suggested the ability of MPs to program monocytes to M2 macrophages. Sadallah et al[54] studied the capability of MPs purified from platelet concentrates and demonstrated that these MPs reduced the secretion of TNF-α and the IL-10 of the LPS- or zymosan A–activated macrophages.

Natural Killer (NK) Cells

Another cell type in the innate immune system is NK cells. These cells play an important role in immunity to viral infections and tumors by secreting cytokines and cytolytic activity. Several study reports have documented the roles of MPs and exosomes in the functioning of NK cells. Clayton et al[55] investigated the effects of tumor-derived exosomes on NKG2D, an activating receptor for NK cells, and demonstrated the ability of exosomes to downregulate the expression of NKG2D molecules on the surface membranes of NK cells and the mediation of this mechanism through TGF-β. Further study isolated tumor-derived exosomes from patients who had acute myelogenous leukemia and examined their immune-regulatory functions. The results demonstrated the ability of the exosomes to decrease the cytotoxic activity of the NK cells isolated from healthy donors, induce Smad phosphorylation, and downregulate NKG2D receptor expression.[56]

The results of the recent study by Sadallah et al[57] also demonstrated that platelet-derived exosomes reduced the expression of NKG2D, NKp30, DNAM-1, and CD107a and the production of interferon (IFN)–γ. Collectively, these studies suggested the roles of exosome-mediated immune evasion in tumors. Further study[58] revealed that neutrophil-derived MPs inhibited production of IFN-γ and TNF-α but induced the secretion of TGF-b1 by NK cells activated by IL-2/IL-12 and mediated by PS interaction.

Dendritic Cells

Of the antigen-presenting cells (APCs), the DCs are the most important, due to their enhanced ability to stimulate naïve T cells.[59] DCs are activated through the recognition of pathogenic antigens by receptors that recognize cell surface patterns, including toll-like receptors and those that sense intracellular pathogens (nucleotide oligomerization domain [NOD]–like receptors).[60,61] Angelot et al[62] showed that incubating endothelial MPs (EMPs) with plasmacytoid DCs resulted in upregulation of costimulatory molecules and secretion of IL-6 and IL-8, suggesting the ability of EMPs to induce maturation of plasmacytoid DCs and production of proinflammatory cytokines. A study report on the effects of MPs on plasmacytoid DCs revealed that EMPs induced the maturation of plasmacytoid DCs and the secretion of IL-6 and IL-8. Also, the same study results[62] showed that EMPs induced naïve CD4 T-lymphocytes to proliferate and produce IFN-γ and TNF-α.

A report on a study of the role in the immune system of MPs isolated from patients who had systemic lupus erythematosus[63] revealed that MPs increased the production of IL-6, TNF, and IFN-α in plasmacytoid and myeloid DCs. A recent study[54] reported that the differentiation of monocytes to DCs that was induced by IL-6 and granulocyte-macrophage colony-stimulating factor (GM-CSF) was altered by MPs isolated from platelet concentrate. These study findings also reported that the immature DCs expressed less human leukocyte antigen–DP (HLA-DP), human leukocyte antigen-DQ (HLA-DQ), and human leukocyte antigen-DR (HLA-DR), and CD80 in presenting the MPs, suggesting that MPs modulate DC activity.

Lymphocytes

T- and B-lymphocytes are important parts of adaptive immunity. T-lymphocytes can be further classified into CD4+ and CD8+ T-lymphocytes. CD4+ T-lymphocytes play a role in regulating the immune response, including activating CD8+ T-lymphocytes and macrophages, maturing plasma cells and memory B cells, and recruiting PMN cells by releasing cytokines. The roles of MPs in the activation, proliferation, and cytokine release of lymphocytes have recently been proposed.

Yari et al[64] collected PMPs from platelet concentrate and found during a coculture experiment that they could induce CD27, CD86, and immunoglobulin production of the B-lymphocyte cell line, suggesting that PMPs can activate B-lymphocytes. Messer et al[65] examined the ability of MPs to induce cytokine release, demonstrating that MPs isolated from the synovial fluid of patients who had rheumatoid arthritis could induce B-lymphocyte activation factor. This study also demonstrated that the MPs isolated from cells treated with actinomycin D could not induce the factor that activated B-lymphocytes. The results of a study[66] examining the roles of EMPs in acute graft-vs-host disease (aGVHD) demonstrated that the injection of EMPs deficient in microRNA-155 into aGVHD mice attenuated the exacerbation of aGVHD manifestations and the differentiation of abnormal T-lymphocytes.

However, the results of a study that compared the immunomodulatory effects of mesenchymal stromal cells (MSCs) on peripheral-blood mononuclear cells[67] showed their inability to inhibit in-vitro proliferation of T-lymphocytes induced by phytohemaggutinin (PHA), compared with MSC and antibody formation of B-lymphocytes, suggesting that MPs have less in-vitro immunomodulation ability than MSCs. The findings of a study comparing the immunosuppressive potency of MPs derived from bone-marrow MSC and adipose-tissue MSC[68] found that both MPs failed to suppress lymphocyte proliferation. A study report by Shen et al[69] stated that MPs derived from apoptotic human PMN neutrophils suppressed CD25 (IL-2Ra)^{neg} CD127 (IL-7Ra)^{pos} Th-lymphocyte proliferation and secretion of IL-2. This report also suggested that the suppression activity of MPs is mediated by downregulation of IL-2 and the IL-2R expression and signaling process. Budoni et al[70] examined the influence of MPs on B-lymphocytes and demonstrated that MPs isolated from MSCs inhibited the B-lymphocyte proliferation and differentiation that are induced by stimulating the peripheral-blood mononuclear culture system with CpG, which suggests that MPs derived from MSCs exert an immunosuppressive effect on B-lymphocytes. Considering these dual roles of MPs, their immunomodulation activity merits further study.

A number of studies, such as one by Del Fattore et al,[71] have also demonstrated that MPs have an apoptosis-inducing activity. These coauthors discovered that MPs are derived from MSCs that are derived from bone marrow–induced apoptosis in CD3 T-lymphocytes. Also, these investigators observed the increased apoptosis and proliferation of regulatory T cells (Tregs).

Wieckowski et al[72] addressed the role of tumor-derived MPs in immune cells, finding that such MPs expressed Fas ligand molecules on their surface membranes. Also, the study report demonstrated that these MPs could promote the expansion of regulatory T-lymphocytes and could induce the apoptosis of CD8+ T-lymphocytes. The apoptosis-inducing ability of MPs was confirmed by Huber et al,[73] who showed that MPs derived from colorectal cancer could induce T-lymphocyte apoptosis through the Fas/Fas L-mediated pathway. This apoptosis-inducing activity of MPs was confirmed by Kim JW et al,[74] who showed that MPs isolated from patients with oral cancer could induce apoptosis in the activated T-lymphocytes through the Fas/Fas-L mechanism and caspase-3 activation. This finding suggests that the MPs had an immune escape mechanism.

It is important to note that in addition to being affected by other MPs, leukocytes can be stimulated to induce MP release. However, the precise mechanism of MP release in leukocytes is not yet fully understood. Various stimulating agents have been reported to induce MP release in leukocytes. According to the findings of one study,[75] that the incubation of neutrophils with antineutrophil cytoplasmic antibodies induced the release of neutrophil-derived MPs. These MPs expressed antineutrophil cytoplasmic antibody (ANCA) autoantigens proteinase 3 and myeloperoxidase, and could promote the generation of thrombin.

Given that C^{a2+} is important for MP shedding, Pintanga et al[76] found that incubating isolated neutrophils with 2 μ m of calcium ionophore A23187 for 20 minutes resulted in the release of PMNs. These MPs expressed CD66b and CD66L, which could induce endothelial cell damage by means of a myeloperoxidase-mediated mechanism.

In the case of monocytes, Wen et al[77] demonstrated that an endotoxin induced the release of monocyte-derived MPs at varying phenotypes and with high messenger RNA (mRNA) contents related to TNF, IL-6, and IL-8. CEM lymphocyte and THP-1 are cell lines commonly used in various laboratories as in-vitro models of lymphocytes and monocytes, respectively. Messer et al[65] found that treatment with a combination of PHA, phorbol myristate acetate (PMA), and actinomycin-D induced the release of CEM-lymphocyte–derived MPs, suggesting that the factors that induce leukocyte activation might also induce MP release. However, MPs isolated using this in-vitro induction could not induce the release of B cell–activating factor, thymic stroma lymphopoietin, or secretory leukocyte protease inhibitor,

DOI: 10.1093/labmed/lmaa043

a result that indicates the different biological roles of MPs induced in vitro and in vivo.

Potential Implications of the Immune-Modulating Activity of MPs for Clinical Medicine

Cardiovascular Diseases

In the past few years, more research[78,79] has focused on the roles of MPs in the pathophysiology of thrombosis. The findings of several studies have demonstrated that the level of MPs is associated with various factors that contribute to cardiovascular disease (CVD). A study that sought to evaluate MPs in patients with obesity who had no other vascular risk factor found higher concentrations of MPs in these patients than in the control individuals.[80] This result was supported by those of Stepanian et al,[81] who quantitated the MPs in women with severe obesity women and found higher concentrations of PMPs, EMPs, and neutrophil-platelet aggregation in this group.

Hypertension is a well-known contributing factor to CVD. The findings of a study that compared the MPs in patients with hypertension revealed significantly higher levels of EMPs and PMPs in the groups with severe hypertension, as well as a correlation between MP level and blood pressure.[82] Another study publication that examined the MP levels in people with hypertension who had type 2 diabetes[83] reported that the levels of PMPs and monocyte-derived MPs in these patients was higher than in the control groups.

Regarding MPs and metabolic syndrome, Diamant et al[84] characterized the MPs in patients with well-regulated type 2 diabetes and found that they exhibited significantly increased LMPs and PMPs. Further, there was a correlation between the number of MPs and body mass index (BMI), fasting plasma glucose, insulin, and serum HDL cholesterol levels.

Hyperlipidemia is also an important contributing factor to the pathophysiology of CVD. A study report on the evaluation of the effects of lipid-lowering treatment on MP concentrations[85] revealed that MP levels in patients who were receiving statins were lower than those in control groups and that these MPs were shed from platelets, endothelia, and leukocytes, suggesting an association between lipedema and MP concentrations in the pathogenesis of CVD.

Age is another factor associated with changes in coagulation and has been found to increase the incidence with CVD complications.[86,87] Forest et al[88] compared the MP levels of elderly people and young people and found that the elderly people in stable condition had lower levels of EMPs than those in the controls. However, elderly people who had infections had increased EMPs, suggesting that changes in MP levels in elderly people are associated with various stimuli.

In addition to MPs from platelets and endothelia, recent research findings have suggested that plasmacytoid DCs play an important role in the progression of atherosclerosis by exerting both pro- and anti-inflammatory cytokine functions. One study report[89] suggested that the PMPs exert an anti-inflammatory effect of plasmacytoid DCs by triggering *liver X receptors* (LXRs), which are nuclear receptors that regulate innate immune responses.

The Framingham risk score (FRS) is a common tool for predicting the risk level of CVD.[90] A study report[91] has suggested 6 risk factors that contribute to CVD: age, sex, total cholesterol, high-density lipoprotein cholesterol (HDL-C), current or past smoking, and systolic blood pressure. The FRS has also been applied to evaluate the risk of CVD in metabolic syndrome.[92] Also, the findings of another study[93] demonstrate the clinical application of the FRS in evaluating patients who have metabolic syndrome. Considering the association between MPs and the parameters in the FRS, adding MP levels as a component of the FRS might increase the reliability and accuracy of the FRS for assessing the risk of CVD. Finally, the FRS can be useful for clinicians to use in deciding on preventive medical treatments for individuals at risk for future cardiovascular events.

Transfusion Medicine

One of the most common post-transfusion complications is transfusion-related acute lung injury (TRALI). TRALI has been shown to be associated with several factors. A case report study by Rizk et al[94] described a 23-year-old man with TRALI after intravenous immunoglobulin (IVIG) infusion that used a rapid infusion procedure. This patient developed noncardiogenic pulmonary edema after 6 hours, and granulocyte-associated immunoglobulin (Ig)G was detected in the blood at 14 weeks and 27 weeks after the infusion. Also, another study report[95] revealed that a patient who had received a high dose of IVIG had experienced TRALI.

A multicenter study in France by Baudel et al[96] suggested that the increased use of IVIG is associated with TRALI. In

addition to IgG, a complement system has been suggested to contribute to TRALI. Dry et al[97] characterized TRALI in an animal model of complement (C5a) and antibody-induced lung injury. Strait et al[98] demonstrated that the activation of macrophages and complement was involved in the pathogenesis of TRALI in a mouse model.

Several study reports have suggested an association between stored RBCs and the TRALI complication. This theory has been further supported by the findings of various studies. Tung et al[99] demonstrated that sheep developed TRALI after transfusion with stored PRBCs but that the sheep that received saline infusion did not develop TRALI. Another study[100] examined the mechanism of TRALI associated with blood storage in a mouse model; its results suggested that plasma and lipids from stored blood products produced pulmonary damage and TRALI. This suggestion was further supported by Silliman et al,[60] in whose study rats received plasma prepared using the whole-blood method or the apheresis method and stored for various numbers of days. The results showed that plasma from day 5 of storage caused lung injury but that rats transfused with plasma from day 0 showed no abnormalities. Further, lipid extracts from day 5 of storage induced lung injury in rats, but lipid extracts from day 0 induced no injury, suggesting that lipids generated during plasma storage contribute to TRALI complications in an animal model.

In the past few years, several study reports, including Jy et al,[101] have demonstrated increases in various MPs in stored blood products. The results of other studies[102,103] demonstrated that these increases were time-dependent: 0 for the first 10 days, a steep increase from days 10 through 15, and few changes at days 35 through 56 of storage.

Several studies have examined the composition of the MPs released during storage. An immunoblotting study by Kriebardis et al[104] showed that the constitution of the RMP membrane included abundant IgG, lipid raft proteins, and other proteins related to the apoptosis pathway. Müller et al[105] also demonstrated that autologous IgG preferentially binds to RMPs.

In addition, the findings of a proteomic study by Bosman et al[106] demonstrated many complements, including fragments of C1q, C1r, C1s, C3, C4, and C9, on the RMPs. Pasini et al[107] suggested the potent proinflammatory effect of RMPs in the presence of immunoglobulin and complement. The results of a study in a murine transfusion model transfused with RMPs[108] suggested a thrombin-dependent mechanism of complement activation by RMPs. Further, Gasser et al[109] reported that LMP could bind to RBCs in a C-dependent fashion, leading to complement activation by the classical pathway and the capture of RBC via CR1. Collectively, these data suggest the potential contribution of IgG, complement, stored RBCs, and RMPs in TRALI complications.

Despite being poorly understood, the mechanisms of TRALI have been attributed to MPs. The results from 2 studies[110,111] showed that CD40 ligand (CD40L) was a primarily platelet-derived proinflammatory mediator found in soluble CD40L (sCD40L) and in cell-associated forms in transfused blood. Ahn et al[112] suggested that increased MP presentation in platelet concentrates is a potential cause of TRALI due to the high expression of CD40L molecules on the surface membranes of MPs. Considering the association of MPs with post-transfusion complications, routine monitoring and quantitation of MPs in blood products might be necessary to minimize complication reactions (**Figure 2**).

Infectious Diseases

Many studies have suggested a relationship between MPs and infectious diseases. Esser et al[113] reported that MPs could carry unpacked viral genome and other viral proteins that need to replicate in the target cells. The findings of another study[114] also demonstrated that MPs could carry chemokine receptor 5 (CCR5) on their surface membranes and could transfer these molecules to CCR5-deficient peripheral-blood mononuclear cells, resulting in infection with macrophage-tropic HIV-1. A recent study that examined the composition of MPs coated with HIV-1 demonstrated the presence of envelope glycoprotein 120 (gp120) and the ability of MPs derived from HIV-1 to bind with galectin-1.[115] Gan and Gould[116] reported an inhibitory budding signal (IBS) from the HIV group-specific antigen (Gag) protein. They also demonstrated that this IBS impaired the budding of CD63 and several other viral and nonviral exosome and microvesicle (EMV) proteins. These findings suggest the ability to inhibit viral release via MPs. Considering these observations, treatment with MP-release inhibitors might be useful to reduce the severity of infectious diseases.

Allergic Diseases

It is well known that the pathophysiology of asthma involves inflammation and cytokine release. The progression

DOI: 10.1093/labmed/lmaa043

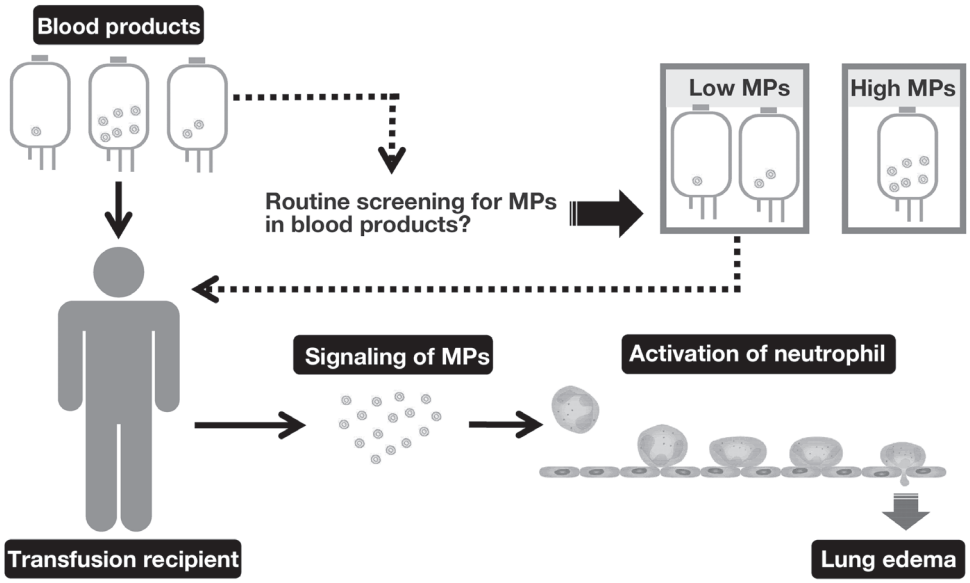

Figure 2

Effect of microparticles (MPs) on post-transfusion complications.

of the disease is established by epithelial cells that orchestrate an inflammatory response to external stimuli. The findings of a study examining the mechanism of communication between epithelial and inflammatory cells[117] have suggested the role of exosomes in the pathophysiology of asthma. In this study report, Kulshreshtha et al demonstrate that epithelial-derived MPs obtained from asthmatic mice induced the proliferation and chemotaxis of undifferentiated macrophages and that the proliferation of monocytes and the alleviation of asthmatic features were inhibited by GW4869, an exosome-production inhibitor. Further investigation using Rab27a/Rab27b double-knockout mice[118] supported the role of exosomes in lung epithelial cells. Although further studies are needed on the molecular mechanisms and roles of MPs and exosomes in this pathophysiologic phenomenon, the current accumulated data suggest that inhibiting the release of MPs or exosomes could be useful in the therapeutic treatment of patients who have asthma and other inflammatory diseases.

Pre-Eclampsia

Pre-eclampsia is a complication of pregnancy that is characterized by high blood pressure, protein in the urea, and edema. The disease is a common cause of maternal and fetal mortality worldwide.[119] Research findings[120] suggest that activation of innate immunity plays an important role in the pathophysiology of this disease. This suggestion was supported by study reports[121–123] showing increased numbers of activated monocytes in pregnant women. Also, changes in the surface expression of CD54 and CD11c and increased intracellular proinflammatory cytokines were demonstrated in pregnant women.[124,125] Compared with monocytes in healthy controls, monocytes from patients with pre-eclampsia showed an increase in the intracellular reactive oxygen species IL-1b, IL-6, and IL-8.[125,126] However, the precise molecular mechanisms of the inflammatory response in pre-eclampsia during pregnancy remain poorly understood.

Considering the etiology of inflammation in women with pre-eclampsia, Messerli et al[127] suggested that placental syncytiotrophoblast-derived MPs activated monocytes. This activation resulted in the upregulation of CD54 expression and increased production of IL-8, IL-6, and IL-1b in a time- and dose-dependent manner. Therefore, the detection of placental syncytiotrophoblast-derived MPs might be an early surrogate marker of pre-eclampsia, and inhibition of the interaction between syncytiotrophoblast-derived MPs and monocytes might prevent this complication of pregnancy.

Cancer

In the past few years, research interest in the role of MPs in the pathophysiology of cancer has increased dramatically.

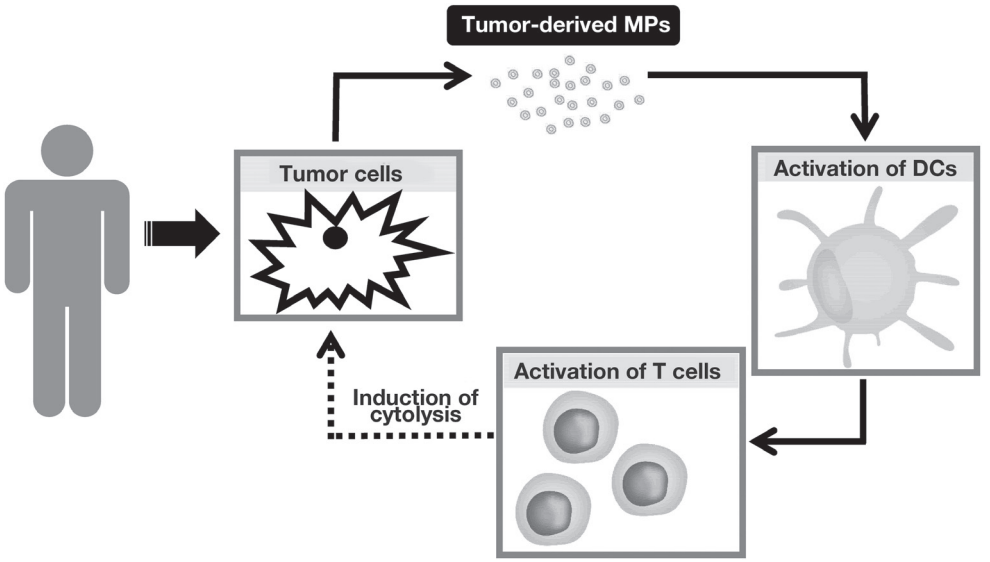

Figure 3

Application of microparticles (MPs) for cancer treatment. DCs indicates dentritic cells.

Study reports suggest a link between MPs and thrombosis complications,[128,129] the development of drug resistance[130,131] and metastasis,[132] tumor angiogenesis,[133] tumor-cell survival,[134] and evasion of immune surveillance in cancer.[73,135]

Apart from these roles in the pathophysiology of cancer, MPs have been suggested for potential application in the therapeutic treatment of patients with cancer patients. Zhang H et al[136] showed that MPs could transfer antigens to DCs, resulting in the induction of protective, adaptive immune responses against the delivered antigen, suggesting that MPs have the abilities to deliver antigens and target DCs. These results suggested that DNA fragments in tumor-derived MPs signal to DCs to produce type I interferon and that this interferon is responsible for tumor-derived MPs inducing DC maturation via the upregulation of CD80, CD86, and MHC II. After taking up these tumor-derived MPs, the DCs underwent maturation, presented tumor-antigen peptides, and stimulated T cells toward Th1 effector T cells, suggesting that tumor-derived MPs induce T cell–dependent antitumor activity.

This suggestion is supported by findings from various clinical studies. El Andaloussi et al[137] examined the immunotherapeutic effect of tumor-derived MPs in treating colon cancer. In this Phase 1 trial, tumor-derived MPs showed the ability to induce an antigen-specific anticancer cytotoxic T-lymphocyte response in patients. Likewise, DC-derived MPs showed the capacity to prime and restore the functions of T cells and NK cells in patients who had non–small-cell lung cancer.[138] One study[139] evaluated the antitumor activity of MSC-derived MPs. Its results showed that these MPs has the ability to induce apoptosis and cell-cycle arrest in various tumor cell lines and to inhibit tumor growth in vivo. Although further studies are required to address the full potential of their clinical application in treating cancer, these data highlight that tumor-derived MPs could function as a novel, cell-free cancer vaccine due to their small size, lack of toxicity, target specificity, and tolerance by host cells (**Figure 3**).

Summary

Overall, it is clear that MPs modulate various immune cells through complex molecular mechanisms. These interactions might result in activation or suppression of the immune system. Understanding of the immunomodulating activity of MPs might provide an alternative approach to treating diseases and minimizing transfusion complications, thus benefiting patients and transfusion recipients in the future. **LM**

Lab Medicine 2021;52;122–135
DOI: 10.1093/labmed/lmaa043

Acknowledgments

This research was supported by the Faculty of Medicine Siriraj Hospital, Mahidol University.

References

1. Herr N, Bode C, Duerschmied D. The effects of serotonin in immune cells. *Front Cardiovasc Med.* 2017;4:48.
2. Prasad AS. Zinc in human health: effect of zinc on immune cells. *Mol Med.* 2008;14(5–6):353–357.
3. Shao K, Lu Y, Wang J, et al. Different effects of tacrolimus on innate and adaptive immune cells in the allograft transplantation. *Scand J Immunol.* 2016;83(2):119–127.
4. Kidd BA, Wroblewska A, Boland MR, et al. Mapping the effects of drugs on the immune system. *Nat Biotechnol.* 2016;34(1):47–54.
5. Pirro M, Schillaci G, Bagaglia F, et al. Microparticles derived from endothelial progenitor cells in patients at different cardiovascular risk. *Atherosclerosis.* 2008;197(2):757–767.
6. Ullal AJ, Pisetsky DS. The release of microparticles by Jurkat leukemia T cells treated with staurosporine and related kinase inhibitors to induce apoptosis. *Apoptosis.* 2010;15(5):586–596.
7. Kolowos W, Gaipl US, Sheriff A, et al. Microparticles shed from different antigen-presenting cells display an individual pattern of surface molecules and a distinct potential of allogeneic T-cell activation. *Scand J Immunol.* 2005;61(3):226–233.
8. Martin S, Tesse A, Hugel B, et al. Shed membrane particles from T lymphocytes impair endothelial function and regulate endothelial protein expression. *Circulation.* 2004;109(13):1653–1659.
9. Morel O, Jesel L, Freyssinet JM, Toti F. Cellular mechanisms underlying the formation of circulating microparticles. *Arterioscler Thromb Vasc Biol.* 2011;31(1):15–26.
10. Martinez MC, Tual-Chalot S, Leonetti D, Andriantsitohaina R. Microparticles: targets and tools in cardiovascular disease. *Trends Pharmacol Sci.* 2011;32(11):659–665.
11. Daleke DL. Regulation of transbilayer plasma membrane phospholipid asymmetry. *J Lipid Res.* 2003;44(2):233–242.
12. Sebbagh M, Renvoizé C, Hamelin J, Riché N, Bertoglio J, Bréard J. Caspase-3-mediated cleavage of ROCK I induces MLC phosphorylation and apoptotic membrane blebbing. *Nat Cell Biol.* 2001;3(4):346–352.
13. Hartjes TA, Mytnyk S, Jenster GW, van Steijn V, van Royen ME. Extracellular vesicle quantification and characterization: common methods and emerging approaches. *Bioengineering (Basel)*. 2019;6(1):7.
14. Yuana Y, Bertina RM, Osanto S. Pre-analytical and analytical issues in the analysis of blood microparticles. *Thromb Haemost.* 2011;105(3):396–408.
15. Théry C, Witwer KW, Aikawa E, et al. Minimal information for studies of extracellular vesicles 2018 (MISEV2018): a position statement of the International Society for Extracellular Vesicles and update of the MISEV2014 guidelines. *J Extracell Vesicles*. 2018;7(1):1535750.
16. Ponomareva AA, Nevzorova TA, Mordakhanova ER, et al. Intracellular origin and ultrastructure of platelet-derived microparticles. *J Thromb Haemost.* 2017;15(8):1655–1667.
17. Almhanawi BH, Khalid B, Ibrahim TA, Tohit ERM. A transmission electron microscopy study of anticoagulant-induced platelet vesiculation. *Porto Biomed J.* 2017;2(1):23–27.
18. Nguyen DB, Thuy Ly TB, Wesseling MC, et al. Characterization of microvesicles released from human red blood cells. *Cell Physiol Biochem.* 2016;38(3):1085–1099.
19. Mørk M, Pedersen S, Botha J, Lund SM, Kristensen SR. Preanalytical, analytical, and biological variation of blood plasma submicron particle levels measured with nanoparticle tracking analysis and tunable resistive pulse sensing. *Scand J Clin Lab Invest.* 2016;76(5):349–360.
20. Shirafuji T, Hamaguchi H, Kanda F. Measurement of platelet-derived microparticle levels in the chronic phase of cerebral infarction using an enzyme-linked immunosorbent assay. *Kobe J Med Sci.* 2008;54(1):E55–E61.
21. Nomura S, Shouzu A, Taomoto K, et al. Assessment of an ELISA kit for platelet-derived microparticles by joint research at many institutes in Japan. *J Atheroscler Thromb.* 2009;16(6):878–887.
22. Noulsri E, Lerdwana S, Kittisares K, Palasuwan A, Palasuwan D. Flow rate calibration to determine cell-derived microparticles and homogeneity of blood components. *Transfus Apher Sci.* 2017;56(4):585–590.
23. Pattanapanyasat K, Noulsri E, Lerdwana S, Sukapirom K, Onlamoon N, Tassaneetrithep B. The use of glutaraldehyde-fixed chicken red blood cells as counting beads for performing affordable single-platform $CD4^+$ T-lymphocyte count in HIV-1-infected patients. *J Acquir Immune Defic Syndr.* 2010;53(1):47–54.
24. Chandler WL, Yeung W, Tait JF. A new microparticle size calibration standard for use in measuring smaller microparticles using a new flow cytometer. *J Thromb Haemost.* 2011;9(6):1216–1224.
25. van der Pol E, van Gemert MJC, Sturk A, Nieuwland R, van Leeuwen TG. Single vs. swarm detection of microparticles and exosomes by flow cytometry. *J Thromb Haemost.* 2012;10(5):919–930.
26. Boilard E, Duchez AC, Brisson A. The diversity of platelet microparticles. *Curr Opin Hematol.* 2015;22(5):437–444.
27. McEntire MC, Wardrop KJ, Davis WC. Comparison of established and novel methods for the detection and enumeration of microparticles in canine stored erythrocyte concentrates for transfusion. *Vet Clin Pathol.* 2017;46(1):54–63.
28. Tilley RE, Holscher T, Belani R, Nieva J, Mackman N. Tissue factor activity is increased in a combined platelet and microparticle sample from cancer patients. *Thromb Res.* 2008;122(5):604–609.
29. Manly DA, Wang J, Glover SL, et al. Increased microparticle tissue factor activity in cancer patients with venous thromboembolism. *Thromb Res.* 2010;125(6):511–512.
30. Shah MD, Bergeron AL, Dong J-F, López JA. Flow cytometric measurement of microparticles: pitfalls and protocol modifications. *Platelets.* 2008;19(5):365–372.
31. Connor DE, Exner T, Ma DD, Joseph JE. Detection of the procoagulant activity of microparticle-associated phosphatidylserine using XACT. *Blood Coagul Fibrinolysis.* 2009;20(7):558–564.
32. Horstman LL, Jy W, Jimenez JJ, Bidot C, Ahn YS. New horizons in the analysis of circulating cell-derived microparticles. *Keio J Med.* 2004;53(4):210–230.
33. Jy W, Horstman LL, Jimenez JJ, Ahn YS. Measuring circulating cell-derived microparticles. *J Thromb Haemost.* 2004;2(10):1842–1851.
34. Mobarrez F, Antovic J, Egberg N, et al. A multicolor flow cytometric assay for measurement of platelet-derived microparticles. *Thromb Res.* 2010;125(3):e110–e116.
35. Kong F, Zhang L, Wang H, et al. Impact of collection, isolation and storage methodology of circulating microvesicles on flow cytometric analysis. *Exp Ther Med.* 2015;10(6):2093–2101.
36. Magnette A, Chatelain M, Chatelain B, Ten Cate H, Mullier F. Pre-analytical issues in the haemostasis laboratory: guidance for the clinical laboratories. *Thromb J.* 2016;14:49.
37. Baron M, Boulanger CM, Staels B, Tailleux A. Cell-derived microparticles in atherosclerosis: biomarkers and targets for pharmacological modulation? *J Cell Mol Med.* 2012;16(7):1365–1376.

38. Doeuvre L, Plawinski L, Toti F, Anglés-Cano E. Cell-derived microparticles: a new challenge in neuroscience. *J Neurochem.* 2009;110(2): 457–468.
39. Nieri D, Neri T, Petrini S, Vagaggini B, Paggiaro P, Celi A. Cell-derived microparticles and the lung. *Eur Respir Rev.* 2016;25(141):266–277.
40. Freyssinet JM. Cellular microparticles: what are they bad or good for? *J Thromb Haemost.* 2003;1(7):1655–1662.
41. Horstman LL, Jy W, Jimenez JJ, Ahn YS. Endothelial microparticles as markers of endothelial dysfunction. *Front Biosci.* 2004;9:1118–1135.
42. Boulanger CM, Tedgui A. Dying for attention: microparticles and angiogenesis. *Cardiovasc Res.* 2005;67(1):1–3.
43. Geiser T, Sturzenegger M, Genewein U, Haeberli A, Beer JH. Mechanisms of cerebrovascular events as assessed by procoagulant activity, cerebral microemboli, and platelet microparticles in patients with prosthetic heart valves. *Stroke.* 1998;29(9):1770–1777.
44. Hajjar E, Korkmaz B, Reuter N. Differences in the substrate binding sites of murine and human proteinase 3 and neutrophil elastase. *FEBS Lett.* 2007;581(29):5685–5690.
45. Martin KR, Kantari-Mimoun C, Yin M, et al. Proteinase 3 is a phosphatidylserine-binding protein that affects the production and function of microvesicles. *J Biol Chem.* 2016;291(20):10476–10489.
46. Xie RF, Hu P, Li W, et al. The effect of platelet-derived microparticles in stored apheresis platelet concentrates on polymorphonuclear leucocyte respiratory burst. *Vox Sang.* 2014;106(3):234–241.
47. Forlow SB, McEver RP, Nollert MU. Leukocyte-leukocyte interactions mediated by platelet microparticles under flow. *Blood.* 2000;95(4):1317–1323.
48. Thom SR, Bennett M, Banham ND, et al. Association of microparticles and neutrophil activation with decompression sickness. *J Appl Physiol (1985).* 2015;119(5):427–434.
49. Niessen A, Heyder P, Krienke S, et al. Apoptotic-cell-derived membrane microparticles and IFN-α induce an inflammatory immune response. *J Cell Sci.* 2015;128(14):2443–2453.
50. Barry OP, Praticò D, Savani RC, FitzGerald GA. Modulation of monocyte-endothelial cell interactions by platelet microparticles. *J Clin Invest.* 1998;102(1):136–144.
51. Gasser O, Schifferli JA. Activated polymorphonuclear neutrophils disseminate anti-inflammatory microparticles by ectocytosis. *Blood.* 2004;104(8):2543–2548.
52. Ismail N, Wang Y, Dakhlallah D, et al. Macrophage microvesicles induce macrophage differentiation and miR-223 transfer. *Blood.* 2013;121(6):984–995.
53. Saha B, Momen-Heravi F, Kodys K, Szabo G. MicroRNA cargo of extracellular vesicles from alcohol-exposed monocytes signals naive monocytes to differentiate into M2 macrophages. *J Biol Chem.* 2016;291(1):149–159.
54. Sadallah S, Eken C, Martin PJ, Schifferli JA. Microparticles (ectosomes) shed by stored human platelets downregulate macrophages and modify the development of dendritic cells. *J Immunol.* 2011;186(11):6543–6552.
55. Clayton A, Mitchell JP, Court J, Linnane S, Mason MD, Tabi Z. Human tumor-derived exosomes down-modulate NKG2D expression. *J Immunol.* 2008;180(11):7249–7258.
56. Whiteside TL. Immune modulation of T-cell and NK (natural killer) cell activities by TEXs (tumour-derived exosomes). *Biochem Soc Trans.* 2013;41(1):245–251.
57. Sadallah S, Schmied L, Eken C, Charoudeh HN, Amicarella F, Schifferli JA. Platelet-derived ectosomes reduce NK cell function. *J Immunol.* 2016;197(5):1663–1671.
58. Pliyev BK, Kalintseva MV, Abdulaeva SV, Yarygin KN, Savchenko VG. Neutrophil microparticles modulate cytokine production by natural killer cells. *Cytokine.* 2014;65(2):126–129.
59. Jenkins MK, Khoruts A, Ingulli E, et al. In vivo activation of antigen-specific CD4 T cells. *Annu Rev Immunol.* 2001;19:23–45.
60. Silliman CC, Bjornsen AJ, Wyman TH, et al. Plasma and lipids from stored platelets cause acute lung injury in an animal model. *Transfusion.* 2003;43(5):633–640.
61. Iwasaki A, Medzhitov R. Toll-like receptor control of the adaptive immune responses. *Nat Immunol.* 2004;5(10):987–995.
62. Angelot F, Seillès E, Biichlé S, et al. Endothelial cell-derived microparticles induce plasmacytoid dendritic cell maturation: potential implications in inflammatory diseases. *Haematologica.* 2009;94(11):1502–1512.
63. Dieker J, Tel J, Pieterse E, et al. Circulating apoptotic microparticles in systemic lupus erythematosus patients drive the activation of dendritic cell subsets and prime neutrophils for NETosis. *Arthritis Rheumatol.* 2016;68(2):462–472.
64. Yari F, Motefaker M, Nikougoftar M, Khayati Z. Interaction of platelet-derived microparticles with a human B-lymphoblast cell line: a clue for the immunologic function of the microparticles. *Transfus Med Hemother.* 2018;45(1):55–61.
65. Messer L, Alsaleh G, Freyssinet J-M, et al. Microparticle-induced release of B-lymphocyte regulators by rheumatoid synoviocytes. *Arthritis Res Ther.* 2009;11(2):R40.
66. Zhang R, Wang X, Hong M, et al. Endothelial microparticles delivering microRNA-155 into T lymphocytes are involved in the initiation of acute graft-versus-host disease following allogeneic hematopoietic stem cell transplantation. *Oncotarget.* 2017;8(14):23360–23375.
67. Conforti A, Scarsella M, Starc N, et al. Microvescicles derived from mesenchymal stromal cells are not as effective as their cellular counterpart in the ability to modulate immune responses in vitro. *Stem Cells Dev.* 2014;23(21):2591–2599.
68. Gouveia de Andrade AV, Bertolino G, Riewaldt J, et al. Extracellular vesicles secreted by bone marrow- and adipose tissue-derived mesenchymal stromal cells fail to suppress lymphocyte proliferation. *Stem Cells Dev*. 2015;24(11):1374–1376.
69. Shen G, Krienke S, Schiller P, et al. Microvesicles released by apoptotic human neutrophils suppress proliferation and IL-2/IL-2 receptor expression of resting T helper cells. *Eur J Immunol.* 2017;47(5):900–910.
70. Budoni M, Fierabracci A, Luciano R, Petrini S, Di Ciommo V, Muraca M. The immunosuppressive effect of mesenchymal stromal cells on B lymphocytes is mediated by membrane vesicles. *Cell Transplant.* 2013;22(2):369–379.
71. Del Fattore A, Luciano R, Pascucci L, et al. Immunoregulatory effects of mesenchymal stem cell-derived extracellular vesicles on T lymphocytes. *Cell Transplant.* 2015;24(12):2615–2627.
72. Wieckowski EU, Visus C, Szajnik M, Szczepanski MJ, Storkus WJ, Whiteside TL. Tumor-derived microvesicles promote regulatory T cell expansion and induce apoptosis in tumor-reactive activated CD8+ T lymphocytes. *J Immunol.* 2009;183(6):3720–3730.
73. Huber V, Fais S, Iero M, et al. Human colorectal cancer cells induce T-cell death through release of proapoptotic microvesicles: role in immune escape. *Gastroenterology.* 2005;128(7):1796–1804.
74. Kim JW, Wieckowski E, Taylor DD, Reichert TE, Watkins S, Whiteside TL. Fas ligand-positive membranous vesicles isolated from sera of patients with oral cancer induce apoptosis of activated T lymphocytes. *Clin Cancer Res.* 2005;11(3):1010–1020.
75. Hong Y, Eleftheriou D, Hussain AAK, et al. Anti-neutrophil cytoplasmic antibodies stimulate release of neutrophil microparticles. *J Am Soc Nephrol.* 2012;23(1):49–62.
76. Pitanga TN, de Aragão França L, Rocha VCJ, et al. Neutrophil-derived microparticles induce myeloperoxidase-mediated damage of vascular endothelial cells. *BMC Cell Biol.* 2014;15:21.
77. Wen B, Combes V, Bonhoure A, Weksler BB, Couraud P-O, Grau GE. Endotoxin-induced monocytic microparticles have contrasting effects on endothelial inflammatory responses. *PLoS One.* 2014;9(3):e91597.
78. Thulin Å, Christersson C, Alfredsson J, Siegbahn A. Circulating cell-derived microparticles as biomarkers in cardiovascular disease. *Biomark Med.* 2016;10(9):1009–1022.

DOI: 10.1093/labmed/lmaa043

79. Alexandru N, Costa A, Constantin A, Cochior D, Georgescu A. Microparticles: from biogenesis to biomarkers and diagnostic tools in cardiovascular disease. *Curr Stem Cell Res Ther.* 2017;12(2):89–102.
80. Goichot B, Grunebaum L, Desprez D, et al. Circulating procoagulant microparticles in obesity. *Diabetes Metab.* 2006;32(1):82–85.
81. Stepanian A, Bourguignat L, Hennou S, et al. Microparticle increase in severe obesity: not related to metabolic syndrome and unchanged after massive weight loss. *Obesity (Silver Spring).* 2013;21(11):2236–2243.
82. Preston RA, Jy W, Jimenez JJ, et al. Effects of severe hypertension on endothelial and platelet microparticles. *Hypertension.* 2003;41(2):211–217.
83. Nomura S, Kanazawa S, Fukuhara S. Effects of efonidipine on platelet and monocyte activation markers in hypertensive patients with and without type 2 diabetes mellitus. *J Hum Hypertens.* 2002;16(8):539–547.
84. Diamant M, Nieuwland R, Pablo RF, Sturk A, Smit JW, Radder JK. Elevated numbers of tissue-factor exposing microparticles correlate with components of the metabolic syndrome in uncomplicated type 2 diabetes mellitus. *Circulation.* 2002;106(19):2442–2447.
85. Suades R, Padró T, Alonso R, Mata P, Badimon L. Lipid-lowering therapy with statins reduces microparticle shedding from endothelium, platelets and inflammatory cells. *Thromb Haemost.* 2013;110(2):366–377.
86. Franchini M. Hemostasis and aging. *Crit Rev Oncol Hematol.* 2006;60(2):144–151.
87. Wilkerson WR, Sane DC. Aging and thrombosis. *Semin Thromb Hemost.* 2002;28(6):555–568.
88. Forest A, Pautas E, Ray P, et al. Circulating microparticles and procoagulant activity in elderly patients. *J Gerontol A Biol Sci Med Sci.* 2010;65(4):414–420.
89. Ceroi A, Delettre FA, Marotel C, et al. The anti-inflammatory effects of platelet-derived microparticles in human plasmacytoid dendritic cells involve liver X receptor activation. *Haematologica.* 2016;101(3):e72–e76.
90. Wannamethee SG, Shaper AG, Lennon L, Morris RW. Metabolic syndrome vs Framingham risk score for prediction of coronary heart disease, stroke, and type 2 diabetes mellitus. *Arch Intern Med.* 2005;165(22):2644–2650.
91. Sohn C, Kim J, Bae W. The Framingham risk score, diet, and inflammatory markers in Korean men with metabolic syndrome. *Nutr Res Pract.* 2012;6(3):246–253.
92. Yousefzadeh G, Shokoohi M, Najafipour H, Shadkamfarokhi M. Applying the Framingham risk score for prediction of metabolic syndrome: The Kerman Coronary Artery Disease Risk Study, Iran. *ARYA Atheroscler.* 2015;11(3):179–185.
93. Jahangiry L, Farhangi MA, Rezaei F. Framingham risk score for estimation of 10-years of cardiovascular diseases risk in patients with metabolic syndrome. *J Health Popul Nutr.* 2017;36(1):36.
94. Rizk A, Gorson KC, Kenney L, Weinstein R. Transfusion-related acute lung injury after the infusion of IVIG. *Transfusion.* 2001;41(2):264–268.
95. Stoclin A, Delbos F, Dauriat G, et al. Transfusion-related acute lung injury after intravenous immunoglobulin treatment in a lung transplant recipient. *Vox Sang.* 2013;104(2):175–178.
96. Baudel JL, Vigneron C, Pras-Landre V, et al. Transfusion-related acute lung injury (TRALI) after intravenous immunoglobulins: French multicentre study and literature review. *Clin Rheumatol.* 2020;39(2):541–546.
97. Dry SM, Bechard KM, Milford EL, Churchill WH, Benjamin RJ. The pathology of transfusion-related acute lung injury. *Am J Clin Pathol.* 1999;112(2):216–221.
98. Strait RT, Hicks W, Barasa N, et al. MHC class I–specific antibody binding to nonhematopoietic cells drives complement activation to induce transfusion-related acute lung injury in mice. *J Exp Med.* 2011;208(12):2525–2544.
99. Tung J-P, Fraser JF, Nataatmadja M, et al. Age of blood and recipient factors determine the severity of transfusion-related acute lung injury (TRALI). *Crit Care.* 2012;16(1):R19.
100. Silliman CC, Voelkel NF, Allard JD, et al. Plasma and lipids from stored packed red blood cells cause acute lung injury in an animal model. *J Clin Invest.* 1998;101(7):1458–1467.
101. Jy W, Ricci M, Shariatmadar S, Gomez-Marin O, Horstman LH, Ahn YS. Microparticles in stored red blood cells as potential mediators of transfusion complications. *Transfusion.* 2011;51(4):886–893.
102. Allan D, Thomas P, Limbrick AR. The isolation and characterization of 60 nm vesicles ('nanovesicles') produced during ionophore A23187-induced budding of human erythrocytes. *Biochem J.* 1980;188(3):881–887.
103. Jy W, Horstman LL, Ahn YS. Microparticle size and its relation to composition, functional activity, and clinical significance. *Semin Thromb Hemost.* 2010;36(8):876–880.
104. Kriebardis AG, Antonelou MH, Stamoulis KE, Economou-Petersen E, Margaritis LH, Papassideri IS. RBC-derived vesicles during storage: ultrastructure, protein composition, oxidation, and signaling components. *Transfusion.* 2008;48(9):1943–1953.
105. Müller H, Lutz HU. Binding of autologous IgG to human red blood cells before and after ATP-depletion. Selective exposure of binding sites (autoantigens) on spectrin-free vesicles. *Biochim Biophys Acta.* 1983;729(2):249–257.
106. Bosman GJCGM, Lasonder E, Luten M, et al. The proteome of red cell membranes and vesicles during storage in blood bank conditions. *Transfusion.* 2008;48(5):827–835.
107. Pasini EM, Kirkegaard M, Mortensen P, Lutz HU, Thomas AW, Mann M. In-depth analysis of the membrane and cytosolic proteome of red blood cells. *Blood.* 2006;108(3):791–801.
108. Zecher D, Cumpelik A, Schifferli JA. Erythrocyte-derived microvesicles amplify systemic inflammation by thrombin-dependent activation of complement. *Arterioscler Thromb Vasc Biol.* 2014;34(2):313–320.
109. Gasser O, Schifferli JA. Microparticles released by human neutrophils adhere to erythrocytes in the presence of complement. *Exp Cell Res.* 2005;307(2):381–387.
110. Inwald DP, McDowall A, Peters MJ, Callard RE, Klein NJ. CD40 is constitutively expressed on platelets and provides a novel mechanism for platelet activation. *Circ Res.* 2003;92(9):1041–1048.
111. Phipps RP, Kaufman J, Blumberg N. Platelet derived CD154 (CD40 ligand) and febrile responses to transfusion. *Lancet.* 2001;357(9273):2023–2024.
112. Ahn ER, Lander G, Jy W, et al. Differences of soluble CD40L in sera and plasma: implications on CD40L assay as a marker of thrombotic risk. *Thromb Res.* 2004;114(2):143–148.
113. Esser MT, Graham DR, Coren LV, et al. Differential incorporation of CD45, CD80 (B7-1), CD86 (B7-2), and major histocompatibility complex class I and II molecules into human immunodeficiency virus type 1 virions and microvesicles: implications for viral pathogenesis and immune regulation. *J Virol.* 2001;75(13):6173–6182.
114. Mack M, Kleinschmidt A, Brühl H, et al. Transfer of the chemokine receptor CCR5 between cells by membrane-derived microparticles: a mechanism for cellular human immunodeficiency virus 1 infection. *Nat Med.* 2000;6(7):769–775.
115. Krishnamoorthy L, Bess JW Jr, Preston AB, Nagashima K, Mahal LK. HIV-1 and microvesicles from T cells share a common glycome, arguing for a common origin. *Nat Chem Biol.* 2009;5(4):244–250.
116. Gan X, Gould SJ. Identification of an inhibitory budding signal that blocks the release of HIV particles and exosome/microvesicle proteins. *Mol Biol Cell.* 2011;22(6):817–830.
117. Kulshreshtha A, Ahmad T, Agrawal A, Ghosh B. Proinflammatory role of epithelial cell-derived exosomes in allergic airway inflammation. *J Allergy Clin Immunol.* 2013;131(4):1194–203, 1203.e1.
118. Bolasco G, Tracey-White DC, Tolmachova T, et al. Loss of Rab27 function results in abnormal lung epithelium structure in mice. *Am J Physiol Cell Physiol.* 2011;300(3):C466–C476.

DOI: 10.1093/labmed/lmaa043

119. Sibai B, Dekker G, Kupferminc M. Pre-eclampsia. *Lancet.* 2005;365(9461):785–799.
120. Redman CW, Sargent IL. Latest advances in understanding preeclampsia. *Science.* 2005;308(5728):1592–1594.
121. Koumandakis E, Koumandaki I, Kaklamani E, Sparos L, Aravantinos D, Trichopoulos D. Enhanced phagocytosis of mononuclear phagocytes in pregnancy. *Br J Obstet Gynaecol.* 1986;93(11):1150–1154.
122. Shibuya T, Izuchi K, Kuroiwa A, Okabe N, Shirakawa K. Study on nonspecific immunity in pregnant women: increased chemiluminescence response of peripheral blood phagocytes. *Am J Reprod Immunol Microbiol.* 1987;15(1):19–23.
123. Luppi P, Haluszczak C, Betters D, Richard CA, Trucco M, DeLoia JA. Monocytes are progressively activated in the circulation of pregnant women. *J Leukoc Biol.* 2002;72(5):874–884.
124. Sacks GP, Redman CW, Sargent IL. Monocytes are primed to produce the Th1 type cytokine IL-12 in normal human pregnancy: an intracellular flow cytometric analysis of peripheral blood mononuclear cells. *Clin Exp Immunol.* 2003;131(3): 490–497.
125. Holthe MR, Staff AC, Berge LN, Lyberg T. Leukocyte adhesion molecules and reactive oxygen species in preeclampsia. *Obstet Gynecol.* 2004;103(5 Pt 1):913–922.
126. Luppi P, Deloia JA. Monocytes of preeclamptic women spontaneously synthesize pro-inflammatory cytokines. *Clin Immunol.* 2006;118(2-3):268–275.
127. Messerli M, May K, Hansson SR, et al. Feto-maternal interactions in pregnancies: placental microparticles activate peripheral blood monocytes. *Placenta.* 2010;31(2):106–112.
128. Thomas GM, Brill A, Mezouar S, et al. Tissue factor expressed by circulating cancer cell-derived microparticles drastically increases the incidence of deep vein thrombosis in mice. *J Thromb Haemost.* 2015;13(7):1310–1319.
129. Geddings JE, Mackman N. Tumor-derived tissue factor-positive microparticles and venous thrombosis in cancer patients. *Blood.* 2013;122(11):1873–1880.
130. Jaiswal R, Gong J, Sambasivam S, et al. Microparticle-associated nucleic acids mediate trait dominance in cancer. *FASEB J.* 2012;26(1):420–429.
131. Lu JF, Luk F, Gong J, Jaiswal R, Grau GER, Bebawy M. Microparticles mediate MRP1 intercellular transfer and the re-templating of intrinsic resistance pathways. *Pharmacol Res.* 2013;76:77–83.
132. Gong J, Luk F, Jaiswal R, Bebawy M. Microparticles mediate the intercellular regulation of microRNA-503 and proline-rich tyrosine kinase 2 to alter the migration and invasion capacity of breast cancer cells. *Front Oncol.* 2014;4:220.
133. Kim CW, Lee HM, Lee TH, Kang C, Kleinman HK, Gho YS. Extracellular membrane vesicles from tumor cells promote angiogenesis via sphingomyelin. *Cancer Res.* 2002;62(21):6312–6317.
134. Abid Hussein MN, Böing AN, Sturk A, Hau CM, Nieuwland R. Inhibition of microparticle release triggers endothelial cell apoptosis and detachment. *Thromb Haemost.* 2007;98(5):1096–1107.
135. Abrahams VM, Straszewski-Chavez SL, Guller S, Mor G. First trimester trophoblast cells secrete Fas ligand which induces immune cell apoptosis. *Mol Hum Reprod.* 2004;10(1):55–63.
136. Zhang H, Tang K, Zhang Y, et al. Cell-free tumor microparticle vaccines stimulate dendritic cells via cGAS/STING signaling. *Cancer Immunol Res.* 2015;3(2):196–205.
137. El Andaloussi S, Lakhal S, Mäger I, Wood MJ. Exosomes for targeted siRNA delivery across biological barriers. *Adv Drug Deliv Rev.* 2013;65(3):391–397.
138. Besse B, Charrier M, Lapierre V, et al. Dendritic cell-derived exosomes as maintenance immunotherapy after first line chemotherapy in NSCLC. *Oncoimmunology.* 2016;5(4):e1071008.
139. Bruno S, Collino F, Deregibus MC, Grange C, Tetta C, Camussi G. Microvesicles derived from human bone marrow mesenchymal stem cells inhibit tumor growth. *Stem Cells Dev.* 2013;22(5):758–771.

DOI: 10.1093/labmed/lmaa043

Science

Potential Use of Antigen-Based Rapid Test for SARS-CoV-2 in Respiratory Specimens in Low-Resource Settings in Egypt for Symptomatic Patients and High-Risk Contacts

Abeer Mohamed Abdelrazik, MD, PhD, Shahira Morsy ELshafie, MD, PhD, Hossam M. Abdelaziz, MD, PhD*

Laboratory Medicine 2021;52:e46-e49

DOI: 10.1093/labmed/lmaa104

ABSTRACT

Objective: Because of the rapidly emerging SARS-CoV-2 pandemic and its wide public health challenges, rapid diagnosis is essential to decrease the spread. Antigen-based rapid detection tests are available; however, insufficient data about their performance are available.

Methods: The lateral-flow immunochromatographic BIOCREDIT COVID-19 antigen test was evaluated using nasopharyngeal swabs in a viral transport medium from patients with confirmed infection, contacts, and exposed healthcare professionals at Fayoum University Hospital in Egypt. Test performance was determined in comparison to the SARS-CoV-2 real-time reverse-transcription polymerase chain reaction (RT-PCR) test.

Results: Three hundred ten specimens from 3 categories—patients with confirmed diagnoses of COVID-19, contacts, and exposed healthcare professionals—were included; 188 specimens were RT-PCR-positive, from which 81 were detected by rapid antigen test. Overall sensitivity was 43.1%. Sensitivity was significantly higher in specimens with high viral loads.

Conclusion: Poor sensitivity of the BIOCREDIT COVID-19 test does not permit its use for diagnosis, and it can only be used in conjunction with RT-PCR for screening.

Keywords: antigen-based rapid test, COVID-19, RT-PCR, SARS-CoV-2

In late 2019, a cluster of patients with a viral pneumonia of unknown etiology was reported in Wuhan, Hubei Province, China.[1] This new viral pneumonia, COVID-19, caused by the novel SARS-CoV-2, spread rapidly and developed into a global pandemic within 3 months of its initial detection.[2,3] The current gold standard and the recommended diagnostic method for the diagnosis of COVID-19 is the detection of viral RNA in respiratory tract specimens by real-time reverse-transcription polymerase chain reaction (RT-PCR), which was introduced in January 2020 and is applied using World Health Organization (WHO) protocols.[4-6]

Several factors may limit the use of RT-PCR, eg, the availability of skilled trained laboratory personnel familiar with molecular techniques, the need for special equipment, and a specific laboratory infrastructure with safety measures and equipment. Moreover, molecular tests are costly and often time-consuming, creating a burden especially for countries with low resources.[7]

There is a strong need for rapid and easy-to-perform tests, particularly in countries with limited access to molecular-level assessments.[5] A rapid antigen detection (RAD) test for SARS-CoV-2 can be interpreted without specialized equipment, and results can be available within 30 minutes. The RAD tests can thereby decrease the workload in laboratories and hospitals and improve the turnaround time for results. However, the WHO has noted that the role of RAD

Abbreviations:

RT-PCR, reverse-transcription polymerase chain reaction; WHO, World Health Organization; RAD, rapid antigen detection; NP, nasopharyngeal; Ct, cycle threshold.

Clinical Pathology Department, Faculty of Medicine, Fayoum University Hospital, Fayoum, Egypt

*To whom correspondence should be addressed.
abdelrazik50@hotmail.com

tests in antigen detection for SARS-CoV-2 requires further evaluation, and the tests are not recommended for clinical diagnosis.[8,9]

The aim of this study was to assess the performance of the BIOCREDIT COVID-19 Ag test as a frontline test in comparison to the molecular RT-PCR technique to evaluate the potential of its use during the peak period of the pandemic, especially in high-risk symptomatic populations such as healthcare workers, reducing the need for expensive molecular confirmatory testing.

Materials and Methods

Patient Selection

This study was performed at Fayoum University Hospital in Egypt and was approved by the Fayoum University Research ethics committee, which is a member of the Egyptian Network Research Ethics Committee. The study included 310 specimens: 160 from patients who tested positive for SARS-CoV-2 by RT-PCR and 150 from exposed healthcare workers and patient contacts. Specimens were all collected during May 2020.

Specimens

Nasopharyngeal (NP) specimens were obtained using flocked NP swabs and transported to the laboratory in universal viral transport media (UTM-RT System, Copan Diagnostics, Murrieta, CA) within 1 to 2 hours of collection.

RT-PCR for SARS-CoV-2

The RT-PCR technique used the SARS-CoV-2/SARS-CoV Multiplex real-time PCR detection kit, DNA technology in the instrument RT-PCR DTlite 4 (Russia), and the extraction was done using the LabTurbo 48C (Taiwan).

BIOCREDIT COVID-19 Ag

PCR-characterized specimens (universal transport medium with swabs) were kept at 4°C and tested within 24 hours by the BIOCREDIT COVID-19 Ag, which is a lateral-flow immunochromatographic assay that uses a dual-color system for the qualitative detection of the SARS-CoV-2 antigen from NP swab specimens. The recommended specimen volume of the BIOCREDIT COVID-19 Ag kit was 90 to 150 μL. To unify the specimen volume, a 100 μL specimen volume average was used.

Statistical Analysis

All statistical calculations were done using SPSS software version 18 under Windows 7. Qualitative data were statistically expressed in the form of frequency and percentages. Numerical data were statistically represented in terms of range, mean, and standard deviation. The Pearson χ^2 and *t*-test were used for comparing categorical variables. A probability value (*P* value) >.05 was considered significant.

Results

A total of 310 specimens were included. Of those, 188 were RT-PCR-positive for SARS-CoV-2 RNA, and 122 were RT-PCR-negative. Among tested patients, 59.4% were men and the median age was 42 years. Positive specimens from patients were taken during the initial phase of the disease with a median duration of symptoms of 3 days. The median cycle threshold (Ct) value of positive RT-PCR specimens was 20.2 (range, 15.8–32.3) (**Table 1**).

The overall sensitivity of the evaluated RAD test was 43.1%. The sensitivity was significantly increased in the subgroup of specimens with Ct values <25.5, indicating high viral loads (**Table 2**). All false negative results according to the RAD test (n = 107) corresponded to specimens with

Table 1. Demographic and Laboratory Features of Included Patients

	All	PCR-Positive	PCR-Negative
Total	310	188	122
Sex			
Male	184 (59.4)	103 (54.8)	81 (66.4)
Female	126 (40.6)	85 (45.2)	41 (33.6)
Age (y), median	42	42	42
Ct value			
Median		20.2	
Range		15.8–32.3	
Mean		22	

Ct, cycle threshold of RT-PCR; PCR, polymerase chain reaction. Data represent absolute numbers (%).

Lab Medicine 2021;52;e46–e49 e47
DOI: 10.1093/labmed/lmaa104

Table 2. Performance Characteristics of RAD Test for the Presence of SARS-CoV-2 in 188 RT-PCR-Positive Specimens

All Specimens					High-Viral-Load Specimens				
Ct Value		Number of Specimens			Ct Value		Number of Specimens		
Mean	Range	Tested	Positive	Sensitivity	Mean	Range	Tested	Positive	Sensitivity
22	15.8–32.3	188	81	43.1%	18	15.8–25.5	76	71	93.4%

Ct, cycle threshold; RAD, rapid antigen detection; RT-PCR, reverse-transcription polymerase chain reaction. High-viral-load specimens are those with Ct values <25.5 for SARS-CoV-2–specific RT-PCR, and normal viral load specimens are those with Ct values >28.0.

RT-PCR Ct values >28. All specimens that tested positive according to the RAD test tested positive according to RT-PCR testing.

Discussion

Different diagnostic test manufacturers have developed rapid tests based on SARS-CoV-2 protein detection in respiratory specimens.[7] The analytical performances of rapid antigen tests depend on different factors including the viral load, the quality of the specimen, and the setting of the people tested.

Rapid tests have different advantages, including low cost, short turnaround time, simple noncomplicating test performance, and the lack of a need for special equipment or skills compared with molecular techniques.[10]

In this study, we assessed the performance characteristics of the rapid antigen test BIOCREDIT COVID-19 Ag for detecting SARS-CoV-2 in respiratory specimens and compared the results with RT-PCR testing. Our data indicated that (i) RAD testing for SARS-CoV-2 had a lower sensitivity than RT-PCR testing, (ii) negative results could not exclude the possibility of SARS-CoV-2 infection with confidence, and (iii) therefore, results should be confirmed by further RT-PCR testing. We also noted that the RAD test can detect SARS-CoV-2 with a high viral load (Ct <25.5), but the sensitivity declines substantially when the viral load decreases with Ct values >28, which is often the case in patients with COVID-19. In this study, the overall sensitivity of the BIOCREDIT COVID-19 Ag test was 43.1%. A similar study revealed an overall sensitivity of 30.2% in 106 SARS-CoV-2 RT-PCR-positive specimens.[6]

Although the RAD test was positive for corresponding RT-PCR-confirmed COVID-19 infection, we recommend checking the specificity more by using the RAD test for other viruses that could cross-react with other human coronaviruses, eg, severe acute respiratory syndrome coronavirus (SARS-CoV) and the Middle East respiratory syndrome coronavirus, which can each cause severe acute respiratory illnesses because of their genetic relationship with SARS-CoV-2.

Conclusion

In summary and based on our data, the application of the RAD test alone in clinical settings is not recommended in favor of continued molecular diagnostics and should not be considered for use in the screening of asymptomatic individuals or for population-based surveillance studies. However, the balance between cost, turnaround time, ease of performance, and sensitivity in adopting an antigen-based assay should be considered in symptomatic patients with a high pretest probability of having COVID-19. The use of these tests should be considered when there is a need for immediate clinical decisions and infection control measures, and negative results in this scenario should be confirmed with a laboratory-based molecular test. **LM**

Acknowledgments

We thank all the technologists of the Laboratory Department, Fayoum University Hospital, for technical assistance and data collection during the current SARS-CoV-2 pandemic. There were no external funding sources for this study. The authors certify that there is no conflict of interest with any organization regarding the material discussed in the article.

References

1. Guarner J. Three emerging coronaviruses in two decades. *Am J Clin Pathol.* 2020;153(4):420–421.
2. Hoffman T, Nissen K, Krambrich J, et al. Evaluation of a COVID-19 IgM and IgG rapid test; an efficient tool for assessment of past exposure to SARS-CoV-2. *Infect Ecol Epidemiol.* 2020;10(1): 1754538.
3. Wang D, Hu B, Hu C, et al. Clinical characteristics of 138 hospitalized patients with 2019 novel coronavirus-infected pneumonia in Wuhan, China. *JAMA.* 2020;323(11):1061–1069.
4. Porte L, Legarraga P, Vollrath V, et al. Evaluation of novel antigen-based rapid detection test for the diagnosis of SARS-CoV-2 in respiratory samples. *Int J Infect Dis.* 2020;99:328–333.
5. SARS-CoV-2 diagnostic pipeline. Foundation for Innovative New Diagnostics website. https://www.finddx.org/covid-19/pipeline. Accessed November 4, 2020.
6. Scohy A, Anantharajah A, Bodéus M, Kabamba-Mukadi B, Verroken A, Rodriguez-Villalobos H. Low performance of rapid antigen detection test as frontline testing for COVID-19 diagnosis. *J Clin Virol.* 2020;129:104455.
7. Mak GC, Cheng PK, Lau SS, et al. Evaluation of rapid antigen test for detection of SARS-CoV-2 virus. *J Clin Virol.* 2020;129:104500.
8. Laboratory testing strategy recommendations for COVID-19: interim guidance, 21 March 2020. World Health Organization website. https://apps.who.int/iris/handle/10665/331509. Accessed November 4, 2020.
9. Balish A, Warnes CM, Wu K, et al. Evaluation of rapid influenza diagnostic tests for detection of novel influenza A (H1N1) virus—United States, 2009. *MMWR Morb Mortal Wkly Rep.* 2009;58(30):826–829.
10. Buchan BW, Ledeboer NA. Emerging technologies for the clinical microbiology laboratory. *Clin Microbiol Rev.* 2014;27(4):783–822.

DOI: 10.1093/labmed/lmaa104

Case Study

Acute Hemolytic Transfusion Reaction Due to Pooled Platelets: A Rare but Serious Adverse Event

Richard Gammon, MD,[1*] *Susan Cook, MT(ASCP)SBB, MS,*[2] *Anthony Trinkle, BS, SBB,*[3] *Korena Thomas, MT(ASCP) CQA(ASQ),*[1] *Kaaron Benson, MD*[2]

Laboratory Medicine 2021;52:202-204

DOI: 10.1093/labmed/lmaa056

ABSTRACT

A female patient aged 65 years with blood group A with relapsed lymphoma had thrombocytopenia; leukocyte-reduced group O prestorage pooled platelet concentrates (PPLTs) were transfused without adverse events. She was discharged home, but 1.5 hours later she returned with fever and dark urine. Hypotension and tachycardia developed; she was admitted to the intensive care unit. Post-transfusion blood and urine samples were obtained. Serial dilutions from 5 donor testing tubes and a simulated PLT pool were performed and read at immediate spin and IgG. Testing confirmed an acute hemolytic transfusion reaction (AHTR): elevated lactate dehydrogenase (996 U/L; normal range 135 U/L–225 U/L) and undetectable haptoglobin (<10 mg/dL; normal range 30 mg/dL–200 mg/dL) levels. Urinalysis showed dark amber urine but no significant quantity of red blood cells. At 37ºC the simulated pool and donor number 5 had high-titer anti-A. As a precaution, the donor was permanently deferred. Research has shown that PLT-associated AHTR has occurred with apheresis platelets but is very rare with whole blood–derived PLTs.

Keywords: hemolysis, antibodies, transfusion practice, transfusion reactions

Patient History

A female patient aged 65 years weighing 52 kg with blood group A and with relapsed lymphoma had thrombocytopenia (5,000 platelets/μL; normal range 150,000 platelets/μL–450,000 platelets/μL); irradiated, leukoreduced pooled platelet concentrates (PPLTs) (5 group O donors) were transfused in 47 minutes. The patient had no adverse events (AEs) and was discharged home but 1.5 hours later returned with fever (103ºF), rigors, dyspnea, cough, chest pressure, nausea, and diarrhea. Hypotension and tachycardia developed; she was transferred to the intensive care unit (ICU). The differential diagnosis of this patient presenting with AE shortly after transfusion included febrile nonhemolytic transfusion reaction, transfusion-transmitted infection, transfusion-related acute lung injury, and an acute hemolytic transfusion reaction (AHTR).

A transfusion reaction investigation was initiated. Testing confirmed an AHTR (**Figure 1**): elevated lactate dehydrogenase (996 U/L; normal range 135 U/L–225 U/L), undetectable haptoglobin (<10 mg/dL; normal range 30 mg/dL–200 mg/dL), prolonged prothrombin time (18.3 sec; normal range 10.2 sec–12.9 sec), international normalized ratio (1.5; normal range 0.8–1.1), Activated partial thromboplastin time (47.3 sec; normal range 25.1 sec–36.5 sec), no evidence of infection in blood or urine cultures, and urinalysis showing dark amber urine with "large" blood on dipstick but only 0–2 red blood cells (RBCs)/high-powered field. The pretransfusion hemoglobin of 8.9 g/dL fell to 7.5 g/dL, and the initial platelet count of 5,000/μL increased to 27,000/μL. The patient developed lactic acidosis (lactate 7.0 mmol/L; normal

Abbreviations

PPLT, pooled platelet concentrates; AHTR, acute hemolytic transfusion reaction; AE, adverse event; ICU, intensive care unit; RBCs, red blood cells; IS, immediate spin.

[1]Scientific Medical and Technical Direction, OneBlood, Orlando, Florida, [2]Department of Pathology and Laboratory Medicine, Moffitt Cancer Center, Tampa, Florida, [3]Immunohematology Reference Laboratory, OneBlood, St. Petersburg, Florida

*To whom correspondence should be addressed.
richard.gammon@oneblood.org

Figure 1

Sample Tubes Before and After Transfusion-Pretransfusion plasma (EDTA) (left), the initial post-transfusion plasma sample (center) and a recollected specimen due to concerns about possible preanalytical error and traumatic venipuncture (right). The center tube shows significant hemoglobinemia that decreased in the right tube collected approximately three hours later.

Table 1. Titer Testing of Donors of Pool and Simulated Pool

Unit	Test	Anti-A	Anti-B
Simulated Pool	IS	256	128
Simulated Pool	37°C	2048	256
Donor 1	IS	32	32
Donor 1	37°C	512	128
Donor 2	IS	128	128
Donor 2	37°C	256	512
Donor 3	IS	128	16
Donor 3	37°C	128	16
Donor 4	IS	64	16
Donor 4	37°C	32	16
Donor 5	IS	256	256
Donor 5	37°C	4096	512

IS, immediate spin.

range 0.5 mmol/L–2.0 mmol/L). The secretor status of the patient was not determined, and A1 typing was not performed. The platelet bag had been discarded and was not available for testing. Serial dilutions (with saline) from the 5 donor test tubes and a simulated platelet pool were prepared and read at immediate spin and IgG (1 hour at 37°C incubation). At 37°C, the simulated pool and donor 5 had high-titer anti-A (**Table 1**). This first-time 16-year-old male donor was permanently deferred as a precaution.

The patient spent 4 days in the ICU requiring extensive support, including 48 hours of pressors. After 1 day in a standard unit, she was discharged home in stable condition. She continued with additional cycles of chemotherapy as an outpatient but her lymphoma continued to progress. She and her family decided on hospice care about 3 weeks after her reaction. She died 1 day after hospice care was begun.

Discussion

This patient presented with fever and many other signs/symptoms about 1.5 hours after a platelet transfusion. Febrile transfusion reactions include serious reactions such as acute hemolysis and bacterial contamination. Immediate action is required and includes stopping the transfusion to limit the amount of potentially harmful blood and sending samples to the blood bank to investigate for acute hemolysis. The patient's vital signs should be carefully monitored for additional evidence of infection, such as the presence of tachycardia.[1,2]

Group ABO–incompatible platelets are routinely provided because of their efficacy, short shelf life, and rarity of these hemolytic events. When platelets are not ABO identical, donor platelets may be incompatible with recipient antibodies, eg, group A platelets to a group O recipient. Platelets do express weak A and B antigens, but the resulting post-transfusion platelet increment is usually adequate, although not as high as ABO-identical platelets. A patient with group O receiving group A platelets may have a post-transfusion increment of approximately 25,000 μL–30,000/μL over baseline value in contrast to an increment of 30,000 μL–35,000/μL with ABO-identical platelets.[3] Donor platelets may be plasma-incompatible

Lab Medicine 2021;52;202–204
DOI: 10.1093/labmed/lmaa056

with recipient RBCs, eg, group O platelets to a recipient with group A. Physicians must be aware of the potential risk of AHTR because of platelet transfusion. An AHTR is rare and is mostly associated with RBC transfusions with clerical error as the underlying etiology. During fiscal years 2013 to 2017, there were 32 fatalities (both ABO and non-ABO etiologies) reported to the U.S. Food and Drug Administration.[4]

Severe AHTRs have occurred rarely and are often associated with donor high-titer anti-A. A review of the literature found 23 published cases of AHTR, all involving the transfusion of group O PPLTs to a recipient with group A or AB. In PPLT-associated AHTRs, anti-A titers ranged from 32 to 16,000, with a mean titer of 512.[5] Donor anti-A and anti-B titers are not routinely performed.[6] These reactions have been seen previously and have almost always occurred in apheresis platelets. The risk of a clinically significant AHTR after ABO-incompatible platelet transfusion has ranged from 1 in 47,800 (0.0021%) at the Japanese Red Cross during an 8-year period[7] to 1 in 9000 (0.01%) at a large cancer treatment hospital in the United States.[8] One study screened 124 group O PPLTs for anti-A and anti-B by both standard tube and manual gel tests.[5] Mean anti-A and anti-B titers in group O PPLTs were, respectively, 16 and 8 by tube and 64 and 32 by gel (P <0.0001). Gel titers were 1 to 2 dilutions higher than tube and sensitive to reagent red cell lots. With the use of at least 64 as a critical titer, 60% of group O PPLTs tested by gel would be considered high-titer. The study concluded that anti-A and anti-B titers in the group O PPLTs studied were comparable to those reported in group O single donor platelets and generally significantly lower than titers reported in AHTR. In addition, the study suggested that a critical direct agglutinin titer of 64 for identifying high-titer units by gel is too low and should be increased to 128 or higher.[5]

Research has shown that AHTRs resulting from platelet transfusion are rare events and have almost exclusively been seen in apheresis platelets with a single donor with a high-titer ABO antibody. This AHTR resulting from pooled platelets was clearly a rare event. Leukoreduced pooled platelets contain 4 to 6 whole blood–derived platelets. Titers of anti-A/AB in 100 unselected group O donors with an arbitrarily chosen high titer of 64 for IgM and a titer of 256 for IgG were 28% and 39%, respectively, which were categorized as dangerous levels.[9] If one of the donations has a high-titer anti-A or anti-B, it should be diluted by the plasma from the other donors. A report of the transfusion of 10,251 leukoreduced pooled platelets revealed no reports of hemolysis.[10]

Thorough evaluations of AE need to consider even rare etiologies. This was the second AHTR because of platelets in 32 years of this hospital's operation, with 12,195 platelet transfusions conducted in 2018. The first event, in 1997, occurred with apheresis platelets. Both events occurred in smaller-sized recipients. This hospital's 2 AHTR events may have been prevented by (i) restricting ABO-incompatible plasma volumes in smaller-sized adults (eg, volume reduction or use of additive solution); (ii) donor anti-A titer screening; or (iii) avoiding transfusing group O platelets to recipients who are not group O. As a precaution, in our hospital we are now volume-reducing ABO-incompatible plasma in platelets to be transfused to all patients who weigh less than 60 kg. **LM**

References

1. Stramer S, Galel S. Infectious disease screening. In: Fung MK, Eder AF, Spitalnik SL, Westhoff CM. eds. *Technical Manual*. 19th ed. Bethesda, MD: AABB Press; 2017:161–206.
2. Savage W, Hod E. Noninfectious hazards of blood transfusion. In: Fung MK, Eder AF, Spitalnik SL, Westhoff CM. eds. *Technical Manual*. 19th ed. Bethesda, MD: AABB Press, 2017:569–598.
3. Cooling L. ABO and platelet transfusion therapy. *Immunohematology.* 2007;23(1):20–33.
4. Fatalities reported to the FDA following blood collection and transfusion. FY 2017. U.S. Food and Drug Administration website. https://www.fda.gov/media/124796/download. Accessed March 2, 2020.
5. Cooling LL, Downs TA, Butch SH, Davenport RD. Anti-A and anti-B titers in pooled group O platelets are comparable to apheresis platelets. *Transfusion.* 2008;48(10):2106–2113.
6. Berséus O, Boman K, Nessen SC, Westerberg LA. Risks of hemolysis due to anti-A and anti-B caused by the transfusion of blood or blood components containing ABO-incompatible plasma. *Transfusion.* 2013;53(Suppl 1):114S–123S.
7. Sato T, Goto N, Tasaki T. Hemolytic transfusion reactions. *N Engl J Med.* 2019;381(14):1396–1398.
8. Mair B, Benson K. Evaluation of changes in hemoglobin levels associated with ABO-incompatible plasma in apheresis platelets. *Transfusion.* 1998;38(1):51–55.
9. Josephson CD, Mullis NC, Van Denmark C, et al. Significant numbers of apheresis-derived group O platelet units have "high-titer" anti-A/A,B: implications for transfusion policy. *Transfusion.* 2004;44(6):805–808.
10. Tormey CA, Sweeney JD, Champion MH, Pisciotto PT, Snyder EL, Wu Y. Analysis of transfusion reactions associated with prestorage-pooled platelet components. *Transfusion.* 2009;49(6):1242–1247.

Management & Administration

SBAR as a Standardized Communication Tool for Medical Laboratory Science Students

Ana L. Oliveira, DrPH, MSPH, MS,[1] *Michelle Brown, PhD, MS, MLS(ASCP)*[CM] *SBB*[CM2,3*]

Laboratory Medicine 2021;52:136-140

DOI: 10.1093/labmed/lmaa061

ABSTRACT

Objective: Laboratory professionals must communicate effectively on an interprofessional team. It is the responsibility of Medical Laboratory Science (MLS) programs to teach communication. The structured communication tool Situation, Background, Assessment, and Recommendation (SBAR) is one way to promote effective communication.

Methods: Students participated in a case-based simulation activity on the importance of teamwork/communication and the use of SBAR and completed a pre/post survey on communicating interprofessionally.

Results: Students reported increased confidence and competence with interprofessional communication after the activity with 4 of 5 questions demonstrating a statistically significant increase in scores post SBAR instruction.

Conclusions: Our study demonstrates that SBAR is a suitable communication tool that can be used to increase our MLS students' confidence and competency in interprofessional communication. Educators should use this communication tool to empower MLS students to be effective members of the healthcare team.

Keywords: SBAR, simulation, medical laboratory science, communication, interprofessional, teamwork, TeamSTEPPS

It is imperative that laboratory professionals of all backgrounds have a strong voice on the multidisciplinary patient care team. This includes participation on diagnostic management teams,[1] interprofessional education,[2] and patient care simulation.[3]

It is vital that laboratory professionals communicate effectively with colleagues outside of the laboratory. Inefficient or ineffective communication among team members has already been identified as a significant contributing factor to adverse events.[4] This is not new information. In 1999, the Institute of Medicine [now the National Academies of Science, Engineering, and Medicine (NASEM)] released a report *Too Err Is Human: Building a Safer Health System*, which disclosed that as many as 98,000 people die each year from medical error. This number is now up to 250,000 deaths per year.[5] Of these deaths, 80% are due to communication errors.[4] More recently, in 2015, an NASEM report, *Improving Diagnosis in Healthcare*, firmly recommended an increased collaboration among medical professionals to decrease diagnostic error.[6]

Today's healthcare requires complex processes and systems and even well-intended, highly skilled professionals are vulnerable to error. In order to improve safety and quality and to decrease human errors, in 2005, the Agency for Healthcare Research and Quality collaborated with the Department of Defense to develop Team Strategies and Tools to Enhance Performance and Patient Safety (TeamSTEPPS). TeamSTEPPS is built upon an evidence-based framework composed of 4 teachable, learnable competencies: communication, leadership, situation monitoring, and mutual support.[7]

The tool Situation, Background, Assessment, and Recommendation/Request (SBAR) is within the communication competency of TeamSTEPPS. Some institutions have added an "I" at the beginning of SBAR, where the "I" stands for identify (**Figure 1**). Each person using the SBAR tool should first begin their interaction

[1]Department of Clinical and Diagnostic Sciences, School of Health Professions, University of Alabama at Birmingham, Birmingham, Alabama [2]Department of Health Services Administration, School of Health Professions, University of Alabama at Birmingham, Birmingham, Alabama [3]Office of Interprofessional Simulation for Innovative Clinical Practice University of Alabama at Birmingham, Birmingham, Alabama

*To whom correspondence should be addressed.
michellebrown@uab.edu

I	**Introduction** **Name and where you are calling from.**
S	**Situation** **Briefly state the patient's name, medical record number, and the reason for the call.**
B	**Background** **Give relevant clinical/technical details.**
A	**Assessment** **Put it all together (current situation, risks, and needs). What is your assessment?**
R	**Recommendation** **Be clear in what you are requesting or recommending.**

Figure 1

Standardized Communication Tool Situation, Background, Assessment, Recommendation (SBAR)

by introducing themselves. According to the American Hospital Association, SBAR is a standardized way of communicating critical information that requires immediate attention and action concerning a patient's condition. SBAR is simple and effective.[8,9]

It is the responsibility of Medical Laboratory Science (MLS) programs to teach effective communication, as much as it is their responsibility to teach microscopy, antibody identification, polymerase chain reaction (PCR), or other cognitive and psychomotor skills. Learning and practicing these skills while in school will foster strong, effective interprofessional communication in practice. The purpose of this study was to determine if the use of the standardized communication tool, SBAR, would increase student's self-perception of confidence and ability to communicate with healthcare professionals outside the laboratory.

Materials and Methods

Study Population and Data Collection

Eighteen students taking the Blood Bank course from the UAB Clinical Laboratory Science program were included in this study. Data were collected using a modified confidence scale (C-Scale) survey with 5 questions related to confidence and competence in interprofessional communication.[10]

Modifications were made to focus the questions on communication rather than using the term "task" in the original C-Scale survey. Participants could choose from a Likert scale (strongly agree, agree, neutral, disagree, and strongly disagree) for their answers to each question. The survey was administered before and after a brief, case-based simulation. A unique identifier was added to the pre- and postsurveys to allow for comparison of results before and after the simulation activity.

Case-Based Simulation

The case-based simulation was incorporated into the student's regularly scheduled course. The activity lasted about 1 h, including a 30 min didactic session on the importance of effective teamwork and communication, a 10 min case-based activity, and a 20 min structured debriefing. Objectives of the didactic session were to: 1) describe the impact of effective teamwork and communication on patient safety, 2) discuss the standardized communication tool, SBAR, and 3) apply SBAR to a common clinical situation. During this portion of the session, reports from the Health and Medicine Division of the NASEM were shared with the students. Additional literature and media was used to demonstrate the growing body of literature focusing on teamwork and communication.

After this didactic teaching, students were given a brief patient case and asked to write what they would say to the nurse during a phone call in response to the situation:

> *You receive a specimen for Monica Jones, MRN 1732937, for a PT/PTT, and it is only filled halfway. This is the second recollect you have had to contact the nurse about today for this same test on the same patient. The first time sent the blood for the PT/PTT in a purple top tube. How would you communicate the need for a recollected specimen to this nurse?*

Students shared their responses with a partner and a few students, then shared their answers with the class. After this first iteration with the simulated case, students were taught the basics of TeamSTEPPS with an emphasis on the SBAR tool. Students were provided with an opportunity for brief deliberate practice with the instructor, and then presented with the same case and asked to respond with an SBAR. Following the second iteration of SBAR use, a structured debriefing was used to explore use of the tool.

After the case-based simulation, students completed the post survey. The survey assessed the student's satisfaction and confidence with their ability to communicate effectively

Lab Medicine 2021;52;136–140 137
DOI: 10.1093/labmed/lmaa061

before and after the training. Understanding how well the students receive the training is the first step in analyzing learning effectiveness.

Data Analysis

In order to evaluate the reliability of the survey questions, Cronbach's Alpha was calculated. The data was tested and found to not be normally distributed, therefore median and range were calculated for all 5 questions pre and post scores. Additionally, the Wilcoxon signed-rank test was used to assess differences in median values for the student's scores pre and post SBAR instruction. Statistical significance was set at 0.05 and all data analysis was performed using SAS (version 9.4).

Results

The overall raw Cronbach's Alpha (reliability) score for the pre-test survey was 0.848. Based on the overall Cronbach's Alpha score and on the individual Cronbach's Alpha scores if each question was removed from the survey (range 0.762–0.837), the survey questions demonstrated good internal consistency in that, collectively, they measure the construct of communication effectiveness (**Table 1**).

All students completed both surveys (100% response rate). Based on the Wilcoxon signed-rank test, the scores increased for all questions after SBAR instruction, and there was a statistically significantly increase in the scores after SBAR instruction for 4 out of the 5 questions ($P < .007$). However, the p-value for question #2 ("I feel that I performed the activity without hesitation") was only marginally statistically significant at 0.058 (**Table 2**). The student's reported an increased perception of confidence and ability to communicate with healthcare professionals outside the laboratory after participating in the case-based simulation.

Table 1. Cronbach's Alpha Score for Pre-Survey to Assess Competence and Confidence in Interprofessional Communication of Medical Laboratory Sciences (MLS) Students (n = 18)

	Survey Question	Cronbach's Alpha if Question Deleted
Q1	I am confident that my communication would be effective	0.837
Q2	I feel that I performed the activity without hesitation	0.805
Q3	My communication would convince the nurse I was competent	0.833
Q4	I felt sure of myself as I completed the activity	0.831
Q5	I feel satisfied with my performance	0.762

$\alpha \geq 0.9$, excellent, $0.9 > \alpha \geq 0.8$ good, $0.8 > \alpha \geq 0.7$, acceptable, below 0.7 is poor. Overall Cronbach's Alpha = 0.848;

Discussion

Standardized communication has been used in nursing and allied health programs for many years,[11,12] however there is a paucity of information on incorporating it into Medical Laboratory Science programs. We reviewed the literature and found an abstract that reported on communication between the laboratory team and the end user, but no communication tools were included.[13] There were also studies looking at the clinical information communicated through electronic health records,[14,15] however this does not parallel he verbal communication we evaluated in this study. Clinicians have reported on which critical results should be reported to the care team have, but fall short of providing recommendations on how to communicate effectively.[16,17] There were also articles on building relationship outside of the laboratory, but these did not focus on tools that could be used to effectively communicate patient information.[18]

Evaluation of the standardized communication tool, SBAR, is underutilized in the laboratory profession. In addition to organizing communication, one advantage of using SBAR is that it concludes with "recommendation." This empowers laboratory staff to speak up and make requests in an organized manner. SBAR is succinct, yet provides detail. A variety of healthcare professionals use SBAR to frame patient care conversations as it has been shown to promote effective communication, improve patient safety, and increase provider satisfaction.[8,9] The laboratory should adopt the use of structured communication tools as well.

SBAR is a tool within the greater TeamSTEPPS platform. American Hospital Association is responsible for the TeamSTEPPS Master Trainer course during which participants learn about SBAR. A publication in Patient Safety and Quality Healthcare from the Chief Medical Officer of

Table 2. Difference Competence and Confidence scores in Interprofessional Communication of Medical Laboratory Sciences (MLS) Students (n = 18) Before and After Learning SBAR Communication Tool (2017)

Survey Question	Median Pre (range)	Median Post (range)	Wilcoxon Rank Test *P*-value
Q1 I am confident that my communication would be effective	4 (3–5)	5 (4–5)	0.000
Q2 I feel that I performed the activity without hesitation	5 (2–5)	5 (4–5)	0.058
Q3 My communication would convince the nurse I was competent	4 (3–5)	5 (3–5)	0.001
Q4 I felt sure of myself as I completed the activity	4 (3–5)	5 (4–5)	0.011
Q5 I feel satisfied with my performance	4 (3–5)	5 (4–5)	0.005

Data was found to not be normally distributed, therefore a non-parametric test, Wilcoxon Rank Test, was used to assess differences in median values for the student's scores pre and post SBAR instruction; SBAR = Situation, Background, Assessment, and Recommendation/Request.

Press Ganey Associates discussed SBAR as an evidence-based practice that can enhance communication skills and improve outcomes.[19] In the current study, we observed a statistically significant ($P < .05$) change in the median scores pre/post learning SBAR with 4 of the 5 questions related to confidence and competence in interprofessional communication. However, the change in median scores for question 2 were marginally significant ($P = .058$). This is anticipated since the students completed the survey after minimal practice with the SBAR tool. To increase proficiency, the program should provide opportunities to apply this new knowledge in an interprofessional setting.

The current study presents many strengths. To our knowledge, this is the first study teaching SBAR in a MLS classroom and therefore preparing students to communicate in the same manner that their peers in other health professions program are being taught to communicate. We had 100% participation in this study and utilized a survey with good internal consistency (overall Cronbach's Alpha score of 0.848).

As with any research study, our study also has limitations. First, students might seem overconfident based on the scores in the pre-survey. Since the necessity of effective interprofessional communication is commonly discussed in class, it may have influenced the student's confidence as they have been told before that effective interprofessional communication is important. Perhaps since we talk about it, students feel they have been prepared. Second, our study was conducted in one medium size MLS program in one state in the USA, therefore our results might not represent all MLS students. Lastly, we did not objectively measure how well students performed SBAR in their communication. Our data represents the subjective measure of how the students felt about their competence of using SBAR and not the objective measure of how well they performed SBAR. We acknowledge that if we are going to expect our students to communicate well interprofessionally, we need to provide adequate education and multiple opportunities for them to practice using their newly acquired skills. Interprofessional simulation is an evidence-based method to accomplish this goal.

In conclusion, our study, in a medium-sized MLS program demonstrates that SBAR is a suitable communication tool that can be used to increase MLS students' confidence and competence in interprofessional communication. SBAR is an effective and underutilized communication tool that can improve interprofessional communication between the laboratory and other healthcare professionals. Therefore, educators should incorporate standardized communication tools into MLS curricula to empower students to be effective members of the healthcare team. **LM**

Acknowledgements

We would like to thank Lucio Olivera, MS for his work on the figures and the University of Alabama at Birmingham (UAB) Biostatistics, Epidemiology and Research Design (BERD) team for their guidance in the statistical analysis.

Author's Contributions

Ana Oliveira: Data analysis, manuscript writing.

Michelle Brown: Project design, data collection, manuscript writing.

DOI: 10.1093/labmed/lmaa061

References

1. Graber ML, Rusz D, Jones ML, et al. The new diagnostic team. *Diagnosis (Berl).* 2017;4(4):225–238.
2. Brown MR, Bostic D. Strengthening the clinical laboratory with simulation-enhanced interprofessional education. *Am Soc Clin Lab Sci.* 2016;29(4):237.
3. Watts P, Langston SB, Brown M, et al. Interprofessional education: a multi-patient, team-based intensive care unit simulation. *Clin Simul Nurs.* 2014;10(10):521–528.
4. Joint Commission on Accreditation of Healthcare Organizations. Joint Commission Center for transforming healthcare releases targeted solutions tool for hand-off communications. *Jt Comm Perspect®.* 2012;32(8):1–3.
5. Makary MA, Daniel M. Medical error-the third leading cause of death in the US. *BMJ.* 2016;353:i2139.
6. National Academies of Sciences, Engineering, and Medicine. *Improving Diagnosis in Health Care.* Washington, DC: National Academies Press; 2015.
7. Weld LR, Stringer MT, Ebertowski JS, et al. TeamSTEPPS improves operating room efficiency and patient safety. *Am J Med Qual.* 2016;31(5):408–414.
8. De Meester K, Verspuy M, Monsieurs KG, Van Bogaert P. SBAR improves nurse-physician communication and reduces unexpected death: a pre and post intervention study. *Resuscitation.* 2013;84(9):1192–1196.
9. Müller M, Jürgens J, Redaèlli M, Klingberg K, Hautz WE, Stock S. Impact of the communication and patient hand-off tool SBAR on patient safety: a systematic review. *BMJ Open.* 2018;8(8):e022202.
10. Grundy SE. The confidence scale: development and psychometric characteristics. *Nurse Educ.* 1993;18(1):6–9.
11. Brust-Sisti LA, Sturgill M, Volino LR. Situation, background, assessment, recommendation (SBAR) technique education enhances pharmacy student communication ability and confidence. *Curr Pharm Teach Learn.* 2019;11(4):409–416.
12. Weinstein AR, Dolce MC, Koster M, et al. Integration of systematic clinical interprofessional training in a student-faculty collaborative primary care practice. *J Interprof Care.* 2018;32(1): 104–107.
13. Biasioli B, Maconi C, Cappelletti P, et al. Laboratory reporting of peripheral blood counts in Italy and evidence based medicine. *Int J Lab Hematol.* 2014;36(s1):30–131.
14. Brousseau G. Integrated clinical information system. *Medinfo.* 1995;8 Pt 1:459.
15. Mohammadzadeh N, Safdari R. The intelligent clinical laboratory as a tool to increase cancer care management productivity. *Asian Pac J Cancer Prev.* 2014;15(6):2935–2937.
16. Genzen JR, Tormey CA. Pathology consultation on reporting of critical values. *Am J Clin Path.* 2011;135(4):505–513.
17. Coffin CM, Spilker K, Lowichik A, et al. Critical values in pediatric surgical pathology: definition, implementation, and reporting in a children's hospital. *Am J Clin Pathol.* 2007;128(6):1035–1040.
18. Freeman V, Finley J. Building and maintaining healthy relationships across the health professions. *Am J Clin Pathol.* 2012;138(suppl_2) :A210.
19. Merlino J. Communication: a critical healthcare competency. Published 2017. Accessed 05 March 2020, Last Accessed 28 July 2020.

Cell-Derived Microparticles in Blood Products from Thalassemic Blood Donors

Egarit Noulsri, PhD,[1*] *Surada Lerdwana, BSc,*[2] *Duangdao Palasuwan, PhD,*[3] *Attakorn Palasuwan, PhD*[3*]

Laboratory Medicine 2021;52:150-157

DOI: 10.1093/labmed/lmaa041

ABSTRACT

Objective: To determine the number of cell-derived microparticles (MPs) in blood products obtained from donors who have thalassemia.

Methods: Packed red blood cells (PRBCs), plasma, and platelet concentrate (PC) were prepared according to routine procedures. We used flow cytometry to quantitate the concentration of MPs.

Results: The results of a comparison of MP levels in unprocessed whole blood showed that the concentration of all MPs in the donors without thalassemia trait (n = 255) was higher than in donors with thalassemia trait (n = 70). After processing, increased concentrations of MPs were documented in both groups. Among the blood components, PRBC showed higher platelet-derived MP concentrations in donors with thalassemia than in donors without thalassemia. However, PC showed higher concentrations of total MPs in donors without thalassemia than in donors with that condition.

Conclusions: Our results suggest little influence of thalassemia-trait status on changes in MP concentrations in blood components.

Keywords: β-thalassemia, transfusion donor, microparticle, quantitation, flow cytometry, laboratory

Cell-derived microparticles (MPs) are small vesicles released from various cells on activation, on injury, or when undergoing apoptosis.[1] These MPs are characterized based on their intracellular origin and are released by red blood cell–derived microparticles (RMPs), platelet-derived microparticles (PMPs), leukocyte-derived microparticles (LMPs), and endothelial cell–derived microparticles (EMPs).[2] Study results[3–5] have suggested that MPs can participate in the coagulation pathway by expressing negatively charged phospholipids, phosphatidylserine (PS), and tissue factor (TF) on their surface membranes. Other study reports[6,7] have also suggested that MPs can modulate immune response.

In transfusion medicine, MPs have been suggested as contributing to post-transfusion complications (for example, transfusion-induced thrombotic complications and transfusion-related acute lung injury [TRALI]).[8–11] Further study results[12–14] have suggested that MP levels are related to the quality of blood products. These results suggest that transfusions containing increased numbers of MPs might contribute to deep vein thrombosis (DVT), pulmonary embolism, and TRALI. These MP-related post-transfusion complications might be minimized or prevented by several proposed approaches, including routine screening for MPs in blood products and filtering blood components after preparation.[15–17] Given the roles of MPs in blood transfusion, it is necessary to examine the factors associated with

Abbreviations:

MP, microparticle; RMP, red blood cell–derived microparticle; PMP, platelet-derived microparticle; LMP, leukocyte-derived microparticle; EMPs, endothelial cell–derived microparticles; PS, phosphatidylserine; TF, tissue factor; TRALI, transfusion-related acute lung injury; DVT, deep vein thrombosis; BC, buffy coat; RBC, red blood cell; PRBC, packed red blood cell; PC, platelet concentrate; PPP, platelet-poor plasma; FFP, fresh frozen plasma; SAGM, saline, adinine, glucose, and mannitol; WBCs, white blood cells; PCR, polymerase chain reaction; PBS, phosphate-buffered saline; RT, room temperature; FSC, forward scatter; SSC, side scatter; FL, fluorescent; HbE, hemoglobin E; SEA, Southeast Asian; Hb, hemoglobin; MCV, mean corpuscular volume; MCH, mean corpuscular hemoglobin; MCHC, mean corpuscular hemoglobin concentration; RDW, red-blood-cell distribution width; HCT, hematocrit

[1]Research Division, Faculty of Medicine Siriraj Hospital, Mahidol University, Bangkok, Thailand, [2]Biomedical Research Incubator Unit, Faculty of Medicine Siriraj Hospital, Mahidol University, Bangkok, Thailand, [3]Oxidation in Red Cell Disorders and Health Task Force, Department of Clinical Microscopy, Faculty of Allied Health Sciences, Chulalongkorn University, Bangkok, Thailand

*To whom correspondence should be addressed.
egarit.nou@mahidol.ac.th

the release of MPs in blood components prepared in routine transfusion laboratories.

Several factors are suggested as being associated with increased levels of MPs in blood components. The results of a study by Noulsri et al[15] showed different concentrations of PMPs in platelet products prepared using platelet-rich plasma, buffy coat (BC), and apheresis instruments, suggesting the effects of blood-component preparation procedures on the release of MPs. The results of further study of the factors causing increased levels of MPs in blood components[18] have also suggested that donor factors and processing and storage are associated with the concentrations of MPs in blood components prepared in routine transfusion laboratories. Regarding transfusion donors, those who have *asymptomatic thalassemia*, an inherited red blood cell (RBC) disorder, generally are eligible to donate for transfusion.[19,20] Given that there is a high prevalence of donors with thalassemia in certain areas of our country, Thailand, the variability associated with donor-provided abnormal RBCs could be attributed to changes in MP levels during blood-component preparation. However, little information is available regarding the levels of MPs in the blood products prepared from donors with thalassemia.

In the current study, we screened transfusion donors to identify those who had thalassemia and quantitated the numbers of MPs in their blood products, including packed red blood cells (PRBCs), platelet concentrate (PC), and plasma. We did so because we believe that knowing the factors that contribute to the release of MPs in blood products is important for managing quality in transfusion laboratories.

Materials and Methods

Reagents and Antibodies

We obtained fluorescent conjugated monoclonal antibodies, annexin V-FITC, CD41-APC, CD235a-PE, CD45-PerCP, and 10 × annexin V-binding buffer for use in our study. CountBright beads were purchased from Thermo Fisher Scientific Inc. In addition, we purchased polystyrene 12-mm × 75-mm tubes and size-standard beads of 1 µm for use in our study.

Transfusion Donors, Specimen Collection, and Complete Blood Count Analysis

This study was approved by the Institutional Review Board of Siriraj Hospital, Mahidol University School of Medicine, Bangkok, Thailand (COA no.359/2016). Written consent was obtained from donors after the procedure was explained in detail, including the time it would take and its possible hazards and benefits. After informed consent was obtained, blood specimens were collected and processed using the standard procedure of the Department of Transfusion Medicine, Faculty of Medicine, Siriraj Hospital, Mahidol University.

The whole blood specimens were drawn into blood-collection tubes containing 3.2% sodium citrate and then subjected to complete blood count determination using a Siemens ADVIA 2120i hematology analyzer (Siemens Healthcare GmbH), which was routinely calibrated as recommended by the manufacturer.

Blood Component Preparation and Specimen Collection

Figure 1 summarizes the overall processes of blood-component preparation and specimen collection. Briefly, whole-blood units were collected into triple blood-collecting systems (JMS Triple Blood Bag; CPD-SAGM Solution; JMS Singapore Pte. Ltd.). Then, each whole-blood unit was centrifuged at 3100*g* for 10 minutes to separate it into 3 layers. The top layer was the platelet-poor plasma (PPP), which was transferred to a satellite bag and stored as fresh frozen plasma (FFP) in a freezer at 20°C or less.

The bottom layer was the PRBCs, which were transferred to another bag attached. A solution of saline, adinine, glucose, and mannitol (SAGM) was added to the RBCs, and it was stored in a cold room at 4°C. The middle layer was the BC, which contains platelets and white blood cells (WBCs). Briefly, 4 bags of the BC from the same ABO blood group were pooled together and centrifuged at *g* for 6 minutes at 22°C, along with 1 empty satellite bag. The platelet concentrate was transferred into an empty platelet-storage bag, and the tubing was sealed.

Specimens were taken from heat-sealed segments immediately after preparation and before storage. The contents of each segment were transferred to a 0.5-mL microcentrifuge tube and then mixed. Next, the specimens were analyzed

DOI: 10.1093/labmed/lmaa041

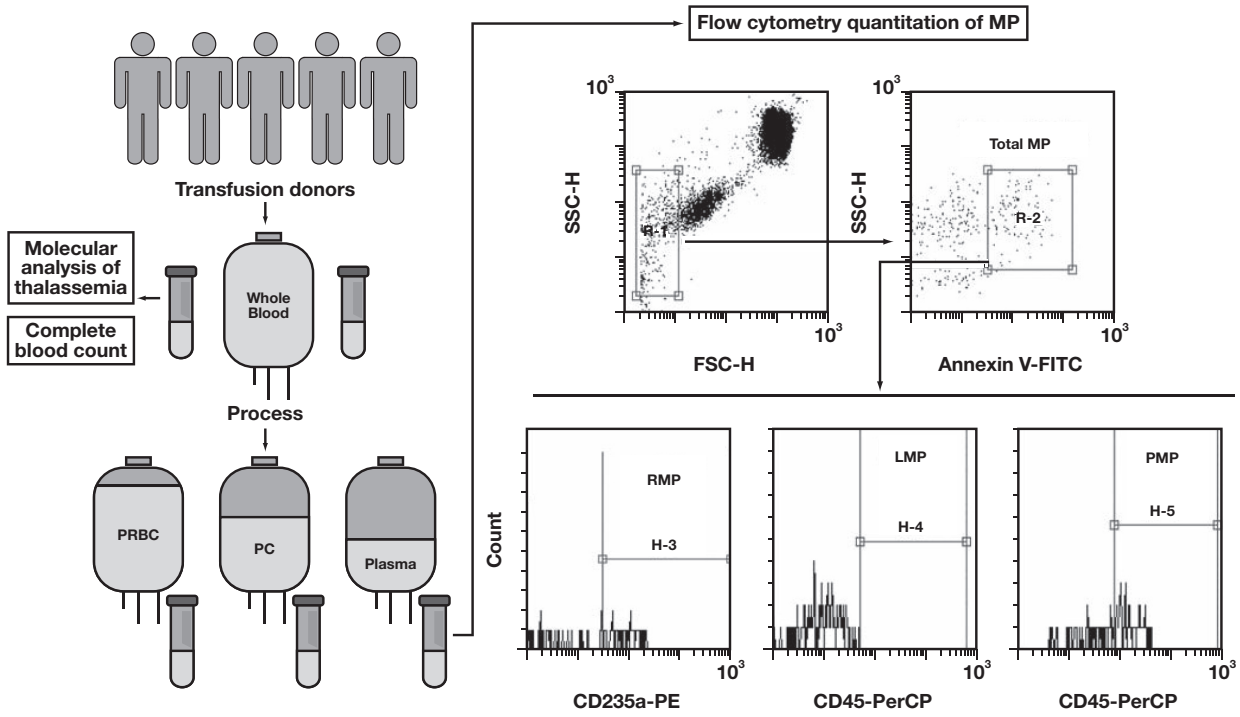

Figure 1

Schematic diagram summarizing the overall experimental design. On collection from transfusion donors, whole blood units are processed according to routine laboratory procedures to prepare packed red blood cells (PRBCs), platelet concentrates (PCs), and fresh plasma. Specimens of unprocessed donor whole blood are subjected to molecular characterization of thalassemia and hematology analysis. The specimens from whole blood and blood products are evaluated using flow cytometry to determine the concentrations of microparticles (MPs) and their origins. For quantitation using flow cytometry, the MP gate is first identified according to forward scatter (FSC) and side scatter (SSC) characteristics (R-1). Then, the gated MPs are analyzed on annexin V vs SSC to determine MPs that test positive for annexin V (R-2), and these populations are defined as total MPs. The MPs that test positive for annexin V are plotted on the histogram of CD235a-PE, CD45-PerCP, and CD41a-APC to determine the numbers of red blood cell–derived microparticles (RMPs) (H-3), leukocyte-derived microparticles (LMPs) (H-4), and platelet-derived microparticles (PMPs) (H-5), respectively.

for concentrations of MPs using flow cytometry within 2 hours after the completion of blood-component processing.

Thalassemia Screening

Hemoglobin typing was performed using HPLC (Variant Hemoglobin Testing System; Bio-Rad Laboratories, Inc.). Multiplex Gap–polymerase chain reaction (PCR) was used to detect α -globin gene variants. Reverse dot-blot hybridization was used to detect β-globin gene mutations.

Flow Cytometry Analysis of MPs

The specimens were diluted to 1:100 using phosphate-buffered saline (PBS). Then, 5 µL of each diluted specimen was incubated with 3 µL of annexin V-FITC, 5 µL of CD41-APC, 5 µL of CD235a-PE, 5 µL of CD45-PerCP, and 20 µL of 1 × annexin-V binding buffer for 15 minutes in the dark at room temperature (RT). Next, 300 µL of annexin-V binding buffer was added to the tube. We analyzed the stained specimens using a FACSCalibur flow cytometer (Becton, Dickinson and Company) equipped with dual 75-mW blue lasers (488 nm) and 40-mW red lasers (640 nm).

The forward scatter (FSC), side scatter (SSC), and fluorescent (FL) parameters were set at logarithmic scale. The threshold was set at FSC to exclude debris and noise. The data were acquired and analyzed using CellQuest software version 4.0 (Becton, Dickinson and Company). The flow cytometer was optimized and calibrated using CaliBrite beads and FACSComp software (Becton, Dickinson and

Company). The MP gate was established on FSC vs SSC according to 1-µm size standard beads (**Figure 1**). The annexin V vs SSC dot plot was used to identify MPs that tested positive for annexin V from the previously gated MPs. The events of RMPs, PMPs, and LMPs were determined on histogram plots of CD235a-PE, CD41a-APC, and CD45-PerCP, respectively. The concentrations of MPs per microliter were calculated as described previously.[17]

Statistical Analysis

The data were analyzed and graphed using GraphPad Prism software, version 5.0.1 (GraphPad Software). All results were expressed as mean, SE, and range. Linear regression was used to determine the association between measured and expected MP concentrations. Statistical significance between the 2 groups was determined using a Student t-test. A *P*-value of less than .05 was considered statistically significant.

Results

Characteristics of Donors with Thalassemia and Hematological Parameters

Our results showed that the prevalence of donors with thalassemia was 21.5%. The mean (SE) ages of the donors with and without thalassemia were 34.9 (11.9) and 36.3 (11.8) years, respectively. The most common type of thalassemia was hemoglobin E (HbE)–related abnormality (14.4%). Also, 8.6% of α-thalassemia abnormality was associated with 3.7-kb deletion, 4.2-kb deletion, and Southeast Asian (SEA) deletion. **Table 1** summarizes the hematology parameters of the donors with and without thalassemia. Overall, the hematology indices of the donors with thalassemia differed significantly from those of the donors without that condition. These parameters were RBCs, hemoglobin (Hb), mean corpuscular volume (MCV), mean corpuscular hemoglobin (MCH), mean corpuscular hemoglobin concentration (MCHC), and red-blood-cell distribution width (RDW). In contrast, there were no significant differences in HCT and WBCs between the 2 groups.

Accuracy and Reliability of MP Quantitation Approach

To address the accuracy and reliability of our MP quantitation, the whole-blood specimens were diluted to 1:10, 1:100, 1:1000, 1:10000, and 1:100000. The total number of platelets in each diluted specimen was determined. The results showed r^2 of 0.98 and a *P* value of less than .001 between the measured concentrations of platelet and their expected values (**Figure 2**).

To establish the MP gating, we incubated whole-blood specimens with A23187 to induce MP release. Then,

Table 1. Hematology Parameters of Tranfusion Donors with and without Thalassemia

Analyte	Mean (SE) (Minimum–Maximum)		*P* Value
	Donors with Thalassemia (*n* = 70)	Donors without Thalassemia (*n* = 255)	
RBCs (× 10^6/µL)	4.8 (0.5) (3.9–6.3)	5.4 (0.5) (4.3–7.1)	<.001[a]
Hemoglobin (g/dL)	13.6 (0.9) (11.5–15.6)	13.9 (1.2) (11.2–18.4)	.02[a]
Hematocrit (%)	41.6 (2.8) (35.9–47.4)	42.3 (3.5) (35.3–53.7)	.12
MCV (fL)	76.7 (5.8) (57.2–86.5)	87 (4.8) (60.9–95.7)	<.001[a]
MCH (pg)	25.1 (1.9) (19.5–28.5)	28.7 (1.8) (18.4–32.9)	<.001[a]
MCHC (g/dL)	32.6 (0.8) (30.1–34.6)	32.9 (0.9) (30.2–35.9)	.01[a]
RDW (%)	14.8 (1) (12.7–17.7)	13.6 (0.9) (11.8–17.3)	<.001[a]
WBCs (× 10^3/µL)	7.5 (1.7) (4.2–12.5)	7.2 (1.6) (3.7–13.9)	.21

RBCs, red blood cells; MCV, mean corpuscular volume; MCH, mean corpuscular hemoglobin; MCHC, mean corpuscular hemoglobin concentration; RDW, red-blood-cell distribution width; WBC, white blood cells.
[a]*Indicates a significant difference between the donors who have and do not have thalassemia.*

Lab Medicine 2021;52;150–157
DOI: 10.1093/labmed/lmaa041

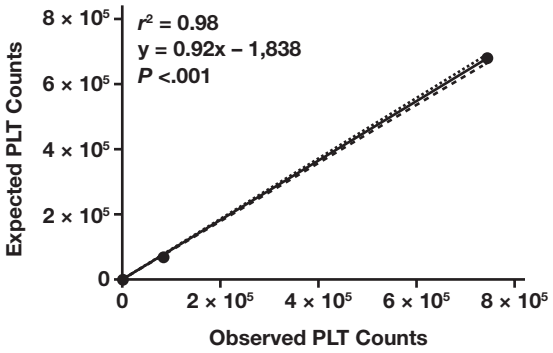

Figure 2

Regression analysis of observed platelet counts (*x*-axis) and expected platelet counts (*y*-axis) according to dilutions.

the treated specimens and untreated control specimens were analyzed using flow cytometry. The percentage of MPs in whole blood treated with A23187 was significantly higher than in the control specimens (33% vs 6%). To address the specificity of the annexin V binding for the identification of MPs, whole-blood specimens were incubated with A23187 to induce MP release. Then, the treated specimens were determined for MP quantitation in the presence and absence of calcium buffer. Our results showed that the percentages of MPs with and without 1 × annexin V-binding buffer were 47% and less than 1%, respectively.

MP Levels in Unprocessed Whole Blood and Blood Products from Donors with and without Thalassemia

Comparison of MP levels in unprocessed whole blood showed that the levels of MPs, RMPs, and PMPs in donors without thalassemia were significantly higher than those levels in donors with the condition (**Table 2**). However, we observed no difference between the groups in the concentrations of LMPs, which were lower than for the other components quantitated. The data also showed that RBCs were the main source of MPs in unprocessed whole blood.

In the blood products, the analysis of PRBCs showed that the concentration of PMPs was significantly higher in donors with thalassemia than in those without the condition. In contrast, analysis of the PC showed that the concentration of total MPs was higher in donors without thalassemia than in donors with the condition. Examination of the fresh plasma showed no significant difference between the groups of donors in concentrations of total MPs, PMPs, and RMPs.

Discussion

In the current cross-sectional study, we identified transfusion donors who had thalassemia and quantitated their MP concentrations in a routine transfusion laboratory. To our knowledge, the current study is the first reported in the literature to analyze the effects on the release of MPs of blood donors with thalassemia. The results suggest that the thalassemia status of blood donors has little effect on the levels of MPs in the blood products prepared in such laboratories.

In the current study, the prevalence of donors with thalassemia was 21.5%. However, Nuinoon et al[20] examined the frequency of the α -thalassemia 1 trait, the β -thalassemia trait, and the HbE-related syndrome in southern Thailand. They found that the overall frequency of blood donors with thalassemia was 12.9% and that the highest frequency was that of heterozygous HbE without α -thalassemia (5.2%). These findings indicate that in Thailand, the frequency of transfusion donors with thalassemia varies in geographic distribution. Our findings showed that the RDW was higher in donors with than in those without thalassemia, suggesting a variation in size of the RBCs in donors with thalassemia. This finding was similar to those of previous studies, which showed increased RDW values in patients with asymptomatic thalassemia and that the ranges of RDW were similar to those observed in our study.[21,22] Also, our findings showed no difference between the groups in the number of WBCs. This finding may be explained by the pathophysiology of asymptomatic thalassemia disease, which shows no abnormality of WBCs in number or function.[23]

Our results regarding fresh whole blood showed that the total numbers of MPs, RMPs, and PMPs in donors without thalassemia were higher than in donors with thalassemia, suggesting that asymptomatic thalassemia has less effect on MP release. After preparation, we found a significant change in only 2 of the 12 parameters measured. First, the numbers of PMPs were higher in PRBCs prepared from donors with thalassemia than in donors without the condition. Second, the total numbers of MPs were higher in PC prepared from donors without than

Table 2. Total Concentrations of Analytes in the Fresh Whole Blood, PRBCs, PC, and FP of Tranfusion Donors with and without Thalassemia

Analyte	Mean (SE) (Minimum–Maximum)		*P* Value
	Donors with Thalassemia (*n* = 70)	Donors without Thalassemia (*n* = 255)	
Fresh Whole Blood			
Total MPs	24,180 (833) (11,643–46,736)	27,590 (697) (6930–86,667)	.02[a]
RMPs	11,200 (386) (4990–20,203)	12,690 (281) (3659–33,180)	.01[a]
PMPs	9,076 (402) (2880–17,008)	11,000 (372) (640–49,770)	.01[a]
LMPs	256 (38) (0-1199)	292 (31) (0-5440)	.57
PRBC			
Total MPs	36,460 (5322) (15,119–383,413)	32,740 (1198) (2520–212,800)	.30
RMPs	18,200 (804) (7714–50,400)	20,080 (476) (1890–56,000)	.06
PMPs	13,270 (4929) (1830–358,773)	8,460 (758) (610–173,973)	<.001[a]
LMPs	239 (56) (0–1000)	216 (19) (0–2016)	.66
PC			
Total MPs	26,990 (1486) (14,720–56,324)	35,170 (1709) (2100–139,153)	.02[a]
RMPs	9500 (346) (5620–14,784)	10,170 (273) (1680–22,017)	.25
PMPs	11,750 (990) (4092–41,768)	14,150 (667) (2773–70,737)	.09
LMPs	237 (44) (0–1027)	241 (25) (0–1943)	.95
FP			
Total MPs	100,200 (12,090) (17,269–527,218)	203,800 (33,870) ($14,490–5.9 \times 10^6$)	.12
RMPs	12,110 (729) (2560–31,342)	10,890 (348) (2,940–58,240)	.12
PMPs	56,330 (8307) (4872–400,280)	137,000 (25,540) ($3840–3 \times 10^6$)	.11
LMPs	260 (48) (0–2033)	212 (22) (0–2439)	.34

PRBCs, packed red blood cells; PC, platelet concentrate; FP, fresh plasma; MPs, microparticles; RMPs, red blood cell–derived microparticles; PMPs, platelet-derived microparticles; LMPs, leukocyte-derived microparticles.
[a]*Indicates a significant difference between the donors with and without thalassemia.*

from donors with thalassemia. This discrepancy suggests that asymptomatic thalassemia has less of an effect on MP production than other variables. Our findings also showed that the concentration of MPs was increased after preparation processes. In particular, the concentration of total MPs was increased as much as 4-fold and 6-fold in plasma prepared from donors with and without thalassemia, respectively. This finding suggests an effect of blood processing on MP release in blood products. Another study[15] quantitated the MP concentrations in various platelet products; its findings included different MP levels in platelet components prepared using different processes. Also, our data showed that RMPs were the major MP population in unprocessed whole blood and PRBCs. However, PMPs were the main MP population in PCs and plasma, suggesting that the origin of MPs is related to the cell concentrations in each blood component.

The findings of a previous study[24] determined the MPs in patients who had hemoglobinopathic manifestations,

DOI: 10.1093/labmed/lmaa041

including thalassemia. Those results showed that the number of MPs in thalassemia intermedia were increased 4-fold, compared with the controls. The results of another investigation[25] demonstrated a significantly increased number of MPs in patients with splenectomized β -thalassemia and showed that this increase was inversely proportional to the levels of hemoglobin, suggesting an association between MPs and severe anemia in β -thalassemia disease.

In our study, the Hb levels in the donors with thalassemia were similar to those in the donors without the condition, suggesting that no anemia is present in donors with thalassemia. However, our further experimentation demonstrated that the levels of total MPs, RMPs, and PMPs in the donors without thalassemia were higher than those in the donors with the condition. This finding might be explained by the differences in the number of donors with thalassemia (n = 70) and of the donors who do not harbor it (n = 255). Regarding the number of MPs, a study examining this number in patients with β -thalassemia found that they had an average of 74,000 particles per µL, whereas the number of MPs in healthy volunteers was 50,000 particles per µL.[26] In the current study, we found the average number of MPs to be 24,000 particles per µL in donors with thalassemia and 27,000 per µL in donors without thalassemia. Although flow cytometry was used to quantitate the MPs, the lower MP concentrations found in our study might be due to the difference in gating strategies and the variability of the cytometer instrument used.

The findings of previous studies[27,28] have characterized the molecular mechanisms of MP release and have shown that the intracellular influx of Ca^{2+} contributes to this mechanism. The results of a number of in-vitro studies[29–31] have also shown that A23187 can induce MP release through this mechanism. In the current study, we stimulated the specimens with A23187 to induce MP release. These specimens were used to establish the MP gating and to address its reliability and accuracy. First, our dilution experiment showed a good correlation between the observed and expected concentrations of platelets. Second, quantitation of the MPs in whole blood treated with A23187 showed that the concentration of MPs was increased more than 100% compared to that in the control specimens. Finally, the number of total MPs decreased less than 1% in the gating without annexin V-binding buffer, suggesting the specificity of annexin V-binding buffer for detecting MPs. Altogether, these data suggest the optimization of our flow-cytometry analysis of MPs in the current study.

The current study had several limitations. Of the 325 transfusion donors, only 70 (21.5%) had thalassemia. Further, nearly all the components were sent to transfusion recipients within 2 weeks after preparation. Given this high requirement, a low number of PRBCs from donors with thalassemia were available with which to investigate the effects of storage on MP release in blood products prepared from donors with thalassemia. Also, there were no clinical data on therapeutic efficiency or complications after transfusion. Further clinical study should be conducted to address whether there is any difference in therapeutic efficacy between the PRBCs from donors with and without thalassemia by using the conventional markers, including post-transfusion Hb/HCT, and the incidence of post-transfusion reactions and MPs.

Conclusions

Our data demonstrated no association between donor with thalassemia and the levels of MPs in blood components. This finding emphasizes the role of individual donor variability and blood-component processing on the heterogeneity of MPs in blood products. **LM**

Acknowledgements

This research was funded by Chulalongkorn University (CU-GES-60-05-30-01). The authors thank the Faculty of Medicine Siriraj Hospital, Mahidol University, for supporting this research project.

References

1. Lötvall J, Hill AF, Hochberg F, et al. Minimal experimental requirements for definition of extracellular vesicles and their functions: a position statement from the International Society for Extracellular Vesicles. *J Extracell Vesicles.* 2014;3:26913.
2. Yáñez-Mó M, Siljander PR-M, Andreu Z, et al. Biological properties of extracellular vesicles and their physiological functions. *J Extracell Vesicles.* 2015;4:27066.
3. Lacroix R, Vallier L, Bonifay A, et al. Microvesicles and cancer associated thrombosis. *Semin Thromb Hemost.* 2019;45(6):593–603.

4. Noulsri E, Ardsiri S, Lerdwana S, Pattanapanyasat K. Comparison of phosphatidylserine-exposing red blood cells, fragmented red blood cells and red blood cell-derived microparticles in β-thalassemia/HbE patients. *Lab Med.* 2019;50(1):47–53.
5. Noulsri E, Lerdwana S, Palasuwan D, Palasuwan A. Quantitation of phosphatidylserine-exposing platelets in platelet concentrate prepared in routine blood transfusion laboratory. *Transfus Apher Sci.* 2020;59(1):102598.
6. Robbins PD, Dorronsoro A, Booker CN. Regulation of chronic inflammatory and immune processes by extracellular vesicles. *J Clin Invest.* 2016;126(4):1173–1180.
7. Ratajczak J, Wysoczynski M, Hayek F, Janowska-Wieczorek A, Ratajczak MZ. Membrane-derived microvesicles: important and underappreciated mediators of cell-to-cell communication. *Leukemia.* 2006;20(9):1487–1495.
8. Hashemi Tayer A, Amirizadeh N, Ahmadinejad M, Nikougoftar M, Deyhim MR, Zolfaghari S. Procoagulant activity of red blood cell-derived microvesicles during red cell storage. *Transfus Med Hemother.* 2019;46(4):224–230.
9. Aung HH, Tung JP, Dean MM, Flower RL, Pecheniuk NM. Procoagulant role of microparticles in routine storage of packed red blood cells: potential risk for prothrombotic post-transfusion complications. *Pathology.* 2017;49(1):62–69.
10. Xie RF, Hu P, Li W, et al. The effect of platelet-derived microparticles in stored apheresis platelet concentrates on polymorphonuclear leucocyte respiratory burst. *Vox Sang.* 2014;106(3):234–241.
11. Xie R, Yang Y, Zhu Y, et al. Microparticles in red cell concentrates prime polymorphonuclear neutrophils and cause acute lung injury in a two-event mouse model. *Int Immunopharmacol.* 2018;55:98–104.
12. Noulsri E. Quantitation of cell-derived microparticles in blood products and its potential applications in transfusion laboratories [online ahead of print]. *Lab Med*. 2020; doi: 10.1093/labmed/lmz100.
13. Amiral J, Seghatchian J. Measurement of extracellular vesicles as biomarkers of consequences or cause complications of pathological states, and prognosis of both evolution and therapeutic safety/efficacy. *Transfus Apher Sci.* 2016;55(1):23–34.
14. Seghatchian J, Amiral J. Unresolved clinical aspects and safety hazards of blood derived- EV/MV in stored blood components: from personal memory lanes to newer perspectives on the roles of EV/MV in various biological phenomena. *Transfus Apher Sci.* 2016;55(1):10–22.
15. Noulsri E, Udomwinijsilp P, Lerdwana S, Chongkolwatana V, Permpikul P. Differences in levels of platelet-derived microparticles in platelet components prepared using the platelet rich plasma, buffy coat, and apheresis procedures. *Transfus Apher Sci.* 2017;56(2):135–140.
16. Chou ML, Lin LT, Devos D, Burnouf T. Nanofiltration to remove microparticles and decrease the thrombogenicity of plasma: in vitro feasibility assessment. *Transfusion.* 2015;55(10):2433–2444.
17. Sugawara A, Nollet KE, Yajima K, Saito S, Ohto H. Preventing platelet-derived microparticle formation–and possible side effects-with prestorage leukofiltration of whole blood. *Arch Pathol Lab Med.* 2010;134(5):771–775.
18. Noulsri E, Palasuwan A. Effects of donor age, donor sex, blood-component processing, and storage on cell-derived microparticle concentrations in routine blood-component preparation. *Transfus Apher Sci.* 2018;57(4):587–592.
19. Francis RO, Jhang JS, Pham HP, Hod EA, Zimring JC, Spitalnik SL. Glucose-6-phosphate dehydrogenase deficiency in transfusion medicine: the unknown risks. *Vox Sang.* 2013;105(4):271–282.
20. Nuinoon M, Kruachan K, Sengking W, Horpet D, Sungyuan U. Thalassemia and hemoglobin E in southern thai blood donors. *Adv Hematol.* 2014;2014:932306.
21. Roth IL, Lachover B, Koren G, Levin C, Zalman L, Koren A. Detection of β-thalassemia carriers by red cell parameters obtained from automatic counters using mathematical formulas. *Mediterr J Hematol Infect Dis.* 2018;10(1):e2018008.
22. Chandra H, Shrivastava V, Chandra S, Rawat A, Nautiyal R. Evaluation of platelet and red blood cell parameters with proposal of modified score as discriminating guide for iron deficiency anemia and β-thalassemia minor. *J Clin Diagn Res.* 2016;10(5):EC31–EC34.
23. Nienhuis AW, Nathan DG. Pathophysiology and clinical manifestations of the β-thalassemias. *Cold Spring Harb Perspect Med.* 2012;2(12):a011726.
24. Westerman M, Pizzey A, Hirschman J, et al. Microvesicles in haemoglobinopathies offer insights into mechanisms of hypercoagulability, haemolysis and the effects of therapy. *Br J Haematol.* 2008;142(1):126–135.
25. Pattanapanyasat K, Noulsri E, Fucharoen S, et al. Flow cytometric quantitation of red blood cell vesicles in thalassemia. *Cytometry B Clin Cytom.* 2004;57(1):23–31.
26. Pattanapanyasat K, Gonwong S, Chaichompoo P, et al. Activated platelet-derived microparticles in thalassaemia. *Br J Haematol.* 2007;136(3):462–471.
27. Morel O, Jesel L, Freyssinet JM, Toti F. Cellular mechanisms underlying the formation of circulating microparticles. *Arterioscler Thromb Vasc Biol.* 2011;31(1):15–26.
28. Morel O, Morel N, Freyssinet JM, Toti F. Platelet microparticles and vascular cells interactions: a checkpoint between the haemostatic and thrombotic responses. *Platelets.* 2008;19(1):9–23.
29. Bassé F, Gaffet P, Bienvenüe A. Correlation between inhibition of cytoskeleton proteolysis and anti-vesiculation effect of calpeptin during A23187-induced activation of human platelets: are vesicles shed by filopod fragmentation? *Biochim Biophys Acta.* 1994;1190(2):217–224.
30. Pasquet JM, Dachary-Prigent J, Nurden AT. Microvesicle release is associated with extensive protein tyrosine dephosphorylation in platelets stimulated by A23187 or a mixture of thrombin and collagen. *Biochem J.* 1998;333 (Pt 3):591–599.
31. Pasquet JM, Dachary-Prigent J, Nurden AT. Calcium influx is a determining factor of calpain activation and microparticle formation in platelets. *Eur J Biochem.* 1996;239(3):647–654.

DOI: 10.1093/labmed/lmaa041

How Reliable Is Automated Urinalysis in Acute Kidney Injury?

Vani Chandrashekar, MD, DNB,[1,*] *Anil Tarigopula, MD, DNB,*[2] *Vikram Prabhakar, DCP, DNB,*[1]

Laboratory Medicine 2021;52:e30-e38

DOI: 10.1093/labmed/lmaa069

ABSTRACT

Objective: Examination of urine sediment is crucial in acute kidney injury (AKI). In such renal injury, tubular epithelial cells, epithelial cell casts, and dysmorphic red cells may provide clues to etiology. The aim of this study was to compare automated urinalysis findings with manual microscopic analysis in AKI.

Methods: Samples from patients diagnosed with AKI and control patients were included in the study. Red blood cells, white blood cells, renal tubular epithelial cells/small round cells, casts, and pathologic (path) cast counts obtained microscopically and by a UF1000i cytometer were compared by Spearman test. Logistic regression analysis was used to assess the ability to predict AKI from parameters obtained from the UF1000i.

Results: There was poor correlation between manual and automated analysis in AKI. None of the parameters could predict AKI using logistic regression analysis. However, the increment in the automated path cast count increased the odds of AKI 93 times.

Conclusion: Automated urinalysis parameters are poor predictors of AKI, and there is no agreement with manual microscopy.

Keywords: urinalysis, acute kidney injury, UF1000i, cast, pathological cast, urine microscopy

Acute kidney injury (AKI) is encountered in hospitalized and critically ill patients.[1] It results from sudden loss of renal excretory functions and can occur in the context of other illnesses. Etiologies for AKI can be prerenal, intrinsic renal, or postrenal.[1] Microscopic findings in urine from patients with AKI vary from a bland urine sediment with few hyaline casts in prerenal AKI to muddy brown casts, coarse granular casts, epithelial cell casts, and renal tubular epithelial cells (RTEC) in renal AKI. Other findings indicative of glomerular pathology include hematuria, red cell fragments, red cell casts, and white cell casts.[1-3]

Urine microscopy has been extensively studied and scored for prediction of acute tubular necrosis, differentiating septic from aseptic AKI, predicting prognosis, and even predicting dialysis.[4-8] Perazella, Coca, Kanbay, et al[4] identified a scoring system incorporating microscopic findings of granular casts and RTEC to differentiate prerenal AKI from renal AKI. Using this scoring system, they were able to predict a worsening of the stages of AKI. With the advent of automation in urinalysis, automated analyzers based on flow cytometry and digital microscopy have replaced time-consuming microscopic evaluation and reagent strip analysis.[9] Studies have correlated automated analyzers with microscopy, and correlations have varied from 0.49 to 0.96 for the various formed elements in urine.[9-11]

There is limited literature regarding the use of automated urine microscopy in AKI.[12,13] Hence, we undertook this study to evaluate the role of the UF1000i cytometer in predicting AKI and to compare automated urinalysis with manual microscopy in patients with AKI.

Abbreviations:

AKI, acute kidney injury; path, pathologic; RTEC, renal tubular epithelial cells; RBCs, red blood cells; WBCs, white blood cells; src, small round cells; IQR, interquartile range; AUC, area under the curve.

[1]Department of Hematology, Clinical pathology, Apollo hospitals, Chennai, India, [2]Department of Centralised Molecular Diagnostics, Apollo Hospitals, Chennai, India

*To whom correspondence should be addressed.
drvani001@gmail.com

Materials and Methods

Urine samples from patients clinically diagnosed with AKI based on the criteria of the Kidney Disease: Improving Global Outcomes working group were included in the

study.[14] According to these criteria, AKI is diagnosed when there is an increase in serum creatinine ≥0.3 mg/dL (≥26.5 μmol/L) within 48 hours or an increase in serum creatinine ≥1.5 times baseline that is known or presumed to have occurred within the prior 7 days, or when urine volume is ˂0.5 mL/kg/h for 6 hours.[14] Patients with AKI due to prerenal as well as renal causes were included in the study group. Urine samples from patients who were not suspected to have AKI (per the working group criteria) were included as control patients. Urine samples which were less than 5mL and samples submitted after one hour of voiding were excluded from the study.

Urine samples from control patients and patients with AKI were centrifuged in graded conical tubes at 1500 rpm for 5 minutes to obtain urine sediment for microscopy. The supernatant was discarded, leaving 0.5 mL of urine sediment. The tube was then flicked, and 1 drop of sediment was placed on a clean slide and coverslipped. The slide was then observed under a bright field microscope. Ten high-power fields (high power field [hpf] 400×), including the edges of the coverslip, were examined to obtain an average numerical score for red blood cells (RBCs), white blood cells (WBCs), casts, and RTEC/hpf. The RBCs were identified as circular or crenated discs, WBCs were identified by cytoplasmic granulation and lobed nucleus, and RTEC were identified by their varied shape—cuboidal to oval to rectangular—with densely granulated cytoplasm and eccentric nuclei. Casts were identified as hyaline when they were cylindrical and acellular, identified as granular when they contained multiple fine or coarse granules, and termed as RBCs, WBCs, and epithelial cell casts when they contained RBCs, WBCs, or RTEC, respectively. The averages of the granular and cellular casts were summed to obtain a manual pathologic (path) cast score. For conversion from hpf to per microliter, the following formula was used: cells counted/microliter = concentration of urine sample × average number of cells or casts counted × chamber volume (volume of sediment between coverslip and slide/number of fields observed; concentration = 5, chamber volume = 0.004 mL, number of fields counted = 10).

The Sysmex UF1000i (Sysmex Co, Japan), is a fluorescence flow cytometer and classifies cells and other formed elements as bacteria, WBCs, RBCs, yeast-like cells, epithelial cells, crystals, casts, path casts (nonhyaline casts), spermatozoa, small round cells (src, which include transitional epithelial cells and RTEC), and mucus. It has a 635 nm laser and 2 analytical channels

Table 1. Median and Range of Various Automated Urinalysis Parameters in Control Patients and Patients with AKI

Control Patients, n = 62	RBC/hpf	WBC/hpf	Cast/hpf	src/hpf	Path cast/hpf
Median (IQR)	1.7 (4.1)	1.7 (10.3)	0.09 (0.45)	0.4 (1.3)	0.05 (0.18)
Minimum	0.20	0.0	0.0	0.0	0.0
Maximum	2507.2	410.0	3.0	67.6	0.9
Patients with AKI, n = 103					
Median (IQR)	13 (32.9)	9.3 (49.2)	0.29 (0.63)	0.60 (1.9)	0.19 (0.35)
Minimum	0.0	0.3	0.0	0.0	0.0
Maximum	1801.0	2562.0	5.0	80.6	5.0

Table 2. Logistic Regression Analysis for Predicting AKI

	Estimate	Standard Error	Odds Ratio	*z*	Wald Statistic	df	*P* Value	Confidence interval (lower)	Confidence interval (upper)
Intercept	–0.082	0.229	0.921	–0.360	0.130	1	.719	0.588	1.443
RBCs	–0.000	0.001	1.000	–0.240	0.058	1	.810	0.998	1.001
WBCs	0.009	0.004	1.009	1.954	3.817	1	.051	1.000	1.018
Casts	–1.238	0.494	0.290	–2.505	6.275	1	.012	0.110	0.764
Path casts	4.536	1.511	93.283	3.002	9.010	1	.003	4.826	1803.149
src	0.008	0.024	1.008	0.318	0.101	1	.751	0.961	1.056

AUC is 0.72, sensitivity = 0.84, specificity = 0.43, and precision is 0.71.

DOI: 10.1093/labmed/lmaa069

that have separate fluorescent dyes. It characterizes formed and unformed elements from unspun urine by fluorescence, forward scatter, impedance, side scatter, and adaptive cluster analysis. For conversion from microliter to high-power field, counts obtained by the UF1000i were divided by a conversion factor of 5.5 (determined by the manufacturer).

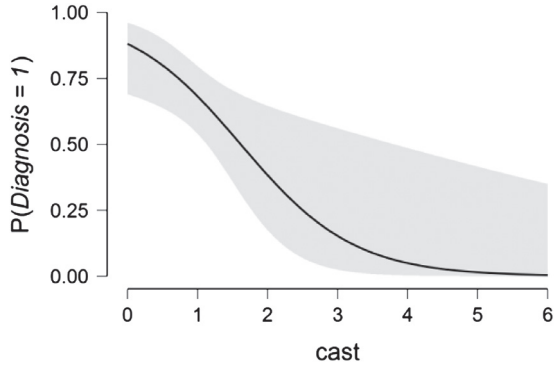

Figure 1

Predicted probability of AKI plotted against cast count. Probability decreases from 1 to 0.75 when cast count increases from 0/hpf to 1/hpf.

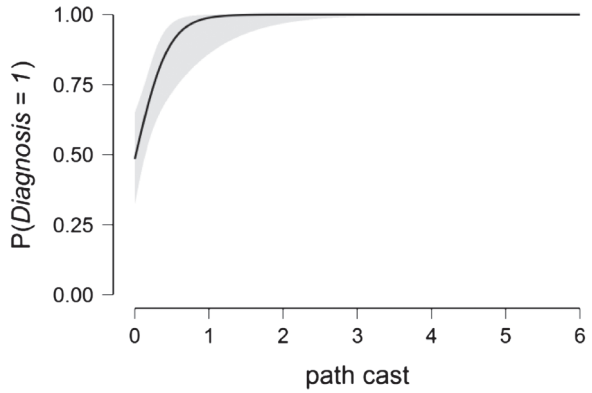

Figure 2

Predicted probability of AKI plotted against path cast count. Probability increases from 0.5 to 1 for increase in path cast count from 0/hpf to 1/hpf.

Continuous variables were expressed as the median when their distribution was not Gaussian, and their variability was expressed as the interquartile range (IQR). Categorical variables were expressed as percentages. Continuous variables were compared using the Wilcoxon signed-rank test, and their associations were studied using the Spearman rank correlation. Associations and differences between continuous variables were considered significant if the 2-tailed *P* value was less than .05. All statistical analysis was carried out using the JASP statistical package (Version 0.12.2). Intermethod comparisons (automated analysis vs microscopic analysis) and the construction of Bland-Altman plots was carried out using GraphPad Prism version 8.0.0 for Windows (GraphPad Software, San Diego, CA; www.graphpad.com).

Results

Control patients included 37 men and 25 women with a median age of 51 years (IQR = 22.5 years; range, 23–80 years). The range and median automated RBC, WBC, cast, src, and path cast count are summarized in **Table 1**. There were 103 patients with AKI, including 73 men and 30 women with a median age of 64 years (IQR = 20 years). The youngest patient was 17 years, and the oldest was 90 years. **Table 1** summarizes the automated urinalysis findings in the patients with AKI.

A logistic model was fitted to the data to test the hypothesis regarding the relationship between AKI diagnosis (coded as 1 when present and 0 when absent) and automated urinalysis parameters. The results showed

Table 3. Comparison of Results of Automated and Manual Urinalysis in Patients With AKI (n = 45)

AKI (auto vs man	RBC auto/hpf	RBC man/hpf	WBC auto/hpf	WBC man/hpf	src auto/hpf	RTEC/ hpf	Cast auto/hpf	Cast man/hpf	Path Cast auto/hpf	Path Cast man/hpf
Median (IQR)	10.1 (32.4)	7.5 (14.2)	7.0 (77.7)	2.0 (6.0)	0.8 (1.9)	0.3 (1.0)	0.28 (0.77)	0.1 (3.0)	0.14 (0.51)	0.6 (1.9)
Minimum	0.6	0.0	0.3	0.1	0.0	0.0	0.02	0.0	0.0	0.0
Maximum	409.4	81.0	2562.2	105.0	80.6	3.5	5.04	10.0	5.04	13.0
P value	*P* <.001		*P* <.001		*P* <.001		*P* =.27		*P* =.002	

Auto, automated; man, manual.
P values are values of significance for Wilcoxon signed-rank test.

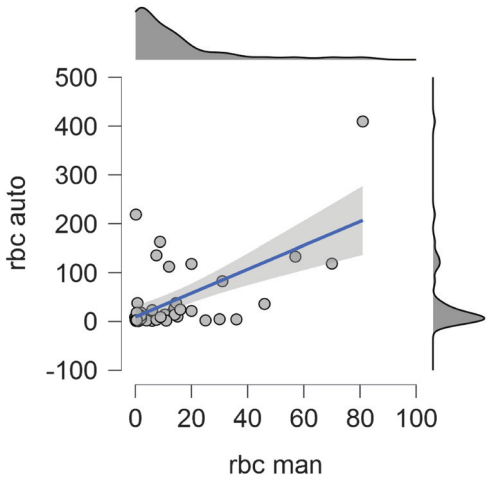

Figure 3

Bivariate relationship between RBC manual and automated counts. At low counts, there is linear positive correlation, whereas at higher counts, there is mild positive correlation with outliers.

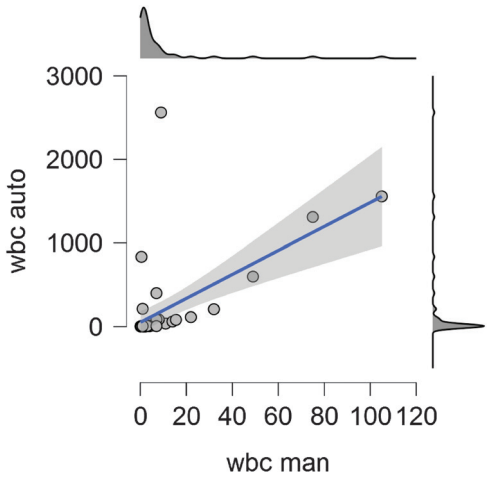

Figure 4

Bivariate relationship between WBC manual and automated counts. At low counts, there is strong linear positive correlation, whereas at higher counts, there is mild positive correlation only.

–predicted logit of AKI = –0.082 + (0.0)* RBC + (0.009)*WBC + (-1.23)*Cast + (4.5)*Path cast + (0.008)*Src (**Table 2** and **Figures 1**, **2**). The log of the odds of a patient having AKI was negatively correlated with cast (P =.01) and positively correlated with path cast (P =.003). The higher the number of casts/hpf, the lower the probability of a patient having AKI, and the higher the number of path casts,

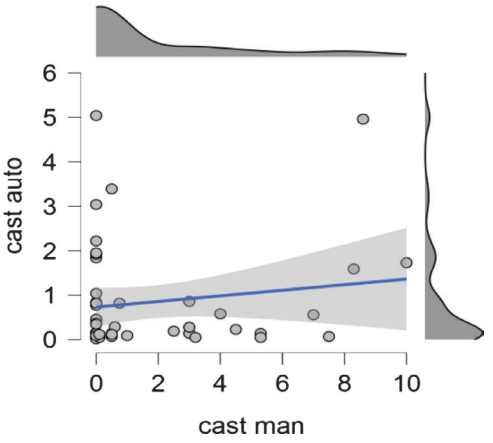

Figure 5

Bivariate relationship between automated and manual cast counts. From the figure, it is evident there is no relationship between the two.

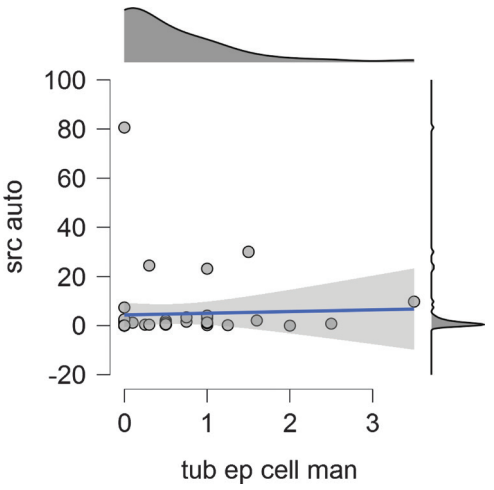

Figure 6

Bivariate relationship between manual renal tubular epithelial cells (RTEC) count and automated small round cell (SRC) count indictes no association between the two parameters.

the higher the likelihood of a patient having AKI. A 1-unit increase in path cast increased the odds for AKI 93.2 times. The RBC, WBC, and src did not influence the log odds of AKI (P ˃.05).

Next we compared the microscopic and automated urinalysis parameters in 45 patients with AKI. The Wilcoxon signed-rank test indicated that the automated median RBC/hpf (10.1 vs 7.5), WBC/hpf (7.0 vs

Lab Medicine 2021;52;e30–e38
DOI: 10.1093/labmed/lmaa069

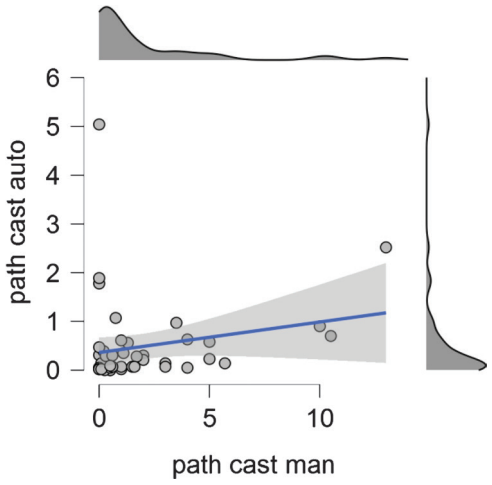

Figure 7

Bivariate relationship between manual and automated path cast count indicates a mild linear positive correlation.

2.0), and automated src (0.8 vs 0.3) ranks in AKI were significantly higher than those revealed through microscopic analysis, $z = 813.5$, $P < .001$; $z = 994$, $P < .001$; and $z = 755.5$, $P < .001$. respectively. Whereas the median microscopic path cast count was significantly higher than the automated path cast/hpf (191; $P = .002$), there was no difference in the median cast count rank ($z = 421$; $P = .27$; **Table 3**). The median and IQR of manual and automated parameters and their associations are summarized in **Table 3** and **Figures 3** to **7**. The Spearman ranked correlation showed a positive correlation between automated WBC and manual WBC count, rho = 0.652 ($P < .001$). No correlation was observed between the automated and manual methods for RBC count (rho = 0.45), cast count (rho = –0.06), src/RTEC (rho = 0.31), and path cast (rho = 0.28; **Figure 8**). The Bland-Altman intermethod comparison between the automated and manual methods showed no agreement between the 2 methods for all the parameters considered. **Figures 9** to **13** show the results of the intermethod comparison between the automated and manual methods. **Images 1–6** show the images of various casts encountered in the urine sediment of patients with AKI.

Discussion

In the present study, which included 165 patients (103 patients with AKI and 62 control patients), we analyzed the automated urinalysis findings in AKI compared with manual microscopy findings (for 45 patients with AKI) and studied the role of UF1000i in predicting AKI. Automated analysis produced significantly higher counts for RBC, WBC, and src ($P < .05$) in patients with AKI. Path casts were significantly higher by manual microscopy. By logistic regression analysis, the area under the curve (AUC) for the prediction of AKI was 0.72 with a sensitivity of 84% and a specificity of 43%. The intermethod comparison between manual and automated analysis showed no agreement between the 2 methods.

Figure 8

Heatmap showing Spearman correlation between automated and manual urinalysis in AKI. Auto, automated; man, manual.

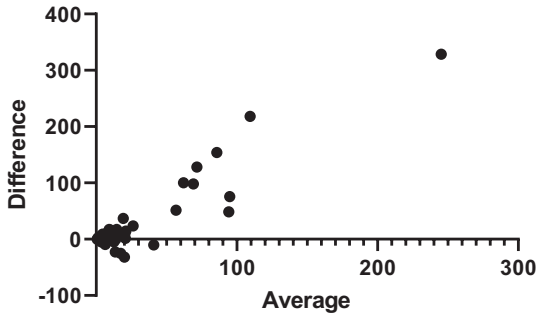

Figure 9

Bland-Altman plot for RBCs showing a proportional error and systematic error. Bias = 28.6, lower limit of agreement = –101.9, and upper limit of agreement = 159.1.

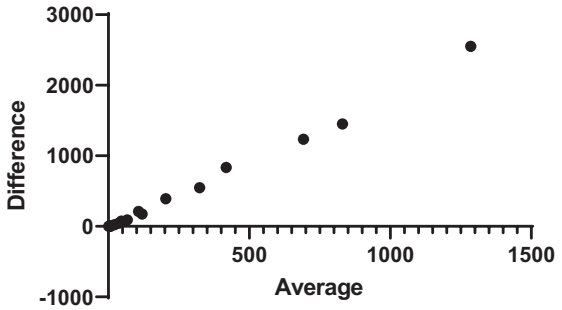

Figure 10

Bland-Altman plot for WBCs showing a proportional error and systematic error. Bias = 175.1, lower limit of agreement = –760.5, and upper limit of agreement = 1111.

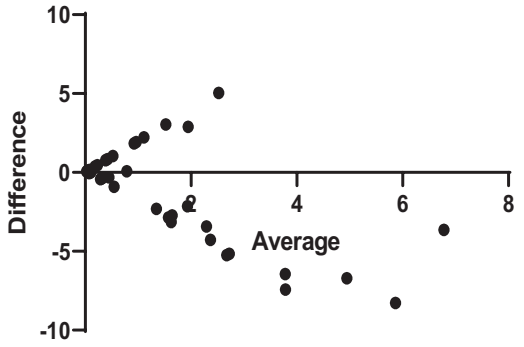

Figure 11

Bland-Altman plot for cast showing a proportional error. Bias = –0.92, lower limit of agreement = –6.5, and upper limit of agreement = 4.7.

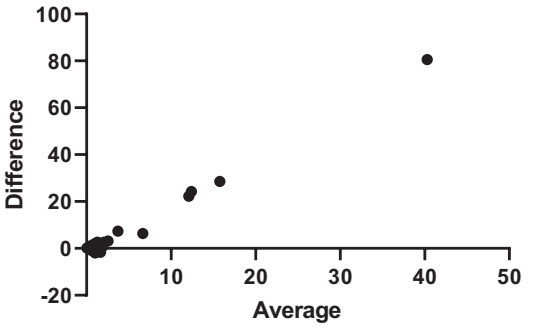

Figure 12

Bland-Altman plot for src and RTEC showing a proportional error and systematic error. Bias = 4.1, lower limit of agreement = –21.8, and upper limit of agreement = 30.1.

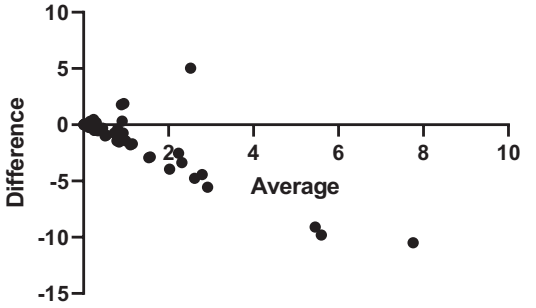

Figure 13

Bland-Altman plot for path cast showing a proportional error. Bias = –1.4, lower limit of agreement = –7.1, and upper limit of agreement = 4.2.

Using a conversion factor of 0.297, Wang and colleagues[15] found that the correlation for the RBC count was 0.86 for RBCs and 0.88 for WBCs. They found that the manual method and the UF1000i count were not significantly different by Passing-Bablok analysis. In our study, we used a conversion factor of 5.5 (as per manufacturer instructions). Various studies have found a good correlation between manual and iQ200 analyzer counts for RBCs, WBCs, and epithelial cells.[10,16-19] One study found a correlation of 0.94 for RBCs, 0.98 for WBCs, 0.85 for casts, and 0.70 for nonsquamous epithelial cells; the sediMAX urine analyzer correlated well with phase contrast microscopy and had an AUC of 80% to 90% for the identification of RBCs, WBCs, and squamous epithelial cells and an AUC of 73% to 74% for the identification of path casts and nonsquamous cells.[20] İnce et al[21] found that urine sediment examination by the

DOI: 10.1093/labmed/lmaa069

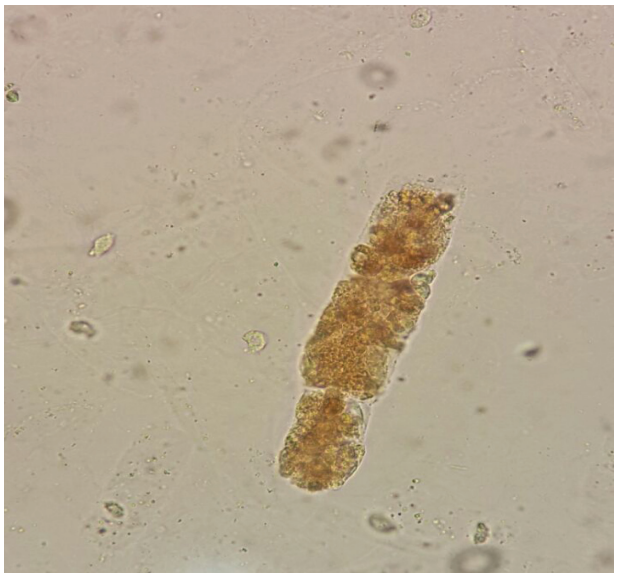

Image 1

Muddy brown granular cast characteristically seen in acute tubular necrosis (400x, unstained).

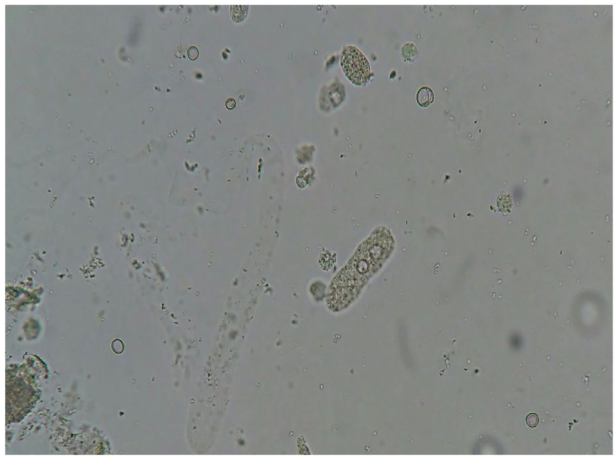

Image 2

Hyaline cast, in the center of the field, and binucleate proximal tubular epithelial cell (sometimes mistaken for granular cast), to the right of the hyaline cast (400x, unstained).

Dirui FUS-200 and Iris iQ200 devices correlated better with each other than with manual microscopy. Manoni et al[22] compared their results with the UF1000i with quantitative microscopy using the Fuchs Rosenthal chamber and found correlation coefficients of 0.98 for RBC, 1.00 for WBC, and 0.69 for casts.

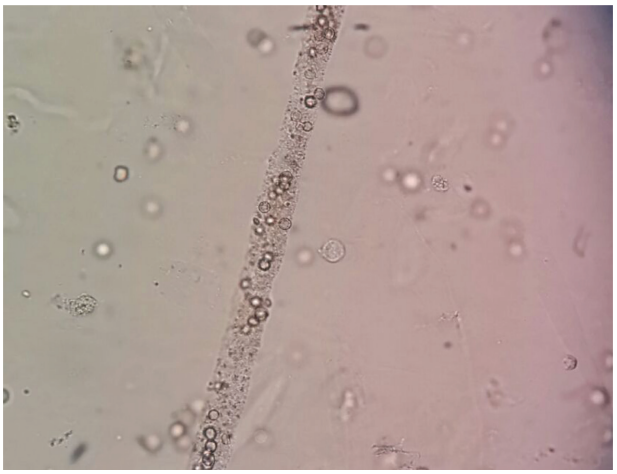

Image 3

Mixed granular and RBC cast (400x, unstained).

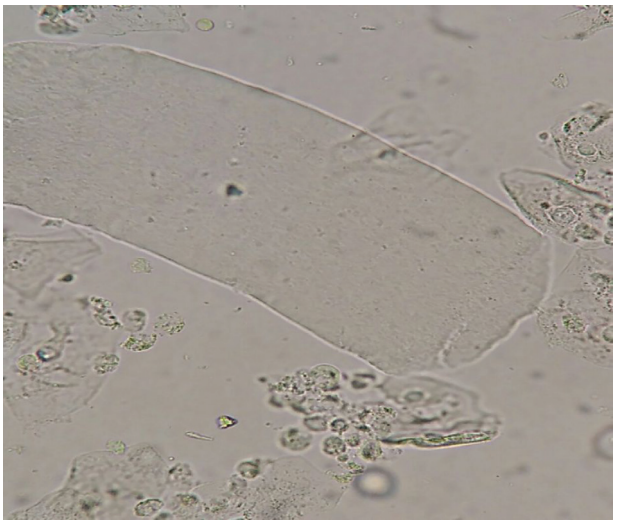

Image 4

Broad waxy cast appearing refractile with a cracked edge (400x).

In our study, the correlation between automated and manual counts for both counts/hpf and per microliter varied from 0.45 for RBCs to 0.65 for WBC, 0.31 for RTEC, –0.06 for casts, and 0.28 for path casts. The reasons for this low level of correlation could be varied. Research has shown that RBCs and certain crystals are not differentiated by the analyzer and tend to be counted together. Manual counting is prone to errors while viewing sediment with numerous RBCs and/or WBCs with significant overlap. The src count includes both RTEC and

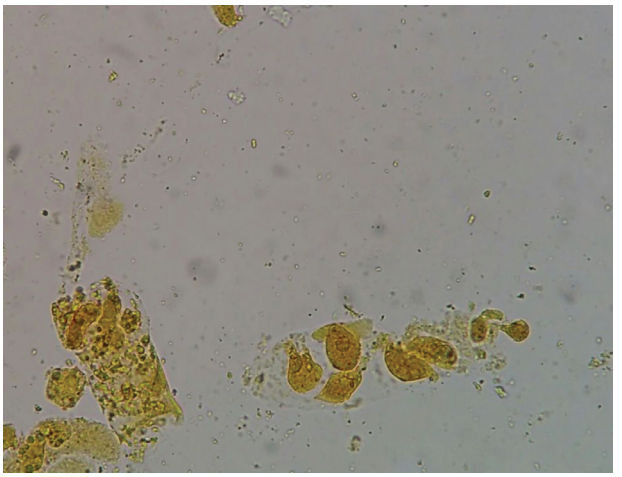

Image 5

Epithelial cell cast, lower right. Tubular epithelial cells have granular cytoplasm and an eccentric nonlobed nucleus (differentiating it from WBCs). Granular cast, left. The casts appear yellow because of bilirubinuria (400x, unstained).

Image 6

Coarse granular cast, left. Uric acid crystals are seen in the right half of the field (400x, unstained).

transitional epithelial cells, whereas microscopically we can distinguish these 2 cell types. Automated RBC, WBC, src, cast, and path cast counts are poor predictors of AKI by logistic regression analysis. However, an increase in path cast by 1 unit increases the chance of having AKI (odds ratio = 93).

Conclusion

In this study on AKI, automated parameters are poorly correlated with visual sediment analysis and are also poor predictors of AKI. This study has some drawbacks. Bright field microscopic examination of urine sediment is not the gold standard for prediction of AKI and is relatively bland in prerenal AKI. We evaluated just 1 sample of urine per patient, whereas repeated measurements would have helped us monitor the changes in automated analysis. **LM**

References

1. Koza Y. Acute kidney injury: current concepts and new insights. *J Inj Violence Res.* 2016;8(1):58–62.
2. Klahr S, Miller SB. Acute oliguria. *N Engl J Med.* 1998;338(10):671–675.
3. Needham E. Management of acute renal failure. *Am Fam Physician.* 2005;72(9):1739–1746.
4. Perazella MA, Coca SG, Kanbay M, Brewster UC, Parikh CR. Diagnostic value of urine microscopy for differential diagnosis of acute kidney injury in hospitalized patients. *Clin J Am Soc Nephrol.* 2008;3(6):1615–1619.
5. Perazella MA, Coca SG, Hall IE, Iyanam U, Koraishy M, Parikh CR. Urine microscopy is associated with severity and worsening of acute kidney injury in hospitalized patients. *Clin J Am Soc Nephrol.* 2010;5(3):402–408.
6. Bagshaw SM, Haase M, Haase-Fielitz A, Bennett M, Devarajan P, Bellomo R. A prospective evaluation of urine microscopy in septic and non-septic acute kidney injury. *Nephrol Dial Transplant.* 2012;27(2):582–588.
7. Marcussen N, Schumann J, Campbell P, Kjellstrand C. Cytodiagnostic urinalysis is very useful in the differential diagnosis of acute renal failure and can predict the severity. *Ren Fail.* 1995;17(6):721–729.
8. Chawla LS, Dommu A, Berger A, Shih S, Patel SS. Urinary sediment cast scoring index for acute kidney injury: a pilot study. *Nephron Clin Pract.* 2008;110(3):c145–c150.
9. Yüksel H, Kiliç E, Ekinci A, Evliyaoğlu O. Comparison of fully automated urine sediment analyzers H800-FUS100 and LabUMat-UriSed with manual microscopy. *J Clin Lab Anal.* 2013;27(4):312–316.
10. Wah DT, Wises PK, Butch AW. Analytic performance of the iQ200 automated urine microscopy analyzer and comparison with manual counts using Fuchs-Rosenthal cell chambers. *Am J Clin Pathol.* 2005;123(2):290–296.

DOI: 10.1093/labmed/lmaa069

11. Cobbaert CM, Arslan F, Caballé Martín I, et al. Automated urinalysis combining physicochemical analysis, on-board centrifugation, and digital imaging in one system: a multicenter performance evaluation of the cobas 6500 urine work area. *Pract Lab Med.* 2019;17:e00139.
12. Sharda N, Bakhtar O, Thajudeen B, Meister Ed, Szerlip H. Manual urine microscopy versus automated urine analyzer microscopy in patients with acute kidney injury. *Lab Med* 2014;45(4):e152–e155.
13. Palsson R, Srivastava A, Waikar SS. Performance of the automated urinalysis in diagnosis of proliferative glomerulonephritis. *Kidney Int Rep.* 2019;4(5):723–727.
14. Kidney Disease: Improving Global Outcomes. KDIGO clinical practice guideline for acute kidney injury. *Kidney Int Suppl* 2012;2(Suppl):1–138.
15. Wang L, Wang H, Zhao C, Chen C. The standardization of the report for urine cell counting-A converting factor for Sysmex UF-1000i. *J Clin Lab Anal.* 2019;33(4):e22857.
16. Chien TI, Kao JT, Liu HL, et al. Urine sediment examination: a comparison of automated urinalysis systems and manual microscopy. *Clin Chim Acta.* 2007;384(1–2):28–34.
17. Linko S, Kouri TT, Toivonen E, Ranta PH, Chapoulaud E, Lalla M. Analytical performance of the Iris iQ200 automated urine microscopy analyzer. *Clin Chim Acta.* 2006;372(1–2):54–64.
18. Park J, Kim J. Evaluation of iQ200 automated urine microscopy analyzer. *Korean J Lab Med.* 2008;28(4):267–273.
19. Budak YU, Huysal K. Comparison of three automated systems for urine chemistry and sediment analysis in routine laboratory practice. *Clin Lab.* 2011;57(1–2):47–52.
20. Zaman Z, Fogazzi GB, Garigali G, Croci MD, Bayer G, Kránicz T. Urine sediment analysis: Analytical and diagnostic performance of sediMAX—a new automated microscopy image-based urine sediment analyser. *Clin Chim Acta.* 2010;411(3-4):147–154.
21. İnce FD, Ellidağ HY, Koseoğlu M, Şimşek N, Yalçın H, Zengin MO. The comparison of automated urine analyzers with manual microscopic examination for urinalysis automated urine analyzers and manual urinalysis. *Pract Lab Med*. March 2016;5:14–20.
22. Manoni F, Tinello A, Fornasiero L, et al. Urine particle evaluation: a comparison between the UF-1000i and quantitative microscopy. *Clin Chem Lab Med.* 2010;48(8):1107–1111.

Corrigendum

In “Comparison of Nucleic Acid Amplification and IgM Tests for the Diagnosis of *Mycoplasma pneumoniae* Infection in Children During a Recent Korean Outbreak” (https://doi.org/10.1093/labmed/lmaa048), Dr. Heungsup Sung was inadvertently omitted as a first corresponding author. His email address is sung@amc.seoul.kr. Lab Medicine regrets the omission.

Science

Absolute Lymphocytes, Ferritin, C-Reactive Protein, and Lactate Dehydrogenase Predict Early Invasive Ventilation in Patients With COVID-19

Salvador Payán-Pernía, MD,[1,*] *Lucía Gómez Pérez, MD,*[1] *Ángel F. Remacha Sevilla, MD, PhD,*[1] *Jordi Sierra Gil, MD, PhD,*[1] *Silvana Novelli Canales, MD, PhD*[1]

Laboratory Medicine 2021;52:141-145

DOI: 10.1093/labmed/lmaa105

ABSTRACT

Objective: Early detection of patients with COVID-19 who will need mechanical invasive ventilation (MIV) may aid in delivering proper care and optimizing the use of limited resources.

Methods: In this single-center retrospective observational study, we aimed to identify simple laboratory parameters that in combination with ferritin (a surrogate marker of severe inflammation) may help predict early (first 48 hours) MIV. A total of 160 patients with COVID-19 in whom serum ferritin, absolute lymphocyte count (ALC), platelet count, C-reactive protein (CRP), and lactate dehydrogenase (LDH) had been analyzed at admission were included.

Results: We found that ferritin, LDH, ALC, and CRP predicted with 88% accuracy the probability of early MIV. Results indicated that LDH showed the greater area under the curve (AUC), with a value of 89.1%. Using the AUC, we established cutoff values for clinical application. Finally, we developed a classification tree based on LDH for its clinical use.

Conclusion: Ferritin, LDH, ALC, and CRP predict with 88% accuracy the probability of early MIV.

Keywords: ferritin, COVID-19, hematology, biomarkers, mechanical ventilation, lactate dehydrogenase

As of October 4, 2020, the World Health Organization reported a total of 34,804,348 confirmed COVID-19 cases of infection globally, including 1,030,738 deaths.[1] The most common clinical features at the onset of the illness caused by SARS-CoV-2 are fever, fatigue, and dry cough. Patients with severe illness may develop dyspnea and hypoxemia within 1 week after onset of the disease, which may quickly progress to acute respiratory distress syndrome (ARDS) or end-organ failure.[2]

Abbreviations:

MIV, mechanical invasive ventilation; ALC, absolute lymphocyte count; CRP, C-reactive protein; LDH, lactate dehydrogenase; AUC, area under the curve; ARDS, acute respiratory distress syndrome; ICU, intensive care unit; IL-6, interleukin-6; MAS, macrophage activation syndrome; RT-PCR, reverse-transcriptase polymerase chain reaction; ROC, receiver operating characteristic

[1]Haematology Department, Hospital de la Santa Creu i Sant Pau, Sant Pau Research Institute, Universitat Autònoma de Barcelona, Barcelona, Spain

*To whom correspondence should be addressed.
sppayan@gmail.com

Since the outbreak in December 2019, the sudden increase in COVID-19 cases of infection is putting high pressure on healthcare services worldwide, with particular significance in intensive care units (ICU). Reported rates of ICU admission represent up to one-quarter of hospitalized patients, but rates vary among countries.[3] These differences may relate to the availability of ICU beds, variations in practice and admission criteria, and differences in predisposing factors and testing availability.

Researchers have learned that ARDS is the most common complication for ICU admission; in a series of 1300 patients admitted to the ICU in the Lombardy region of Italy, 88% required endotracheal intubation and mechanical ventilation.[3] Similarly, two-thirds of patients with COVID-19 who required critical care in the United Kingdom had mechanical ventilation within 24 hours of admission.[4] Therefore, early detection of patients who will need mechanical invasive ventilation (MIV) may aid in delivering proper care and optimizing the use of limited resources, and this is of particular interest in lower- and middle-income countries.

Several laboratory parameters have been associated with worse outcomes in patients with COVID-19: elevated liver enzymes, ferritin, IL-6, lactate dehydrogenase (LDH), C-reactive protein (CRP), D-dimer, prothrombin time, troponin, and creatine phosphokinase, along with lymphopenia and acute kidney injury.[5-7]

Hyperferritinemia has been linked to macrophage activation syndrome (MAS), which is present in serious inflammatory disease[8]; MAS is quite possibly the origin of the severest clinical manifestations of SARS-CoV-2 infection.[9]

In this setting, we aimed to identify simple laboratory parameters that in combination with ferritin may help to predict early (first 48 hours) MIV by orotracheal intubation.

Methods

This retrospective observational study was performed at Hospital de la Santa Creu i Sant Pau, a first-level hospital in Barcelona, Spain. The study was conducted according to the Declaration of Helsinki and approved by the institutional ethics committee. For patient enrollment, all consecutive blood tests that included ferritin between March 15, 2020 and April 6, 2020 were reviewed. In this way, patients diagnosed with COVID-19 in whom serum ferritin, ALC, platelet count, CRP, and LDH had been analyzed at admission were selected. In all patients, these parameters were determined in the same sample or with a maximum time difference of 24 hours. We assessed ALC on a Sysmex XN-10 (Sysmex Corporation, Kobe, Japan) analyzer. Serum ferritin was measured on an Architect c16000 System (Abbott Laboratories, IL) using a 2-step chemiluminescent microparticle immunoassay. We determined CRP and LDH in serum using the Alinity c system (Abbot Laboratories, IL), the former using a particle-enhanced immunoturbidimetric assay, the latter using spectrophotometry.

One hundred sixty patients aged 23 to 75 years were recruited. Informed consent was obtained from all participants. One hundred fifty-eight patients had a laboratory-confirmed SARS-CoV-2 infection according to World Health Organization guidance[10]: a positive result of real-time reverse-transcriptase polymerase chain reaction (RT-PCR) assay of a nasopharyngeal swab. In 2 patients, RT-PCR was negative and the diagnosis of COVID-19 was made presumptively based on a compatible clinical presentation and an exposure risk. Patients who received tocilizumab, a monoclonal antibody against IL-6, at any time during their hospital stay were excluded for the study because this agent has been associated with a decrease in CRP and ferritin levels.[11] Patients with active neoplasia were also excluded because of iron overload.

Demographic, clinical, laboratory, and outcome data were extracted from electronic medical records. An image on chest radiograph was considered typical of COVID-19 in the presence of consolidation and ground-glass opacities, with bilateral, peripheral, and lower lung zone distributions. All patients were evaluated until death or hospital discharge.

Descriptive analyses of the variables were expressed as mean (range) or the number of patients (%). We chose MIV as the dependent variable, and the independent variables were LDH, ALC, platelet count, ferritin, and CPR. To analyze the association between the independent variables and MIV, the Pearson χ^2 test was used, considering a type I error < 5%. A binomial logistic regression analysis was used for the joint evaluation of variables associated with MIV. The significant variables with P <.05 in the univariate analysis were selected for the regression analysis performed by the stepwise backward method (likelihood ratio). The variables that kept $P \leq .05$ after adjustments remained in the multiple regression model. A receiver operating characteristic (ROC) analysis was performed to measure the diagnostic/predictive accuracy of each significant variable.

Moreover, we developed a classification tree analysis using the chi-squared automated interaction detection (CHAID) growing method. This nonparametric analysis examines interactions among variables to create a decision tree without assuming that independent and dependent variables are linked by linear relationships. All statistical analyses were carried out using SPSS, version 21.0. Because the sample size was small (n = 160), we could not conduct an internal validation analysis.

Results

Table 1 shows the demographic and clinical characteristics of the 160 patients included in the study. Overall, 58.10% were men. The median age was 57 years (minimum: 23;

Table 1. Patient Characteristics

		Frequency (n)	Percentage (%)
Age, y, mean (minimum–maximum)			
57 (23–75)			
Sex			
Female		67	41.90
Male		93	58.10
Total		160	100.00
COVID-19 diagnosis			
Possible		2	1.30
Confirmed		158	98.80
Total		160	100.0
Typical X-ray pattern			
Yes		158	98.80
No		2	1.30
Total		160	100.00
Lactate dehydrogenase, U/L, mean (minimum–-maximum)	405 (147–5250)		
Ferritin, μg/L, mean (minimum–-maximum)	993 (107–5127)		
CRP, mg/L, mean (minimum–-maximum)	125.3 (5.6–404.3)		
Platelets, × 10^9/L, mean (minimum–-maximum)	223.2 (59.-495)		
Lymphocytes, × 10^9/L, mean (minimum–-maximum)	1.11 (0.11–2.85)		
Thrombotic event			
Yes		5	3.10
No		155	96.90
Total		160	100.00
MIV			
Yes		32	20.00
No		128	80.00
Total		160	100.00

Abbreviations: CRP, C-reactive protein; MIV, mechanical invasive ventilation.

Table 2. Variables Included in the Logistic Regression Model

Step 1	B	SE	Wald	df	Sig.	Exp (B)	95% CI for Exp (B)	
							Lower	Upper
Absolute lymphocytes (× 10^9/L)	–2.750	0.960	8.201	1	0.004	0.064	0.010	0.420
Lactate dehydrogenase (U/L)	0.007	0.002	10.941	1	0.001	1.007	1.003	1.011
C-reactive protein (mg/L)	0.006	0.003	3.970	1	0.046	1.007	1.000	1.013
Ferritin (μg/L)	0.001	0.000	4.026	1	0.045	1.001	1.000	1.001
Constant	–3.615	1.220	8.777	1	0.003	0.027	…	…

In the logistic regression model, all predictors were included in the first step. B is the coefficient in the model; SE is the standard error corresponding to B; Wald is the χ^2 distributed with 1 degree of freedom (df); Sig. is the corresponding P value; Exp (B) is the exponentiation of the B coefficient, which is an odds ratio (OR); and the 95% confidence intervals (CIs) around the OR are also presented.

maximum: 75). A total of 32 patients (20%) required endotracheal intubation and mechanical ventilation, which happened in 96.9% of these patients within 48 hours after the emergency room admission.

Four independent variables were selected for logistic regression model fitting (**Table 2**): LDH, ALC, ferritin, and CRP. The platelet count was excluded ($P > .05$). Although each variable in the equation remained statistically significant, CRP and ferritin were close to the limit of significance ($P = .046$ and $P = .045$, respectively). Without including independent variables in the model, the probability of not being intubated was 80%. After the inclusion of the independent variables, the model's capacity to predict no intubation improved to 88%.

In the ROC analysis, LDH showed the greater AUC, with a value of 89.1%, followed by CRP (80.5%), ALC (77.6%), and ferritin (77.5%). Using the AUC, we established cutoff

Lab Medicine 2021;52;141–145
DOI: 10.1093/labmed/lmaa105

Table 3. AUC Scores for Significant Variables and Cutoff Values Predictive of MIV

Variables	AUC Score (%)	Cutoff Value	Sensitivity (%)	Specificity (%)	MIV (yes/no)
LDH (U/L)	89.1	<219	100.0	11.7	No
		<310	93.8	52	
		>1102	6.3	100	Yes
		>506	69.0	94	
CRP (mg/L)	80.5	<65.65	100.0	39	No
		>76.45	96.9	44	Yes
Absolute lymphocytes ($\times 10^9$/L)	77.6	<0.37	100	19	Yes
		<0.53	95	28	Yes
		>1.28	36.7	93.7	No
		>1.56	21.9	100	No
Ferritin (μg/l)	77.5	<300	93.8	18.0	No
		>3496	18.8	99.2	Yes

Abbreviations: AUC, area under the curve; CRP, C-reactive protein; LDH, lactate dehydrogenase; MIV, mechanical invasive ventilation.

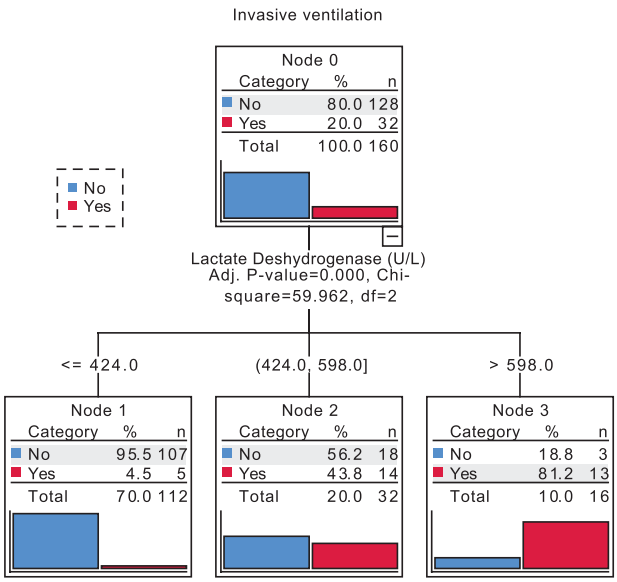

Figure 1

Classification tree. The root node (node 0) shows the binary (Yes/No) distribution of the outcome of the dependent variable, MIV. The χ^2 test is then applied to ensure that the branch is associated with a statistically significant predictor of MIV—in this case, LDH. As seen in node 1, LDH ≤424.0 U/L could predict that 95.5% of those patients did not need MIV; in addition, 70% of all patients had LDH ≤424.0 U/L. On the other hand, as shown in node 3, LDH >598.0 U/L could anticipate that 81.2% of patients needed MIV; only a minority of all patients (10%) reached those LDH levels. MIV, mechanical invasive ventilation; LDH, lactate dehydrogenase.

values for clinical application, as shown in **Table 3**. We found that LDH might represent the most useful discrimination variable for clinical application: when it was <219 U/L, patients did not need MIV, with a sensitivity of 100% and a specificity of 11.7%. No patients with CRP <65.65 mg/L or an ALC >1.56 × 10^9/L needed MIV. Ferritin levels <300 μg/L predicted no MIV with a sensitivity of 93.8%.

On the classification tree analysis (**Figure 1**), LDH >598 U/L increased the likelihood of MIV, and an <424 U/L defined a category with the lowest probability of MIV.

Discussion

Our work provides an approximation for the prediction of early (first 48 hours) MIV in patients with COVID-19 by means of simple laboratory tests that can be easily collected in any hospital. Although our results are concordant with those published by other authors about risk factors for severe disease and death, they refer specifically to the risk of MIV, which is of particular interest in the context of the high pressure on ICUs. Therefore, our data can help prioritize patients quickly when healthcare resources are limited.

We found that LDH is the biomarker that better can predict early MIV; with a sensitivity of 100%, patients will not be intubated if LDH on admission is <219 U/L. Based on LDH, we developed a classification tree to estimate the risk of MIV quickly. Research has shown that LDH is an intracellular enzyme found in nearly all organ systems that catalyzes the interconversion of pyruvate and lactate, with concomitant interconversion of Reduced nicotinamide adenine dinucleotide and Nicotinamide adenine dinucleotide. Abnormal values can not only result from cardiac damage or hemolysis but also from multiple organ injury and decreased oxygenation with upregulation of the glycolytic pathway.

Because LDH is present in lung tissue, elevated levels seen in COVID-19 and other viral respiratory infections, such as Middle East Respiratory Syndrome, may represent the extent of lung injury that influences clinical outcomes.[12]

In severe COVID-19 infection, a deviation of the protective immune response into a dysfunctional program occurs, leading to cytokine release syndrome with severe inflammation and, eventually, multisystemic failure. A better understanding of the mechanisms lying at the root of immune response failure is needed; serum levels of inflammatory markers, such as CRP, ferritin, IL-6, and other cytokines, are increased in COVID-19.[13] In the setting of ongoing inflammation, evidence supports a role for ferritin in modulating the immune response, via its induction of anti-inflammatory cytokines and limitation of free radical damage. Alternatively, emerging work suggests a potential causative role of ferritin in the inflammatory pathology of disease.[14] Transcriptional induction of the *CRP* gene mainly occurs in hepatocytes in the liver in response to increased levels of inflammatory cytokines, especially IL-6. Similar to ferritin, evidence suggests that CRP is an important regulator of inflammatory processes and not just a marker.[15]

Lymphopenia, the fourth marker to predict early MIV, is a common feature in patients with COVID-19 and is more pronounced in severe cases of infection. It affects mainly T cells, including CD4 Th1 and Tregs, but particularly CD8. Although circulating CD8 in patients with severe COVID-19 has exhibited phenotypes associated with abnormal functionality and exhaustion, CD4 cells have been shown to express activation markers. In addition, natural killer lymphocytes have decreased in patients with both moderate and severe cases of the disease.[9,16] Injured alveolar epithelial cells could lead to the infiltration of lymphocytes.[16]

Conclusion

This study identifies 4 simple laboratory parameters that predict with 88% accuracy the probability of early MIV, enabling early intervention and optimization of healthcare resources. **LM**

References

1. Coronavirus disease 2019 (COVID-19) weekly epidemiological update and weekly operational update. World Health Organization. https://www.who.int/emergencies/diseases/novel-coronavirus-2019/situation-reports. Updated November 15, 2020. Accessed November 15, 2020.
2. Wang D, Hu B, Hu C, et al. Clinical characteristics of 138 hospitalized patients with 2019 novel coronavirus-infected pneumonia in Wuhan, China. *JAMA.* 2020;323(11):1061–1069.
3. Grasselli G, Zangrillo A, Zanella A, et al.; COVID-19 Lombardy ICU Network. Baseline characteristics and outcomes of 1591 patients infected with SARS-CoV-2 admitted to ICUs of the Lombardy region, Italy. *JAMA.* 2020;323(16):1574–1581.
4. Mahase E. Covid-19: most patients require mechanical ventilation in first 24 hours of critical care. *BMJ.* 2020;368:m1201.
5. Henry BM, de Oliveira MHS, Benoit S, Plebani M, Lippi G. Hematologic, biochemical and immune biomarker abnormalities associated with severe illness and mortality in coronavirus disease 2019 (COVID-19): a meta-analysis. *Clin Chem Lab Med.* 2020;58(7):1021–1028.
6. Ruan Q, Yang K, Wang W, Jiang L, Song J. Clinical predictors of mortality due to COVID-19 based on an analysis of data of 150 patients from Wuhan, China. *Intensive Care Med.* 2020;46(5):846–848.
7. Mehta P, McAuley DF, Brown M, Sanchez E, Tattersall RS, Manson JJ; HLH Across Speciality Collaboration, UK. COVID-19: consider cytokine storm syndromes and immunosuppression. *Lancet.* 2020;395(10229):1033–1034.
8. Rosário C, Zandman-Goddard G, Meyron-Holtz EG, D'Cruz DP, Shoenfeld Y. The hyperferritinemic syndrome: macrophage activation syndrome, Still's disease, septic shock and catastrophic antiphospholipid syndrome. *BMC Med.* 2013;11:185.
9. Merad M, Martin JC. Pathological inflammation in patients with COVID-19: a key role for monocytes and macrophages. *Nat Rev Immunol.* 2020;20(6):355–362.
10. Laboratory testing strategy recommendations for COVID-19: interim guidance. World Health Organization. https://www.who.int/publications/i/item/laboratory-testing-strategy-recommendations-for-covid-19-interim-guidance. Updated March 21, 2020. Accessed November 15, 2020.
11. Sciascia S, Aprà F, Baffa A, et al. Pilot prospective open, single-arm multicentre study on off-label use of tocilizumab in patients with severe COVID-19. *Clin Exp Rheumatol.* 2020;38(3):529–532.
12. Henry BM, Aggarwal G, Wong J, et al. Lactate dehydrogenase levels predict coronavirus disease 2019 (COVID-19) severity and mortality: a pooled analysis. *Am J Emerg Med*. 2020;38(9):1722–1726.
13. García LF. Immune response, inflammation, and the clinical spectrum of COVID-19. *Front Immunol.* 2020;11:1441.
14. Kernan KF, Carcillo JA. Hyperferritinemia and inflammation. *Int Immunol.* 2017;29(9):401–409.
15. Sproston NR, Ashworth JJ. Role of C-reactive protein at sites of inflammation and infection. *Front Immunol.* 2018;9:754.
16. Liu J, Li S, Liu J, et al. Longitudinal characteristics of lymphocyte responses and cytokine profiles in the peripheral blood of SARS-CoV-2 infected patients. *EBioMedicine.* 2020;55:102763.

DOI: 10.1093/labmed/lmaa105

Neurogranin as a Novel Biomarker in Alzheimer's Disease

Luisa Agnello, PhD,[1#] Caterina Maria Gambino, PhD,[1#] Bruna Lo Sasso, PhD,[1,2] Giulia Bivona, MD,[1,2] Salvatore Milano, BS,[2] Anna Maria Ciaccio,[4] Tommaso Piccoli, MD,[3] Vincenzo La Bella, MD,[3] Marcello Ciaccio, MD[1,2]*

Laboratory Medicine 2021;52:188-196

DOI: 10.1093/labmed/lmaa062

ABSTRACT

Background: In this study, we investigated the possible role of 2 novel biomarkers of synaptic damage, namely, neurogranin and α-synuclein, in Alzheimer disease (AD).

Methods: The study was performed in a cohort consisting of patients with AD and those without AD, including individuals with other neurological diseases. Cerebrospinal fluid (CSF) neurogranin and α-synuclein levels were measured by sensitive enzyme-linked immunosorbent assays (ELISAs).

Results: We found significantly increased levels of CSF neurogranin and α-synuclein in patients with AD than those without AD. Neurogranin was correlated with total tau (tTau) and phosphorylated tau (pTau), as well as with cognitive decline, in patients with AD. Receiver operating characteristic (ROC) curve analysis showed good diagnostic accuracy of neurogranin for AD at a cutoff point of 306 pg per mL with an area under the curve (AUC) of 0.872 and sensitivity and specificity of 84.2% and 78%, respectively.

Conclusions: Our findings support the use of CSF neurogranin as a biomarker of synapsis damage in patients with AD.

Keywords: neurogranin, α-synuclein, CSF, synaptic loss, biomarker, synapsis

Alzheimer disease (AD), one of the most prevalent neurodegenerative disorders worldwide, is characterized by memory loss and cognitive impairment. The pathological hallmarks of the disease are the extracellular amyloid-β (Aβ) peptides deposition, the intracellular neurofibrillary tangles consisting of phosphorylated tau (pTau) protein, the loss of synapses, and neuroinflammation.[1,2]

Abbreviations:

AD, Alzheimer disease; Aβ, amyloid-β; pTau, phosphorylated tau; MCI, mild cognitive impairment; CSF, cerebrospinal fluid; tTau, total tau; MMSE, Mini-Mental State Examination; PET, positron emission tomography; CLEIA, chemiluminescence enzyme immunoassay; ELISA, enzyme-linked immunosorbent assay; IQR, interquartile; ANOVA, analysis of variance; ROC, receiver operating characteristic; AUC, area under the curve; CI, confidence interval; PD, Parkinson disease; F, female; M, male; … , nonapplicable.

[1]Department of Biomedicine, Neurosciences and Advanced Diagnostics, Institute of Clinical Biochemistry, Clinical Molecular Medicine and Laboratory Medicine, University of Palermo, Palermo, Italy, [2]Department of Laboratory Medicine, University Hospital "P. Giaccone," Palermo, Italy, [3]Department of Biomedicine, Neurosciences and Advanced Diagnostics, Neurology Unit, University of Palermo, Palermo, Italy, and [4]University of Palermo, Palermo, Italy

*To whom correspondence should be addressed.
marcello.ciaccio@unipa.it

[#]These authors contributed equally to this work.

Cognitive decline is closely associated with synapse loss and neuropathological lesions in many brain regions as a consequence of direct effects of Aβ and tau proteins on synaptic structural plasticity, as well as indirect effects of the inflammatory response on the neuronal process.[3] AD has a slowly progressive clinical course which, based on the symptoms, can generally be divided into 3 phases: initial, intermediate, and terminal.[4] Dementia represents the end stage of the disease. Also, a preclinical stage and a prodromal stage, the latter of which is also referred to as mild cognitive impairment (MCI) due to AD, can be identified, especially in the field of clinical research.

The preclinical stage is defined by the presence of typical AD alterations detected by cerebrospinal fluid (CSF) biomarkers in the absence of signs and/or symptoms of the disease.[5] MCI due to AD, however, is characterized by the presence of an initial memory disorder but no significant impact on the life of the patient. We note that

neuropathological alterations in AD occur several years before the onset of cognitive decline, making CSF biomarkers a useful tool for supporting the early diagnosis of the disease and the differential diagnosis between AD and other forms of dementia.[6,7]

Currently, 3 CSF molecules, known as core CSF biomarkers, including total tau (tTau), pTau, and Aβ42 peptide, have been internationally recognized as research clinical diagnostic tools for AD.[8–10] Specifically, the typical AD biochemical profile is defined by decreased Aβ42 levels associated with increased tTau and pTau levels.[11,12] Alterations of such biomarkers reflect the main pathophysiological mechanisms of the disease. Specifically, the decrease in Aβ42 levels is the consequence of amyloid-plaque deposition, whereas the increase in pTau and tTau levels reflects the formation of neurofibrillary tangles and related neuronal damage.

Although Aβ42 changes are typically observed only in AD, tau changes are not characteristic of the disease. Indeed, elevated tau levels can be detected in several neurodegenerative disorders, such as Creutzfeldt-Jacob disease, Wernicke encephalopathy, severe malaria, hydrocephalus, and brain cancer,[13–16] referred to collectively as "tauopathies".[17] Therefore, additional specific biomarkers reflecting synaptic plasticity are needed; several molecules have been studied as possibilities.[18–22] Among molecules involved in synaptic dysfunction or neurodegeneration,[23–25] neurogranin and α-synuclein seem to be promising as novel molecular biomarkers for AD.

The aim of the present study is to assess the diagnostic value of CSF neurogranin and α-synuclein in a cohort consisting of patients with and without AD. Also, we evaluated the relationship of these analytes with CSF core biomarkers. The combination of these biomarkers may increase the diagnostic accuracy of AD testing, as well as allowing us to better understand the pathogenesis of the disease, to identify potential drug targets, design clinical trials, and improve clinical practice in AD diagnostic workup.[26]

Materials and Methods

Study Design

We performed a retrospective observational study at the Palermo University Hospital "P Giaccone" that included individuals being treated at the Neurology Unit who underwent lumbar puncture for CSF analysis. The study population consisted of 29 patients with AD (mean [SD], age 67.8 [6.4] years) and 59 patients without AD (62.5 [11.3] years), including individuals with neurological acute/subacute inflammatory disorders and tumors, which usually result in significant neuronal/axonal death and, thus, neurodegeneration. The severity of dementia in patients with AD was assessed using the Mini-Mental State Examination (MMSE).

All clinical and biological assessments were carried out in accordance with the Declaration of Helsinki, and the study was approved by the local Ethics Committee. All participants gave written consent. The informed consent contains a statement that "the biological material [collected] may also be used for research purposes."

The diagnosis of AD or other neurological diseases was made by an expert neurologist based on medical history, clinical examination, neuropsychological testing, neuroimaging, fluorodeoxyglucose positron emission tomography (PET) and CSF biomarkers findings, according to the clinical diagnostic criteria of McKhann et al and Albert et al.[27,28]

CSF Biochemical Analysis

CSF specimens were obtained by lumbar puncture in the L3/4 or L4/5 interspace using a 25-gauge needle, collected in polypropylene tubes, centrifuged at 500 g for 20 minutes, aliquoted in propylene tubes, and stored at –80°C until biochemical analysis, according to international consensus protocols.[29] CSF Aβ40, Aβ42, pTau, and tTau levels were measured by chemiluminescence enzyme immunoassay (CLEIA; Lumipulse G β-amyloid 1–40, Lumipulse G β-amyloid 1–42, Lumipulse G pTau 181, and Lumipulse G Total Tau, Fujirebio Inc.) on a fully automatic platform (Lumipulse G1200 analyzer, Fujirebio Inc.). CSF neurogranin and α-synuclein levels were measured via enzyme-linked immunosorbent (ELISA) assay, according to manufacturer instructions.[30,31]

Statistical Analysis

Statistical analysis was performed by MedCalc statistical software, v. 19.4.1 (MedCalc Software Ltd). Demographic and biochemical variables, as well as CSF biomarker levels, in AD and non-AD groups were expressed as mean (SD) or median (interquartile [IQR]) ranges, as appropriate. Nonparametric testing was performed using Mann-Whitney

Lab Medicine 2021;52;188–196 189
DOI: 10.1093/labmed/lmaa062

rank sum testing or, where appropriate, with the Kruskal-Wallis 1-way analysis of variance (ANOVA) on ranks.

Differences among AD and non-AD groups were compared using Mann-Whitney U and Fisher exact testing. To explore the association between biomarkers and clinical variables, we applied Spearman correlation analysis and multivariate linear regression models. Diagnostic accuracy for AD was evaluated by receiver operating characteristic (ROC) curve analysis and reported as area under the curve (AUC) and 95% confidence interval (95% CI). The best statistical threshold for neurogranin and α-synuclein in AD diagnosis was estimated using the Youden method, selecting the cut point at which the quantity Youden index (sensitivity + specificity – 1) is maximized. Results were considered significant for *P* values less than .05.

Results

The demographical characteristics of patients with and without AD are shown in **Table 1**. Among the patients without AD, 5 had acute polyradiculoneuritis, 5 had myelitis, 1 had bipolar disorder, 1 had trigeminal neuralgia, 3 had conversion disorder, 3 had progressive idiopathic polyneuropathy, 6 had hydrocephalous, 1 had cerebral metastasis, 3 had muscular dystrophy, 8 had neuropathy, 4 had encephalitis, 4 had vascular encephalopathy, 4 had cervical myelopathy, 1 had cerebral aneurysm, 2 had brain cancer, 1 had amyloidosis, 4 had leukoencephalopathy, 1 had epilepsy, and 2 had multiple sclerosis.

As expected, patients with AD showed lower concentrations of CSF Aβ42 and higher levels of CSF tTau and pTau than patients without AD (Aβ42: 632.6 vs 817 pg/mL; tTau: 832.5 vs 231.9 pg/mL; pTau: 80.3 vs 32.4 pg/mL, respectively; $P < .001$ for each). We also observed statistically differences in the Aβ42/Aβ40 ratio between patients with and those without AD (0.05 vs 0.38; $P < .001$). Also, patients with AD had significantly higher levels of CSF neurogranin and α-synuclein than patients without AD (median [IQR], 460 [410–647] vs 187 [163.38–267.93] pg/mL, $P < .001$; and 2844 [2326.9–3524.5] vs 2152 [2058.4–2787.8], $P = .01$, respectively). Finally, no significant correlation between sex and neurogranin and α-synuclein was observed in our study ($r = 0.20$, $P = .12$ and $r = 0.122$, $P = .36$, respectively).

CSF Neurogranin Concentrations in Relation to Core AD Biomarkers

Spearman correlation analysis was performed to investigate the relationship among CSF neurogranin levels and clinical characteristics and core CSF biomarkers in the whole cohort and within each group, as shown in **Table 2**. We observed that CSF neurogranin level is slightly correlated with age ($r = 0.231$; $P = .04$) in all patients, but such correlation was not seen in each subgroup (patients with and without AD) when analyzed separately.

In the AD group, a statistically significant correlation was found between CSF neurogranin and MMSE ($r = – 0.555$, $P = .02$), as shown in **Table 2**. Also, CSF neurogranin level showed strong positive correlation with tTau and pTau in the entire cohort of patients ($r = 0.828$, $P < .001$;

Table 1. Demographic, Clinical, and Biomarker Data by Diagnostic Group

Variable	AD Group (n = 29)	Non-AD Group (n = 59)	*P* Value[a]
Age at onset, y (mean [SD])	67.8 [6.4]	62.5 [11.3]	**.01**
Sex, F/M, no. (% F)	15/14 (51.7%)	46/13 (77.9%)	**.01**
Education (y), median (IQR)	10 (5–16)	8 (5–14)	.62
MMSE, range (IQR)	18.76 (7.4)	…	…
CSF Aβ42 (pg/mL), mean (SD)	632.6 (128.3)	817 (174)	**<.001**
CSF Aβ42/Aβ40 ratio, mean (SD)	0.05 (0.02)	0.38 (0.08)	**<.001**
CSF tTau (pg/mL), mean (SD)	832.5 (432.5)	231.9 (322.4)	**<.001**
CSF pTau (pg/mL), mean (SD)	80.3 (35.1)	32.4 (17.9)	**<.001**
CSF pTau/Aβ42, mean (SD)	0.144 (0.06)	0.08 (0.07)	**.01**
CSF neurogranin (pg/mL), median (IQR)	460 (410–647)	187 (163.38–267.93)	**<.001**
CSF α-synuclein (pg/mL), median (IQR)	2844 (2326.9–3524.5)	2152 (2058.4–2787.8)	**.01**

AD, Alzheimer disease; F, female; M, male; IQR, interquartile range; MMSE, Mini-Mental State Examination; … , nonapplicable; CSF, cerebrospinal fluid; Aβ, amyloid-β; tTau, total tau; pTau, phosphorylated tau.
[a]*Bolding indicates statistical significance.*

$r = 0.762$, $P < .001$, respectively) and in each diagnostic group ($r = 0.828$, $P < .001$; $r = 0.664$, $P = .005$, in patients with AD; $r = 0.858$, $P < .001$; $r = 0.715$, $P < .001$, in patients without AD). Negative correlation between CSF neurogranin and the Aβ42/Aβ40 ratio was found in patients without AD ($r = –0.442$, $P = .006$; **Table 2**) but not in patients with AD. Finally, weak correlation between neurogranin and Aβ42 was observed for patients without AD ($r = 0.356$; $P = .02$), but not for patients with AD.

CSF α-Synuclein Concentrations in Relation to Core AD Biomarkers

Table 3 shows the correlation among CSF α-synuclein and core AD biomarkers. A strong positive correlation between α-synuclein levels and tTau and pTau levels was found in the whole cohort ($r = 0.619$, $P < .001$; $r = 0.574$, $P = .001$, respectively). Such correlation was also statistically significant in patients without AD ($r = 0.585$, $P < .001$; $r = 0.761$, $P < .001$, respectively) but not in patients with AD ($r = 0.514$, $P = .04$; $r = 0.435$, $P = .09$, respectively).

Similarly, a strongly negative correlation was observed between α-synuclein and the Aβ42/Aβ40 ratio in the whole cohort and in patients without AD ($r = –0.432$, $P = .001$; $r = –0.407$, $P = .01$, respectively) but the negative correlation did not reach statistical significance in patients with AD. Moreover, for patients without AD, we found a weak correlation between CSF Aβ42 and α-synuclein levels ($r = 0.350$; $P = .01$). No significant correlation was found between CSF α-synuclein and MMSE in patients with AD.

Correlation among CSF Neurogranin, α-Synuclein, tTau, and pTau

We observed that CSF neurogranin and α-synuclein levels were strongly correlated in the whole cohort and within each diagnostic group ($r = 0.711$, $P < .001$; $r = 0.642$, $P = .003$; $r = 0.706$, $P < .001$), as shown in **Figure 1**. We used a stepwise multiple logistic regression analysis to identify optimal biomarker panels for patients with AD. Using neurogranin as the dependent variable, all included CSF biomarkers (α-synuclein, tTau, and pTau) were significantly associated with neurogranin among patients with AD ($r^2 = 0.829$;

Table 2. Correlations of CSF Neurogranin Levels with Clinical Variables and Core CSF Biomarkers

Variable	All Patients (n = 88)		AD Group (n = 29)		Non-AD Group (n = 59)	
	r	*P* Value	*R*	*P* Value	*r*	*P* Value
Age, y	0.231	.04	–0.073	.77	0.137	.30
MMSE	…	…	–0.555	.02	…	…
CSF Aβ42	0.222	.09	0.055	.84	0.356[a]	.02
CSF Aβ42/CSF Aβ40	–0.567[b]	<.001	–0.394	.13	–0.442[a]	.006
CSF tTau	0.828[b]	<.001	0.858[b]	<.001	0.715[b]	<.001
CSF pTau	0.762[b]	<.001	0.664[a]	.005	0.588[a]	.003

CSF, cerebrospinal fluid; AD, Alzheimer disease; MMSE, Mini-Mental State Examination; … , nonapplicable; Aβ, amyloid-β; tTau, total tau; pTau, phosphorylated tau.
[a]*The correlation coefficient is expressed as* r = P ≤ *.01.*
[b]*The correlation coefficient is expressed as* r = P ≤ *.001.*

Table 3. Correlations of CSF α-Synuclein Levels with Clinical Variables and Core CSF Biomarkers[a]

Variable	All Patients (n = 88)		AD Group (n = 29)		Non-AD Group (n = 59)	
	r	*P* Value	*R*	*P* Value	*r*	*P* Value[b]
Age, y	0.165	.15	–0.300	.23	0.200	.13
MMSE	…	…	–0.147	.57	…	…
CSF Aβ42	0.287	.02	0.205	.44	0.350[c]	.01
CSF Aβ42/CSF Aβ40	–0.432[c]	.001	–0.166	.54	–0.407[c]	.01
CSF tTau	0.619[d]	<.001	0.514	.04	0.585[d]	**<.001**
CSF pTau	0.574[d]	<.001	0.435	.09	0.761[d]	**<.001**

CSF, cerebrospinal fluid; AD, Alzheimer disease; MMSE, Mini-Mental State Examination; … , nonapplicable; Aβ, amyloid-β; tTau, total tau; pTau, phosphorylated tau.
[a]*Associations were investigated using Spearman correlation analyses.*
[b]*Bolding indicates statistical significance.*
[c]*The correlation coefficient is expressed as* r = P ≤*.01.*
[d]*The correlation coefficient is expressed as* r = P ≤*.001.*

DOI: 10.1093/labmed/lmaa062

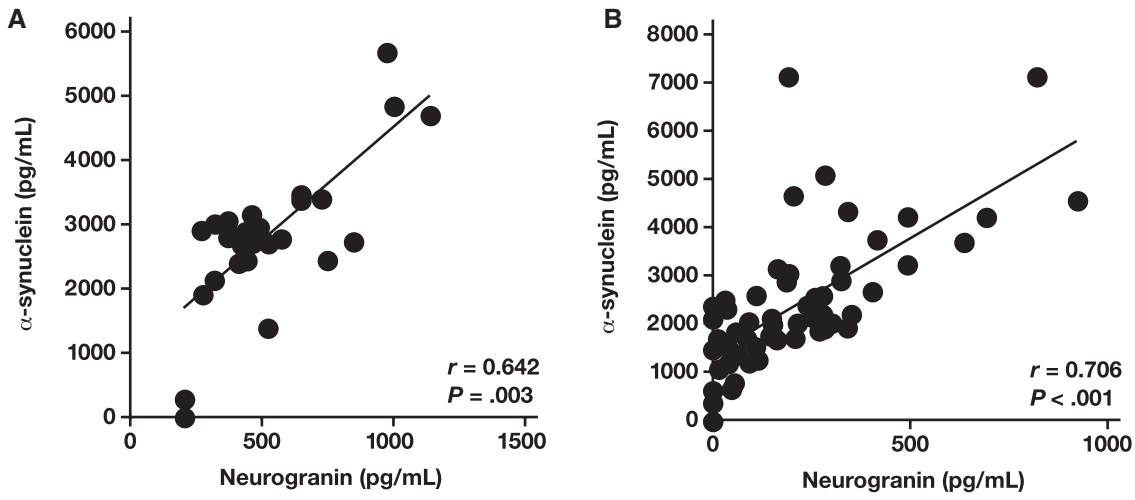

Figure 1

Protein profiles of neurogranin and α-synuclein in cerebrospinal fluid (CSF) specimens from patients with Alzheimer disease (AD; **A**) and patients with non-AD neurodegenerative disorders (**B**).

$P < .001$). In the adjusted analysis for cognition, all of these variables remained associated ($r^2 = 0.779$, $P < .001$). When using α-synuclein as a dependent variable, statistically significant association was found among CSF biomarkers ($r^2 = 0.512$; $P = .03$). However, we did not find significant correlation when using adjusted analysis ($r^2 = 0.39$; $P > .05$; data not shown).

ROC Curve Analysis of CSF Neurogranin and α-Synuclein

Per the ROC curve analysis for the AD diagnosis, the AUC of neurogranin was 0.872 (95% CI, 0.777–0.937; Figure 2). The statistical best cut point for neurogranin associated with AD, as calculated via the Youden index, was 306 pg per mL, with sensitivity of 84.2%, specificity of 78%, and Youden index of 0.621. The AUC of α-synuclein for AD diagnosis was 0.681 (0.656–0.782). The statistical best cut point for α-synuclein associated with AD was 2683 pg per mL with sensitivity of 73.3%, specificity of 72.9%, and Youden index of 0.465.

Discussion

Synaptic dysfunction and loss are early events in cognitive impairment in patients with AD.[32] Therefore, biomarkers reflecting synaptic integrity in the brain could be useful for accurate early diagnosis and disease prognosis.

The main findings of our study can be summarized as follows. First, CSF levels of neurogranin and α-synuclein are significantly increased in patients with AD than patients without AD. Second, neurogranin and α-synuclein levels are significantly correlated in the entire population and in each subgroup (patients with and without AD). Third, neurogranin was significantly correlated with pTau and tTau in the entire population and in each subgroup. Moreover, neurogranin was correlated with MMSE in patients with AD. Fourth, α-synuclein was significantly correlated with pTau and tTau in the entire population. However, such correlation was maintained only in patients without AD when separately analyzing the 2 subgroups. Moreover, α-synuclein was not correlated with MMSE in patients with AD. Fifth, per ROC curve analysis, neurogranin, but not α-synuclein, showed good diagnostic accuracy for AD diagnosis. Thus, our findings encourage the use of neurogranin as a synaptic dysfunction biomarker specific for AD. Although α-synuclein also reflects the synaptic damage in neurodegenerative diseases, it seems not to be specific for AD.

Neurogranin is a calmodulin-binding protein expressed exclusively in the brain, particularly in dendritic spines of postsynaptic neurons, with an important role in synaptic plasticity, long-term potentiation, learning, and memory.[33,34] Recently, some authors[35–41] reported that

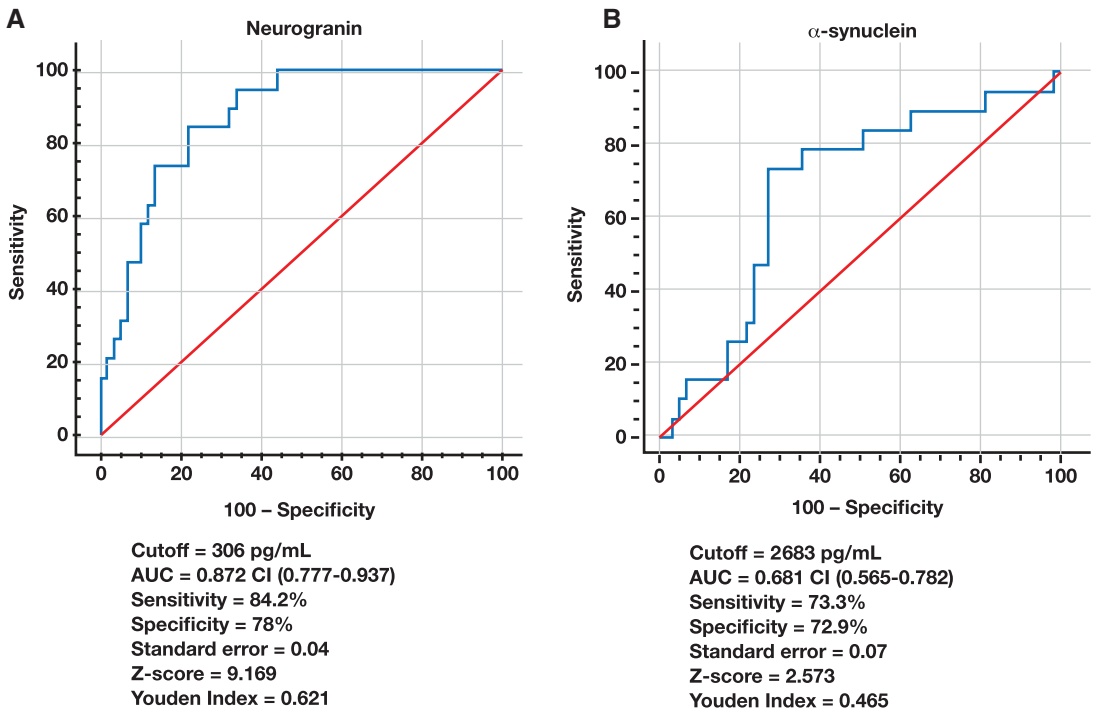

Figure 2

Receiver operating characteristic (ROC) curves of cerebrospinal fluid (CSF) neurogranin and α-synuclein for Alzheimer disease (AD) diagnosis. Data are expressed in pg/mL; AUC, area under the curve, 95% CI, 95% confidence interval.

CSF neurogranin levels are significantly higher in patients with AD compared with healthy controls; thus, neurogranin has emerged as a promising CSF biomarker for synapse damage in AD.

The interest on the postsynaptic proteins in AD has been further supported by evidence that increased CSF neurogranin levels are indicative of future cognitive deterioration because they increase in patients with MCI that will convert to AD, compared with patients whose health remains stable.[42–44] In contrast, initial study findings[45] revealed that neurogranin levels were markedly reduced in the hippocampus and frontal lobes in patients with AD. Also, a recent study report[46] revealed decreased neurogranin levels as biomarker of future cognitive deterioration.

Our results, in line with those of Portelius et al[47] and Wellington et al,[48] highlighted that the increased CSF neurogranin levels are specific to AD. A possible explanation is that although synapse degeneration is a common event of all neurodegenerative processes, neurogranin is mainly expressed in the brain regions involved in AD, namely, the amygdala, hippocampus, and neocortex.[49] Also, we found a negative correlation between CSF neurogranin concentration and cognitive function, as evaluated by the MMSE, in patients with AD. Because tau alterations are not characteristic of AD, neurogranin, as a biomarker of synaptic degeneration specific of AD, could be assessed together with CSF core biomarkers for supporting the early diagnosis of AD. However, contrasting data have been reported,[50,51] so further investigations are needed.

We noted that there is high variability in the CSF neurogranin levels revealed by different studies. Our results are in agreement with those of Kvartsberg et al[42] but contrast with those of Kester et al,[41] which report lower neurogranin levels. These differences probably could be linked to variability among kits from different manufacturers. Thus, future studies to determine cutoff levels are imperative.

An alternative or complementary potential biomarker for AD is α-synuclein, a presynaptic protein expressed in cortical

DOI: 10.1093/labmed/lmaa062

and subcortical areas, which is involved in neurotransmitter synthesis and release, as well as synaptic plasticity.[52] It has been strongly implicated in Parkinson disease (PD) pathogenesis and other Parkinsonian syndromes, such as multiple system atrophy and dementia with Lewy bodies.[53] Recent evidence[54] suggest that α-synuclein might be involved in AD cognitive decline by interacting with Aβ and tau peptides and promoting their aggregation with consequent neuronal damage.

Although it is confirmed[55,56] that patients with PD have decreased CSF α-synuclein levels, findings in patients with AD are inconsistent, with authors[57–61] reporting no variation, or lower or higher CSF α-synuclein concentrations. In our study, we found that CSF α-synuclein significantly increases in patients with AD. However, it did not show good diagnostic accuracy for AD and it was not correlated with tau levels or MMSE scores. These findings suggest that CSF α-synuclein probably is unfit as a diagnostic biomarker for AD.

We were intrigued to find a highly significant correlation between neurogranin and pTau levels, as well as tTau levels, in patients with and without AD. Tau is a cytoskeletal protein associated with microtubules, primarily expressed in axons of the neurons of the central nervous system, where it promotes the bind and stability of microtubules.[62] Tau can undergo several post-translational modifications, including phosphorylation. The hyperphosphorylation of tau occurring in AD is the result of Aβ-mediated mitochondrial oxidative stress.[63] It is well known[64] that hyperphosphorylation of tau reduces its affinity to microtubules, promoting its aggregation into neurofibrillary tangles, which cause defective axonal transport and neuronal damage, leading to neuronal loss. Hence, tau levels reflect the intensity of AD neurodegeneration.

In our study results, we found a statically significant correlation between neurogranin and tau levels in patients with AD, highlighting the promising role of this protein as an AD biomarker. Also, in line with Bruno et al,[65] we discovered that CSF α-synuclein levels were associated with CSF neurogranin concentrations. Based on multiple regression analysis, we found that neurogranin was significantly associated with CSF tTau, pTau, and α-synuclein in patients with AD. Taken together, our findings support the hypothesis that CSF neurogranin could represent a biomarker of neurodegeneration in patients with AD. The increase in neurogranin levels could be the consequence of synaptic injury, leading to cognitive deterioration.

A few limitations of the present study should be addressed. First, we did not include healthy control individuals because we had difficulty obtaining CSF specimens from healthy subjects. A second limitation was the small number of patients with AD in the cohort. Ideally, we would have examined CSF specimens from a larger number of patients, and this process should have involved longitudinal specimen gathering.

Conclusions

Our results support a role for CSF neurogranin as a biomarker for AD, reflecting synaptic loss. Further investigations in larger populations are encouraged, to confirm our results and to support the introduction of neurogranin into the panel of CSF biomarkers for AD diagnosis and monitoring of cognitive decline. **LM**

References

1. Perl DP. Neuropathology of Alzheimer's disease. *Mt Sinai J Med.* 2010;77(1):32–42.
2. Vickers JC, Mitew S, Woodhouse A, et al. Defining the earliest pathological changes of Alzheimer's disease. *Curr Alzheimer Res.* 2016;13(3):281–287.
3. Jackson J, Jambrina E, Li J, et al. Targeting the synapse in Alzheimer's disease. *Front Neurosci.* 2019;13:735.
4. Wilson RS, Segawa E, Boyle PA, Anagnos SE, Hizel LP, Bennett DA. The natural history of cognitive decline in Alzheimer's disease. *Psychol Aging.* 2012;27(4):1008–1017.
5. Yildirim E, Soncu Buyukiscan E, Demirtas-Tatlidede A, Bilgiç B, Gurvit H. An investigation of affective theory of mind ability and its relation to neuropsychological functions in Alzheimer's disease. *J Neuropsychol.* 2020; doi: 10.1111/jnp.12207.
6. Ito K, Ahadieh S, Corrigan B, French J, Fullerton T, Tensfeldt T; Alzheimer's Disease Working Group. Disease progression meta-analysis model in Alzheimer's disease. *Alzheimers Dement.* 2010;6(1):39–53.
7. Jack CR Jr, Knopman DS, Jagust WJ, et al. Hypothetical model of dynamic biomarkers of the Alzheimer's pathological cascade. *Lancet Neurol.* 2010;9(1):119–128.
8. Blennow K, Zetterberg H. The past and the future of Alzheimer's disease fluid biomarkers. *J Alzheimers Dis.* 2018;62(3):1125–1140.

9. Ritchie C, Smailagic N, Noel-Storr AH, Ukoumunne O, Ladds EC, Martin S. CSF tau and the CSF tau/ABeta ratio for the diagnosis of Alzheimer's disease dementia and other dementias in people with mild cognitive impairment (MCI). *Cochrane Database Syst Rev.* 2017;3:CD010803.
10. Agnello L, Piccoli T, Vidali M, et al. Diagnostic accuracy of cerebrospinal fluid biomarkers measured by chemiluminescent enzyme immunoassay for Alzheimer disease diagnosis. *Scand J Clin Lab Invest.* 2020;80(4):313–317.
11. Lafirdeen ASM, Cognat E, Sabia S, et al. Biomarker profiles of Alzheimer's disease and dynamic of the association between cerebrospinal fluid levels of β-amyloid peptide and tau. *PLoS One.* 2019;14(5):e0217026.
12. Mattsson N, Lönneborg A, Boccardi M, Blennow K, Hansson O; Geneva Task Force for the Roadmap of Alzheimer's Biomarkers. Clinical validity of cerebrospinal fluid Aβ42, tau, and phospho-tau as biomarkers for Alzheimer's disease in the context of a structured 5-phase development framework. *Neurobiol Aging.* 2017;52:196–213.
13. Andreasen N, Blennow K. CSF biomarkers for mild cognitive impairment and early Alzheimer's disease. *Clin Neurol Neurosurg.* 2005;107(3):165–173.
14. Goodall CA, Head MW, Everington D, Ironside JW, Knight RSG, Green AJE. Raised CSF phospho-tau concentrations in variant Creutzfeldt-Jakob disease: diagnostic and pathological implications. *J Neurol Neurosurg Psychiatry.* 2006;77(1):89–91.
15. Medana IM, Lindert RB, Wurster U, et al. Cerebrospinal fluid levels of markers of brain parenchymal damage in Vietnamese adults with severe malaria. *Trans R Soc Trop Med Hyg.* 2005;99(8):610–617.
16. Matsushita S, Miyakawa T, Maesato H, et al. Elevated cerebrospinal fluid tau protein levels in Wernicke's encephalopathy. *Alcohol Clin Exp Res.* 2008;32(6):1091–1095.
17. Molinuevo JL, Blennow K, Dubois B, et al. The clinical use of cerebrospinal fluid biomarker testing for Alzheimer's disease diagnosis: a consensus paper from the Alzheimer's Biomarkers Standardization Initiative. *Alzheimers Dement.* 2014;10(6):808–817.
18. Bivona G, Lo Sasso B, Iacolino G, et al. Standardized measurement of circulating vitamin D [25(OH)D] and its putative role as a serum biomarker in Alzheimer's disease and Parkinson's disease. *Clin Chim Acta.* 2019;497:82–87.
19. Bivona G, Gambino CM, Iacolino G, Ciaccio M. Vitamin D and the nervous system. *Neurol Res.* 2019;41(9):827–835.
20. Nagaraj S, Laskowska-Kaszub K, Dębski KJ, et al. Profile of 6 microRNA in blood plasma distinguish early stage Alzheimer's disease patients from non-demented subjects. *Oncotarget.* 2017;8:16122–16143.
21. Goetzl EJ, Boxer A, Schwartz JB, et al. Altered lysosomal proteins in neural-derived plasma exosomes in preclinical Alzheimer disease. *Neurology.* 2015;85(1):40–47.
22. Bivona G, Agnello L, Bellia C, et al. Non-skeletal activities of vitamin D: from physiology to brain pathology. *Medicina (Kaunas).* 2019;55(7):341.
23. Sharma N, Singh AN. Exploring biomarkers for Alzheimer's disease. *J Clin Diagn Res.* 2016;10(7):KE01–KE6.
24. Zetterberg H, Bendlin BB. Biomarkers for Alzheimer's disease—preparing for a new era of disease-modifying therapies. *Mol Psychiatry.* 2020; doi: 10.1038/s41380-020-0721-9.
25. Hameed S, Fuh J-L, Senanarong V, et al. Role of fluid biomarkers and PET imaging in early diagnosis and its clinical implication in the management of Alzheimer's disease. *J Alzheimers Dis Rep.* 2020;4(1):21–37.
26. Boccardi M, Nicolosi V, Festari C, et al. Italian consensus recommendations for a biomarker-based aetiological diagnosis in mild cognitive impairment patients. *Eur J Neurol.* 2020;27(3):475–483.
27. McKhann GM, Knopman DS, Chertkow H, et al. The diagnosis of dementia due to Alzheimer's disease: recommendations from the National Institute on Aging-Alzheimer's Association workgroups on diagnostic guidelines for Alzheimer's disease. *Alzheimers Dement.* 2011;7(3):263–269.
28. Albert MS, DeKosky ST, Dickson D, et al. The diagnosis of mild cognitive impairment due to Alzheimer's disease: recommendations from the National Institute on Aging-Alzheimer's Association workgroups on diagnostic guidelines for Alzheimer's disease. *Alzheimers Dement.* 2011;7(3):270–279.
29. del Campo M, Mollenhauer B, Bertolotto A, et al. Recommendations to standardize preanalytical confounding factors in Alzheimer's and Parkinson's disease cerebrospinal fluid biomarkers: an update. *Biomark Med.* 2012;6(4):419–430.
30. Vanderstichele H, Demeyer L, Janelidze S, et al. Recommendations for cerebrospinal fluid collection for the analysis by ELISA of neurogranin trunc P75, α-synuclein, and total tau in combination with Aβ(1-42)/Aβ(1-40). *Alzheimers Res Ther.* 2017;9(1):40.
31. De Schaepdryver M, Jeromin A, Gille B, et al. Comparison of elevated phosphorylated neurofilament heavy chains in serum and cerebrospinal fluid of patients with amyotrophic lateral sclerosis. *J Neurol Neurosurg Psychiatry.* 2018;89(4):367–373.
32. Shankar GM, Walsh DM. Alzheimer's disease: synaptic dysfunction and Aβ. *Mol Neurodegener.* 2009;4:48.
33. Díez-Guerra FJ. Neurogranin, a link between calcium/calmodulin and protein kinase C signaling in synaptic plasticity. *IUBMB Life.* 2010;62(8):597–606.
34. Shinohara M, Fujioka S, Murray ME, et al. Regional distribution of synaptic markers and APP correlate with distinct clinicopathological features in sporadic and familial Alzheimer's disease. *Brain.* 2014;137(5):1533–1549.
35. Remnestål J, Just D, Mitsios N, et al. CSF profiling of the human brain enriched proteome reveals associations of neuromodulin and neurogranin to Alzheimer's disease. *Proteomics Clin Appl.* 2016;10(12):1242–1253.
36. Tarawneh R, D'Angelo G, Crimmins D, et al. Diagnostic and prognostic utility of the synaptic marker neurogranin in Alzheimer disease. *JAMA Neurol.* 2016;73(5):561–571.
37. Galasko D, Xiao M, Xu D, et al; Alzheimer's Disease Neuroimaging Initiative (ADNI). Synaptic biomarkers in CSF aid in diagnosis, correlate with cognition and predict progression in MCI and Alzheimer's disease. *Alzheimers Dement (N Y).* 2019;5:871–882.
38. De Vos A, Jacobs D, Struyfs H, et al. C-terminal neurogranin is increased in cerebrospinal fluid but unchanged in plasma in Alzheimer's disease. *Alzheimers Dement.* 2015;11(12):1461–1469.
39. Hellwig K, Kvartsberg H, Portelius E, et al. Neurogranin and YKL-40: independent markers of synaptic degeneration and neuroinflammation in Alzheimer's disease. *Alzheimers Res Ther.* 2015;7:74.
40. Janelidze S, Hertze J, Zetterberg H, et al. Cerebrospinal fluid neurogranin and YKL-40 as biomarkers of Alzheimer's disease. *Ann Clin Transl Neurol.* 2016;3(1):12–20.
41. Kester MI, Teunissen CE, Crimmins DL, et al. Neurogranin as a cerebrospinal fluid biomarker for synaptic loss in symptomatic Alzheimer disease. *JAMA Neurol.* 2015;72(11):1275–1280.
42. Kvartsberg H, Duits FH, Ingelsson M, et al. Cerebrospinal fluid levels of the synaptic protein neurogranin correlates with cognitive decline in prodromal Alzheimer's disease. *Alzheimers Dement.* 2015;11(10):1180–1190.
43. Mattsson N, Insel PS, Palmqvist S, et al; for the Alzheimer's Disease Neuroimaging Initiative. Cerebrospinal fluid tau, neurogranin, and neurofilament light in Alzheimer's disease. *EMBO Mol Med.* 2016;8(10):1184–1196.
44. Portelius E, Zetterberg H, Skillbäck T, et al; Alzheimer's Disease Neuroimaging Initiative. Cerebrospinal fluid neurogranin: relation to cognition and neurodegeneration in Alzheimer's disease. *Brain.* 2015;138(11):3373–3385.
45. Davidsson P, Blennow K. Neurochemical dissection of synaptic pathology in Alzheimer's disease. *Int Psychogeriatr.* 1998;10(1):11–23.

DOI: 10.1093/labmed/lmaa062

46. Bos I, Vos SJB, Schindler SE, et al. Vascular risk factors are associated with longitudinal changes in cerebrospinal fluid tau markers and cognition in preclinical Alzheimer's disease. *Alzheimers Dement.* 2019;15(9):1149–1159.
47. Portelius E, Olsson B, Höglund K, et al. Cerebrospinal fluid neurogranin concentration in neurodegeneration: relation to clinical phenotypes and neuropathology. *Acta Neuropathol.* 2018;136(3):363–376.
48. Wellington H, Paterson RW, Portelius E, et al. Increased CSF neurogranin concentration is specific to Alzheimer disease. *Neurology.* 2016;86(9):829–835.
49. Yilmaz A, Fuchs D, Price RW, et al. Cerebrospinal fluid concentrations of the synaptic marker neurogranin in neuro-HIV and other neurological disorders. *Curr HIV/AIDS Rep.* 2019;16(1):76–81.
50. Villar-Pique A, Zerr I, Llorens F. Cerebrospinal fluid neurogranin as a new player in prion disease diagnosis and prognosis. *Neural Regen Res.* 2020;15(5):861–862.
51. Blennow K, Diaz-Lucena D, Zetterberg H, et al. CSF neurogranin as a neuronal damage marker in CJD: a comparative study with AD. *J Neurol Neurosurg Psychiatry.* 2019;90(8):846–853.
52. Cheng F, Vivacqua G, Yu S. The role of α-synuclein in neurotransmission and synaptic plasticity. *J Chem Neuroanat.* 2011;42(4):242–248.
53. Selnes P, Stav AL, Johansen KK, et al. Impaired synaptic function is linked to cognition in Parkinson's disease. *Ann Clin Transl Neurol.* 2017;4(10):700–713.
54. Twohig D, Nielsen HM. α-synuclein in the pathophysiology of Alzheimer's disease. *Mol Neurodegener.* 2019;14(1):23.
55. Hong Z, Shi M, Chung KA, et al. DJ-1 and α-synuclein in human cerebrospinal fluid as biomarkers of Parkinson's disease. *Brain.* 2010;133(3):713–726.
56. Tokuda T, Salem SA, Allsop D, et al. Decreased α-synuclein in cerebrospinal fluid of aged individuals and subjects with Parkinson's disease. *Biochem Biophys Res Commun.* 2006;349(1):162–166.
57. Larson ME, Sherman MA, Greimel S, et al. Soluble α-synuclein is a novel modulator of Alzheimer's disease pathophysiology. *J Neurosci.* 2012;32(30):10253–10266.
58. Wang DS, Bennett DA, Mufson E, Cochran E, Dickson DW. Decreases in soluble α-synuclein in frontal cortex correlate with cognitive decline in the elderly. *Neurosci Lett.* 2004;359(1-2):104–108.
59. Reesink FE, Lemstra AW, van Dijk KD, et al. CSF α-synuclein does not discriminate dementia with Lewy bodies from Alzheimer's disease. *J Alzheimers Dis.* 2010;22(1):87–95.
60. Tateno F, Sakakibara R, Kawai T, Kishi M, Murano T. Alpha-synuclein in the cerebrospinal fluid differentiates synucleinopathies (Parkinson Disease, dementia with Lewy bodies, multiple system atrophy) from Alzheimer disease. *Alzheimer Dis Assoc Disord.* 2012;26(3):213–216.
61. Twohig D, Rodriguez-Vieitez E, Sando SB, et al; Dominantly Inherited Alzheimer Network (DIAN). The relevance of cerebrospinal fluid α-synuclein levels to sporadic and familial Alzheimer's disease. *Acta Neuropathol Commun.* 2018;6(1):130.
62. Rodríguez-Martín T, Cuchillo-Ibáñez I, Noble W, Nyenya F, Anderton BH, Hanger DP. Tau phosphorylation affects its axonal transport and degradation. *Neurobiol Aging.* 2013;34(9):2146–2157.
63. Lejri I, Agapouda A, Grimm A, Eckert A. Mitochondria- and oxidative stress-targeting substances in cognitive decline-related disorders: from molecular mechanisms to clinical evidence. *Oxid Med Cell Longev.* 2019;2019:9695412.
64. Cuchillo-Ibanez I, Seereeram A, Byers HL, et al. Phosphorylation of tau regulates its axonal transport by controlling its binding to kinesin. *FASEB J.* 2008;22(9):3186–3195.
65. Bruno D, Reichert Plaska C, Clark DPA, et al. CSF α-synuclein correlates with CSF neurogranin in late-life depression. *Int J Neurosci.* 2020;__:1–5.

Comparison of Nucleic Acid Amplification and IgM Tests for the Diagnosis of *Mycoplasma pneumoniae* Infection in Children During a Recent Korean Outbreak

Hye-Young Lee, MD,[1,2] Seunghwan Sul, MT,[1] Jeong Young Lee, MT,[1] Mi-Na Kim, MD, PhD,[1] Jinho Yu, MD, PhD,[3] Heungsup Sung, MD, PhD[1,]*

Laboratory Medicine 2021;52:181-187

DOI: 10.1093/labmed/lmaa048

ABSTRACT

Objective: In the absence of standardized methods for *Mycoplasma pneumoniae* detection, we evaluated the diagnostic value of polymerase chain reaction (PCR) and IgM assays for detecting *M. pneumoniae* infection in children during a recent Korean outbreak.

Methods: The diagnostic performances of PCR and IgM assays for *M. pneumoniae* in 1,109 clinical specimens were evaluated by the Japanese Respiratory Society (JRS) scoring system as an interim reference standard.

Results: The level of agreement between both tests was fair. As analyzed by the JRS scoring system, the sensitivity of PCR was 45.2% in the group aged <5 years, 86.8% in the group aged 5 years to 10 years group, and 72.2% in the group aged 10 years to 18 years; the sensitivity of the IgM assay was 66.8%, 71.4%, and 55.6% in each group, respectively.

Conclusion: The sensitivity of PCR is relatively low but is superior to that of IgM assays such that diagnostic performance can be improved by both test methods in patients aged <5 years .

Keywords: *Mycoplasma pneumoniae*, polymerase chain reaction, anti-*Mycoplasma pneumoniae* IgM, outbreak, sensitivity, diagnostic performance

Mycoplasma pneumoniae (*M. pneumoniae*) is a major causative pathogen of respiratory tract infection, accounting for as much as 10% to 40% of all community-acquired pneumonia (CAP).[15,5] *M. pneumoniae* pneumonia is prevalent in children and young adults.[6-8] Because β-lactam antibiotics used in other types of CAP are ineffective in this type of pneumonia,[9,10] the timely and accurate diagnosis of *M. pneumoniae* infection and subsequent initiation of adequate antibiotic therapy are crucial. Most patients present with gradual disease onset, and the nonspecificity of the clinical symptoms, such as fever, chill, cough, and headache, can make the clinical diagnosis challenging.[11,12] Therefore, laboratory methods for correctly determining pneumonia etiology are necessary.

Several laboratory diagnostic tests have been suggested for *M. pneumoniae* detection,[13-15] but a consensus reference method remains to be determined. *M. pneumoniae* culture is accurate and mostly reliable but has limitations for the diagnosis of *M. pneumoniae* infection because of the particular nature of this organism's growth in culture.[11,12] Using a 4-fold rise of IgG titer in paired specimens collected 2 to 3 weeks apart, the traditional gold standard for *M. pneumoniae* diagnosis, is time consuming and delays diagnostic decision-making.[11,12] In routine practice, serology has been commonly used, but cross-reaction or delayed immune response can cause false-positive or false-negative results.[1,12] Recently,

Abbreviations

PCR, polymerase chain reaction; JRS, Japanese Respiratory Society; CAP, community-acquired pneumonia; PPV, positive predictive value; NPV, negative predictive value.

[1]Department of Laboratory Medicine, University of Ulsan College of Medicine and Asan Medical Center, Seoul, Korea, [2]Department of Laboratory Medicine, U2Bio Laboratories, Seoul, Republic of Korea, [3]Department of Pediatrics, University of Ulsan College of Medicine and Asan Medical Center, Seoul, Korea

*To whom correspondence should be addressed.
sung@amc.seoul.kr

polymerase chain reaction (PCR) has been developed and clinically utilized to diagnose *M. pneumoniae* infection.[6,9,14] Although several studies have shown that PCR is more useful than serological tests to detect early *M. pneumoniae* infection, the presence of asymptomatic carriers can affect the PCR results and clinical interpretations.[4,6,9,14]

In this study, in the absence of standardized test methods for *M. pneumoniae* detection, we evaluated the diagnostic value of PCR and IgM assays for detecting *M. pneumoniae* infection in children of different age groups in the clinical setting of a recent outbreak in Korea. In addition to investigating assay performance, we evaluated the clinical and laboratory characteristics of patient groups with discrepant results on PCR and IgM testing.

Materials and Methods

Study Setting and Population

This retrospective study was performed in a single tertiary-care hospital in Korea between July 2014 and June 2017. The outbreak of *M. pneumoniae* infection occurred during the study period, and clinical specimens (sputum and endotracheal aspirates for PCR or serum for IgM) from 1,109 patients with suspected respiratory tract infection and compatible symptoms (fever and cough with or without respiratory distress) were tested for infection with *M. pneumoniae*; we performed both PCR and IgM tests on those patients for the ease and speed of diagnosis in an actual clinical setting in a pediatric emergency department. Most pediatric patients were also screened for blood culture and respiratory virus PCR when feasible. The exclusion criteria included nosocomial infections and the use of antibiotics in the 48 hours before diagnosis. Patients' guardians denied previous *M. pneumoniae* infection on the medical records. This study was approved by the institutional review board of the Asan Medical Center (2018-1294). Informed consent was waived by the institutional review board because this study was performed retrospectively and extra clinical specimens were not required.

Data Collection

The clinical and laboratory data were reviewed via electronic medical records. The analyzed clinical data included age, sex, presence of underlying illness (comorbidity), symptoms, febrile days, and history of prior antibiotics use. Laboratory results such as peripheral leukocyte counts, hemoglobin, platelet count, C-reactive protein, and coinfection were also reviewed and analyzed.

Applying Clinical Criteria for *M. pneumoniae* Pneumonia

Patients with positive PCR and/or a positive IgM assay result were considered to have a laboratory diagnosis of *M. pneumoniae* infection. To compare the performance of DNA detection by PCR and IgM assay, we used the Japanese Respiratory Society (JRS) scoring system, which is a diagnostic tool for the identification of *M. pneumoniae* infection based on clinical and laboratory findings[2,16,17]; if either positive result for PCR or IgM was applied as the gold standard, then each specificity and positive predictive value (PPV) indicated 100% so that it provided a limitation on the proper assessment of the 2 methods.

The sensitivity and specificity of the JRS system are 88.7% and 77.5%, with positivity on both culture and PCR as the gold standard.[16,17] The JRS scoring system includes 6 parameters[16,17]: (i) aged <60 years, (ii) absence of or only minor underlying diseases, (iii) persistent cough, (iv) adverse findings on chest auscultation, (v) absence of identifiable etiological agent in sputum by rapid diagnostic testing, and (vi) a peripheral white blood cell count $<10 \times 10^9$/L. A score of ≥4 points indicates a high probability of *M. pneumoniae* pneumonia, and a score of ≤3 points shows that *M. pneumoniae* pneumonia is less likely and typical bacterial pneumonia is more plausible.[16]

PCR for *M. pneumoniae* DNA and Chemiluminescent Assay for *M. pneumoniae* IgM

Respiratory and peripheral blood specimens were collected immediately after admission. *M. pneumoniae* DNA testing was conducted with the AmpliSens *Mycoplasma pneumoniae/Chlamydia pneumoniae*-FRT PCR kit (InterLabService Ltd, Moscow, Russia), as previously reported.[18] Serological testing was performed with the LIAISON *Mycoplasma pneumoniae* IgM kit (DiaSorin, Dublin, Ireland) for the detection of *M. pneumoniae* IgM antibodies, according to the manufacturer's instructions. An index value >10 was regarded as a positive result.

Data Analysis

The overall agreement of the PCR and IgM assays for detecting *M. pneumoniae* infection and the diagnostic performance of both laboratory methods among different age groups (aged <5 years, aged 5 years–10 years, and aged 10 years–18 years) were evaluated. The patients who tested positive were classified into 3 groups: group 1, PCR(+)/IgM(+); group 2, PCR(+)/IgM(-); and group 3, PCR(-)/IgM (+). Comparisons were made between group 1 vs group 2, group 1 vs group 3, and group 2 vs 3. The assay agreement and diagnostic performance were evaluated with the JRS scoring system as the interim reference standard. The clinical data are presented as medians or as positive rates. Laboratory data are expressed as mean ± SD. To perform the comparisons, we used the Pearson χ^2 test or Fisher exact test for categorical variables and the Mann-Whitney *U* test for continuous variables, when appropriate. Significance across more than 2 groups was determined using the 1-way analysis of variance or Pearson χ^2 test. Paired proportions of discordant PCR and serological results in each age group were analyzed by the McNemar test. A *P* value <.005 was defined as clinically significant. All statistical analyses were 2-tailed and performed with SPSS version 19 (SPSS Inc, Chicago, IL).

Results

Comparison of *M. pneumoniae* PCR and IgM

Overall, PCR and serology showed a fair level of agreement (k = 0.34, minimal correlation level). Approximately 64.0% of patients (710/1,109) tested positive for PCR and/or IgM. We found that approximately 39.0% of patients (433/1,109) had PCR positivity and 55.0% (610/1,109) had IgM positivity. Of the patients with positive PCR results, 46.9% (333/710) also had positive IgM results. When the patients with positive PCR results were classified into the 3 age groups (aged <5 years [85 cases], aged 5 years–10 years [256 cases], and aged 10–18 years [92 cases]), some differences in assay performance emerged; 76 (89.4%), 196 (76.6%), and 61 (66.3%) cases, respectively, were positive for IgM (**Figure 1**). The proportion of IgM positivity decreased with age among patients with positive PCR results.

Because there was no reference standard for the laboratory diagnosis of *M. pneumoniae*, we analyzed the PCR and IgM assay results using the JRS scoring system as an interim reference standard. As shown in **Table 1**, the estimated sensitivity and specificity of PCR were 56.3% and 96.1%, respectively. The PPV of PCR was 72.0%, and the negative predictive value was 92.6%. In contrast, the IgM assay had a sensitivity of 59.4% and a specificity of 88.4%. The PPV and negative predictive value (NPV) of IgM were 47.5% and 92.3%, respectively.

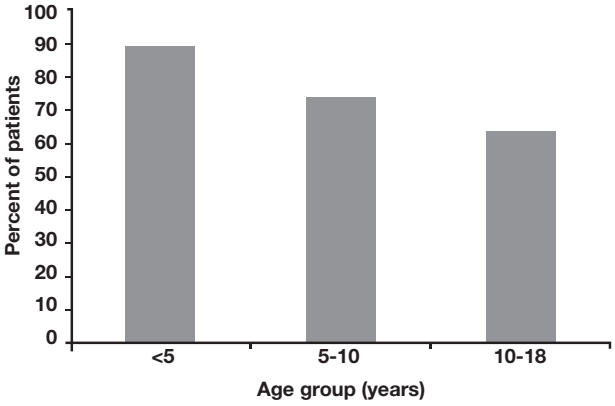

Figure 1

Proportion of IgM positivity in positive PCR results for *M. pneumoniae* in children with different age groups.

Table 1. Diagnostic Values of Laboratory Test Methods with JRS Score as the Interim Gold Standard

	Sensitivity	Specificity	PPV	NPV	Accuracy
PCR					
<5 y	45.2	85.5	68.8	68.9	68.9
5–10 y	86.8	58.3	79.8	70.0	77.0
10–18 y	72.2	89.2	79.6	84.7	83.0
Total	56.3	96.1	72.0	92.6	91.2
IgM					
<5 y	66.8	54.6	50.9	70.0	59.6
5–10 y	71.4	40.6	60.8	42.9	60.8
10–18 y	55.6	76.3	57.7	74.7	68.7
Total	59.4	88.4	47.5	92.3	84.1
PCR or IgM					
<5 y	73.5	51.9	51.9	73.5	60.8
5–10 y	97.3	35.4	74.1	87.2	75.9
10–18 y	77.8	69.9	60.0	84.4	72.8
Total	73.9	87.2	50.4	95.0	85.2

JRS, Japanese Respiratory Society; PCR, polymerase chain reaction; PPV, positive predictive value; NPV, negative predictive value.
All values are expressed as percentages.

DOI: 10.1093/labmed/lmaa048

Notably, some assay performance differences according to age group were found. The PCR sensitivity was 45.2% in the group aged <5 years, 86.8% in the group aged 5 years to 10 years, and 72.2% in the group aged 10 years to 18 years. Correspondingly, the IgM assay sensitivity was 66.8%, 71.4%, and 55.6%, respectively. When either positive result for PCR or IgM was applied as the gold standard, the PCR sensitivity was 34.4% in the group aged <5 years, 75.1% in the group aged 5 years to 10 years, and 75.4% in the group aged 10 years to 18 years (see Supplemental Table 1). These results tended to be similar when we applied the JRS scoring system as a gold standard. We also found that the IgM assay sensitivity in each group was 96.4%, 82.4%, and 74.6%, respectively, based on the corresponding criteria (see Supplemental Table 1).

The positive rate with PCR was lower than the positive rate with IgM assay in the group aged <5 years (P <.001 by McNemar test) (**Table 2**). No significant difference between PCR and IgM assay performance was found with the specimens from children aged >5 years.

Clinical and Laboratory Findings

Table 3 shows the clinical and laboratory characteristics of 3 patient groups classified by PCR and IgM assay results. The mean patient age in each group was 5.0 ± 3.2 years (group 1), 6.5 ± 3.6 years (group 2), and 3.1 ± 3.6 years (group 3). Notably, the comorbidity rate was higher in group 3 than in any other group (group 1 vs group 3, P <.001; group 2 vs group 3, P =.002). Group 1 had higher rates of macrolide use (n = 160, 48.0%), a JRS score ≥4 (n = 247, 74.2%), and a longer febrile period (6.5 days ± 3.6). Patients in group 3 had more coinfections than those in group 1 and group 2 (group 1 vs group 3, P <.001; group 2 vs group 3, P <.001). In the analysis of the interval between symptom onset and specimen collection days, 59.2%, 82.0%, and 79.4% of specimens of each group, respectively, were obtained within 7 days. In addition, 47.1%, 18.0%, and 20.6% respectively of specimens of each group were obtained for intervals ≥7 days. Etiologies for patients with coinfections are described in Supplement Table 2. In the comparison of laboratory findings (WBC and platelet counts, hemoglobin, and C-reactive protein), WBC counts in group 3 were found to be higher than in groups 1 and 2 (group 1 vs group 3, P =.002; group 2 vs group 3, P <.001).

Discussion

Although the diagnosis of *M. pneumoniae* pneumonia in routine clinical practice has been based on serological methods,[1,2] PCR tests for *M. pneumoniae* infection are increasingly being adopted in the clinical laboratory.[8,12,14] Several previous studies of the diagnostic performance of PCR and IgM for *M. pneumoniae* showed that PCR is superior to serology for rapid and accurate diagnosis of infection with this pathogen.[1,5,14,19] However, little is known about the diagnostic performance of methods for diagnosing *M. pneumoniae* infection in the outbreak setting.

Epidemics of *M. pneumoniae* infection generally occur every 3 to 7 years[20]; the recent Korean *M. pneumoniae* outbreak occurred during 2015, in the middle of the study period. According to the Centers for Disease Control and Prevention guidelines for influenza diagnostic testing, the interpretation of negative results should consider the clinical characteristics of the patient because false-negative test results are likely to occur.[21] Real-time-PCR or other molecular assays are preferred in an outbreak setting to improve sensitivity for influenza.[17,21] However, there is currently no well-established standard laboratory method for the diagnosis of *M. pneumoniae* infection, and an optimal detection method

Table 2. Correlation Between PCR and IgM Performance in Positive Rates Across Different Age Groups

Age Group, y (n)	PCR/IgM (%)			*P* Value
	Positive/Positive	Positive/Negative	Negative/Positive	
<5 (401)	156 (38.9)	30 (7.5)	215 (53.6)	<.001
5–10 (239)	146 (61.1)	52 (21.8)	41 (17.2)	.3
10–18 (70)	31 (44.3)	18 (25.7)	21 (30.0)	.749
Total (710)	333 (46.9)	100 (14.1)	277 (39.0)	<.001

JRS, Japanese Respiratory Society; PCR, polymerase chain reaction.
The McNemar test was used for the correlation analysis. Positive cases were defined as having a JRS score ≥4.

Table 3. Clinical and Laboratory Characteristics of Patient Groups According to PCR and IgM Test Results

	Group 1 (n = 333)	Group 2 (n = 100)	Group 3 (n = 277)	*P* Value by Group			
				1 vs 2	1 vs 3	2 vs 3	1 vs 2 vs 3
Age, y	5.0 ± 3.2	6.7 ± 3.6	3.1 ± 3.6	<.001	<.001	<.001	<.001
Male sex (%)	155 (46.5)	52 (53.0)	123 (44.4)	.273	.6	.087	.244
Comorbidity (%)	28 (8.4)	9 (9.0)	65 (23.5)	.853	<.001	.002	<.001
Clinical diagnosis[a] (%)	247 (74.2)	78 (78.0)	102 (36.8)	.438	<.001	<.001	<.001
Prior antibiotics use (%)							
Macrolides	160 (48.0)	28 (28.0)	64 (23.1)	<.001	<.001	.515	<.001
Other antibiotics	149 (44.7)	37 (37.0)	102 (36.8)	.170	.048	.975	.103
Coinfection (%)	136 (41.1)	37 (37.0)	161 (58.1)	.186	<.001	<.001	<.001
Febrile days	6.5 ± 3.6	4.3 ± 2.2	4.5 ± 5.1	<.001	<.001	.502	<.001
Intervals between symptom onset and specimen collection, d (%)							
0–7	176 (52.9)	82 (82.0)	220 (79.4)	…	…	…	…
≥7	157 (47.1)	18 (18.0)	57 (20.6)	…	…	…	…
Laboratory findings							
WBC, × 10^9/L	9,090 ± 4252	7,389 ± 2723	13,192 ± 21,120	<.001	.002	<.001	<.001
Hemoglobin, g/dL	12.4 ± 1.1	12.4 ± 1.2	12.2 ± 1.5	.838	.045	.146	.076
Platelets, × 10^9/L	304.1 ± 105.7	242.6 ± 78.5	310.7 ± 119.7	<.001	.467	<.001	<.001
CRP, mg/dL	3.7 ± 4.3	4.1 ± 3.3	3.9 ± 5.5	.329	.76	.56	.758

CRP, C-reactive protein ; JRS, Japanese Respiratory Society; PCR, polymerase chain reaction; WBC, white blood cells.
[a]Clinical diagnosis was according to the JRS scoring system. Data are presented as n (%), mean ± standard deviation, or median with lower and upper quartiles. Group 1, PCR (+)/IgM (+); group 2, PCR(+)/IgM(-); group 3, PCR(-)/IgM(+).

for *M. pneumoniae* infection during an outbreak is needed to improve diagnostic precision and to guide prompt implementation of adequate antibiotic therapy.[2,5] In this study, we investigated the overall diagnostic performance of PCR and IgM assays for *M. pneumoniae* detection against symptomatic patients in the context of a recent Korean outbreak.

Our results showed a great discrepancy between *M. pneumoniae* PCR and IgM test results, which accords with earlier reports.[1,7,19] Only 9.0% of patients who underwent both tests (333/1,109) showed simultaneous positive results. In our analysis, the sensitivity of both PCR and IgM was low (56.3% and 59.4%, respectively), possibly because clinical diagnosis by the JRS scoring system overestimates *M. pneumoniae* infection; with this interim reference standard, the sensitivity of 2 laboratory test methods may be underestimated. Although PCR and IgM sensitivity were low in this study, this result did not preclude comparing the performance of the 2 test methods.

We also described the overall sensitivity, specificity, NPV, and PPV of PCR and IgM in the corresponding age groups. The sensitivity of PCR was relatively low in patients aged <5 years, whereas it was higher in the other age groups. When a positive result for either PCR or IgM was applied as the gold standard, the PCR sensitivity was relatively lower in the group aged <5 years than in the other groups, and the overall trends of sensitivity for each group were similar when we applied the JRS scoring system as a gold standard. This result may reflect the difficulty in obtaining good-quality respiratory specimens in young children; simultaneous performance with serological testing would improve the diagnostic sensitivity. On the other hand, in accordance with earlier researcht, it showed greater PCR sensitivity in the groups aged 5 years to 10 years and 10 years to 18 years.[14] This finding is consistent with the study of Thurman et al,[5] in which a total of 97 symptomatic individuals had an IgM serology test that was more sensitive than PCR and IgM/IgG testing, whereas the PCR method was the most accurate method against asymptomatic patients.[5]

During an outbreak, it is essential to not miss the detection of patients with clinically compatible symptoms showing negative test results. Confirmatory testing by a more sensitive and specific test method should be conducted in the absence of a well-established standard laboratory method for the diagnosis of *M. pneumoniae* infection. However, the clinical presentation observed in our patient population did not differ greatly from that described in other studies.[1,9,19] In the present

DOI: 10.1093/labmed/lmaa048

study, we found a significant difference in the coinfection rate in group 3 compared with the other 2 groups. We found that 82.0% of group 2 patients (PCR[+]/IgM[-]) did not seems to have enough time to develop a detectable immune response for IgM. Considering the delay in seroconversion, a negative result by the IgM may be because of collection before the development of a detectable immune response. One could also consider the possibility of asymptomatic carriers in group 2 (PCR[+]/IgM[-]).[1,3] However, our study cohorts were all symptomatic, and *M. pneumoniae* carriage is known to be rare during an outbreak of *M. pneumoniae* pneumonia.[14]

The several limitations of the present study are as follows. First, the sampling timing varied from case to case. Because collecting specimens after symptom onset, at diagnosis, and during the convalescent period was not easy in our actual clinical setting, we performed PCR and IgM tests only at the time of admission to the pediatric emergency department for ease and speed of diagnosis. Therefore, some patients may not have been provided enough time to mount an IgM antibody response, or bacteria may have been eliminated before detection by PCR. However, based on the analysis being conducted 7 days before and after symptom onset for the 3 groups, we confirmed that combining the PCR test and IgM testing may be a pragmatic and sensitive approach to confirming *M. pneumoniae* infection at the time of admission of symptomatic pediatric patients during an outbreak.

Second, because of the absence of gold standards for *M. pneumoniae* infection, we applied the JRS scoring system as a clinical interim reference in spite of its imperfection. Third, even if the patients' parents denied a previous history of *M. pneumoniae* infection for patients, some patients may not have had a previous history but others (especially older children) were more likely to suffer from asymptomatic or undiagnosed *M. pneumoniae* infections. In addition, some patients (again, especially older children) may have detectable levels of *M. pneumoniae* IgM for several months after *M. pneumoniae* infection, leading to false-positive IgM results.

Conclusion

In the present study, we confirm that PCR sensitivity is relatively low in patients younger than age 5 years, and simultaneous detection with IgM assays may improve the diagnostic performance in this age group. Our findings, showing the diagnostic values of PCR and IgM in *M. pneumoniae* detection among different age groups in the context of an *M. pneumoniae* infection outbreak, further characterize the diagnostic performance of these assays.

Supplementary Data

Supplemental tables can be found in the online version of this article at www.labmedicine.com. **LM**

Acknowledgments

This work was supported by the Bio and Medical Technology Development Program of the National Research Foundation (NRT) of Korea grant funded by the Korea government (NRF-2016M3A9B6918716). The authors declare that there is no conflict of interests regarding the publication of this article.

References

1. Chang HY, Chang LY, Shao PL, et al. Comparison of real-time polymerase chain reaction and serological tests for the confirmation of *Mycoplasma pneumoniae* infection in children with clinical diagnosis of atypical pneumonia. *J Microbiol Immunol Infect.* 2014;47(2):137–144.
2. Qu J, Gu L, Wu J, et al.; Beijing Network for Adult Community-Acquired Pneumonia (BNACAP). Accuracy of IgM antibody testing, FQ-PCR and culture in laboratory diagnosis of acute infection by *Mycoplasma pneumoniae* in adults and adolescents with community-acquired pneumonia. *BMC Infect Dis.* 2013;13:172.
3. Defilippi A, Silvestri M, Tacchella A, et al. Epidemiology and clinical features of *Mycoplasma pneumoniae* infection in children. *Respir Med.* 2008;102(12):1762–1768.
4. Dorigo-Zetsma JW, Zaat SA, Wertheim-van Dillen PM, et al. Comparison of PCR, culture, and serological tests for diagnosis of *Mycoplasma pneumoniae* respiratory tract infection in children. *J Clin Microbiol.* 1999;37(1):14–17.
5. Thurman KA, Walter ND, Schwartz SB, et al. Comparison of laboratory diagnostic procedures for detection of *Mycoplasma pneumoniae* in community outbreaks. *Clin Infect Dis.* 2009;48(9):1244–1249.
6. Liu FC, Chen PY, Huang F, Tsai CR, Lee CY, Wang LC. Rapid diagnosis of *Mycoplasma pneumoniae* infection in children by polymerase chain reaction. *J Microbiol Immunol Infect.* 2007;40(6):507–512.
7. Martínez MA, Ruiz M, Zunino E, Luchsinger V, Avendaño LF. Detection of *Mycoplasma pneumoniae* in adult community-acquired pneumonia by PCR and serology. *J Med Microbiol.* 2008;57(Pt 12):1491–1495.
8. Chou RC, Zheng X. A comparison of molecular assays for *Mycoplasma pneumoniae* in pediatric patients. *Diagn Microbiol Infect Dis.* 2016;85(1):6–8.
9. Kashyap B, Kumar S, Sethi GR, Das BC, Saigal SR. Comparison of PCR, culture & serological tests for the diagnosis of *Mycoplasma pneumoniae* in community-acquired lower respiratory tract infections in children. *Indian J Med Res.* 2008;128(2):134–139.
10. Dumke R, Strubel A, Cyncynatus C, et al. Optimized serodiagnosis of *Mycoplasma pneumoniae* infections. *Diagn Microbiol Infect Dis.* 2012;73(2):200–203.
11. Daxboeck F, Krause R, Wenisch C. Laboratory diagnosis of *Mycoplasma pneumoniae* infection. *Clin Microbiol Infect.* 2003;9(4):263–273.

12. Waites KB, Balish MF, Atkinson TP. New insights into the pathogenesis and detection of *Mycoplasma pneumoniae* infections. *Future Microbiol.* 2008;3(6):635–648.
13. Daxboeck F, Khanakah G, Bauer C, Stadler M, Hofmann H, Stanek G. Detection of *Mycoplasma pneumoniae* in serum specimens from patients with mycoplasma pneumonia by PCR. *Int J Med Microbiol.* 2005;295(4):279–285.
14. Nilsson AC, Björkman P, Persson K. Polymerase chain reaction is superior to serology for the diagnosis of acute *Mycoplasma pneumoniae* infection and reveals a high rate of persistent infection. *BMC Microbiol.* 2008;8:93.
15. Riordan A. In children with respiratory symptoms are *Mycoplasma pneumoniae* PCR and serology clinically significant? *Arch Dis Child Educ Pract Ed.* 2014;99(4):157.
16. Yin YD, Zhao F, Ren LL, et al. Evaluation of the Japanese Respiratory Society guidelines for the identification of *Mycoplasma pneumoniae* pneumonia. *Respirology.* 2012;17(7):1131–1136.
17. Yanagihara K, Kohno S, Matsusima T. Japanese guidelines for the management of community-acquired pneumonia. *Int J Antimicro Agents*. 2001;18:S45–S48.
18. Edelstein I, Rachina S, Touati A, et al. *Mycoplasma pneumoniae* monoclonal P1 type 2c Outbreak, Russia, 2013. *Emerg Infect Dis.* 2016;22(2):348–350.
19. He XY, Wang XB, Zhang R, et al. Investigation of *Mycoplasma pneumoniae* infection in pediatric population from 12,025 cases with respiratory infection. *Diagn Microbiol Infect Dis.* 2013;75(1):22–27.
20. Hong KB, Choi EH, Lee HJ, et al. Macrolide resistance of *Mycoplasma pneumoniae*, South Korea, 2000-2011. *Emerg Infect Dis.* 2013;19(8):1281–1284.
21. Rapid diagnostic testing for influenza: information for clinical laboratory directors. Centers for Disease Control and Prevention website. https://www.cdc.gov/flu/professionals/diagnosis/rapidlab.htm. Accessed March 5, 2020.

DOI: 10.1093/labmed/lmaa048

Science

Gonorrhea and Chlamydia Specimen Positivity Rate by Polymerase Chain Reaction at a Regional Veteran Affairs Medical Center

Jeffrey M. Petersen, MD,[1,2*] *Sahil Patel, MS, MT (AMT),*[1] *Sharvari Dalal, MD,*[1,2] *Darshana Jhala, MD*[1,2]

Laboratory Medicine 2021;52:e23-e29

DOI: 10.1093/labmed/lmaa046

ABSTRACT

Objective: Sexually transmitted infections because of *Neisseria gonorrhoeae* (NG) and/or *Chlamydia trachomatis* (CT) remain a major public health problem. Although the literature describes the population-based epidemiology of CT/NG, it does not appear to contain reference points for the statistical analyses of specimen positivity rates by nucleic acid testing (NAT) with polymerase chain reaction (PCR) that would be collected by a laboratory following best laboratory and regulatory practice. For facilities that diagnose NG and CT by a real-time PCR assay, an understanding of the expected specimen positivity rate of gonorrhea and chlamydia would be helpful for monitoring the assay for quality assurance. Therefore, on behalf of the Michael J. Crescenz Veteran Affairs Medical Center (VAMC), we present this novel quality assurance study on its CT/NG specimen positivity rates conducted by NAT with PCR.

Methods: Quality assurance/improvement quarterly data from April 1, 2012 to September 30, 2019 were reviewed to obtain both the test volume of PCR for CT/NG and the number of positive test results at the VAMC to collate and perform statistical analyses. Testing had been performed using the Abbott m2000 RealTime System (Abbott Park, IL).

Results: A total of 22,709 PCR tests for CT/NG had been performed on the veteran population; of these, 502 tests were positive for NG and 744 were positive for CT. Quarterly percentage rates ranged from 1.67% to 5.30% for CT and from 1.00% to 3.25% for NG, with average rates of 3.35% and 2.22% for CT and NG, respectively.

Conclusion: The establishment of an expected rate of specimen positivity of CT/NG by NAT with PCR at the VAMC is a significant novel reference point in the quality assurance (QA) literature and provides a benchmark that aids tremendously in QA for the microbiology/molecular laboratory.

Keywords: polymerase chain reaction, molecular diagnostics, sexually transmitted diseases, quality assurance, quality improvement, regulatory compliance, reference statistics, quality, CAP Microbiology Checklist

Chlamydia and gonorrhea are major public health problems that are sexually transmitted.[1] With a total of 1,758,668 cases of *Chlamydia trachomatis* (CT) and 583,405 cases of *Neisseria gonorrhoeae* (NG) diagnosed and reported in 2018 to the Centers for Disease Control and Prevention (CDC), these 2 sexually transmitted infections (STIs) are the first and second most common notifiable conditions in the United States.[2-4] As infection with CT/NG can lead to morbidity (for instance, pelvic inflammatory disease or facilitation of transmission of human immunodeficiency virus infection), clinical laboratory testing is performed to provide a diagnosis to assist in clinical treatment and to allow for appropriate public health reporting.

Quality assurance (QA) is an essential part of ensuring the accuracy and reliability of laboratory testing, and part of QA is guided by the College of American Pathologists (CAP) for laboratories accredited by CAP.[1,3,5] A regulatory item on the College of American Pathologists Microbiology Checklist (standard MIC.63252 under Molecular Microbiology) states that "when appropriate, statistics (*e.g.* percentage of results that are positive for *Chlamydia trachomatis* and/or *Neisseria gonorrhoeae*) are maintained and monitored"

Abbreviations:

NG, *Neisseria gonorrhoeae*; CT, *Chlamydia trachomatis*; NAT, nucleic acid testing; PCR, polymerase chain reaction; VAMC, Veteran Affairs Medical Center; QA, quality assurance; QA/QI, quality assurance/quality improvement.

[1]Department of Pathology and Laboratory Medicine, Michael J. Crescenz Veteran Affairs Medical Center, Philadelphia, Pennsylvania, [2]Department of Pathology and Laboratory Medicine, Philadelphia, Pennsylvania

*To whom correspondence should be addressed.
Jeffrey.petersen@va.gov

(https://elss.cap.org/elss/ShowProperty?nodePath=/UCMCON/Contribution%20Folders/DctmContent/education/OnlineCourseContent/2017/LAP-TLTM/checklists/cl-mic.pdf; p. 77).[6] This standard is understandable; although nucleic acid testing (NAT) by polymerase chain reaction (PCR) can be highly sensitive and specific, false results can occur for a number of reasons, including contaminating environmental amplicons in the laboratory, errors in specimen collection, errors in test operation, or contamination of specimens in the clinic.[3] Therefore, it is important for clinicians and laboratory professionals to understand test limitations and for laboratories to perform appropriate QA and quality control as part of standard laboratory practice.[1,3-5] Currently, laboratories can perform QA by monitoring their CT and/or NG statistics and undertaking appropriate investigation and/or actions if significant statistical deviations from the past are identified.

However, for the QA of NAT testing for CT/NG, resources in the literature for specimen positivity rates by laboratories for comparison are scarce; available relevant literature instead would include broad population-based epidemiological data, manufacturer's instructions if addressed, clinical gestalt, and anecdotal reports of reasonable positivity rates from colleagues.[1-4,7-9] This scarceness is reinforced further in that other than the abstract presentation of the data from this article,[1] there has been no published literature specifically on the specimen positivity rate as part of a laboratory's statistical QA monitoring program in compliance with MIC.63252[6] in either the veteran or general nonveteran population. Documentation of this information would be useful especially for the veteran population because it is known epidemiologically that veterans have higher rates of STIs compared with the general population.[7-9] Although the specimen positivity rate defined at a veteran affairs medical center (VAMC) may potentially be higher than that obtained at a similar hospital serving a different general nonveteran population, a documented study would serve as a reference point for the veteran population studied. Therefore, the quality assurance/quality improvement (QA/QI) statistical monitoring at a major regional VAMC is presented to support this material as a benchmark.

Materials and Methods

The QA/QI quarterly data from April 1, 2012 to September 30, 2019 were reviewed to obtain both the test volume of NAT testing by PCR for CT/NG and the number of positive test results at the VAMC. Quarters for each year began on October 1; therefore, quarter 1 of 2013 began on October 1, 2012 and ended on December 31, 2012. Consequent quarter dates would be as follows: quarter 2 (January 1 to March 31), quarter 3 (April 1 to June 30), and quarter 4 (July 1 to September 30). Testing had been performed using the Abbott m2000 RealTime System (Abbott Park, IL) using properly validated standard laboratory protocols for NAT testing by PCR as recommended by the manufacturer. These protocols included running appropriate quality control with samples known to be positive for organisms (CT/NG), negative quality control samples, and an internal quality control to help rule out the presence of an inhibitor of the PCR reaction. These QA/QI data were presented as a regular graphical and tabulated report at the Laboratory Quality Management Committee (LQMC) at the VAMC. If any significant statistical deviations were detected in the data on review by the medical director or the LQMC, then an appropriate investigation would be undertaken to resolve this deviation, take appropriate corrective action if needed, and ensure quality patient and laboratory care. In addition, because of previous experience in CT/NG testing at the VAMC and published epidemiological evidence, an upper CT/NG specimen positivity rate cutoff of ≤6% had been established internally by an educated assessment such that a rate above 6% using NAT by PCR would be investigated for QA.[1,2,4,6-9] Similarly, an unusual drop in the specimen positivity rate that approached 0% would also be investigated. In addition, after each batched run of NAT by PCR for CT/NG, the run data were reviewed by the medical director for quality assurance. The deidentified QA/QI data included all test results including repeat tests/runs, quality controls, and training or proficiency samples.

The QA/QI quarterly data were compiled in a Microsoft Excel (Redmond, WA) spreadsheet, and from this file the graphs and tables were prepared. Additional statistical analyses by a 2-tailed *t*-test were also performed periodically to verify the lack of statistically significant differences, which would have a calculated *P* value of less than .05.

In addition, on further review, to further provide a reference to the specific patient population at the VAMC that underwent NAT testing by PCR for CT/NG, demographic data on the patients tested were obtained through a Vista/Fileman (U.S. Department of Veterans Affairs, Washington, DC) search. The total number of unique patients who were veterans (some patients were tested multiple times) and their age, sex, and ethnicity were recorded for reference.

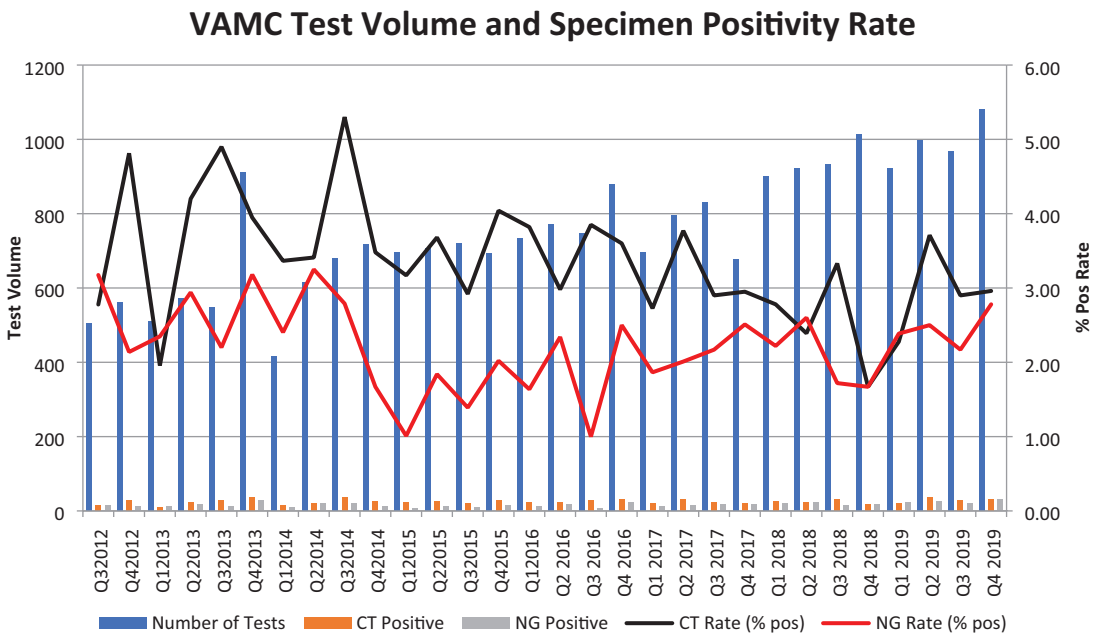

Figure 1

Graphical analysis of quarterly data of specimen positivity rate (by NAT for CT/NG) and test volume. Note that the percent positivity rate remained comparable from quarter to quarter with no significant deviations (such as a rate of zero or a statistically significant unexplained increase). Pos, positive; VAMC, veteran affairs medical center; CT, *Chlamydia trachomatis;* NG, *Neisseria gonorrhoeae.*

To ensure that each demographic data point represented a unique patient data point, extra collected demographic data on veterans for a repeat visit or testing were removed from the demographic tabulation. Age was represented as the age of the veteran at the time of the search. This demographic data extraction also included CT/NG test results, allowing for a determination of the number of unique test results given to patients.

Results

A total of 22,709 NAT tests by PCR for CT/NG had been performed on the veteran population at the VAMC; of these, 502 were positive for NG and 744 were positive for CT. Quarterly percentage rates on a quarterly basis ranged from 1.67% to 5.30% (CT) and 1.0% to 3.25% (NG) with average rates of 3.35% and 2.22% for CT and NG respectively (see **Figure 1** and **Figure 2**). At all times, the specimen positivity rate stayed below the VAMC's expected rate of less than 6%, a figure based on prior epidemiological studies and the VAMC's institutional experience with the known patient population.[1-4,7-9] Statistical calculations comparing year to year verified no statistically significant differences in the specimen positivity rates. The entirety of the data are tabulated in the supplementary data (See Supplemental Table 1). The statistical analyses throughout the entire study period were maintained and never showed a significant deviation from what was expected.

For demographic recording purposes, the aggregate totals by sex, race/ethnicity, and age for the total unique veteran patient population, the population that had tested negative for both CT and NG, and the population that had tested positive for at either CT, NG, or both were computed. These data are self-reported by patients and tabulated in **Figure 3**. Many of the patients underwent repeat testing over the study period, resulting in the number of tests outnumbering the number of patients. In addition, a total of 396 patients had tested negative for both CT and NG but had also tested positive for either CT or NG at another testing visit; these patients were therefore included in both the population that had tested negative for both at least once and the population that had tested positive for either CT or NG at least once. This information on patients who were veterans was meant to provide a demographic benchmark of the population at this VAMC.

Lab Medicine 2021;52;e23–e29 e25
DOI: 10.1093/labmed/lmaa046

Statistical Parameter	Value for CT Rate	Value for NG Rate
Minimum percentage positive	1.67%	1.00%
Maximum percentage positive	5.30%	3.25%
Average	3.35%	2.22%
Standard Deviation	0.827%	0.576%
Median	3.35%	2.21%
Variance	0.661%	0.320%

Figure 2

Tabulated overall calculated statistical results including minimum and maximum, average percent positivity, standard deviation, median, and variance from quarter 3 of 2012 to quarter 4 of 2019. CT, *Chlamydia trachomatis;* NG, *Neisseria gonorrhoeae.*

Discussion

Research has shown that STIs resulting from CT/NG remain a major public health problem and are common worldwide.[1,2,4,7-9] The prevalence of CT/NG varies from population to population; these population differences may result in part from differences in access to healthcare and in risk factors for infection. The veteran population, particularly members of the subpopulation who are patients at VAMCs throughout the country, has been shown to be more prone to serious illnesses such as infections and to differ significantly from nonveterans in several population-based health metrics.[10-12] In particular, STIs including CT/NG in the veteran and military population have been shown to have a higher incidence compared with the general population.[1,2,4,7-9] The presence of this epidemiological evidence is helpful to laboratory professionals in the community at large who are attempting to determine a reasonable specimen positivity rate because the patients who are to be tested may be part of at least 1 of the described populations.[1]

However, although one could attempt to extrapolate that the specimen positivity rate assessed by NAT for a particular higher-risk population (such as the veteran population being treated at the VAMC) may be higher than in other populations, there are limitations to depending solely on epidemiological data to ascertain a reasonable specimen positivity rate calculated by NAT. One very important limitation to the epidemiological data is that most persons infected by CT/NG are asymptomatic, and the number of undiagnosed, untreated, and unreported infections may exceed the total number of diagnosed and reported infections.[13] Determining the incidence and prevalence of a disease within a population is dependent on being able to recognize the cases of infection in the population.[14] In addition, the epidemiology of a disease in the population can differ significantly from the clinical data derived from sick patients seen in a clinic or hospital, which is where samples for CT/NG NAT testing are taken.[14] Because of this variance, epidemiological conclusions on the risk for the target population at large would be significantly limited if they were drawn from clinical data only, because these data may have a selection bias that stems from differences between the subpopulation that has access to and seeks medical care vs the rest of the population that has not sought medical attention. For the laboratory that is newly performing NAT testing for CT/NG, establishing a reasonable CT/NG specimen positivity rate based solely on epidemiological data from the populations at large is therefore not without peril.

Moreover, one must consider that sometimes patients may have more than 1 specimen (eg, to cover both genital and extragenital potential sites of infection) and that some patients may be positive at more than 1 site, which may lead the specimen positivity rate to be higher than what would be suggested by the epidemiological data.[15] Therefore, actual specimen positivity rate data have an important role in addition to epidemiological data. Similar reference point data from other laboratory CT/NG NAT, if there are significant similarities in the patient population, may be quite useful as a reference value to a laboratory newly monitoring its CT/NG NAT statistics per MIC.63252.[6] For quality patient and laboratory care, it is not enough to simply monitor and track statistics; it is also important to be able to know when an observed statistical trend indicates the need for further QA investigation and review. The data presented here from the VAMC are one such benchmark regarding a veteran population that may provide substantive information

Total Patient Demographics		Demographics for Patients who Tested Negative for Both CT/NG*		Demographics for Patients with a Positive Test Result*	
Demographic Characteristic	Number	Demographic Characteristic	Number	Demographic Characteristic	Number
Gender		*Gender*		*Gender*	
FEMALE	2444	FEMALE	2430	FEMALE	79
MALE	5270	MALE	5115	MALE	486
Race/Ethnicity		*Race/Ethnicity*		*Race/Ethnicity*	
AMERICAN INDIAN OR ALASKA NATIVE	23	AMERICAN INDIAN OR ALASKA NATIVE	22	AMERICAN INDIAN OR ALASKA NATIVE	1
ASIAN	84	ASIAN	80	ASIAN	11
BLACK OR AFRICAN AMERICAN	4905	BLACK OR AFRICAN AMERICAN	4788	BLACK OR AFRICAN AMERICAN	386
DECLINED TO ANSWER	213	DECLINED TO ANSWER	211	DECLINED TO ANSWER	18
NATIVE HAWAIIAN OR OTHER PACIFIC ISLANDER	36	NATIVE HAWAIIAN OR OTHER PACIFIC ISLANDER	36	NATIVE HAWAIIAN OR OTHER PACIFIC ISLANDER	4
UNKNOWN BY PATIENT	62	UNKNOWN BY PATIENT	61	UNKNOWN BY PATIENT	3
WHITE	2391	WHITE	2347	WHITE	142
Age Distribution		*Age Distribution*		*Age Distribution*	
<=20	0	<=20	0	<=20	0
21-30	658	21-30	627	21-30	94
31-40	1985	31-40	1932	31-40	208
41-50	1151	41-50	1132	41-50	77
51-60	1717	51-60	1683	51-60	89
61-70	1607	61-70	1584	61-70	77
71-80	519	71-80	513	71-80	17
81-90	71	81-90	68	81-90	3
91-100	6	91-100	6	91-100	0
Grand Total	7714	Grand Total	7545	Grand Total	565

Figure 3

Basic demographic data (sex, race/ethnicity and age distribution) of unique patients who were veterans in the total population and who tested either negative or positive for CT or NG. The number of unique patients is lower than the number of tests run because many patients had repeat testing over the study period, some tests needed to be rerun on the same specimen for diagnosis, and there was additional testing of control/proficiency/training material. *Some patients who tested positive for either CT/NG or both at 1 time also tested negative on other visits. Population with negative test results also includes patients who had tested positive at another visit. The race/ethnicity is self-reported by patients.

for a laboratory with a newly implemented CT/NG NAT assay without a long prior history of statistical results for comparison.[1]

In addition, QA plays a very important role in the proper implementation of NAT for clinical diagnosis.[3,16-18] All diagnostic tests, including nucleic acid amplification tests or NAT, can generate inaccurate results because of issues with specimen collection, test operation, or the laboratory environment. Given the sensitivity of NAT tests to even a few amplicons of the target genetic sequence, environmental amplicons or carryover contamination from previously amplified products in the laboratory or clinical setting can be a source of false-positive results. Because PCR by its nature can lead to the amplification of even a few target sequences of DNA by DNA polymerase, even a very tiny amount of

DOI: 10.1093/labmed/lmaa046

contamination or environmental amplicon can potentially turn into a significantly increased amount of contamination that can ruin NAT by PCR run to detect CT/NG.[3,16-18] However, if inhibitors of the PCR reaction are introduced, either because of specimen preparation or perhaps from the specimen's nature itself, false-negative results can occur. Because of these limitations, particularly the vulnerability to contamination either from the clinic/hospital or within the laboratory, efforts are warranted to both attempt to detect the possibility of false results through QA monitoring and to ensure that such contamination does not occur.[3] Prevention of contamination can be as simple as following standard well-established QA protocols for the molecular laboratory and ensuring clean equipment and workspaces.[3,16-18] Monitoring quality control and statistics for the patient results may help identify whether there is a potential issue with false results.[3]

Nonetheless, NAT by PCR is generally regarded to be superior in overall performance in detecting CT/NG compared with culture and other nonculture diagnostic methods; unlike other methods, NAT offers extended sensitivities to detect organisms (sensitivity well above 90%) with a concurrent very high specificity of ≥99%.[3] False results can still occur because of specimen collection, test operation, and the laboratory environment. Monitoring the rate of positive and indeterminate results in accordance with MIC.63252 may alert the laboratory to trends that require investigation to assure result accuracy. In addition to checking past laboratory results, for facilities that diagnosis NG and CT by real-time PCR assay, an understanding of the expected rate of CT/NG specimen positivity at other institutions can be helpful for monitoring the assay (particularly if past data at the facility are limited because the assay was recently implemented), both for epidemiological purposes and as a check on the assay to detect abnormal trends that may require additional investigation. These internal QA investigations, after laboratory professionals detect a potential issue from their statistical or quality control data, may either show that there is no problem with false results (eg, if the patient population tested by the clinics served by the laboratory drastically shifted in characteristics or risk of infection) or may identify a potential concern that can be addressed with corrective action to ensure continued quality care. The improvements made would be part of the QA/QI that is standard laboratory practice. Ultimately, the monitoring of CT/NG statistics is an example of how compliance with a regulatory standard can help the laboratory provide optimal patient and laboratory care.

We acknowledge that epidemiological evidence for multiple different populations, both veteran and nonveteran, exists in the literature to help delineate the expected prevalence of CT/NG infection in each population.[1,2,4,7-9] For example, the VAMC's expected upper rate of ≤6% is derived partly from prior experience in the VAMC laboratory and from epidemiological studies showing that 6% is at around the upper 95% confidence interval limit for non-Hispanic black individuals in the Centers for Disease Control and Prevention epidemiological data and is slightly less than the 6.7% National Health and Nutrition Examination Survey prevalence rate noted in epidemiological data of men with a high risk of infection in corrections facilities; because the testing population at the VAMC includes veterans who are not individually at high risk of infection simply undergoing screening, the expected institutional upper rate of 6% appeared reasonable to guide the clinical gestalt of the reviewing microbiology director. However, because the epidemiology of the population as a whole does not always extrapolate to specimen positivity rates or even to the selected subpopulation from the population that is seen in the clinic or hospital, literature on the expected specimen positivity rates still has a very important role in providing a guidepost to other laboratories, particularly if the other laboratory has a similar patient population but does not have many previous statistics for review because it has newly implemented NAT for CT/NG by PCR.[14] Other than the abstract presentation of the data from the VAMC,[1] there are no other studies in the literature focused on the statistical monitoring of specimen positivity rates of CT/NG by PCR for MIC.63252. Nonetheless, this study also presents future directions that could be undertaken to further illuminate the literature for laboratories seeking resources on expected specimen positivity rates from other hospitals.[1]

The VAMC experience is limited in that it is restricted to the veteran population only; given that veterans have been documented epidemiologically to have more STIs including CT/NG compared with the general population, a study of CT/NG specimen positivity rates in a nonveteran hospital serving the general population may show different specimen positivity rates. Such a study would significantly help mitigate the scarcity of the literature regarding published statistical reference points of CT/NG positivity rates.

In summary, this novel study publishes the specimen positivity rate of CT.NG infection at the VAMC to provide a reference point in the literature for such monitoring and alerts for trends that may require further investigation, which aids

tremendously in facilitating QA in the microbiology/molecular laboratory.

Conclusion

The establishment of the expected rate of positive laboratory-diagnosed CT and NG at the VAMC makes a significant contribution to the literature concerning veterans and provides a valuable reference for similar facilities monitoring the QA of their PCR assay for these STIs. From the VAMC, the specimen positivity rates on a quarterly basis ranged from 1.67% to 5.30% (CT) and 1.0% to 3.25% (NG) with average rates of 3.35% and 2.22%, respectively. At no point did the rates show a statistically significant difference from year to year or exceed the standard VAMC upper limit gestalt of 6%. **LM**

Acknowledgments

The data from this article were presented as a finalist laboratory practice abstract presentation at the national meeting of the American Society for Clinical Pathology; September 11, 2019; Phoenix, Arizona.

References

1. Petersen J, Patel S, Dalal S, Jhala D. Laboratory-diagnosed gonorrhea and chlamydia infection rate in the veteran population: the Corporal Michael J. Crescenz Veteran Affairs Medical Center (CMCVAMC) Experience. *Am J Clin Pathol.* 2019;152(Supplement_1):S136–S137. https://doi.org/10.1093/ajcp/aqz126.007
2. 2018 STD surveillance report. Centers for Disease Control and Prevention website. https://www.cdc.gov/nchhstp/newsroom/2019/2018-STD-surveillance-report.html. Updated October 8, 2019. Accessed June 23, 2020.
3. Papp J, Schacter J, Gaydos C, et al. Recommendations for the laboratory-based detection of *Chlamydia trachomatis and Neisseria gonorrhoeae* – 2014. *MMWR Recomm Rep*. 2014;63(2):1–19.
4. Centers for Disease Control and Prevention. Gonorrhea—United States, 1998. *MMWR Morb Mortal Wkly Rep.* 2000;49(24):538–542. https://www.cdc.gov/mmwr/preview/mmwrhtml/mm4924a5.htm
5. Ehrmeyer SS. Satisfying regulatory and accreditation requirements for quality control. *Clin Lab Med.* 2013;33(1):27–40.
6. Standard MIC.63252. College of American Pathologists microbiology checklist, molecular microbiology. https://elss.cap.org/elss/ShowProperty?nodePath=/UCMCON/Contribution%20Folders/DctmContent/education/OnlineCourseContent/2017/LAP-TLTM/checklists/cl-mic.pdf. Updated August 21, 2017. Accessed June 23, 2020.
7. Goyal V, Mattocks KM, Sadler AG. High-risk behavior and sexually transmitted infections among U.S. active duty servicewomen and veterans. *Journal of Women's Health*. Nov 2012;21(11):1155–1169.
8. Evans MW, Borrero S, Yabes J, Rosenfeld EA. Sexual behaviors and sexually transmitted infections among male veterans and nonveterans. *Am J Mens Health.* 2017;11(4):791–800.
9. Satterwhite CL, Joesoef MR, Datta SD, Weinstock H. Estimates of Chlamydia trachomatis infections among men: United States. *Sex Transm Dis.* 2008;35(11 Suppl):S3–S7.
10. Agha Z, Lofgren RP, VanRuiswyk JV, et al. Are patients at veterans affairs medical centers sicker? *Arch Intern Med*. 2000;160(21):3252–3257.
11. Eibner C, Krull H, Brown KM, et al. Current and projected characteristics and unique health care needs of the patient population served by the department of veterans affairs. *Rand Health Q.* 2016;5(4):13.
12. Morgan RO, Teal CR, Reddy SG, Ford ME, Ashton CM. Measurement in veterans affairs health services research: veterans as a special population. *Health Serv Res.* 2005;40(5 Pt 2):1573–1583.
13. Turner CF, Rogers SM, Miller HG, et al. Untreated gonococcal and chlamydial infection in a probability sample of adults. *JAMA.* 2002;287(6):726–733.
14. Coggon D, Rose G, Barker DJP. *Epidemiology for the Uninitiated. 4th ed*. London, UK: The BMJ. 1997. https://www.bmj.com/about-bmj/resources-readers/publications/epidemiology-uninitiated
15. van Liere GA, Hoebe CJ, Wolffs PF, Dukers-Muijrers NH. High co-occurrence of anorectal chlamydia with urogenital chlamydia in women visiting an STI clinic revealed by routine universal testing in an observational study; a recommendation towards a better anorectal chlamydia control in women. *BMC Infect Dis.* 2014;14:274.
16. Valentine-Thon E. Quality control in nucleic acid testing-where do we stand? *J Clin Virol*. 2002;25(Supplement_3):S13–S21.https://doi.org/10.1016/S1386-6532(02)00196-8
17. Vaneechoutte M, Van Eldere J. The possibilities and limitations of nucleic acid amplification technology in diagnostic microbiology. *J Med Microbiol.* 1997;46(3):188–194.
18. Kubista M, Andrade JM, Bengtsson M, et al. The real-time polymerase chain reaction. *Mol Aspects Med.* 2006;27(2-3):95–125.

Special Report

Criticality of In-House Preparation of Viral Transport Medium in Times of Shortage During COVID-19 Pandemic

Jeffrey Petersen, MD,[1,2] *Sharvari Dalal, MD,*[1,2] *Darshana Jhala, MD*[1,2,*]

Laboratory Medicine 2021;52:e39-e45

DOI: 10.1093/labmed/lmaa099

ABSTRACT

Objective: With the COVID-19 pandemic, there have been supply challenges necessitating that laboratories must prepare their own viral transport medium (VTM), which provides stability for clinical specimens for diagnostic viral testing.

Methods: Within a veteran affairs medical center clinical laboratory, VTM was prepared with a Hanks Balanced Salt Solution (HBSS) 500 mL bottle with phenol red, sterile heat-inactivated fetal bovine serum (FBS), gentamicin sulfate (50 mg/mL), and amphotericin B (250 μg/mL). An antimicrobial mixture was made of 50 mL each of amphotericin B and gentamicin sulfate. Ten mL of FBS and 2 mL of the antimicrobial mixture were mixed into the HBSS bottle, from which 3 mL aliquots were made. Sterility and efficacy check were assessed. These preparations were conducted at our VAMC's clinical laboratory to assure adequate VTM supply during the COVID-19 shortage.

Results: The VTM was successfully prepared in-house, supporting uninterrupted testing for the facility and other affiliated medical facilities/centers and community living centers.

Conclusion: This quality assurance/improvement report represents the first published manuscript on feasible VTM preparation exclusively within a clinical microbiology laboratory during the COVID-19 pandemic.

Keywords: viral transport media preparation, SARS-CoV-2, emergency preparedness, molecular pathology, COVID-19, quality control, quality assurance, supply shortage, clinical pathology, laboratory workflow

From its unassuming beginnings in Wuhan, China, SARS-CoV-2, the viral agent that causes the COVID-19 disease, has become an international pandemic.[1-6] With the unprecedented outbreak of the respiratory illness caused by SARS-CoV-2, there have been challenges to the maintenance of adequate supplies in terms of both personal protective equipment and testing materials.[7,8] In particular, the dire nationwide shortage of commercial viral transport medium (VTM, a formulation of a buffered salt solution, complex protein and amino acids, and antimicrobial agents), a critical medium for the transport of specimens for reverse transcriptase polymerase chain reaction (RT-PCR) testing, has created a situation in which testing laboratories need to manufacture their own in-house VTM because commonly used commercial VTM is simply unavailable.[7-11] Despite the shortage, VTM remains a critical and pivotal reagent for preserving stability to achieve a reliable test result.[12] Maintaining the stability of the collected virus is of utmost importance to perform COVID-19 RT-PCR with optimal results because the virus must still be sufficiently present and preserved in the specimen at the time of testing.

Given the lack of supply from commercial vendors, in-house manufacture has become an uncharted route forced upon medical centers and laboratories with the intention of proceeding with testing using VTM despite the dire shortages.[7-10] Consequently, a variety of transport media including saline, phosphate buffered saline, minimum essential medium, and other media with variable formulations have been shared and documented.[11,13-15] In nonshortage

Abbreviations:

VTM, viral transport medium; HBSS, Hanks Balanced Salt Solution; FBS, fetal bovine serum; RT-PCR, reverse transcriptase polymerase chain reaction; VAMC, veteran affairs medical center; CDC, Centers for Disease Control and Prevention.

[1]Corporal Michael J. Crescenz Veteran Affairs Medical Center, Philadelphia, Pennsylvania, [2]Department of Pathology and Laboratory Medicine, University of Pennsylvania, Philadelphia, Pennsylvania

*To whom correspondence should be addressed.
darshana.jhala@va.gov

times, VTM is generally considered the standard of care and offers advantages over other simpler formulations because of its documented ability to prevent overgrowth of bacteria/fungi and ensure prolonged stability of viral genetic material.[11-15] It has an established role in ensuring the stability of viral genetic material with simpler temperature and handling needs falling within the usual standard of care compared with the other media types such as saline.[11-15] Indeed, in a study by Rogers et al,[15] a trend toward an increasing cycle threshold value likely resulting from the degradation of viral genetic material in a small sampling was noted with saline stored at room temperature for prolonged periods of time in contrast to storage in VTM. Therefore, although there may be some degree of equivalence in various transport media in supporting the diagnosis of viral genetic material by RT-PCR, the use of VTM is preferred and is closer to general standard practice outside of shortage times.[15]

Despite the extraordinary nature of the current crisis, peer-reviewed literature to guide laboratories on the emergency manufacture, initial laboratory validation, and quality control of VTM for the COVID-19 pandemic is sparse. More important, peer-reviewed literature on VTM preparation and quality control has not been published by a clinical laboratory without research department infrastructure, specifically one in a regional veteran's hospital.[1,9,12] To fill this gap in the peer-reviewed literature for this critical component, this study shares the viewpoint and experience of pathologists at a regional veteran affairs medical center (VAMC) in both manufacturing and performing quality control of its VTM. These preparations were performed at our VAMC's clinical microbiology laboratory to assure adequate VTM supply during the COVID-19 shortage.

Method of Preparation

There has been variation leading to a lack of clarity in reference to VTM formulations, including the usage of phenol red and quality control processes. Phenol red, with its corresponding color change from pink to yellow in the presence of increasing acidity, has its use in the detection of potential bacterial contamination and was thus chosen to be included in the VAMC's preparation.[11] Within the clinical microbiology laboratory, VTM was prepared using a strict aseptic technique with a 500 mL bottle of Hanks Balanced Salt Solution (HBSS) with phenol red, sterile heat-inactivated fetal bovine serum (FBS), gentamicin sulfate (50 mg/mL), and amphotericin B (250 μg/ml), see **Figure 1**. First, 50 mL of amphotericin B and 50 mL of gentamicin sulfate were mixed into an antimicrobial mixture. Next, 10 mL of FBS was mixed with the HBSS bottle. Then 2 mL of the antimicrobial mixture was also mixed into the HBSS bottle. The HBSS bottle was then capped and mixed by inverting the bottle. Each bottle was then additionally labeled as follows: "2% FBS, 100 μg/mL Gentamicin, 0.5 μg/mL Amphotericin B, [current date], Expires [1 month from current date]."

Afterward, 3 mL aliquots were made from the bottle to constitute individual tubes of VTM for clinical use. These tubes were further labeled as follows:

Viral Transport Medium
For Transport of specimens only
Not to be taken internally
Store at 2 to 8°C. Do not freeze.
Ingredients: Hanks balanced salt solution, fetal bovine serum, gentamicin, amphotericin B
Expires [1 year after current date of manufacture]

All tubes and any remaining medium in the bottle were stored in the refrigerator (2 to 8°C).

Method of Quality Control for Sterility

One viral transport tube aliquot per bottle was utilized for the sterility check (see **Figure 2**). After the first initial visual inspection to verify that the color of the liquid in the tube was appropriate (pink from the phenol red), the aliquot tube was incubated in the CO_2 incubator at 37°C for 24 hours.

After incubation for 24 hours, the tubes were visually inspected for signs of growth such as color change (with phenol red specifically, a yellowing of the initial pink color indicative of acidification, frequently because of bacterial growth), turbidity, or presence of floccules when tapped or vortexed. If no signs of growth were observed, then within a biosafety cabinet, 1 mL of the viral transport medium was inoculated into a sheep blood agar plate, a chocolate agar plate, and a thioglycolate broth vial. Both the remaining aliquot tube and the plated medium

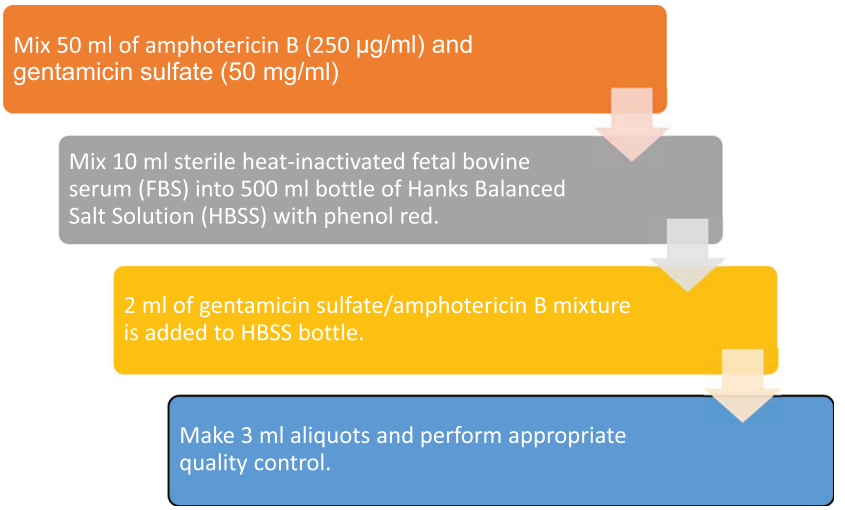

Figure 1

Flowchart of summary of 4 steps of VTM preparation. This figure was shown as part of an abstract presentation of these data.[1] VTM, viral transport medium.

were returned to the CO_2 incubator for incubation at 37°C for 48 hours. At both the 24- and 48-hour marks, plates and tubes were examined for signs of bacterial growth. Any observed growth at any stage of this sterility testing were fully worked up to identify the contaminating organism(s). All the bottle tests for sterility conducted by the VAMC clinical laboratory passed with no growth observed.

Initial Laboratory Validation

Additional RT-PCR tests were performed on the first bottle received for testing to confirm that the in-house manufacture of VTM was efficacious for clinical use (see **Figure 2**). These validations were performed just once before in-house VTM was authorized for clinical use. These additional runs were performed over 3 days and included both positive and negative aliquots spiked with corresponding control material from the Seracare (Milford, MA) AccuPlex SARS-CoV-2 Reference Material Kit. The runs were performed on the Abbott (Abbott Park, IL) RealTime SARS-CoV-2 Assay on the Abbott m2000 testing platform and on the Cepheid (Sunnyvale, CA) Xpert Xpress SARS-CoV-2 Assay. Because VTM would be utilized clinically and might be placed temporarily in conditions other than refrigerator temperatures, positive spiked specimens were stored temporarily at room temperature, refrigerator temperatures (2 to 8°C), and frozen temperatures (–20°C) to verify that RNA material was still preserved in the VTM for testing at the various temperatures.

The first day of testing involved 3 positively spiked and 3 negatively spiked specimens stored in the refrigerator routinely. The second day involved 3 positively spiked specimens stored at room temperature before testing, 3 positively spiked specimens kept in the refrigerator, and 3 negatively spiked specimens kept in the refrigerator. The third day involved 3 positively spiked specimens kept in the refrigerator, 3 positively spiked specimens frozen at –20°C before testing, and 3 negatively spiked specimens kept in the refrigerator. In this first-time validation, all test results were as expected and thus achieved validation for using in-house VTM for clinical application.

Method of Quality Control for Efficacy and RNA Contamination

Positive efficacy checks were performed to ensure that the in-house VTM from each bottle did not lead to degradation of viral

Lab Medicine 2021;52;e39–e45 e41
DOI: 10.1093/labmed/lmaa099

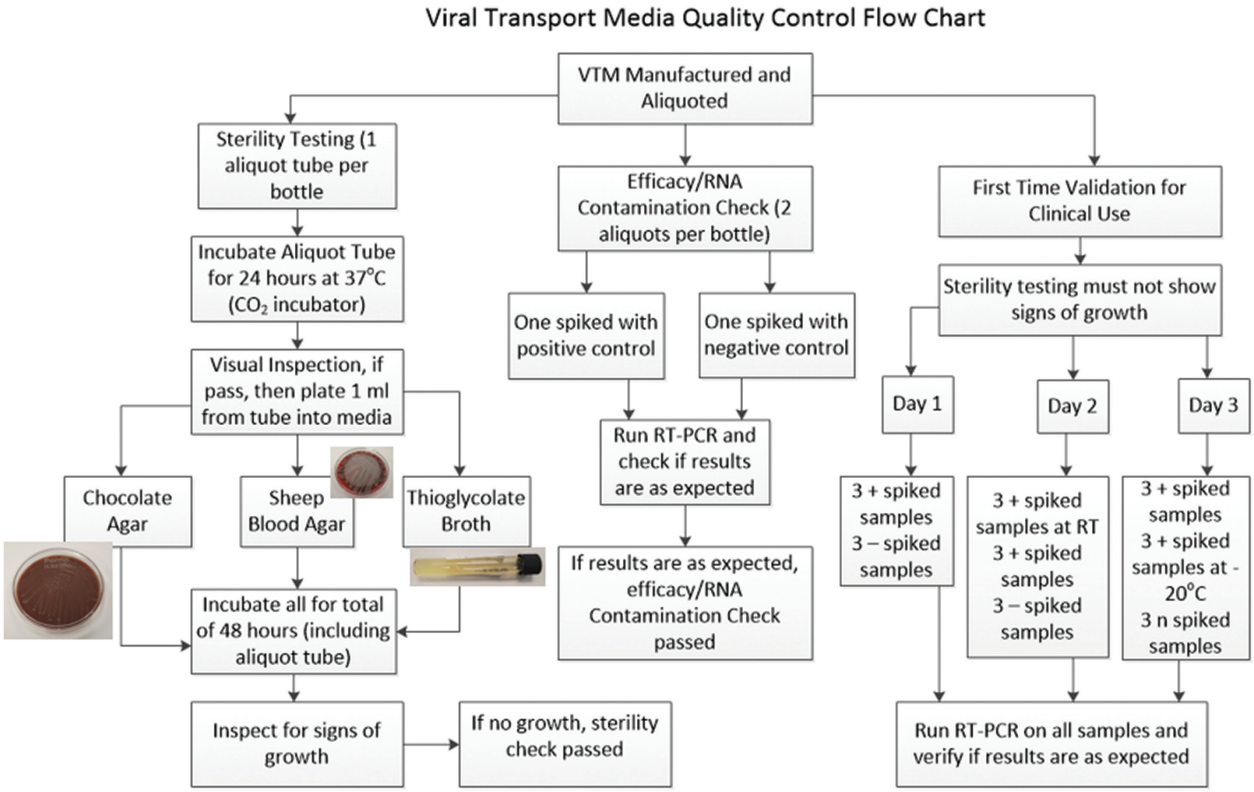

Figure 2

Flowchart of quality control program for the VTM including sterility testing in the lefthand branch, efficacy check in the middle branch, and the first-time validation in the righthand branch. For the validation, all spiked specimens without a specified temperature were done at refrigerator temperature (4 to 10°C temperatures). RT, room temperature; RT-PCR, reverse transcriptase polymerase chain reaction; VTM, viral transport medium. This figure was shown in an abstract presentation of these data.[1]

RNA that would preclude accurate testing. Negative RNA contamination tests were performed to verify that the manufacturing process did not introduce viral RNA that could lead to false positive results. Two aliquots from each bottle of VTM were thus taken (see **Figure 2**). One aliquot was spiked with positive control material and the other aliquot with negative control material. The laboratory staff then performed RT-PCR testing on each aliquot to confirm that the expected results were obtained (positive in the aliquot spiked with positive control material, negative in the aliquot spiked with negative control material).

Differences in Preparation

Methods to produce VTM have been made publicly available previously.[9,11] The primary similarity among these methods is that VTM is ultimately a mixture of a buffered salt solution, complex protein and amino acids, and antimicrobial agents to ensure the stability of the viral specimen for later nucleic acid testing. However, given the different circumstances of each practice setting and laboratory/clinical needs, there are also important differences. For instance, some preparations of VTM exclude phenol red for simplicity, but at the VAMC laboratory it was determined that including this quality marker was important to ensure the lack of bacterial contamination of the specimens produced (see **Image 1**).[9,11] In addition, a CO_2 incubator at an increased temperature of 37°C was utilized to provide a stable conducive environment to efficiently detect bacterial or fungal contamination compared to a lower room or refrigerator temperature incubation.[10,15]

Methods to validate and perform quality control have varied from institution to institution and in the literature

Image 1

Left: One of the prepared aliquots of transport media. Note the pink color because of the phenol red. In the presence of acidity (perhaps because of bacterial growth), this color would show yellowing, and thus this coloration remains a quality control tool. This image was shown in an abstract presentation of these data.[1] Right: One aliquot of prepared VTM was generously inoculated with a large quantity of *Escherichia coli* and then incubated in the CO_2 incubator at 37ºC for 24 hours. Because of bacterial growth, the VTM has a yellow appearance.

(both peer-reviewed and non-peer-reviewed).[9] One publicly available standard operating procedure by the Centers for Disease Control and Prevention (CDC), for instance, does not include an efficacy check to verify that viral genetic material is preserved by the media created and that the medium is not inadvertently contaminated by interfering genetic material.[9] Although the CDC has a publicly available protocol with its viewpoint, there is no peer-reviewed consensus in reference to sterility quality control.[9,11] Other institutions have found quality testing for efficacy/genetic material to be important and have included it in their algorithms, with variation in specifics.[11] Three culture mediums (sheep blood agar, chocolate agar, and thioglycolate broth) were used at the VAMC for thoroughness in sterility testing

Lab Medicine 2021;52;e39–e45
DOI: 10.1093/labmed/lmaa099

and to ensure sensitivity in detecting microorganism contamination. The length of time that the products of each step of the preparation process can be kept before expiration has also lacked clarity among multiple institutions; given the CDC protocol and the standard length of time available for commercial VTM before expiration, the VAMC laboratory established the expiration date of each aliquot as being 1 year after manufacture. The expiration date of any intermediate products (ie, the bottle mixture to be aliquoted) was set at 1 month so that intermediate steps will be completed expediently.

Finally, it is important to note that the preparation of VTM in this report took place within the clinical microbiology laboratory of a regional VAMC. This preparation setting led to the selection of the batch size of 1 bottle, or approximately 500 mL; under a prolonged shortage, other larger laboratories can potentially consider scaling up solutions to include larger batches and multiple reagents, and supporting quality assurance common to good manufacturing practice. Other than Petersen et al,[1] no published reports are available in the peer-reviewed literature for VTM preparation in the clinical laboratory of a regional VAMC. We have found only a single study on the preparation of VTM in a university hospital setting using a well-equipped research division and laboratories.[11] Published reports of a clinical laboratory preparing VTM in these unprecedented times present a unique perspective and act as a reference for other laboratories faced with the similar need for preparation.

Conclusion

In this first publication (other than the abstract presentation of these data[1]) on VTM manufacture, validation, and quality control within a regional VAMC's clinical microbiology laboratory during this unprecedented crisis of COVID-19, VTM production and related quality testing/validation have proven to be feasible and highly useful.[1] It is possible for VTM adequate to meet the needs of the regional VAMC to be prepared with appropriate sterility and efficacy to meet the unprecedented demand for SARS-CoV-2 testing with its concomitant severe supply shortages. This report presents the first published experience in the preparation and quality control of VTM within the clinical laboratory of a medical center specifically for SARS-CoV-2 testing during the COVID-19 pandemic; this information is a potentially useful reference point for other similar regional medical centers faced with this ongoing pandemic and worldwide health emergency. The in-house preparation of VTM in the face of severe supply shortages remains critical, and maintaining the stability of the virus to be detected is of utmost importance to ensure optimal laboratory results, appropriate laboratory diagnosis to confirm COVID-19 infection, and successful performance of testing in-house. **LM**

Acknowledgments

Data from this study were presented as a virtual poster at the American Society for Clinical Pathology National Conference; September 9 to September 12, 2020 (see reference 1).

References

1. Petersen J, Dalal S, Jhala D. In-House Viral Transport Medium (VTM) manufacture in the time of shortage, supply and crisis of COVID-19 at Veteran Affairs Medical Center (VAMC). *Am J Clin Pathol*. 2020;154(Supplement_1):S161–S162.
2. Director-General's remarks at the media briefing on 2019-nCoV on 11 February 2020. World Health Organization. https://www.who.int/dg/speeches/detail/who-director-general-s-remarks-at-the-media-briefing-on-2019-ncov-on-11-february-2020. Accessed April 16, 2020.
3. Outbreak of 2019 Novel Coronavirus (2019-nCoV) in Wuhan, China. Updated January 20, 2020. Centers for Disease Control and Prevention. https://www.cdc.gov/csels/dls/locs/2020/outbreak-of-2019-novel-coronavirus-2019-ncov-in-wuhan-china.html. Accessed April 16, 2020.
4. Country and technical guidance—coronavirus disease (COVID-19). World Health Organization. https://www.who.int/emergencies/diseases/novel-coronavirus-2019/technical-guidance. Accessed April 16, 2020.]
5. Zhou P, Yang XL, Wang XG, et al. A pneumonia outbreak associated with a new coronavirus of probable bat origin. *Nature.* 2020;579(7798):270–273.
6. Wu Z, Mcgoogan JM. Characteristics of and important lessons from the Coronavirus Disease 2019 (COVID-19) outbreak in China: summary of a report of 72,314 cases from the Chinese Center for Disease Control and Prevention. *JAMA* 2020;323(13):1239–1242.
7. Ranney ML, Griffeth V, Jha AK. Critical supply shortages—the need for ventilators and personal protective equipment during the Covid-19 pandemic. *N Engl J Med.* 2020;382(18):e41.
8. Thomas K. Coronavirus test obstacles: a shortage of face masks and swabs [Internet]. New York Times. https://www.nytimes.com/2020/03/18/health/coronavirus-test-shortages-face-masks-swabs.html. Published March 18, 2020; updated July 23, 2020. Accessed April 13, 2020.
9. Preparation of viral transport medium. Centers for Disease Control and Prevention. https://www.cdc.gov/coronavirus/2019-ncov/downloads/Viral-Transport-Medium.pdf. Accessed April 10, 2020.

10. Callahan CJ, Lee R, Zulauf KE, et al. Open development and clinical validation of multiple 3D-printed sample-collection swabs: rapid resolution of a critical COVID-19 Testing Bottleneck. Preprint. Posted online May 7, 2020. medRxiv 20065094. doi: 10.1101/2020.04.14.20065094

11. Smith KP, Cheng A, Chopelas A, et al. Large-scale, in-house production of viral transport media to support SARS-CoV-2 PCR testing in a multihospital health care network during the COVID-19 pandemic. *J Clin Microbiol*. 2020;58(8):e00913-20.

12. Johnson FB. Transport of viral specimens. *Clin Microbiol Rev.* 1990;3(2):120–131.

13. Rodino KG, Espy MJ, Buckwalter SP, et al. Evaluation of saline, phosphate buffered saline, and minimum essential medium as potential alternatives to viral transport media for SARS-CoV-2 testing. *J Clin Microbiol*. 2020;58(6):e00590-20.

14. Druce J, Garcia K, Tran T, Papadakis G, Birch C. Evaluation of swabs, transport media, and specimen transport conditions for optimal detection of viruses by PCR. *J Clin Microbiol.* 2012;50(3):1064–1065.

15. Rogers AA, Baumann RE, Borillo GA, et al. Evaluation of transport media and specimen transport conditions for the detection of SARS-CoV-2 by use of real-time reverse transcription-PCR. *J Clin Microbiol* 2020;58(8):e00708-20.

16. Cote RJ. Media composition, microbial, laboratory scale. In: Flickinger, MC, ed. *Encyclopedia of Industrial Biotechnology*. John Wiley and Sons; 2010.

DOI: 10.1093/labmed/lmaa099

Overview

Variation in LOD Across SARS-CoV-2 Assay Systems: Need for Standardization

*Youvraj Sohni, MSc, PhD**

Laboratory Medicine 2021;52:107-115

DOI: 10.1093/labmed/lmaa103

ABSTRACT

Multiple SARS-CoV-2 emergency use authorization (EUA) tests are being used for clinical testing across various clinical testing laboratories for meeting the diagnostic challenges of the ongoing pandemic. However, cross-assay variations in performance characteristics need to be recognized. A better understanding is needed of the clinical implications of cross-assay variation in performance characteristics, particularly in the limit of detection (LOD) of the SARS-CoV-2 assays used for clinical testing. Herein, a snapshot of the diversity of SARS-CoV-2 EUA analytical assay systems including methodologies, assay designs, and technology platforms is presented. Factors affecting the variations in LOD are discussed. Potential measures that may standardize across the various assay systems are suggested. Development of international standards and reference materials for the establishment of performance characteristics may substantially alleviate potential clinical decision-making challenges. Finally, cross-assay variation in LODs among the diverse SARS-CoV-2 diagnostic assays impacts clinical decision-making with multiple assay systems in use and lack of standardization across platforms. International standards in parallel with continued cross-platform studies and collaborative efforts across pertinent healthcare entities will help mitigate some of the clinical decision-making challenges.

Keywords: SARS-CoV-2, RT-PCR, LOD, C_T, Standards, COVID-19

In response to the ongoing public health emergency for COVID-19, the U.S. Food & Drug Administration (FDA) has issued emergency use authorization (EUA) for several SARS-CoV-2 diagnostic assays developed by IVD manufacturers, academic centers, and commercial reference laboratories. Several of these EUA assays are now part of the SARS-CoV-2 clinical testing workflow. The list of assays that receive EUA continues to increase, and the complete list of these assays can be accessed from the FDA website.[1]

The need for widespread availability of accurate diagnostic testing for SARS-CoV-2 is critical for appropriate and timely clinical decision-making. Multiple testing options are needed as SARS-CoV-2 testing capacity increases across the various clinical testing laboratories. In the foreseeable future, a limited manufacturing allocation of testing kits and related consumables compels individual clinical laboratories to use multiple assay systems to meet SARS-CoV-2 testing needs.[2,3]

It is reasonable to expect that cross-assay variation in performance characteristics of the EUA assays currently in use will have a bearing on the results of patient testing and subsequent clinical decision-making. In the context of the ongoing pandemic, ensuring that patient testing is not compromised is essential. Therefore, the clinical implications of cross-assay variation in performance characteristics must be recognized. This is particularly relevant for those patient specimen testing results that are close to the limit of detection (LOD) of the assay systems in use. These high cycle threshold (C_T) SARS-CoV-2 results may not meet the 95% confidence interval (CI) detection criteria, and such test results may be discordant when comparatively tested across different assay systems. The potential impact on SARS-CoV-2 transmission and the clinical significance of such patient results is yet to be completely understood.

Abbreviations:

EUA, emergency use authorization; LOD, limit of detection; FDA, U.S. Food & Drug Administration; IVD, in vitro diagnostics; C_T, cycle threshold; CI, confidence interval; CDC, Centers for Disease Control and Prevention; NP, nasopharyngeal; RT-PCR, reverse-transcription polymerase chain reaction; OP, oropharyngeal; TMA, transcription-mediated amplification; POC, point of care; NGS, next-generation sequencing; LDT, laboratory-developed test; IFU, instructions for use; $TCID_{50}$, median tissue culture infectious dose; BAL, bronchoalveolar lavage.

Science and Technology, LabCorp, Elon, North Carolina

*To whom correspondence should be addressed.
sohniy@labcorp.com

Clinical Implications

A significant majority of those with SARS-CoV-2 infections present with mild symptoms, are asymptomatic with positive results, or never develop any signs or clinical symptoms of COVID-19.[4] Thus a better understanding of the spectrum of the disease is needed because SARS-CoV-2 infection can be detected before the development of clinical symptoms. Although an ideal objective for a test is to eliminate the possibility of presumed false-negative patient results, the challenge is knowing the clinical implications of SARS-CoV-2 testing results that fall within the window of difference in LOD between the assay systems used in the clinical testing workflow.

Currently the EUA assays in use for SARS-CoV-2 diagnostics are all qualitative tests and generally provide a binary test with a positive or negative result. A third presumptive positive result is part of some tests (for example, the Cepheid GeneXpert assay; Cepheid, Sunnyvale, CA). As per the Centers for Disease Control and Prevention (CDC) recommendations, viral testing for SARS-CoV-2 is considered to be diagnostic when conducted among individuals with symptoms consistent with COVID-19. In addition, diagnostic testing may be considered for asymptomatic individuals with known or suspected recent exposure to SARS-CoV-2 to control transmission or to determine the resolution of infection. Viral testing is considered as screening when conducted among asymptomatic individuals without known or suspected exposure to SARS-CoV-2 for early identification and as surveillance when conducted among asymptomatic individuals to detect transmission hot spots or characterize disease trends. The CDC also recommends testing for all close contacts of persons with SARS-CoV-2 infection and for those in some high-risk settings.[5]

Assays with a relatively low LOD may detect SARS-CoV-2 in specimens with low viral loads that may be missed by assays with higher LODs. Viral loads in throat swab and sputum specimens peak at approximately 5–6 days after symptom onset, but specimens taken from an individual with a recently acquired SARS-CoV-2 infection can have low viral loads. One small study suggests that viral load detected in an asymptomatic patient may be similar to that in symptomatic patients, which in turn suggests the transmission potential of asymptomatic or minimally symptomatic patients.[6,7] Ultimately, correlating virus counts and therapeutic measures with outcomes may result in different strategies of care or isolation.

SARS-CoV-2 Shedding and Reverse-Transcription Polymerase Chain Reaction

Viral RNA may be detected from patient specimens weeks after the infectious stage has ended post-onset of symptoms. Sun et al[8] reported persistent shedding of viral RNA in nasopharyngeal (NP) swabs and feces specimens, with the estimated time until loss of RNA detection ranging from 45.6 days for NP swab specimens to 46.3 days for fecal specimens in mild cases of infection and from 48.9 days for NP swab specimens to 49.4 days for fecal specimens in severe cases of infection. However, the authors noted that the median time for throat specimens from mild cases of infection was 15.6 days (95% CI, 11.8–20.7 days) and that the 95th percentile was 32.8 days (95% CI, 25.9–42.3 days). Therefore, Sun et al.[8] suggested that the detection of viral RNA for mild cases of infection in throat swab specimens at the 50th day after illness onset should be a low-probability event, beyond the 95th percentile limit, as for fecal specimens. Similarly, according to van Kampen et al,[9] the probability of detecting infectious virus drops below 5% 15 days post-onset of symptoms. Lan et al[10] reported positive reverse-transcription polymerase chain reaction (RT-PCR) results in throat swab specimens from patients who recovered from mild COVID-19 for 50 days at maximum.

Chen et al[11] studied viral shedding at multiple timepoints in stool specimens and analyzed its correlation with clinical manifestations and the severity of illness. Those authors found that SARS-CoV-2 RNA in stool specimens was not associated with the presence of gastrointestinal symptoms and the severity of illness. A majority of patients may remain positive for viral RNA in the feces after the pharyngeal swabs are returned negative. The results show the presence of SARS-CoV-2 RNA in the feces of patients with COVID-19 and suggest the possibility of SARS-CoV-2 transmission via the fecal-oral route.[9] Gupta et al[12] reported that the duration for fecal shedding of viral RNA ranged from 1 to 33 days and in one patient was up to 47 days from symptom onset, longer after the clearance of respiratory specimens. In spite of viral RNA concentration, virus isolation from stool specimens was not successful from patient specimens collected between days 6 and 12. There appears to be active replication of the virus in the throat during the first 5 days after the onset of symptoms with no virus replication in stool specimens.[13]

An RT-PCR assay may have the analytical sensitivity for detecting a few hundred copies of viral RNA, but that does not indicate the infectious status of the patient. For these reasons, identifying such patients with low levels of detectable viral RNA that straddle the LOD of the assay of choice needs more clarity. It may be challenging to interpret RT-PCR tests for SARS-CoV-2 infection particularly early in the course of infection when these results underlie clinical decision-making to minimize onward transmission.

C_T Values and Infectivity

A relatively lower C_T value increases the probability of the presence of infectious virus, but the C_T value itself is not enough to determine whether the virus can be cultured from the specimens. Thus a limitation of PCR and other nucleic acid-based diagnostics is that they do not establish infectivity. Studies have shown that viral infectivity, as defined by culturability, is decreased when RT-PCR C_T values are >24, with the odds ratio for infectivity being decreased by 32% for every 1-unit increase in C_T.[14] Wölfel et al[13] were able to isolate virus during the first week of symptoms particularly from a majority of sputum specimens but could not isolate the virus from specimens taken after day 8. The infectivity of the virus culture does appear to correlate with viral load, and specimens that contain $<10^6$ copies/mL do not yield an isolate.[13,15]

In addition, Huang et al[15] reported that the mean C_T values of culturable oropharyngeal (OP) and NP specimens were similar whereas culturable sputum specimens had relatively lower C_T values. Specimens for a successful viral culture contained higher viral RNA counts, but note that viral genome integrity is an important factor for culturability and infectivity assessment. In their study, Huang et al[15] stated that a genome copy number of 5 to 6 $\log_{10}$ genome copies/mL appears to be the minimal viral load necessary for virus isolation. Detection of SARS-CoV-2 by RT-PCR is still the diagnostic gold standard, and the World Health Organization recommends 2 negative tests at least 24 hours apart as 1 of the key criteria for a clinically recovered patient.[16] In their study, Bullard et al[14] showed a link between in vitro viral growth, C_T value, and symptom-to-test. Thus, these authors suggested that a C_T value >24 in conjunction with duration of symptoms >8 days could be used together to determine the duration of infectivity in patients.

Nucleic acid amplification kits may sometimes produce false-negative results that do not match clinical features. The false-negative rate is a function of time with virus exposure and subsequent pathogenesis whether infection is presymptomatic, asymptomatic, or paucisymptomatic. In a recent case study, Lv et al[17] reported a successively RT-PCR-negative patient with COVID-19. The authors emphasized the importance of clinical signs and symptoms, other laboratory findings, and chest computed tomography images that should be considered in spite of RT-PCR-negative results. They also reported the dynamic change process of SARS-CoV-2 target genes by RT-PCR testing during the course of infection of a patient with COVID-19 from successive negative results to a successive single positive *N* gene to 2 positive *ORF1a/b* and *N* genes.

If clinical suspicion is high, then infection should not be ruled out on the basis of RT-PCR alone and the clinical and epidemiologic situation should be carefully considered.[18] Because RT-PCR positivity persists beyond the period of infectivity, clinical criteria that include isolation of hospitalized patients for 14 days from symptom onset or 72 hours symptom-free would be the prudent approach. Early discharge followed by home isolation of patients after day 10 of symptoms appears to have little risk of infectivity.[13,14]

Factors such as comorbidities and/or age are certainly part of the consideration in addition to other clinical findings that inform clinical decision-making. Children with SARS-CoV-2 infection have milder clinical symptoms and fewer laboratory and radiologic abnormalities. Nonetheless, understanding the perinatal outcomes of infants born to women infected with SARS-CoV-2 during pregnancy is important for early identification of children with SARS-CoV-2 to provide optimal medical care and control the pandemic.[19]

Finally, the CDC advises clinicians to use their judgment to determine if a patient has signs or symptoms compatible with COVID-19 and whether the patient should be tested. Clinicians are encouraged to consider testing for other causes of respiratory illness in addition to testing for SARS-CoV-2 depending on patient age, season, or clinical setting. Further details and updated recommendations may be accessed on the CDC website.[5]

Lab Medicine 2021;52;107–115
DOI: 10.1093/labmed/lmaa103

SARS-CoV-2 Assays

Table 1 is a representation of some of the molecular SARS-CoV-2 EUA assays that are run on a diverse array of platforms. Several of the assay systems have integrated automated nucleic acid extraction and analytical steps. The automated high-throughput testing platforms such as the Roche (Indianapolis, IN) cobas 6800/8800 feature integrated specimen prep and RT-PCR. Similarly, the Hologic (San Diego, CA) Panther/Fusion systems are high-throughput and automated but employ transcription-mediated amplification (TMA) methodology.

At the other end of the spectrum, designated point-of-care (POC) devices such as the Abbott ID NOW (Lake Forest, IL) and the Mesa Biotech (San Diego, CA) Accula platform exist, with the latter designed to be a molecular lateral flow assay readout system. The Cepheid Xpert Xpress SARS-CoV-2 assay also has the option to be used in a POC format. The POC-type devices include those that are deemed waived to be tested at the point of collection.

Some IVD manufacturers have integrated the SARS-CoV-2 EUA assay to be part of respiratory panel testing. The BioFire (Salt Lake City, UT) Respiratory Panel 2.1 is a multiplexed nucleic acid test intended for the simultaneous qualitative detection and differentiation of nucleic acids from multiple viral and bacterial respiratory organisms including SARS-CoV-2. Similarly, the QIAstat Respiratory panel (Qiagen, Germantown, MD) is designed to allow the discrimination of respiratory pathogens including SARS-CoV-2.

Other novel technologies continue to be applied to develop SARS-CoV-2 assays and have received EUA for SARS-CoV-2 testing. The Rheonix (Ithaca, NY) assay uses a proprietary microfluidic Rheonix CARD cartridge technology that integrates specimen preparation and target detection using RT-PCR. Digital PCR-based assays have received EUA, including the Gnomegen (San Diego, CA) COVID-19 RT-Digital PCR Kit, which is validated on the Gnomegen real-time PCR instrument, and the QuantStudio 3D Digital PCR Systems (Applied Biosystems, Foster City, CA). Similarly, the Bio-Rad (Hercules, CA) SARS-CoV-2 ddPCR test is a droplet digital PCR assay.

The majority of the EUA assays are based on RT-PCR methodology, although isothermal nucleic acid amplification methodology such as TMA along with next-generation sequencing (NGS) and clustered regularly interspaced short palindromic repeats–based methodologies have also received EUA for SARS-CoV-2 clinical diagnostic testing. For example, the Illumina (San Diego, CA) COVIDSeq Test on the NovaSeq 6000 platform is an NGS assay in which the viral genome is sequenced. It is entirely conceivable that novel and cutting-edge technologies would be used in SARS-CoV-2 diagnostic testing. Many such technology platforms would be amenable for use in niche testing areas for SARS-CoV-2 depending on patient testing requirements.

In many instances, commercial IVD manufacturers have developed and validated current EUA assays on their own hardware systems for both nucleic acid extraction and the analytical method. Alternatively, other commercial manufacturers have developed kits that have been validated on generic platforms for either manual or automated nucleic acid extraction followed by analytical runs on, eg, RT-PCR platforms sold by other manufacturers.

As expected, cross-comparison studies have shown that there is variation in analytical sensitivity across these different methodologies and technology platforms.[6,20-23]

Cross-Platform Comparison Studies

Earlier in the pandemic, Carter et al[20] reviewed molecular assay methodologies used for EUA tests. Subsequently, several studies have emerged in which performance characteristics across several SARS-CoV-2 EUA assays were compared and useful cross-comparison data with respect to LOD were provided.[22,23]

Cradic et al[2] evaluated the clinical performance of 3 molecular assays using NP swab specimens and compared the Abbott (Lake Forest, IL) ID NOW COVID-19, the DiaSorin Molecular (Cypress, CA) Simplexa COVID-19 Direct, and the Roche cobas 6800 SARS-CoV-2 assays. The Simplexa and Roche cobas assays reportedly had approximately 10 to 100 times lower LODs than the Abbott ID NOW. Based on these evaluations, Cradic et al[2] proposed a multiplatform testing approach in relation to the patient population and the assay performance characteristics including assay sensitivity.

Table 1. Representative SARS-CoV-2 EUA Assay Systems.

Test/Instrument	Methodology	Gene Targets	Claimed LOD
Roche cobas SARS-CoV-2/cobas 6800/8800 systems	RT-PCR	*ORF1a/b*	0.007 $TCID_{50}$/mL
Thermofisher TaqPath COVID-19 Combo Kit/Applied Biosystems 7500, QuantStudio 5 and 7 systems	RT-PCR	*ORF1a/b, N, S*	10 GCE/reaction
Hologic Panther Fusion SARS-CoV-2 Assay/Panther Fusion	TMA	*ORF1*	0.01 $TCID_{50}$/mL
Abbott Real-Time SARS-CoV-2 Assay/m2000sp plus m2000rt systems	RT-PCR	*N, RdRp*	3.1 GE/reaction or 100 copies/mL
DiaSorin Molecular Simplexa COVID-19 Direct/Liaison MDX	RT-PCR	*ORF1, S*	500 copies/mL
Cepheid Xpert Xpress SARS-CoV-2 Test/GeneXpert Dx or GeneXpert Infinity systems	RT-PCR	*N2* and *E*	250 copies/mL
BioFire COVID-19 Test/FilmArray 2.0, FilmArray Torch System	RT-PCR	*ORF1a/b, ORF8*	0.022 $TCID_{50}$/mL or 330 copies/mL
Mesa Biotech/Accula SARS-CoV-2	Molecular LFA	*N*	200 copies/mL
Abbott ID NOW COVID-19	Isothermal	*RdRp*	125 GE/mL
Luminex NxTAG CoV Extended Panel Assay/Luminex MAGPIX	RT-PCR	*ORF1a/b, N, E*	5×10^3 GCE/mL
NeuMoDx SARS-CoV-2 Assay/288 Molecular System and NeuMoDx 96 Molecular System	RT-PCR	*Nsp2, N*	150 copies/mL
QIAstat-Dx Respiratory SARS-CoV-2 Panel	RT-PCR	*Orf1b (Rdrp), E*	500 copies/mL
Luminex ARIES SARS-CoV-2 Assay	RT-PCR	*ORF1a/b, N*	333 copies/mL
Gnomegen COVID-19 RT-Digital PCR Detection Kit/Gnomegen Real-Time Digital PCR Instrument or QuantStudio 3D Digital PCR System	RT-digital PCR	*N1/N2*	8 copies/reaction
InBios Smart *Detect* SARS-CoV-2 rRT-PCR Kit/7500 Fast Dx Real-Time PCR Instrument (Applied Biosystems) or CFX96 Touch Real-Time PCR Detection System (BioRad)		*E, N, ORF1b/ RdRp*	1100 GE/mL or 12.5 GE/reaction
BD SARS-CoV-2 Reagents/BD MAX System	RT-PCR	*N1, N2*	40 GE/mL
Atila Biosystems iAMP COVID-19 Detection Kit/BioRad CFX96 Real-Time System	Isothermal amplification	*N, ORF1a/b*	4 copies/ μL
Rheonix COVID-19 MDx Assay/Rheonix Encompass MDx Workstation	RT-PCR	*N1*	0.025 $TCID_{50}$/mL 625 GE/mL)
Bio-Rad SARS-CoV-2 ddPCR Test/QX200 and QXDx Droplet Digital PCR systems	ddPCR	*N1, N2*	625 copies/mL
BioFire Respiratory Panel 2.1 (RP2.1)/BioFire FilmArray System	RT-PCR	*S, M*	500 copies/mL or 0.069 $TCID_{50}$/mL
Sherlock CRISPR SARS-CoV-2 kit	RT-LAMP/CRISPR-based detection	*N, O*	4.5 copies/μL
Abbott Alinity m SARS-CoV-2 assay/Alinity m System	RT-PCR	*RdRp, N*	100 copies/mL
HDPCR SARS-CoV-2 Assay/Applied Biosystems QuantStudio 12K system	RT-PCR	*N1, N2*	250 copies/mL
Illumina COVIDSeq Test/NovaSeq 6000 Sequencing System	NGS	Virus genome	1000 copies/mL
BioCode SARS-CoV-2 Assay/BioCode MDx-3000	RT-PCR	*N*	0.0117 $TCID_{50}$/mL

CRISPR, clustered regularly interspaced short palindromic repeats; ddPCR, digital droplet polymerase chain reaction; EUA, emergency use authorization; FDA, U.S. Food and Drug Administration; GCE, genome copy equivalent; GE, genome equivalents; IFU, instructions for use; LFA, lateral flow assay; LOD, limit of detection; NGS, next-generation sequencing; RT-LAMP, reverse-transcription loop-mediated isothermal amplification; RT-PCR, reverse-transcription polymerase chain reaction; $TCID_{50}$, median tissue culture infectious dose; TMA, transcription-mediated amplification. Complete assay list may be accessed on the FDA website. The information summarized herein has been derived from the manufacturer's IFU, also accessible on the FDA website. Test/instrument, gene targets, and claimed LOD units are as reported in the manufacturer's IFU. Roche Diagnostics, Indianapolis, IN; Thermofisher Scientific, Waltham, MA/Applied Biosystems, Foster City, CA; Hologic, Inc., San Diego, CA; Abbott Diagnostics, Lake Forest, IL; Diasorin Molecular, Cypress, CA; Cepheid, Sunnyvale, CA; Biofire, Salt Lake City, UT; Mesa Biotech, Inc., San Diego, CA; Abbott Diagnostics, Lake Forest, IL; Luminex Corporation, Austin, TX; NeuMoDx Molecular, Inc., Ann Arbor, MI; Qiagen, Germantown, MD; Gnomegen, San Diego, CA; InBios, Seattle, WA; Becton Dickinson and Company, Sparks, MD; Atila Biosystems, Mountain View, CA; Rheonix Inc., Ithaca, NY; Bio-Rad Laboratories, Hercules, CA; Biofire, Salt Lake City, UT; Sherlock Biosciences, Cambridge, MA; Abbott Diagnostics, Lake Forest, IL; Applied Biosystems, Foster City, CA; Illumina, San Diego, CA; Applied BioCode, Santa Fe Springs, CA.

Craney et al[24] compared the diagnostic performance of 2 high-throughput assay systems, the Roche cobas 6800 and the Hologic Panther Fusion, using 389 nasopharyngeal specimens. The overall percentage agreement between the platforms was 96.4% ($\kappa = 0.922$). Remarkably, as reported, no significant difference existed between the corresponding C_T values generated on the 2 systems (*P* value = .88). The authors suggested that these assay systems can be considered comparable in terms of their clinical performance.

Lieberman et al[3] compared the analytical performance of the CDC primer set LDT and the Cepheid, DiaSorin Simplexa, Hologic Panther, and Roche cobas assays using a total of 169 NP swabs. The CDC-LDT and Cepheid Xpert Xpress SARS-CoV-2 assays were the most sensitive assays for SARS-CoV-2, with 100% agreement across specimens. However, as per Lieberman et al,[3] the Hologic Panther Fusion, the DiaSorin Simplexa, and the Roche cobas 6800 assays only failed to detect positive specimens near the

DOI: 10.1093/labmed/lmaa103

LOD of the CDC-LDT assay. The authors highlighted the importance of having multiple viral detection testing platforms available in a public health emergency.

Zhen, Manji, et al[22] stressed the importance of accurate testing results in patient management and, to that end, the importance of false negative results because they inevitably lead to more exposures that can be potentially devastating. Zhen, Smith, et al[23] compared the performance characteristics of 4 PCR methods that yielded comparable results ($\kappa \geq 0.96$); however, they did observe a notable difference when it came to overall LOD, with the GenMark (Carlsbad, CA) having the overall highest LOD of all 4 platforms evaluated and the DiaSorin Simplexa having the lowest LOD (39 ± 23 copies/mL), closely followed by the Hologic Panther Fusion (83 ± 36 copies/mL). Their modified CDC assay showed a final LOD of 779 ± 27 copies/mL. The clinical correlation was also consistent with LOD findings where both the DiaSorin Simplexa and Hologic Panther Fusion assays had 100% positive agreement and detected all specimens deemed positive by the consensus test result, which was 3 of 4 evaluated assays as the gold standard.

As is to be expected, differences exist in LODs across assays, as reported in these studies. More such studies[25,26] continue to be published with data that will better define the applicability and optimal use of these different assays in laboratory testing to inform clinical decision-making.

Factors Affecting LOD

Test manufacturers seeking EUA are required to establish performance characteristics such as accuracy, precision, analytical sensitivity, and analytical specificity. The analytical sensitivity of an assay is the ability of an assay to detect very low concentrations of a given analyte in a biological specimen. The LOD is the lowest actual concentration of an analyte that can be consistently detected in typically ≥95% of specimens tested; thus it is an important performance characteristic. Analytical performance at the low concentration limit is critical for infectious disease diagnostics.

As the representative assays presented in **Table 1** indicate, there is considerable variability in the manner in which molecular assay LODs are reported in manufacturer IFUs. Per manufacturer IFUs, the claimed LOD is reported as median tissue culture infectious dose ($TCID_{50}$)/mL, copies/mL, genome copy equivalent/mL, or copies/reaction. The genome equivalent is the amount of DNA necessary to be present in a purified specimen to guarantee that all genes are present.

The calculation for $TCID_{50}$/mL depends on the cell line being used for culture and is based on the degree of cytopathic effect observed in the tissue culture. Viral counts reported by $TCID_{50}$ tend to be much lower than RT-quantitative PCR measurements (Bar-On[27]). The RNA counts can overestimate infectious virions because the presence of viral RNA does not necessarily imply the presence of infectious virions. To assess the concentration of infectious viruses, researchers typically measure $TCID_{50}$, which involves infecting replicate cultures of susceptible cells with dilutions of the virus and noting the dilution at which half the replicate dishes become infected.

Several key variables define what is ultimately the LOD for a particular assay system because individual assay performance characteristics vary. Although LOD can be determined by calculating the point at which a signal can be discriminated from the background, it is more often determined empirically by testing serial dilutions of target analyte such as viral stocks.

In addition to the physicochemical factors that impact assay performance, some assay technologies involve direct specimen testing but most are methods that have a preanalytical specimen extraction step. The direct specimen assay systems include the Diasorin Simplexa Covid-19 Direct Assay on the Liaison MDX and the Atila Biosystems (Mountain View, CA) iAmp COVID-19 Detection Kit, which is run on the Bio-Rad CFX Real-Time System using an isothermal amplification method.

Among these assay systems, there is a variation in the input specimen volume for a given SARS-CoV-2 molecular assay that also affects what is ultimately determined to be the LOD for the assay.

Gene Targets

As shown in **Table 1**, assay designs vary across the assays and instruments on which they have been validated. The SARS-CoV-2 RNA transcript encodes multiple genes such as the replicase complex *ORF1ab,* the spike protein, the viral envelope,

the membrane, and the nucleocapsid proteins. Although gene targets are selected for their SARS-CoV-2 specificity, the assay designs have included 1 or more gene sequences among the *ORf1a/b,* nucleocapsid, spike protein, envelope, membrane, and RNA-dependent RNA polymerase genes.

The specificity of gene targets for SARS-CoV-2 is a critical part of assay design. This specificity is necessary for SAR-CoV-2 detection and discrimination among other related SARS viruses. Coronaviruses have a significantly lower mutation rate than those observed in other RNA viruses, such as the influenza virus, because of the presence of intrinsic proofreading activity during viral replication.[28-33] It is possible that successful SARS-CoV-2 replication cycles may accumulate mutations that could ultimately contribute to differences in clinical outcomes between patients with differing viral populations. Gussow et al[32] and Artesi et al[34] identified a C-to-U transition at position 26,340 of the SARS-CoV-2 genome that spans the envelope gene. Moreover, they stressed the importance of targeting 2 genomic regions to minimize the chance for false negative results. It is thus prudent to monitor circulating SARS-CoV-2 variants that may adversely impact the performance of RT-PCR diagnostic assays.[35]

Assay Protocol

Currently, the assays with EUA are all qualitative, providing a binary positive or negative answer (or a third answer as presumptive positive or indeterminate in a few assay systems). Most RT-PCR assay systems are set up for a C_T value <40 to be clinically reported as PCR-positive. However, this situation does not always occur because some assay systems continue amplification cycles beyond 40. It is likely that a patient test result that may be positive has a late C_T (eg, >40 C_T) and may remain undetected on a different assay platform. Nevertheless, a PCR-positive result indicates the presence of viral RNA and may not necessarily indicate the presence of viable virus. Thus, it is difficult to correlate the C_T values from one assay system to another in an accurate manner.[36,37]

It is assumed during PCR that each template molecule is duplicated once per cycle. However, for templates expressed at very low levels variance exists in the results from PCR reactions with scattered C_T values between replicate PCR reactions.[38] As can be envisaged for low copy number templates, comparison across different assay designs, instruments, target genes, and PCR physicochemical characteristics is difficult.

Specimen Types

The SARS-CoV-2 molecular tests discussed are performed after sampling using NP swabs or other upper respiratory tract specimens, including OP swabs or saliva. Aside from the diversity of assay designs, target genes, molecular methodologies, and platforms used to detect SARS-CoV-2, specific specimen types, which include NP and OP swabs, BAL, and sputum impact the LOD of an assay. In addition, alternate specimen types such as saliva and cotton swabs have also been validated for specific assays and intended uses, as has the use of saline as an alternative transport medium vs conventional viral transport medium. Limited allocations of swabs (and reagents) have compelled manufacturers (and clinical laboratories) to validate alternate swabs and transport to be used for patient specimen collection and testing.[39]

The timeline of testing for PCR positivity may vary with the type of specimen. However, BAL fluid specimens seem to show the highest positive rates, followed by sputum, nasal swabs, fibrobronchoscope brush biopsy, pharyngeal swabs, feces, and blood.[40] False-negative results may occur because of inappropriate timing of specimen collection in relation to illness onset and deficiency in sampling technique, especially of NP swabs. Research has shown that PCR positivity declines more slowly in sputum and may still be positive after NP swabs are negative. The persistence of PCR in sputum and stool has been found to be similar as assessed.[13]

International Standards

There is a dire need for the development of international standards for a SARS-CoV-2 RNA copy number. Development of such standards would permit comparison of the myriad assay systems such that the assay LOD can be reported in a standardized manner. This would be very useful for clinical practitioners and laboratory and other healthcare professionals.

To support its evaluation of diagnostic tests for COVID-19, the FDA has announced that it will provide a SARS-CoV-2 reference panel to ensure the quality of the tests, validation

Lab Medicine 2021;52;107–115 113
DOI: 10.1093/labmed/lmaa103

of new assays, test calibration, and monitoring of assay performance. The FDA panel will be available to commercial and laboratory developers who are interacting with the FDA through the pre-EUA process.

The Coronavirus Standards Working Group, bringing together commercial, academic, and public-sector interests, has been formed to develop tools that ensure the reliability and accuracy of this vital COVID-19 testing.[41] As stated on its website, this working group will develop an annotated inventory of resources, identify gaps, and conduct international collaborative experiments to evaluate and establish comparability of the diverse control materials and test methods available. A commendable objective is to pool knowledge to collaboratively produce the most-needed reference materials, reference samples, and reference measurement methods to underpin an enduring and reliable COVID testing enterprise.

Bustin and Nolan[42] stated in 2020 that current RT-PCR testing for SARS-CoV-2 has several shortcomings because of the shortage in the availability of suitable assays, reagents, equipment, and testing capacity. Interestingly, they recommended centralized RNA extraction procedures in containment level 3 facilities with dissemination of analytical testing of noninfectious RNA to nationwide laboratories. They suggested that these procedures be considered by public health organizations such as the CDC and Public Health England in the United Kingdom for protocols for emergency testing systems that can be rapidly adopted in emergency situations.

Conclusion

Worldwide multifarious assay systems are currently in use to test for SARS-CoV-2. To effectively implement clinical countermeasures, it is imperative to recognize the clinical decision-making that may be influenced by variation in the performance characteristics of the diverse assay systems in use for SARS-CoV-2 diagnostic testing. The assay results, particularly those that fall near the LOD, may not be commutable from one platform to another. As discussed herein, efforts to standardize across the different assays, platforms, and technologies would enhance clinical diagnostic testing to the ultimate benefit of patients. It is anticipated that cross-platform comparison studies will continue to add to our knowledge base. Simultaneous ongoing efforts to learn more about SARS-CoV-2 pathogenesis would lead to improved diagnostic testing such that successful preventive, diagnostic, and prognostic countermeasures may be implemented for controlling the ongoing pandemic. **LM**

References

1. https://www.fda.gov/medical-devices/coronavirus-disease-2019-covid-19-emergency-use-authorizations-medical-devices/vitro-diagnostics-euas#individual-molecular. Individual EUAs for molecular diagnostic tests for SARS-CoV-2. U.S Food & Drug Administration. Last updated November 6, 2020. Accessed November 13, 2020.
2. Cradic K, Lockhart M, Ozbolt P, et al. Clinical evaluation and utilization of multiple molecular in vitro diagnostic assays for the detection of SARS-CoV-2. *Am J Clin Pathol.* 2020;154(2):201–207.
3. Lieberman JA, Pepper G, Naccache SN, et al. Comparison of commercially available and laboratory developed assays for in vitro detection of SARS-CoV-2 in clinical laboratories. *J Clin Microbiol.* 2020;58:e00821-20.
4. Tan C, Xiao Y, Meng X, et al. Asymptomatic SARS-CoV-2 infections: What do we need to know? *Infect Control Hosp Epidemiol.* Published online ahead of print May 6, 2020. doi:10.1017/ice.2020.201.
5. https://www.cdc.gov/coronavirus/2019-ncov/hcp/testing-overview.html. Overview of testing for SARS-CoV-2 (COVID-19). Centers for Disease Control and Prevention. Updated October 21, 2020. Accessed November 13, 2020.
6. Zou L, Ruan F, Huang M, et al. SARS-CoV-2 viral load in upper respiratory specimens of infected patients. *N Engl J Med.* 2020;382:12.
7. He X, Lau EHY, Wu P, et al. Temporal dynamics in viral shedding and transmissibility of COVID-19. *Nat Med.* 2020;26(9):672–675.
8. Sun J, Xiao J, Sun R, et al. Prolonged persistence of SARS-CoV-2 RNA in body fluids. *Emerg Infect Dis.* 2020;26(8):1834–1838.
9. van Kampen JJA, van de Vijver DAMC, Fraaij PLA, et al. Shedding of infectious virus in hospitalized patients with coronavirus disease-2019 (COVID-19): duration and key determinants. Preprint. Posted online June 9, 2020. *medRxiv*. doi: 10.1101/2020.06.08.20125310.
10. Lan L, Xu D, Ye G, et al. Positive RT-PCR test results in patients recovered from COVID-19. *JAMA*. 2020;323(15):1502–1503.
11. Chen Y, Chen L, Deng Q, et al. The presence of SARS-CoV-2 RNA in the feces of COVID-19 patients. *J Med Virol.* 2020;92(7):833–840.
12. Gupta S, Parker J, Smits S, et al. Persistent viral shedding of SARS-CoV-2 in faeces—a rapid review. *Colorectal Dis.* 2020;22(6):611–620.
13. Wölfel R, Corman VM, Guggemos W, et al. Virological assessment of hospitalized patients with COVID-2019. *Nature.* 2020;581(7809):465–469.
14. Bullard J, Durst K, Funk D, et al. Predicting infectious SARS-CoV-2 from diagnostic samples. *Clin Infect Dis*. Published online May 22, 2020. doi: 10.1093/cid/ciaa638.
15. Huang C-G, Lee K-M, Hsiao M-J, et al. Culture-based virus isolation to evaluate potential infectivity of clinical specimens tested for COVID-19. *J Clin Microbiol.* 2020; 58:e01068-20.
16. https://www.who.int/publications/i/item/who-2019-nCoV-surveillanceguidance-2020.7. Public health surveillance for COVID-19: interim guidance. World Health Organization. Updated August 7, 2020. Accessed November 13, 2020.
17. Lv DF, Ying QM, Weng YS, et al. Dynamic change process of target genes by RT-PCR testing of SARS-Cov-2 during the course of a

coronavirus disease 2019 patient. *Clin Chim Acta.* 2020;506:172–175.

18. Kucirka L, Lauer S, Laeyendecker O, Boon D. Variation in false negative rate of RT-PCR based SARS-CoV-2 tests by time since exposure. *Ann Intern Med.* 2020;173(4):262–267.
19. Zimmermann P, Curtis N. Coronavirus infections in children including COVID-19. An overview of the epidemiology, clinical features, diagnosis, treatment and prevention options in children. *Pediatric Infect Dis J.* 2020;39(5):355–368.
20. Carter LJ, Garner LV, Smoot JW, et al. Assay techniques and test development for COVID-19 diagnosis. *ACS Cent Sci.* 2020;6(5):591–605.
21. Gorzalski AJ, Tian H, Laverdure C, et al. High-throughput transcription-mediated amplification on the Hologic Panther is a highly sensitive method of detection for SARS-CoV-2. *J Clin Virol.* 2020;129:104501.
22. Zhen WR, Manji E, Smith GJ, Berry GJ. Comparison of four molecular in vitro diagnostic assays for the detection of SARS-CoV-2 in nasopharyngeal specimens. *J Clin Microbiol*. 2020;58(8):e00743-20.
23. Zhen W, Smith E, Manji R, et al. Clinical evaluation of three sample-to-answer platforms for the detection of SARS-CoV-2. *J Clin Microbiol*. 2020;58(8):e00783-20.
24. Craney AR, Velu P, Satlin MJ, et al. Comparison of two high-throughput reverse transcription-polymerase chain reaction systems for the detection of severe acute respiratory syndrome coronavirus 2. *J Clin Microbiol.* 2020;58(8):e00890-20.
25. Rhoads DD, Cherian SS, Roman K, et al. Comparison of Abbott ID Now, DiaSorin Simplexa, and CDC FDA EUA methods for the detection of SARS-CoV-2 from nasopharyngeal and nasal swabs from individuals diagnosed with COVID-19. *J Clin Microbiol.* 2020;58(8):e00760-20.
26. Harrington A, Cox B, Snowden J, et al. Comparison of Abbott ID Now and Abbott m2000 methods for the detection of SARS-CoV-2 from nasopharyngeal and nasal swabs from symptomatic patients. *J Clin Microbiol.* 2020;58(8):e00798-20.
27. Bar-On YM, Flamholz A. SARS-CoV-2 (COVID-19) by the numbers. *Elife* 2020;9:e57309.
28. Denison MR, Graham RL, Donaldson EF, Eckerle LD, Baric RS. Coronaviruses: an RNA proofreading machine regulates replication fidelity and diversity. *RNA Biol.* 2011;8(2):270–279.
29. Fehr AR, Perlman S. Coronaviruses: an overview of their replication and pathogenesis. *Coronaviruses* 2020;1282:1–23.
30. Sanjuán R, Nebot MR, Chirico N, Mansky LM, Belshaw R. Viral mutation rates. *J Virol.* 2010;84(19):9733–9748.
31. Minskaia E, Hertzig T, Gorbalenya AE, et al. Discovery of an RNA virus exoribonuclease that is critically involved in coronavirus RNA synthesis. *PNAS* 2006;103:5108–5113.
32. Gussow AB, Auslander N, Faure G, Wolf YI, Zhang F, Koonin EV. Genomic determinants of pathogenicity in SARS-CoV-2 and other human coronaviruses. *Proc Natl Acad Sci U S A.* 2020;117(26):15193–15199.
33. Cimons M. SARS-CoV-2 is mutating slowly, and that's a good thing. https://hub.jhu.edu/2020/06/10/sars-cov-2-dna-suggests-single-vaccine-will-be-effective/. Accessed November 13, 2020.
34. Artesi M, Bontems S, Göbbels P, et al. A recurrent mutation at position 126340 of SARS-CoV-2 is associated with failure of the E-gene qRT-PCR utilized in a commercial dual-target diagnostic assay. *J Clin Microbiol.* 2020;58(10):e01598-20.
35. Hu J, He C-L, Gao Q-Z, et al. D614G mutation of SARS-CoV-2 spike protein enhances viral infectivity. Preprint. Posted online June 19, 2020. *bioRxiv* 178509. doi: 10.1101/2020.06.20.161323.
36. Sethuraman N, Jeremiah SS, Ryo A. Interpreting diagnostic tests for SARS-CoV-2. *JAMA.* 2020;323(22):2249–2251.
37. Nalla AK, Casto AM, Huang MW, et al. Comparative performance of SARS-CoV-2 detection assays using seven different primer/probe sets and one assay kit. *J Clin Microbiol.* 2020;58(6):e00557-20.
38. Bustin SA, Nolan T. Data analysis and interpretation. In: Bustin SA, ed. *A-Z of Quantitative PCR*. La Jolla, CA: IUL Press; 2004: 447–448.
39. Rodino KG, Espy MG, Buckwalter SP, et al. Evaluation of saline, phosphate buffered saline and minimum essential medium as potential alternatives to viral transport media for SARS-CoV-2 testing. *J Clin Microbiol*. 2020;58(6):e00590-20.
40. Wang W, Xu Y, Gao R, et al. Detection of SARS-CoV-2 in different types of clinical specimens. *JAMA*. 2020;323(18):1843–1844.
41. https://jimb.stanford.edu/covid-19-standards. Coronavirus Standards Working Group: a COVID-19 diagnostic standards development partnership. The Joint Initiative for Metrology in Biology. Accessed November 13, 2020.
42. Bustin SA, Nolan T. RT-qPCR testing of SARS-CoV-2: a primer. *Int J Mol Sci.* 2020;21:3004.

DOI: 10.1093/labmed/lmaa103

Science

The Utility of Elevated Serum Lactate Dehydrogenase in Current Clinical Practice

Kritika Krishnamurthy, MBBS, MD,[1,*] *Ana Maria Medina, MD,*[1,2] *Lydia Howard, MD*[1,2]

Laboratory Medicine 2021;52:e17-e22

DOI: 10.1093/labmed/lmaa059

ABSTRACT

Objective: Because of its wide tissue distribution, elevation of serum lactate dehydrogenase (LD) is a nonspecific finding. Although serum LD is still included in the prognosis and staging of metastatic melanoma and germ cell tumors, its nonspecificity has led to decreased usefulness.

Methods: In this study, we analyzed the serum LD assays performed in a 726-bed hospital during a 1-year period and reviewed charts of patients with serum LD of >3 standard deviations (SD).

Results: Of 312 patients with elevated serum LD, only 9 were patients with melanoma and germ cell tumors. The other 303 patients had other malignancies, chronic conditions, and sepsis.

Conclusion: Elevated serum LD (even >3 SD) is an extremely nonspecific finding that does not contribute to clinical management in a majority of patients. As such, serum LD testing should be retired from routine clinical order sets and restricted in use.

Keywords: lactate dehydrogenase, LD, serum LD, serum markers

The ability of the glycolytic pathway to produce adenosine triphosphate in the absence of oxygen allows tissues to survive in a hypoxic environment by preventing anoxic damage. Under anaerobic conditions, nicotinamide adenine dinucleotide hydride (NADH) is reoxidized by lactate dehydrogenase (LD) with the simultaneous reduction of pyruvate to lactate.[1] This reversible reaction is used for the estimation of LD activity in the clinical laboratory by determining the rate of NADH production spectrophotometrically at 340 nm.[2]

Research has shown that LD (molecular weight 134 kDa) is a peptide tetramer composed of 2 types of chains, H and M, which combine in differing proportions to form 5 isoenzymes: LD-1 is composed of 4 H subunits (H_4), LD-2 is composed of H_3M, LD-3 is composed of H_2M_2, LD-4 is composed of HM_3, and LD-5 is composed of M_4. The LD cytoplasmic enzyme is ubiquitous, but isoenzyme activity varies according to tissue type. In the heart, kidney, and erythrocytes, LD-1 and LD-2, the electrophoretically faster isoenzymes, predominate and the slower-moving LD-4 and LD-5 predominate in skeletal muscle.[3] The variable distribution of LD isoenzymes in different tissues has been used as a means of determining which tissue or organ is contributing to an increase in serum concentration. A much chronicled example is the use of the serum LD isoenzyme ratio in the diagnosis of myocardial infarction (MI), the "flipped" LD-1/LD-2.[3] However, LD isoenzyme distribution is assessed electrophoretically and thus is time consuming and not routinely performed at hospital laboratories,[3] whereas total serum LD can be determined spectrophotometrically in routine laboratory settings.

Because enzyme concentrations in various tissues are approximately 5000 to 15,000 times those found physiologically in normal serum,[1] even minimal tissue damage leading to leakage of serum LD results in significantly elevated total serum LD activity; this measurement has long been used as a marker for tissue damage in a variety of pathological

Abbreviations:

LD, lactate dehydrogenase; SD, standard deviation; NADH, nicotinamide adenine dinucleotide hydride; MI, myocardial infarction; ICD-10, International Classification of Diseases, 10th revision; CK-MB, creatine kinase MB.

[1]Arkadi M. Rywlin M.D. Department of Pathology and Laboratory Medicine, Mount Sinai Medical Center, Miami Beach, Florida, [2]Florida International University, Herbert Wertheim College of Medicine, Miami, Florida

*To whom correspondence should be addressed.
kritikakrishnamurthy@yahoo.com

conditions. Because of its wide tissue distribution, serum LD elevation is a nonspecific finding. However, because of the advent of more specific markers, serum LD concentrations are no longer used as a marker for tissue damage.[4,5]

Serum LD seems to have limited clinical implications in terms of patient management in modern medicine. Its use in the assessment of liver diseases has been largely undermined by the superiority of transaminases and alkaline phosphatase. Similarly, the creatine kinase assay is far more specific and hence superior in the assessment of muscular disorders.[1] The best indications for serum LD seem to be for confirming clinical hemolysis and using it to stage and guide management of certain tumors, such as malignant melanoma and germ cell tumors, as a biomarker.[1]

Despite its decreased usefulness, serum LD remains a test frequently ordered by clinicians and continues to be ordered often for hospitalized patients. In this study, we analyzed the serum LD assays performed in our hospital during a 1-year period and assessed the diagnostic and prognostic utilities of elevated serum LD and the cost of serum LD testing in modern medical practice.

Materials and Methods

This study was approved by the institutional review board at Mount Sinai Medical Center, Miami Beach, Florida. We retrospectively reviewed all the serum LD assays that were performed in the clinical chemistry laboratory at the Arkadi M. Rywlin M.D. Department of Pathology and Laboratory Medicine at Mount Sinai Medical Center between January 1, 2017, and December 31, 2017.

Serum LD concentrations were determined using a Siemens Dimension vista 1500 system (Siemens Healthcare Diagnostics Ltd, Cambridge, UK) with standard automated biochemical assays that were recommended by the International Federation of Clinical Chemistry and Laboratory Medicine.

This system uses L-lactate buffered at a pH of 9.4 as a substrate. The LD oxidizes the substrate in the presence of NAD^+ to yield pyruvate and NADH, which absorbs light at 340 nm. The LD activity is measured as a rate reaction at 340/700 nm, proportional to the amount of LD in the specimen. The normal value range of the assay is 87 U/L to 241 U/L (mean 164 U/L; standard deviation [SD] 38.5 U/L) in men and 84 U/L to 246 U/L (mean 165 U/L; SD 40.5 U/L) in women. Patients with serum LD concentrations >3 SD were included in this study. In view of the well-established ubiquity of LD, the cutoff of >3 SD was selected to enhance the selection for patients with significant tissue damage and to weed out elevations of diffuse or nonspecific etiology.

The charts of the patients with serum LD >3 SD were reviewed from the electronic medical record (using Epic, May 2019) to establish the main diagnosis for the current hospitalization and indication for serum LD testing based on *International Classification of Diseases,* 10th revision (ICD-10) codes and the documented treatment plan of the ordering physicians. Based on the clinical history and ICD-10 codes, the patients were classified into neoplastic and non-neoplastic groups. The progress notes of the ordering physicians and their clinical care teams were reviewed to see if the serum LD results were mentioned or discussed as a part of the treatment plan or algorithm.

The χ^2 test and Mann-Whitney *U* test for nonparametric variables were performed using IBM SPSS statistics version 22.0 software (**Figure 1**).

Results

A total of 3864 serum LD assays were performed in 3171 patients at Mount Sinai Medical Center from January 1, 2017, to December 31, 2017. Of these, 403 patients had serum LD concentrations of >2 SD and 316 patients had serum LD concentrations >3 SD (men >279.5 U/L; women >286.5 U/L) at least once. Of these 316 cases, 4 specimens were labeled as hemolyzed, based on the red discoloration of separated serum that was visually matched against a color chart by the technologist, and were excluded from the study.

Of the remaining 312 patients with serum LD >3 SD, 35 had neoplastic disorders with a median serum LD value of 502 U/L (295 U/L–5533 U/L) and 277 had non-neoplastic disorders with a median serum LD value of 396.75 U/L (283 U/L–9584 U/L) (**Table 1**). There was no statistically significant difference in serum LD concentrations between these 2 groups. Of the 35 patients with neoplastic disorders, 16 had carcinoma, 17 had hematologic malignancy, and 2 were being treated for sarcoma. Of the 16 patients with carcinoma, no significant difference was seen with primary site or cancer stage. Of the 277 patients with

Table 1. Distribution of Patients with Serum LD >3 SD Classified by Admitting Diagnosis and Dysfunctional Organ System

Disorder	Admitting Diagnosis/ Dysfunctional Organ System	Patients with Serum LD >3 SD	Median	Range	
				Min	Max
Neoplastic	Carcinoma	17[a]	657.00	297	3962
	Hematologic malignancies, myeloproliferative and myelodysplastic syndromes	17	502.00	280	5533
	Sarcomas	2	370.00	295	445
Non-neoplastic					
Sepsis		55[a]	469.00	283	5502
Noninfectious	Non-neoplastic kidney disease	14	363.50	292	1933
	Non-neoplastic liver, gallbladder, and pancreatic disease	15	485.00	311	4391
	MI (NSTEMI + STEMI)	5	387.00	345	1399
	Non-neoplastic hematologic disorders	31	402.00	288	9584
	Autoimmune disease	2	383.50	336	431
	Heart disease (excluding MI)	40[a]	467.50	283	6990
	Neurological disorders	10	430.50	305	3415
	Multiorgan diseases	47	399.50	285	9897
	Pediatric illness	5	669.00	564	1220
	Muscular disorders	5	330.00	297	1704
	Non-neoplastic respiratory disorders	33[a]	359.00	290	1894
	Non-neoplastic gastrointestinal disorders	12	372.50	291	751
	Psychiatric disorders	6	394.00	295	547
Total		312	416.50	280	9897

[a] *One case excluded because of hemolyzed specimen.*
MI, Myocardial Infarction; NSTEMI, Non ST elevated MI; STEMI, ST elevated MI.

non-neoplastic disorders, 54 had sepsis and the remaining 223 were being treated for noninfectious diseases. The median serum LD concentration in the septic group was 469 U/L (283 U/L–5502 U/L), and the median serum LD in the noninfectious group was 394 U/L (283 U/L–9584 U/L). No statistically significant difference was identified between the septic and noninfectious groups.

The nonseptic/noninfectious group included 14 patients with kidney disease, 15 patients with liver and pancreatobiliary disease, 31 patients with anemia and pancytopenia excluding hematologic malignancies, 2 patients with autoimmune disease, 44 patients with heart disease (including 5 MI), 32 patients with COPD and other respiratory disorders, 10 patients with neurologic disorders, 12 patients with gastrointestinal disorders, 6 patients with psychiatric illnesses, 5 patients with muscular disorders, 5 pediatric patients with various conditions, and 47 patients with multiple diagnoses. Statistical analysis failed to highlight any significant difference among any of the groups. Thus, serum LD elevations panned varied disease states, highlighting the nonspecificity and lack of diagnostic utility.

Of the 312 patients with elevated serum LD, 57 were repetitively tested for serum LD concentrations at variable intervals. Of these, 7 (12%) patients had neoplastic disorders and the remainder had non-neoplastic disorders. A single repeat test was conducted for 36 patients, 2 repeat tests were done for 12 patients, 3 repeat tests for 6 patients, and ≥4 for 3 patients. No particular clinical diagnosis, indication, or rationale was identified for repetitive testing. The serum LD concentrations showed a declining trend in 30 patients, a rising trend in 22 of these patients, and no significant change in 5 patients who underwent repeated testing. None of the trends were associated with any specific condition and seemed to be random.

Each serum LD test was performed at a cost of $2.50. The net cost of running 3864 serum LD tests was $9660.00, excluding the cost of quality control testing and wastage.

Discussion

Historically, the flipped pattern (ie, LD-1/LD-2 >1.0)[3] of serum LD isoenzymes was used for the late diagnosis

DOI: 10.1093/labmed/lmaa059

of MI. however, this flipped pattern was not specific to MI and could occur in hemolytic diseases and various tumors, causing diagnostic ambiguity. As a diagnostic marker for MI, serum LD started fading with the introduction of creatine kinase MB (CK-MB), which not only proved to be more specific but also has an earlier peak at 24 hours as compared with serum LD, which peaks in 72 hours.[6] However, CK-MB concentrations normalize in 3 to 4 days and are not helpful in late-presenting patients. Serum LD has held a distinct advantage in the regard that it remains elevated for 10 days to 14 days after MI. The advent of the cardiac troponin assay has been substantial because it is highly specific; cardiac troponin levels peak at 12 hours and remain elevated for 7 days, thus displacing serum LD in the diagnosis of MI.[7] This finding was apparent in our study, where out of 312 patients with elevated LD only 5 were diagnosed with MI. In none of these 5 patients were serum LD concentrations discussed as part of the clinical algorithm or treatment plan. Although we did not analyze the charts of patients with serum LD <3 SD, serum LD levels are generally elevated in patients with MI. Thus, it can be surmised that in patients with MI, serum LD level evaluation has been eclipsed by the use of cardiac troponins and has disappeared from the clinician's arsenal.[5]

Serum LD was also tested as a marker of declining liver function. In our study, serum LD was found elevated in patients with varied gastrointestinal complaints, including but not limited to cholecystitis, pancreatitis, and cirrhosis. Given its ubiquitous distribution and the superior specificity of transaminases and alkaline phosphatases, serum LD has little to no value in the diagnosis or prognosis of liver disease.[8] The role of elevated serum LD in the absence of transaminase elevation when diagnosing space-occupying lesions of the liver has been voided by the development of markers such as 5'nucleotidase and gamma glutamyltanferase.[9] In a study by Puri et al,[10] a significant positive correlation was found between erythrocyte fructose 6 phosphate concentrations and serum LD-5 concentrations, supporting the use of LD-5 as a marker of dietary fructose–associated hepatotoxicity. However, there is no strong evidence yet in support of the role of fructose in hepatic dysfunction. We have very limited experience in this field, and given that LD-5 is present in muscles, any type of muscle injury would lead to its elevation and thus the specificity of LD-5 as a marker would be poor.

Serum LD is often used for expeditious confirmation of in vivo hemolysis in the clinical setting. However, hemolysis that occurs because of preanalytical handling also results in a false increase in serum LD[11] concentrations, thus invalidating its diagnostic utility. Therefore, in our study, hemolyzed specimens were excluded. Serum LD concentrations may also be elevated because of increased erythrocyte precursor turnover in megaloblastic anemia. Deficiency of folate or vitamin B12 causes the erythrocyte precursor cell to break down in the bone marrow, also resulting in the release of large quantities of LD-1 and LD-2.[12] Serum LD was elevated to >3 SD in patients with anemia in this study, but it was not significantly different among the types of anemia. Notably, it was also elevated in cases of pancytopenia and myelofibrosis. It is evident that lack of specificity hinders the use of serum LD in differentiating among the different types of anemias.

In addition to hemolysis, another factor that leads to specious elevation of serum LD is macro-LD. Macroenzymes are complexes of serum enzymes with a protein leading to a prolonging of the enzyme's half-life.[13] Macro-LD is LD complexed with IgG or IgM. It is a rare form but occurs in approximately 1 of 10,000 people, causing a false elevation in serum LD level.[14]

Cancer cells undergo metabolic reprogramming to sustain higher proliferative rates. Under aerobic conditions, normal cells seem to generate most of their energy through mitochondrial oxidative phosphorylation, whereas tumor cells produce a substantial amount of their energy through glycolysis. This Warburg effect followed by an increased turnover of tumor cells leads to elevation of serum LD.[15] Thus, serum LD concentrations have been used in the prognosis and management of tumors. With the discovery of newer and more specific tumor markers, the use of serum LD is fast declining. In our study, serum LD was elevated in equal numbers of epithelial and nonepithelial malignancies with no significant difference between the 2 types. It still holds value in certain tumors such as testicular nonseminomatous germ cell tumors, where it is included in American Joint Committee on Cancer recommendations for use in conjunction with alpha-fetoprotein and human chorionic gonadotropin as a serological marker for diagnosis, staging, and long-term follow-up.[16] Serum LD also remains the best available prognosticator in metastatic melanoma and continues to be included in TNM staging.[17] Daneshmandi et al[18]

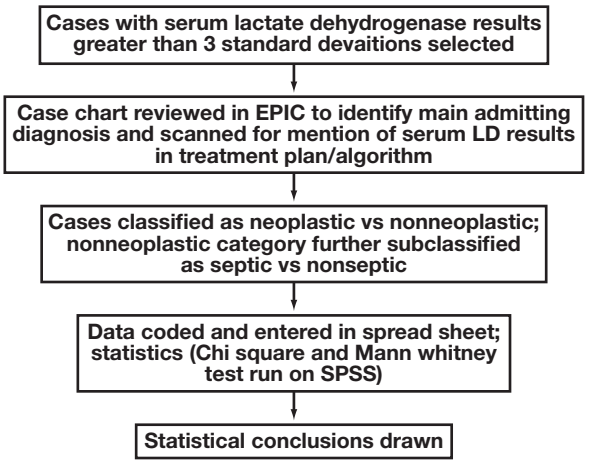

Figure 1

Workflow diagram of data collection.

showed that the efficacy of anti-programmed cell death-1 treatment was improved by blocking LD-A. Serum LD is also ocassionally elevated in lymphoid neoplasms and is commonly used for prognostication, assessing treatment response, and monitoring for tumor recurrence in patients with non-Hodgkin's lymphoma and acute leukemias.[19,20]

Unfortunately, very few cases of germ cell tumors, melanomas, and non-Hodgkin lymphomas underwent regular serum LD at our hospital for us to comment on its utility in these cancers, which remains a limitation of this study. Given the large-scale studies that prove its effectiveness, melanomas, germ cell tumors, non-Hodgkin's lymphoma, and acute leukemias may be the rare medical conditions that do merit serum LD for staging purposes. However, for diagnosis and follow-up, serum LD cannot be used as a stand-alone test and will need to be supplemented with other confirmatory investigations.

Elevated serum LD seems to have no value in the assessment of renal disease, neuromuscular disorders, pulmonary diseases, or autoimmune disorders, with each of these entities having superior and more specific markers. Although in our study serum LD was elevated in multiple patients with the above-mentioned conditions, the concentrations had no impact on patient management.

Serum LD may be elevated in a number of disorders, but its ubiquitous distribution is a severe handicap to its meaningful clinical utility. In addition, false elevation because of hemolysis and macro-LD further abrogate its value as a clinical marker. Although it still serves some purpose in prognostication, follow-up, and staging of certain tumors such as melanoma, non-Hodgkins lymphoma and germ cell tumor, serum LD elevation in other conditions is clinically irrelevant in the presence of better, more specific markers. This study focused on serum LD elevation, and only patients with serum LD >3 SD were reviewed. The study did not address the clinical value of a negative test ruling out serum LD elevation. Although this missing element is a limitation of the study, the authors emphasize the ubiquitous distribution of serum LD and its lack of specificity, which diminishes its clinical utility. Serum LD is used to assess for significant tissue damage. Our review of the current literature failed to reveal any conditions except those previously mentioned where the absence of serum LD elevation alone is clinically useful. In addition, this study was conducted among hospitalized patients, who are in general thoroughly investigated. As such, any potential screening role of serum LD among outpatients has not been addressed in this study.

Of the 312 patients with elevated serum LD, only 9 had melanoma and germ cell tumors, comprising 0.3% of the elevated serum LD cases. If serum LD concentrations >2 SD were assessed and the same percentage extrapolated, only 19 patients with elevated serum LD would impact clinical management, costing approximately $1750 in a single institution in a single year. Assuming similar practices across most hospitals, this cost would increase exponentially. The remaining 3855 serum LD tests (ie, the total 3864 minus the 9 melanomas and germ cell tumors) performed at our laboratory over the year examined, with a cost of $9637.50, were extraneous in the clinical course and management of patients. These unnecessary tests are not only a waste of financial and human resources from the standpoint of test performance but may also lead to wastage of specimens, especially in patients from whom obtaining adequate blood specimens is difficult such as neonates.

Conclusion

As such, serum LD testing should be retired from routine clinical order sets for hospitalized patients and restricted to use in melanomas, germ cell tumors, non-Hodgkin's

Lab Medicine 2021;52;e17–e22 e21
DOI: 10.1093/labmed/lmaa059

lymphoma, and acute leukemias. This measure would reduce an unnecessary economic burden and provide more efficient patient management. **LM**

References

1. Panteginini M, Bais R. Serum enzymes. In: Burtis C, Bruns D, eds. *Teitz Fundamentals of Clinical Chemistry and Molecular Diagnostics*. 7th ed. St. Louis, MO: Elsevier Saunders; 2014:318–336.
2. Schumann G, Bonora R, Ceriotti F, et al. IFCC primary reference procedures for the measurement of catalytic activity concentrations of enzymes at 37 degrees C. Part 3. Reference procedure for the measurement of catalytic concentration of lactate dehydrogenase. *Clin Chem Lab Med.* 2002;40(6):643–648.
3. Pincus MR, Abraham NZ, Carty RP. Clinical enzymology. In: McPherson RA, Pincus MR, eds. *Henry's Clinical Diagnosis and Management*. 22nd ed. Philadelphia, PA: Elsevier Saunders; 2011:273–295.
4. Martins JT, Li DJ, Baskin LB, Jialal I, Keffer JH. Comparison of cardiac troponin I and lactate dehydrogenase isoenzymes for the late diagnosis of myocardial injury. *Am J Clin Pathol.* 1996;106(6):705–708.
5. Randall DC, Jones DL. Eliminating unnecessary lactate dehydrogenase testing. A utilization review study and national survey. *Arch Intern Med.* 1997;157(13):1441–1444.
6. Roe CR. Diagnosis of myocardial infarction by serum isoenzyme analysis. *Ann Clin Lab Sci.* 1977;7(3):201–209.
7. Bodor GS. Biochemical markers of myocardial damage. *EJIFCC.* 2016;27(2):95–111.
8. Reichling JJ, Kaplan MM. Clinical use of serum enzymes in liver disease. *Dig Dis Sci.* 1988;33(12):1601–1614.
9. Jialal I, Sokoll LJ. Clinical utility of lactate dehydrogenase: a historical perspective. *Am J Clin Pathol.* 2015;143(2):158–159.
10. Puri BK, Kingston MC, Monro JA. Fructose-associated hepatotoxicity indexed by the lactate dehydrogenase isoenzyme LDH-5. *Med Hypotheses.* 2019;124:40–41.
11. Rousseau N, Pige R, Cohen R, Pecquet M. What is the acceptable hemolysis index for the measurements of plasma potassium, LDH and AST? *Ann Biol Clin (Paris).* 2016;74(3):323–328.
12. Beck WS. Erythrocyte disorders—anemias related to disturbance of DNA synthesis (megaloblastic anemias). In: Williams WJ, Beutler E, Erslev AJ, Lichtman MA, eds. *Hematology.* 3rd ed. New York, NY: McGraw-Hill; 1983: 434.
13. Galasso PJ, Litin SC, O'Brien JF. The macroenzymes: a clinical review. *Mayo Clin Proc.* 1993;68(4):349–354.
14. Mifflin TE, Bruns DE, Wrotnoski U, et al. University of Virginia case conference: macroamylase, macrocreatinekinase and other macroenzymes. *Clin Chem*. 1985;31(10):1243–1248.
15. Icard P, Lincet H. A global view of the biochemical pathways involved in the regulation of the metabolism of cancer cells. *Biochim Biophys Acta.* 2012;1826(2):423–433.
16. Gilligan TD, Seidenfeld J, Basch EM, et al.; American Society of Clinical Oncology. American Society of Clinical Oncology clinical practice guideline on uses of serum tumor markers in adult males with germ cell tumors. *J Clin Oncol.* 2010;28(20):3388–3404.
17. Petrelli F, Ardito R, Merelli B, et al. Prognostic and predictive role of elevated lactate dehydrogenase in patients with melanoma treated with immunotherapy and BRAF inhibitors: a systematic review and meta-analysis. *Melanoma Res.* 2019;29(1):1–12.
18. Daneshmandi S, Wegiel B, Seth P. Blockade of lactate dehydrogenase-A (LDH-A) improves efficacy of anti-programmed cell death-1 (PD-1) therapy in melanoma. *Cancers (Basel)*. 2019;11(4):E450.
19. Endrizzi L, Fiorentino MV, Salvagno L, Segati R, Pappagallo GL, Fosser V. Serum lactate dehydrogenase (LDH) as a prognostic index for non-Hodgkin's lymphoma. *Eur J Cancer Clin Oncol.* 1982;18(10):945–949.
20. Yadav C, Ahmad A, D'Souza B, et al. Serum lactate dehydrogenase in non-Hodgkin's lymphoma: a prognostic indicator. *Indian J Clin Biochem.* 2016;31(2):240–242.

Machine Learning Prediction of SARS-CoV-2 Polymerase Chain Reaction Results with Routine Blood Tests

Thomas Tschoellitsch, MD,[1] *Martin Dünser, MD,*[1] *Carl Böck, MSc,*[1] *Karin Schwarzbauer, MSc,*[2] *Jens Meier, MD*[1,*]

Laboratory Medicine 2021;52:146-149

DOI: 10.1093/labmed/lmaa111

ABSTRACT

Objective: The diagnosis of COVID-19 is based on the detection of SARS-CoV-2 in respiratory secretions, blood, or stool. Currently, reverse transcription polymerase chain reaction (RT-PCR) is the most commonly used method to test for SARS-CoV-2.

Methods: In this retrospective cohort analysis, we evaluated whether machine learning could exclude SARS-CoV-2 infection using routinely available laboratory values. A Random Forests algorithm with 28 unique features was trained to predict the RT-PCR results.

Results: Out of 12,848 patients undergoing SARS-CoV-2 testing, routine blood tests were simultaneously performed in 1357 patients. The machine learning model could predict SARS-CoV-2 test results with an accuracy of 86% and an area under the receiver operating characteristic curve of 0.74.

Conclusion: Machine learning methods can reliably predict a negative SARS-CoV-2 RT-PCR test result using standard blood tests.

The diagnosis of COVID-19 is based on the detection of SARS-CoV-2 in respiratory secretions, blood, or stool.[1,2] Currently, reverse-transcription polymerase chain reaction (RT-PCR) is the most commonly used method to test for SARS-CoV-2.[3] Key limitations of this technique are its restricted availability and time requirement, often leaving clinicians unaware of the patient's virus status for 12 hours or longer.

Materials and Methods

In this retrospective cohort analysis, we evaluated whether machine learning could exclude SARS-CoV-2 PCR infection using routinely available laboratory values. Therefore, we extracted demographic, clinical, and laboratory data and concurrent (ie, within a 24-hour window) SARS-CoV-2 RT-PCR test results (Cobas SARS-CoV-2, Roche, Freiburg, Germany and Real-Time PCR Assay, BioProducts Genesig, Camberley, United Kingdom) from the electronic charts of patients in whom a SARS-CoV-2 test was performed at the Kepler University Hospital in Linz, Austria, from March 1, 2020, until April 30, 2020. Laboratory results used were from within 24 hours of admission. We trained a machine learning model (the Random Forests algorithm)[4] using R version 3.6.3[5] and the packages RandomForest 4.6–14, Boruta 7.0.0, Psych 2.0.9, pROC 1.16.2, ROCR 1.0–11, Amelia 1.7.6, and Caret 6.0–86[6], ranger 0.12.1 using laboratory data with 1353 unique features of which 28 were used in the final model. The following standard laboratory values were included: blood count, electrolytes, C-reactive protein, creatinine, blood urea nitrogen, liver enzymes, bilirubin, cholinesterase, and prothrombin time.

Thereafter, the dataset underwent extensive data preprocessing and data cleaning. The data cleaning included detection of typos and out-of-range values and the imputation of missing values; features with more than 25% of missing values were excluded. The remaining missing values were imputed using Strawman imputation, which replaces missing data by median values (continuous variables) or the most frequently occurring

Abbreviations:

RT-PCR, reverse-transcription polymerase chain reaction; ROC, receiver operating characteristic; WHO, World Health Organization.

[1]Department of Anesthesiology and Critical Care Medicine, Kepler University Hospital GmbH and Johannes Kepler University, Faculty of Medicine, Linz, Austria, [2]Institute for Machine Learning, Johannes Kepler University, Linz, Austria

*To whom correspondence should be addressed.
jens.meier@kepleruniklinikum.at

value (categorical values). The Strawman imputation method yielded results comparable to other, more complicated methods (eg, the "missForest" technique[7]). Censored numerical data were truncated (eg, "<0.1" was replaced by 0.1). Categorical features with >2 values were one-hot encoded (ie, a binary encoding for every category). Ordinal features were encoded as positive integers. Binary and numerical features were included as they were.

For the determination of our model performance, we conducted nested cross-validation. The hyperparameter search was conducted in the inner five-fold cross-validation loop via grid-search. The model performance is estimated in the outer loop in five folds. The study protocol was approved by the Ethics Committee of Upper Austria (No. 1104/2020).

Results

Out of 12,848 patients undergoing SARS-CoV-2 testing, routine blood tests were performed concurrently in 1528 patients who were then included in the statistical analysis (**Table 1**). Of the 1528 study participants, 65 tested positive for SARS-CoV-2. After data cleaning 1357 study participants were analyzed.

As calculated from the confusion matrix (**Table 2**), the machine learning model was able to detect SARS-CoV-2 test results with an accuracy of 81%, an area under the ROC curve of 0.74 (**Figure 1A**), a sensitivity of 60%, and a specificity of 82%. The positive and negative predictive values were 13%

Table 1. Patient Characteristics and Routine Blood Results

Variable	All Patients Mean (SD)	SARS-CoV-2 Test Negative Mean (SD)	SARS-CoV-2 Test Positive Mean (SD)
n	1528	1463	65
Age (y)	56.3 (26.6)	55.9 (26.7)	64 (21)
Female sex, n (%)	50.1	50.1	44.6
Hospitalized, n (%)	19.5	19.3	23.1
Hb (g/dL)	13.0 (2.3)	13.0 (2.3)	13.1 (2.2)
Hct (% red blood cells in whole blood)	38 (7)	38 (7)	38 (6)
MCH (pg/cell)	29.7 (2.7)	29.7 (2.7)	30.2 (2.5)
MCHC (g/dL)	33.8 (1.4)	33.7 (1.4)	34.5 (1.4)
MCV (fL)	88.1 (6.9)	88.1 (2.7)	87.5 (6.1)
MPV (fL)	9.8 (1.5)	9.8 (1.5)	10.3 (1.4)
RDW-CV (%)	14.1 (2.1)	14.2 (2.1)	13.6 (1.9)
Erythrocytes (10^{12}/L)	4.4 (0.8)	4.4 (0.8)	4.3 (0.8)
Normoblasts (cells/L)	0.0 (0.6)	0 (0.1)	0 (0)
White blood cell count (10^9/L)	10.0 (7.3)	10.1 (7.4)	6.7 (5.1)
Platelets (10^9/μL)	255 (96)	258 (95)	200 (106)
Sodium (mmol/L)	137 (5)	137 (5)	134 (5)
Chloride (mmol/L)	101 (5)	101 (5)	98 (6)
Potassium (mmol/L)	4.0 (0.6)	4.0 (0.6)	3.8 (0.4)
Total calcium (mmol/L)	2.3 (0.2)	2.3 (0.2)	2.2 (0.2)
Creatinine (mg/dL)	1.2 (1.0)	1.2 (1.0)	1.1 (0.5)
GFR (mL/min)	70 (27)	70 (27)	70 (24)
BUN (mg/dL)	20 (17)	21 (17)	20 (16)
Total bilirubin (mg/dL)	0.7 (0.9)	0.7 (0.9)	0.7 (0.7)
ALT (U/L)	39 (119)	40 (122)	28 (17)
gGT (U/L)	74 (183)	75 (186)	53 (59)
LDH (U/L)	264 (188)	262 (190)	304 (137)
Cholinesterase (kU/L)	6.7 (2.3)	6.8 (2.3)	6.2 (2.3)
Alkaline phosphatase (U/L)	106 (132)	108 (134)	78 (39)
Prothrombin time (%)[a]	84 (25)	84 (26)	86 (22)

ALT, alanine aminotransferase; BUN, blood urea nitrogen; GFR, glomerular filtration rate; gGT, gamma glutamyl transferase; Hb, hemoglobin; Hct, hematocrit; LDH, lactate dehydrogenase; MCH, mean corpuscular hemoglobin; MCHC, mean corpuscular hemoglobin concentration; MCV, mean corpuscular volume; MPV, mean platelet volume; RDW-CV, red blood cell distribution width; SD, standard deviation.

SI conversion factors: To convert Hb or MCHC to g/L, multiply values by 10, Hct % × 0.01 → Proportion of 1.0, creatinine mg/dL × 88.4 → μmol/L, GFR mL/min × 60 → mL/s, BUN mg/dL × 0.357 → mmol/L, total bilirubin mg/dL × 17.104 → μmol/L, ALAT, gGT, LDH, alk. Phosphatase U/L × 0.0167 → μkat/L.

Data are given as mean values ± SD, if not otherwise indicated.

[a]Normal range 78%–123% for our laboratory.

Lab Medicine 2021;52;146–149 147
DOI: 10.1093/labmed/lmaa111

and 98%, respectively (F1 score = 0.21). The importance of single features for the model is displayed in **Figure 1B**.

Discussion

Our results suggest that machine learning methods can predict SARS-CoV-2 RT-PCR results using routine blood values with fair accuracy. Although from a bedside perspective the value of such a model to predict a positive SARS-CoV-2 test result was poor, the high negative predictive value of 99% allows clinicians to reliably predict a negative SARS-CoV-2 test result with acceptable safety. The machine learning algorithm used, Random Forests, although not new, is a proven and effective method.

Table 2. Confusion Matrix for Model Results

Confusion Matrix	Actual Positive	Actual Negative
Predicted positive (%)	34 (6.8 ± 3.2)	232 (46.4 ± 9.6)
Predicted negative (%)	20 (4 ± 0.7)	1071 (214.2 ± 9.1)
Accuracy: 86.1% (%)	PPV: 20.0	NPV: 98.8

NPV, negative predicted value; PPV, positive predicted value.
First number: All folds; parentheses: mean and standard variance per fold.

When evaluating the feature importance reported by the machine learning models, leukocyte count ranked as the most important feature. Elevated white blood cell counts have been observed early on in COVID-19 and have been linked to inflammation, similar to an increase in the neutrophil-to-lymphocyte ratio.[8] Another highly ranked feature, hemoglobin level, has been associated with mortality from COVID-19.[9] Serum calcium changes are considered to be important for various functions of viruses such as structure and gene expression and release, along with promoting inflammation pathways linked to lung cell damage and edema formation.[10,11]

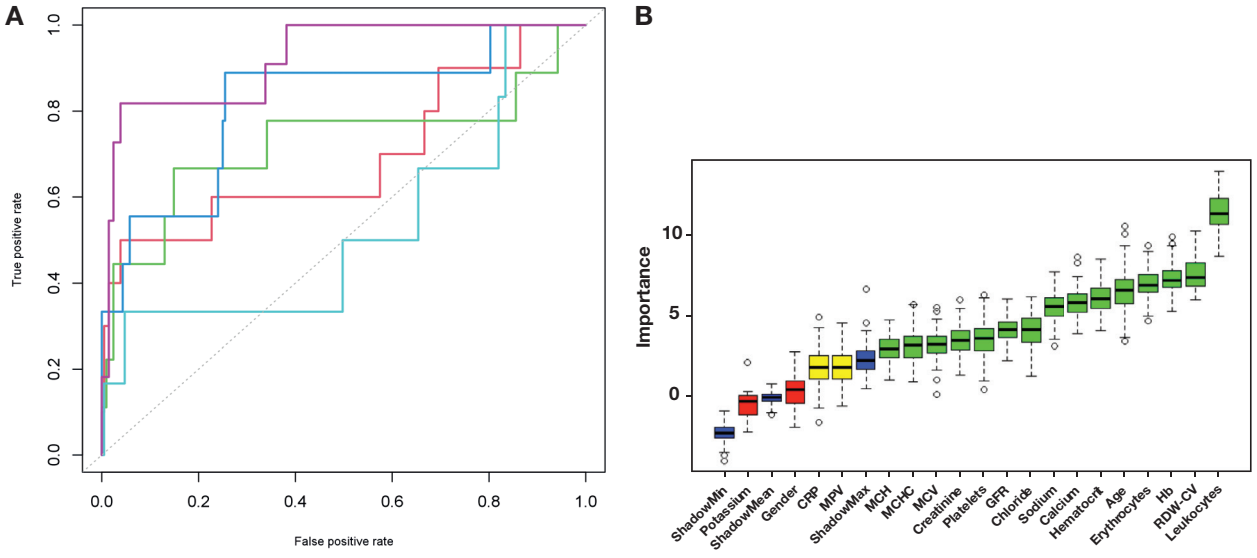

Figure 1

Machine learning model results. A, ROC, AUC (SD): 0.898 (0.002); every fold displayed in individual color. B, Relative feature importance of Random Forests algorithm obtained from the Boruta package of R.[5] ShadowMin, shadowMax, and shadowMean refer to features created by the Boruta algorithm[2,3] by shuffling the original features' values (so-called shadow features) and training a model for prediction on the combined original and shuffled feature values; using this model, the *Z*-scores for the shadow features' importances are calculated. Those features that are ranked more important than their shadow counterpart are marked as important. The Boruta algorithm is used as a validation method for feature importances calculated by the Random Forest algorithm. Blue boxplots are minimal, average, and maximum *Z*-scores of shadow features; red, yellow, and green boxplots are features that were rejected, remain tentatively important, and are confirmed important, respectively. Box upper and lower horizontal edges are first and third quartiles, whiskers denote the 1.5 interquartile range of feature importance, and circles are outliers. AUC, area under the curve; CRP, C-reactive protein; MCH, mean corpuscular hemoglobin; MCHC, mean corpuscular hemoglobin concentration; MCV, mean corpuscular volume; GFR, glomerular filtration rate; Hb, hemoglobin; RDW-CV, red blood cell distribution width; ROC, receiver operating characteristic; SD, standard deviation.

Our results may have relevant clinical implications, particularly for settings where SARS-CoV-2 RT-PCR testing is not readily available and/or personal protection equipment is in short supply.

Although World Health Organization (WHO) considerations have defined acceptable and desirable price ranges for large-volume SARS-CoV-2 RT-PCR testing, demand vs general availability and currently reported current prices commonly exceed these recommendations by a factor of 10 or higher.[12,13] On the contrary, commonly reported reference costs of routinely ordered laboratory tests that were identified as features of high importance in our prediction model are well below the WHO-designated desirable range for SARS-CoV-2 RT-PCR tests.[14] It can therefore be considered beneficial from an economic point of view to employ the presented model as support for clinical decision-making.

When interpreting the results of our analysis, 2 limitations must be considered. First, RT-PCR test results can be false-negative and false-positive.[15] This potential impairs the validity of the model to predict true-negative RT-PCR results. Second, although 1357 study patients were included in our analysis, the sample size may still be considered low for machine learning methods, especially regarding the asymmetry of the classification problem. Inclusion of more patients may therefore have yielded more valid results.

Conclusion

In conclusion, machine learning methods can reliably predict a negative SARS-CoV-2 RT-PCR test result using standard blood values.

References

1. Corman VM, Landt O, Kaiser M, et al. Detection of 2019 novel coronavirus (2019-nCoV) by real-time RT-PCR. *Eurosurveill.* 2020;25(3):2000045.
2. Chen Y, Chen L, Deng Q, et al. The presence of SARS-CoV-2 RNA in the feces of COVID-19 patients. *J Med Virol*. 2020;92(7):833–840.
3. Cheng MP, Papenburg J, Desjardins M, et al. Diagnostic testing for severe acute respiratory syndrome–related coronavirus 2: a narrative review. *Ann Intern Med.* 2020;172(11):726–734.
4. Breiman L. Random forests. *Mach Learn.* 2001;45(1):5–32.
5. R: The R Project for Statistical Computing [computer program]. The R Foundation. 2020. https://www.r-project.org/. Accessed November 24, 2020.
6. The Comprehensive R Archive Network [computer program]. The R Foundation. 2020. https://cran.r-project.org/. Accessed November 24, 2020.
7. Stekhoven DJ, Bühlmann P. MissForest—non-parametric missing value imputation for mixed-type data. *Bioinformatics.* 2012;28(1):112–118.
8. Qin C, Zhou L, Hu Z, et al. Dysregulation of immune response in patients with coronavirus 2019 COVID-19 in Wuhan, China. *Clin Infect Dis.* 2020;71(15):762–768.
9. Sayad B, Afshar ZM, Mansouri F, Rahimi Z. Leukocytosis and alteration of hemoglobin level in patients with severe COVID-19: association of leukocytosis with mortality. *Health Sci Rep.* 2020;3(4):e194.
10. Zhou Y, Frey TK, Yang JJ. Viral calciomics: interplays between Ca2+ and virus. *Cell Calcium.* 2009;46(1):1–17.
11. Cappellini F, Brivio R, Casati M, Cavallero A, Contro E, Brambilla P. Low levels of total and ionized calcium in blood of COVID-19 patients. *Clin Chem Lab Med.* 2020;58(9):e171–e173.
12. Ramdas K, Darzi A, Jain S. "Test, re-test, re-test": using inaccurate tests to greatly increase the accuracy of COVID-19 testing. *Nat Med.* 2020;26(6):810–811.
13. COVID-19 target product profiles for priority diagnostics to support response to the COVID-19 pandemic v.1.0. World Health Organization website. https://www.who.int/publications/m/item/covid-19-target-product-profiles-for-priority-diagnostics-to-support-response-to-the-covid-19-pandemic-v.0.1. Published September 28, 2020. Accessed November 24, 2020.
14. Estimated costs of 51 commonly ordered laboratory tests in Canada - PubMed [Internet]. [cited 2020 September 26]. Available from: https://pubmed.ncbi.nlm.nih.gov/30615855/.
15. Wikramaratna PS, Paton RS, Ghafari M, Lourenço J. Estimating the false-negative test probability of SARS-CoV-2 by RT-PCR. Preprint. Posted online October 14, 2020. medRxiv. https://www.medrxiv.org/content/10.1101/2020.04.05.20053355v3.

DOI: 10.1093/labmed/lmaa111

ABL Kinase Domain Mutations in Iranian Chronic Myeloid Leukemia Patients with Resistance to Tyrosine Kinase Inhibitors

Mahboobeh Shojaei, PhD,[1] Hamid Rezvani, MD,[2] Azita Azarkeivan, MD,[1] Behzad Poopak, PhD[3]*

Laboratory Medicine 2021;52:158-167

DOI: 10.1093/labmed/lmaa052

ABSTRACT

Objective: Tyrosine kinase inhibitors (TKIs) are considered standard first-line treatment in patients with chronic myeloid leukemia. Because ABL kinase domain mutations are the most common causes of treatment resistance, their prevalence and assessment during treatment may predict subsequent response to therapy.

Methods: The molecular response in *Bcr-Abl1*^{IS} was tested via quantitative real-time polymerase chain reaction. We used the direct sequencing technique to discover the mutations in the ABL kinase domain. The IRIS trial established a standard baseline for measurement – (100% BCR-ABL1 on the 'international scale') and a major molecular response (good response to therapy) was defined as a 3-log reduction in the amount of BCR-ABL1 – 0.1% BCR-ABL1 on the international scale.

Results: We observed 11 different mutations in 13 patients, including E255K, which had the highest mutation rate. A lack of hematologic response was found in 22 patients, who showed a significantly higher incidence of mutations.

Conclusion: Detection of kinase domain mutations is a reliable method for choosing the best treatment strategy based on patients' conditions, avoiding ineffective treatments, and running high-cost protocols in patients with acquired resistance to TKIs.

Keywords: chronic myeloid leukemia, mutation, TKI, sequencing

Chronic myeloid leukemia (CML) is a clonal myeloproliferative neoplasm, resulting from the t(9;22)(q34;q1) translocation, forming the chimeric gene *Bcr-Abl1* on chromosome 22.[1,2] The encoded Bcr-Abl1 protein deregulates tyrosine kinase activity and plays a major role in the pathogenesis of CML. The expression of this chimeric protein may be essential for the development of the disease. Constitutive tyrosine kinase activity promotes cell growth and proliferation through the phosphorylation of downstream signaling molecules.[3,4]

Understanding the molecular basis of CML has allowed the development of targeted drugs against cancer cells.[5] Imatinib mesylate (IM), as a first-generation tyrosine kinase inhibitor (TKI), is used for the treatment of all newly diagnosed patients with CML. Once IM reaches the target cancer cells, the drug works by inhibiting the tyrosine kinase activity of the Bcr-Abl1 fusion protein.

However, despite significant treatment achievements, drug resistance is still one of the major obstacles to effective management for patients with CML. It is estimated that approximately 20% to 40% of patients receiving IM therapy demand drug substitutions, possibly because of a lack of tolerance or resistance responses.[6] Therefore, the second generation of TKIs, including nilotinib (NI) and dasatinib (DA), has helped patients overcome drug resistance alongside IM therapy. In a

Abbreviations:

TKI, tyrosine kinase inhibitor; CML, chronic myeloid leukemia; IM, imatinib mesylate; NI, nilotinib; DA, dasatinib; CHR, complete hematologic response; Ph+, Philadelphia positive; PCyR, partial cytogenetic response; CCyR, complete cytogenetic response; MR, molecular response; RT-PCR, real-time polymerase chain reaction; WBC, white blood cell; PB, peripheral blood; MCH, mean corpuscular hemoglobin; MCV, mean corpuscular volume; NS, not significant.

[1]Iranian Blood Transfusion Organization, High Institute of Research and Education in Transfusion Medicine, Tehran, Iran, [2]Hematology and Oncology Center, Taleghani Hospital, Shahid Beheshti University of Medical Sciences, Tehran, Iran, [3]Department of Hematology, Tehran Medical Sciences Branch, Islamic Azad University, Tehran, IR Iran and Head of Payvand Clinical & Specialty Laboratory, Dr. Poopak Research Center

*To whom correspondence should be addressed.
bpoopak@gmail.com

related development, resistance to first- and second-generation CML drugs led to the emergence of a third-generation TKI, ponatinib.[7]

There are 2 major reasons for drug resistance in CML (primary and secondary) following treatment. Primary resistance is referred to when the expected response to therapy is not obtained among newly diagnosed patients. Secondary resistance is defined by the achievement and then subsequent loss of a hematologic or cytogenetic response. Mutations in BCR-ABL are rarely responsible for primary resistance and Mutations are often responsible for secondary resistance. A number of different guidelines have been used to identify potential patients who are treatment resistant. The National Comprehensive Cancer Network criteria for inadequate response to treatment include lack of complete hematologic response (CHR) after 3 months of treatment (Philadelphia positive [Ph+] cells >95%), lack of partial cytogenetic response (PCyR) after 6 months of treatment (Bcr-Abl1 >10%), and lack of complete cytogenetic response (CCyR) after 12 months of treatment (Bcr-Abl1 >1%) (https://www.nccn.org). On the other hand, the European LeukemiaNet[8] (ELN) recommendations for determining CML treatment resistance are as follows: no CHR or Philadelphia positive (Ph+) cells >95% after 3 months of treatment, Bcr-Abl1 >10% or Ph+ cells >35% after 6 months of treatment, Bcr-Abl1 >1% or Ph+ cells ≥1% after 12 months of treatment, and loss of CHR, CCyR, or PCyR or confirmed loss of major molecular response (MR) after 12 months of treatment.[8]

Numerous factors are involved in developing acquired resistance to TKIs, which can be divided into 2 groups dependent on (constitutive expression of *Bcr-Abl1* because of kinase domain mutations) or independent of the *Bcr-Abl1* oncogene.[9] The *Bcr-Abl1* mutations are the major reason for resistance to TKI therapy: 40% to 90% of patients with a high risk of treatment-resistant CML carry at least 1 mutation in the *Bcr-Abl1* kinase domain.[10] Approximately 100 different types of mutations can be linked to IM resistance and lead to more than 50 amino acid changes in the Bcr-Abl1 oncoprotein.[11] Based on *Bcr-Abl1* domains, the mutations occur at 4 different sites: the P-loop domain, IM binding site, catalytic domain, and activation loop.[12] It has also been reported that the level of IM resistance in various mutations depends on the type of alterations and their positions in the ABL kinase domain.[13,14] In addition, many studies have emphasized the importance of the identified mutation profile in selecting the correct protocol for further treatment; eg, the ELN committee has considered the *Bcr-Abl1* mutation analysis as a requirement before choosing medication for patients with IM-resistant CML .[8,15]

The measurement of Bcr-Abl1 mutation frequencies in different populations may facilitate patient assessments, specifying the most appropriate treatment and ultimately improving patient outcomes. However, there is a shortage of available information on the genetic profile of patients with treatment-resistant CML in Iran.[16] Therefore, the purpose of this study was to evaluate ABL kinase domain mutations among Iranian patients with CML with resistance to TKIs.

Materials and Methods

Study Design

We performed a descriptive cross-sectional study of patients with CML with resistance to TKIs. All patients were selected based on the 2013 ELN recommendations.[8] The study population consisted of 63 patients with CML treated with different protocols who were referred to the Payvand Clinical and Specialty Laboratory, Tehran, Iran, from February 2016 to January 2017. We excluded 13 of the 63 patients from the analysis because they achieved a deep and durable MR to treatment. Our research was approved by the medical ethics committee of the Research Center of Iranian Blood Transfusion Organization, Tehran, Iran, and all the patients signed an informed consent form before entering the study.

Analysis of the Bcr-Abl1 transcripts was conducted as follows. Ten mL peripheral blood was collected in EDTA-evacuated tubes. The total RNA in the buffy coat was then extracted according to the ELN protocol,[8] using guanidinium thiocyanate and isopropanol. The RNA quantity and purity were characterized by optical absorption biophotometry to prevent protein contamination (260:280 ratio). Subsequently, cDNA synthesis was carried out according to the instructions supplied by the reverse transcription reagent kit (Fermentas, Spain). We used quantitative real-time polymerase chain reaction (RT-PCR) for the measurement of the Bcr-Abl1 transcripts and *ABL* as a control gene. The Bcr forward (5'-TGACCAACTCGTGTGTGAAACTC) and ABL kinase reverse (5'-TCCACTTCGTCTGAGATACTGGATT) primers were included in the commercial Metabion kit. For the Bcr-Abl1 mutation analysis, specimens with confirmed treatment failure were analyzed in terms of the ABL kinase domain mutation. The PCR method was run by the ABL kinase forward (5' CGCAACAAGCCCACTGTCT) and reverse primers.

DOI: 10.1093/labmed/lmaa052

PCR Conditions

The cDNA specimens were amplified using the respective master mix in a 48-well thermal cycler (PEQ Star, Germany). In a reaction volume of 2.5 μL, 1X Long PCR buffer (complete) and 2 μL MgCl2; 0.5 mM dNTP, 1.25 μL forward primer and 1.25 μL reverse primer, 0.4 μL Taq polymerase and 5 μL cDNA were added.

The annealing temperature was 95°C. To ensure the amplification of the target band, PCR products underwent electrophoresis on a 1% agarose gel, poststained with SYBR Green dye. The length of the amplified band was 863 bp. The PCR products with primers were directly sequenced after the formation of the desired band on an electrophoresis gel.

Bioinformatics Analysis

For quick and easy comparison between the mutated and normal specimens, MEGA6 Software was used to detect any probable mutation of the *ABL* gene transcript by aligning the *ABL* gene sequence of the patients with the *ABL* reference gene.

Statistical Analysis

In the beginning, descriptive statistics were performed on the obtained results. The Kolmogorov-Smirnov test was conducted to evaluate the normality of data. Through the quantitative data analysis, independent *t*-test, and Mann-Whitney *U* test were conducted, depending on our variables and results. A χ^2 statistic was used to investigate the qualitative data of the patients. All statistical analyses were performed using SPSS v.19.0. A *P* value <.05 was considered statistically significant.

Results

We analyzed 50 patients with CML who did not respond to the first-line TKI therapy adequately. Given the high dispersion of age (range, ages 6 years–90 years), the median age of the patients was 41 years. In terms of gender distribution, 36 patients (72%) were male with an average of 2.57 men/women (**Table 1**).

Patients were divided into 3 groups based on the time of CML development. As shown in **Table 1**, most patients (those with and without the ABL kinase domain mutation) experienced treatment failure in <5 years since the onset of disease. Half of the patients with the mutation were prescribed first-generation TKIs and the other half were treated with second-generation TKIs (see **Table 1**).

The hematologic examination was performed first to evaluate the patients' response to treatment. The values of the hematologic parameters are shown in **Table 2**. The average white blood cell (WBC) count was 58.48 and 16.09 among the groups with and without the mutation, respectively. Twenty-two patients (44%) with a WBC count $>10\times10^9$/L, a platelet count $>450\times10^9$/L, a basophil count >5% of total WBC, and an accumulation of immature myeloid cells in the peripheral blood (PB) were considered as the nonhematologic responders to treatment (**Table 3**).

We used the RT-PCR technique to study the levels of MR and the Bcr-Abl1/ABL ratio to predict patients' responses to particular treatments. Finally, the patients were categorized into 3 groups: *Bcr-Abl1*^{IS} >10%, *Bcr-Abl1*^{IS} ≥1% (MR1), and *Bcr-Abl1*^{IS} ≥0.1% (MR2). The total average of the Bcr-Abl1/ABL ratio for all the patients who were treatment resistant was 41.9 (**Table 4**).

Direct sequencing of *ABL* gene transcripts of all the specimens was conducted after the loss of response to therapy. Among patients with loss of treatment response, 11 different mutations were found in 13 patients (26%); E255K mutation was the most frequent (20%) followed by G250E and F359V, each with a frequency of 13.5%. The presence of 2 simultaneous mutations was revealed in 2 patients (E255K/F486S vs E255K/M244V). The incidence of mutations and their locations are shown in **Table 2**. Considering the 26% prevalence of mutations in the treatment-resistant population, at least 5 good responders to therapy were required to compare the mutation patterns. Consequently, we established a control group of 6 patients and found no mutation after specimen sequencing.

We also compared the hematologic indices of WBC and platelets between patients with and without mutations (see **Table 3**). Among the patients with mutations, 5 (38.4%) had a normal WBC count and 8 (61.6%) had an elevated WBC count. The average values of neutrophils, monocytes, and lymphocytes were significantly higher among patients with mutations. According to these findings, the emergence of mutations was significantly higher among patients with a lack of hematologic response (see **Table 3**). The mutation pattern of individuals with a lack of hematologic response is shown in **Table 5**.

Table 1. Patient Characteristics

Variables	With Mutations	Without Mutations	Total
Sex (M:F)	1:6	3:1	2:57
Median age, y (range)	37.5 (13–59)	47.5 (6–90)	41 (6–90)
First-line therapy (%)			
Hydroxyurea	-	2 (5.3)	2 (4)
Interferon	-	1 (2.6)	1 (2)
IM	13 (100)	34 (89.4)	46 (92)
NI	-	1 (2.6)	1 (2)
Second-line therapy (%)			
Without change	7 (53)	18 (47.4)	24 (48)
IM	-	3 (7.9)	3 (6)
NA	6 (47)	12 (31.6)	18 (36)
DA	-	1 (2.6)	1 (2)
Multiple drug therapy[a]	-	4 (10.5)	4 (8)
Disease duration (%)			
<5 y	9 (69)	27 (71)	36 (72)
6–10 y	3 (23)	9 (33.3)	11 (22)
>10 y	1 (8)	2 (5.2)	3 (6)

[a]*IM + hydroxyurea, IM + interferon, IM + NI, DA + NI.*

Table 2. Mutation Spectrum in Studied Patients

Mutation Type	T315I	S417F	E459K	F486S	Y253H	M244V	K247 R	E255V	G250E	F359V	E255K
Location	ATP binding	C-terminal loop	C-terminal loop	C-terminal loop	P loop	P loop	P loop	P loop	P loop	SH2 contact	P loop
Frequency (%)[a]	1 (6.6)	1 (6.6)	1 (6.6)	1 (6.6)	1 (6.6)	1 (6.6)	1 (6.6)	1 (6.6)	2 (13.5)	2 (13.5)	3 (20)

[a]*Two patients had 2 mutations simultaneously (E255K/M244V and E255K/F486S).*

Table 3. Comparison of Patient Characteristics and Hematologic Response Between Patients with and Without Mutation

Variables	Mutation		*P* Value
	Yes (n = 13)	No (n = 37)	
Age, y	37.83 ± 13	43.89 ± 17	NS
Sex (%)			
Male	9 (69.3)	28 (73.7)	NS
Female	4 (30.7)	10 (26.3)	NS
Disease duration, y	5.1 ± 3	4.47 ± 3.9	NS
WBC (%)			
<4 x 10^3/μL	0	5 (13.5)	.035
4–11 x 10^3/μL	5 (38.4)	25 (64.9)	—
>11 x 10^3/μL	7 (61.6)	8 (21.6)	—
Mean	58.48 ± 102	16.09 ± 34	.026
Neutrophils (μL)	19.23 ± 20 x 10^3	11.5 ± 29	.017
Monocytes (μL)	3.3 ± 5.2 x 10^3	0.92 ± 1.4	.018
Lymphocytes (μL)	7.7 ± .9 x 10^3	3.12 ± 4.2	.026
Hemoglobin (g/dL)	11.6 ± 2.8	12.5 ± 2.2	NS
Platelets (/μL)	326.3 ± 296.8 x 10^3	292.1 ± 296.4	NS
MCV (fL)	91.6 ± 6.3	90.5 ± 8.7	NS
MCH (pg)	29.6 ± 2.3	29.8 ± 2.8	NS
Hematologic response (%)			
Yes	4 (31)	24 (65)	.03
No	9 (69)	13 (35)	

MCH, mean corpuscular hemoglobin; MCV, mean corpuscular volume; NS, not significant.

Lab Medicine 2021;52;158–167
DOI: 10.1093/labmed/lmaa052

Table 4. MR

Variables		With Mutations		Without Mutations	Total
MR (%)					
>10		11 (85)		23 (62)	34 (68)
MR1		2 (15)		9 (24)	11 (22)
MR2		0		5 (14)	5 (10)
Response (%)					
Failure		13 (100)		34 (92)	47 (94)
Warning		0		3 (8)	3 (6)
Optimal		0		0	0
Bcr/ABL transcript analysis					
ABL/Bcr-ABL transcript	Mean	Median	Standard deviation	Min	Max
	41.9	20	53	0.12	223

Table 5. Relation Between Mutation Kind and Hematologic Response

Factor		BCR-ABL/ABL	*P* Value
Hematologic response	Yes	28.59	.028
	No	62.3	
Mutation	Yes	83.15	.005
	No	30.02	
Pearson correlation			
Characteristics			
Age, y	50	Correlation: 0.343	.015
Disease duration, mo	50	Correlation: 0.133	.35

Table 6. Correlation Between BCR-ABL/ABL Transcript Patient Characteristics, Hematologic Response, and Mutation Occurrence

Nonhematologic Response	Variables		(%)Frequency
	MR	Failure	22 (100)
		Optimal	0 (0)
	Mutation	Yes	9 (38)
		No	13 (61.9)
	Mutation Kind	E255K and F486S	1 (4.5)
		E255K and M244K	1 (4.5)
		E255K	1 (4.5)
		E255V	1 (4.5)
		E459K	1 (4.5)
		F359V	2 (9)
		G250E	1 (4.5)
		T315I	1 (4.5)
		Wild-type	13 (59)

To determine the association between the mutation occurrence and hematologic response with *Bcr-Abl1*^{IS}, the mean difference in *Bcr-Abl1*^{IS} levels was evaluated in patients with mutations, those without mutations, and those lacking hematologic response (**Table 6**).

Discussion

As a first-generation TKI, IM revolutionized the treatment of patients with CML.[17,18] It is the first-line therapy for

hundreds of thousands of patients throughout the world, and sustained treatment response is achieved in most patients. Although it is thought to be an effective treatment protocol in 60% of patients, nearly 20% of patients with CML have shown a relatively poor response to IM therapy, and most other patients continue to experience treatment-resistant conditions.[19] In recent years, meeting the challenges of patients with IM resistance has led to failures in the management of patients with CML.[13,17,18] The development of multiple *Bcr-Abl1* kinase domain mutations is one of the greatest challenges of IM therapy.[19] Therefore, strategies for identifying these mutations have become a major issue in terms of providing prognostic information and selecting the appropriate treatment afterward.[12,13,17,18]

According to the 2013 ELN recommendations,[8] all patients with CML harboring *Bcr-Abl1* kinase domain mutations encounter treatment resistance and may undergo partial or complete treatment failure depending on the type of mutation.[20] More than 90 different mutations have been identified in patients with acquired resistance to TKIs. Previous research has shown that the substitutions of 15 amino acids are the main reason behind the 80% to 90% prevalence of resistance mutations. In addition, 7 mutant codons (G250E, Y253H, E255K, T315I, M351T, F359, and H396) are responsible for approximately 60% to 70% of such conditions.[21] A comprehensive study by Khorashad, de Lavallade, et al[22] on 319 patients showed that the emergence of *Bcr-Abl1* kinase domain mutations is the only factor that independently contributes to the loss of CCyR. They also discovered a greater risk of disease progression among patients with these mutations compared with those without the mutations.[22] Appropriate information on risk factors related to kinase domain mutations is extremely helpful in improving the effectiveness of monitoring IM resistant patients.

Numerous studies have been conducted concerning the impact of *Bcr-Abl1* kinase domain mutations on the outcome of patients with CML. Various research has estimated differing overall prevalence of such mutations in patient populations, likely because of a distinct study profile (prospective vs retrospective studies.), patient selection, or molecular methods for identification of the disease-causing mutations.[13,18,23-26] Some mutations cause partial or complete treatment failure, so identifying such changes facilitates the choice of proper treatment methods in patients who are therapy resistant.[27]

Hematologic examinations showed that almost 44% of our patients failed to achieve hematologic response, and the lack of MR and increased levels of *Bcr-Abl1* expression in all the patients resulted in the possibility of domain kinase mutations. Earlier reports showed that a significant increase in the *Bcr-Abl1* ratio is strongly associated with the occurrence of acquired mutations.[28] In contrast, mutation probability is very low among patients with decreased levels of *Bcr-Abl1* ratio or stable conditions.[12,29,30] Almost all our patients with a mutation exhibited elevated levels of the *Bcr-Abl1* transcript, which reflected the importance of ABL kinase domain mutation analysis among the poor molecular responders to treatment. A lack of hematologic response was found in 69% of patients with ABL kinase domain mutations, making a statistically significant difference between patients with and without these mutations. This issue points out the indispensable role of patient follow-up over a 3-month period. Based on available medical records, none of our patients had continuous follow-up support for assessing response to therapy. Considering that all the patients had evidence of molecular relapse and that hematologic relapse occurred in only 22 out of 50 studied cases, we could, as in other investigations, assume that a hematologic relapse is a delayed event compared with molecular relapse in patients at high risk of treatment-resistant conditions. Therefore, the most important implication of these findings is that the hematologic examination alone is not a potential predictive marker for clinical response to treatment.

Our findings further indicated that 26% of patients who had a poor MR and treatment failure harbored mutations within the ABL kinase domain region. The prevalence of such mutations was evaluated in individuals with the appropriate response to treatment as a control group to confirm the role of ABL kinase domain mutations on developing resistance to therapy. Considering the 26% prevalence of mutations, at least 5 good responders to therapy were required to compare the mutation patterns. We determined that there were no ABL kinase domain mutations among 6 control patients with the proper response to treatment. Thus, these findings show the role of such mutations in the development of resistance observed during treatment of patients with CML.

It has also been suggested that the mutation rate and pattern are different within various population subgroups. According to a recent study conducted on 32 patients with CML with hematologic relapse, more than 90% of patients developed mutations after IM therapy.[24] Kagita

DOI: 10.1093/labmed/lmaa052

et al[27] showed that 46.03% of patients with drug-resistant CML harbored ABL kinase domain mutations, in which T315I was the most common cause of treatment failure in the Indian population. In another study of CML in India, a range of *Bcr-Abl1* mutations in 44% of patients with drug resistance (39% within the kinase domain, 4% within the SH2-SH3 domain, and 1% with *Bcr-Abl1* amplification) was described.[28] Pagnano et al[31] carried out a study in Latin America suggesting a 41% prevalence of mutations among patients with CML who were unresponsive to different protocols, with T315I as the most problematic mutation. This finding is consistent with the 31% mutation frequency found in a study on the Spanish population by Marcé and colleagues.[32] Although the prevalence of mutations in all above-mentioned studies was higher than in this study, Elias et al[33] reported a 22.4% frequency of ABL kinase domain mutations among Malaysian patients with CML. On the other hand, the mutation frequency was only 11.9% in a Dutch CML screening population undergoing IM therapy.[34]

Although the T315I mutation had the highest incidence of *Bcr-Abl1* changes in many surveys, E255K, G250E, and F359V were the most common mutations presented in our study. In total, 50% of patients developed mutations within the P-loop domain, and 30% had C-terminal domain changes. Per the study of Rostami et al[16] in Valiasr Hospital, Tehran, Iran, the P-loop domain has been considered the most prevalent mutated site in the *Bcr-Abl1* transcript. Chahardouli et al[35] revealed that drug-binding and P-loop domains, with a prevalence of 29% and 26%, respectively, were the most frequent mutated sites among the patients with CML who were referred to Shariati Hospital, Tehran, Iran. Collectively, the P-loop domain is the most frequently mutated site among the Iranian CML population, specifically affecting the risk of disease progression.[22] It is also associated with extremely poor prognosis among patients treated using IM.[25,26,36]

Half of our patients were previously treated with IM, and the other half were prescribed NI, whereas all the patients in other studies only continued their treatment protocol with IM. Hochhaus, Saglio, et al[37] suggested that the incidence of mutations in patients with NI treatment was lower than in those treated using IM. Based on the common mutations of TKIs, DA is the most appropriate drug affecting the majority of mutations, and ponatinib should be specifically prescribed in cases with T325I mutation.[38,39] According to the 2013 ELN recommendations,[8] NI or DA could be prescribed as first-line therapy in patients diagnosed with CML. Several studies have shown that the emergence of new mutations in individuals who had taken DA was much lower than in those with IM treatment.[22,40-42] On the other hand, P-loop domain mutation is more prevalent among patients treated using IM than in patients treated using DA.[42] Therefore, the results of the present research highlight the importance of identifying such mutations.

Among the patients with treatment resistance, the emergence of mutations was associated with an increased level of WBC, and less common neutrophils, lymphocytes, and monocytes. There was a positive association between the WBC count and *Bcr-Abl1*, which is only statistically significant with monocytes. However, it has been shown that the *Bcr-Abl1* transcript level has a significant positive relationship with the WBC count.[27] This difference could result from the smaller sample size of our study than in similar research. Because the Bcr-Abl1/ABL ratio was significantly different between the patients with mutations and those without mutations, it was assumed that the occurrence of mutations causes Bcr-Abl1/ABL stability against the therapy and therefore leads to an increased number of WBC in the PB. According to our test results, mutations detected in the ABL kinase domain were the cause of the rising Bcr-Abl1/ABL ratio and resistance in patients with CML undergoing their first tyrosine kinase therapy. In patients using IM therapy, an increasing Bcr-Abl1/ABL ratio with respect to the international scale established by the ELN[8] is a means of detecting patients with IM resistance. In 85% of patients with mutations in our study, the Bcr-Abl1/ABL ratio was more than 10%. In addition, 15% of patients with mutations were detected in MR1.

It has been understood that the more that the disease progresses, the more likely it is that the mutations will occur in the kinase domain.[23-26] We found that 72% of our patients experienced treatment failure in <5 years since the onset of disease, which is not consistent with previous findings. This result may have numerous reasons, including patient ethnicity, environmental effects on the emergence of mutations, and the type of treatment protocols in other similar studies. Furthermore, the frequency of mutations in our research was lower than in most studies, probably because of the smaller sample size of our patient groups. Technical limitations seem to be another important factor in this regard. We used the direct sequencing technique, with a sensitivity of 20% to 25%, to assess the mutation pattern.[43,44] The advantages

Table 7. Sensitivity of Different TKIs Based on BCR-ABL Mutations

Drug Sensitivity	IM	NI	DA	Ponatinib
Sensitive	BCR-ABL, N	BCR-ABL, N	BCR-ABL, N	BCR-ABL, N
		G250E	G250E	T315I
			F359V	F359V
			Y253H	Y253H
Semi-sensitive	G250E[a]	E255K	E255K	E255K
		E255V	E255V	E255V
		Y253H	—	—
Resistant	T315I	T315I	T315I	—
	E255K	F359V	—	—
	E255V	—	—	—
	Y253H	—	—	—

[a]*Mutations E459K, K247R, S417F, F486S, and M244V not shown, treated with high dose of IM, NI, DA, or ponatinib.*

of using high-sensitivity counting techniques include the precise identification of novel mutations. Note that there is not enough information regarding the patients' history and their treatment protocols.

Numerous studies have assessed the identification of an appropriate treatment strategy related to ABL kinase domain mutations, summarized in **Table 7**.[38,39,45] Comparing these findings with the mutation pattern found in our research indicated that most patients did not receive a specific treatment protocol in accordance with the type of mutation in the ABL kinase domain that they had shown. Therefore, evaluating the *Bcr-Abl1* kinase domain mutations may modify the therapeutic approach and the appropriate drug selection process of patients with CML.

Conclusion

Our results showed that patients with therapy-resistant CML had a lower incidence of mutations in the ABL kinase domain with a different pattern as compared with most other studies. Regular monitoring at specified intervals by consideration of approved guidelines is necessary to detect resistance in patients and the best management of therapeutic agents.

Acknowledgments

We express our deepest gratitude for the support of all Payvand Clinical and Specialty Laboratory staff who backed our work step by step and gave us access to their vast experience and reservoir of creative ideas. Dr. Behzad Poopak designed and supervised the project, and Mahboobeh Shojaei performed experimental works, data collection, analysis, and interpretation of results. She also conducted the literature review and drafted the manuscript. Fariba Karami and Nazanin Arjmand helped perform the experiments.

Funding

All funding of this research project were funded by Dr. Behzad Poopak.

References

1. Sahin F, Saydam G, Cömert M, et al. Turkish chronic myeloid leukemia study: retrospective sectional analysis of CML patients. *Turk J Haematol.* 2013;30(4):351–358.
2. Bertacchini J, Ketabchi N, Mediani L, Capitani S, Marmiroli S, Saki N. Inhibition of Ras-mediated signaling pathways in CML stem cells. *Cell Oncol (Dordr).* 2015;38(6):407–418.
3. Sinclair A, Latif AL, Holyoake TL. Targeting survival pathways in chronic myeloid leukaemia stem cells. *Br J Pharmacol.* 2013;169(8): 1693–1707.
4. Shahrabi S, Azizidoost S, Shahjahani M, Rahim F, Ahmadzadeh A, Saki N. New insights in cellular and molecular aspects of BM niche in chronic myelogenous leukemia. *Tumour Biol.* 2014;35(11):10627–10633.
5. Fialkow PJ, Jacobson RJ, Papayannopoulou T. Chronic myelocytic leukemia: clonal origin in a stem cell common to the granulocyte, erythrocyte, platelet and monocyte/macrophage. *Am J Med.* 1977;63(1):125–130.
6. Khorashad JS, Kelley TW, Szankasi P, et al. BCR-ABL1 compound mutations in tyrosine kinase inhibitor-resistant CML: frequency and clonal relationships. *Blood.* 2013;121(3):489–498.
7. Hochhaus A, Ernst T, Eigendorff E, La Rosée P. Causes of resistance and treatment choices of second- and third-line treatment in chronic

myelogenous leukemia patients. *Ann Hematol.* 2015;94(Suppl 2):S133–S140.

8. Baccarani M, Deininger MW, Rosti G, et al. European LeukemiaNet recommendations for the management of chronic myeloid leukemia: 2013. *Blood.* 2013;122(6):872–884.
9. Soverini S, Branford S, Nicolini FE, et al. Implications of BCR-ABL1 kinase domain-mediated resistance in chronic myeloid leukemia. *Leuk Res.* 2014;38(1):10–20.
10. Yang K, Fu LW. Mechanisms of resistance to BCR-ABL TKIs and the therapeutic strategies: a review. *Crit Rev Oncol Hematol.* 2015;93(3):277–292.
11. Balabanov S, Braig M, Brümmendorf TH. Current aspects in resistance against tyrosine kinase inhibitors in chronic myelogenous leukemia. *Drug Discov Today Technol.* 2014;11(March):89–99.
12. Hughes T, Deininger M, Hochhaus A, et al. Monitoring CML patients responding to treatment with tyrosine kinase inhibitors: review and recommendations for harmonizing current methodology for detecting BCR-ABL transcripts and kinase domain mutations and for expressing results. *Blood.* 2006;108(1):28–37.
13. Branford S, Rudzki Z, Walsh S, et al. Detection of BCR-ABL mutations in patients with CML treated with imatinib is virtually always accompanied by clinical resistance, and mutations in the ATP phosphate-binding loop (P-loop) are associated with a poor prognosis. *Blood.* 2003;102(1):276–283.
14. Corbin AS, La Rosée P, Stoffregen EP, Druker BJ, Deininger MW. Several Bcr-Abl kinase domain mutants associated with imatinib mesylate resistance remain sensitive to imatinib. *Blood.* 2003;101(11):4611–4614.
15. Jabbour E, Hochhaus A, Cortes J, La Rosée P, Kantarjian HM. Choosing the best treatment strategy for chronic myeloid leukemia patients resistant to imatinib: weighing the efficacy and safety of individual drugs with BCR-ABL mutations and patient history. *Leukemia.* 2010;24(1):6–12.
16. Rostami G, Hamid M, Yaran M, Khani M, Karimipoor M. Incidence and clinical importance of BCR-ABL1 mutations in Iranian patients with chronic myeloid leukemia on imatinib. *J Hum Genet.* 2015;60(5):253–258.
17. Gorre ME, Mohammed M, Ellwood K, et al. Clinical resistance to STI-571 cancer therapy caused by BCR-ABL gene mutation or amplification. *Science.* 2001;293(5531):876–880.
18. Hochhaus A, Kreil S, Corbin AS, et al. Molecular and chromosomal mechanisms of resistance to imatinib (STI571) therapy. *Leukemia.* 2002;16(11):2190–2196.
19. Hughes T, White D. Which TKI? An embarrassment of riches for chronic myeloid leukemia patients. *Hematology Am Soc Hematol Educ Program.* 2013;2013:168–175.
20. Etienne G, Dulucq S, Lascaux A, et al. ELN 2013 response status criteria: relevance for de novo imatinib chronic phase chronic myeloid leukemia patients? *Am J Hematol.* 2015;90(1):37–41.
21. Rejali L, Poopak B, Hasanzad M, et al. Characterizing of four common BCR-ABL kinase domain mutations (T315I, Y253H, M351T and E255K) in Iranian chronic myelogenous leukemia patients with imatinib resistance. *Iran J Cancer Prev.* 2015;8(3):e2334.
22. Khorashad JS, de Lavallade H, Apperley JF, et al. Finding of kinase domain mutations in patients with chronic phase chronic myeloid leukemia responding to imatinib may identify those at high risk of disease progression. *J Clin Oncol.* 2008;26(29):4806–4813.
23. Branford S, Rudzki Z, Walsh S, et al. High frequency of point mutations clustered within the adenosine triphosphate-binding region of BCR/ABL in patients with chronic myeloid leukemia or Ph-positive acute lymphoblastic leukemia who develop imatinib (STI571) resistance. *Blood.* 2002;99(9):3472–3475.
24. Shah NP, Nicoll JM, Nagar B, et al. Multiple BCR-ABL kinase domain mutations confer polyclonal resistance to the tyrosine kinase inhibitor imatinib (STI571) in chronic phase and blast crisis chronic myeloid leukemia. *Cancer Cell.* 2002;2(2):117–125.
25. Soverini S, Martinelli G, Rosti G, et al. ABL mutations in late chronic phase chronic myeloid leukemia patients with up-front cytogenetic resistance to imatinib are associated with a greater likelihood of progression to blast crisis and shorter survival: a study by the GIMEMA Working Party on Chronic Myeloid Leukemia. *J Clin Oncol.* 2005;23(18):4100–4109.
26. Soverini S, Colarossi S, Gnani A, et al.; GIMEMA Working Party on Chronic Myeloid Leukemia. Contribution of ABL kinase domain mutations to imatinib resistance in different subsets of Philadelphia-positive patients: by the GIMEMA Working Party on Chronic Myeloid Leukemia. *Clin Cancer Res.* 2006;12(24):7374–7379.
27. Kagita S, Uppalapati S, Jiwatani S, et al. Incidence of Bcr-Abl kinase domain mutations in imatinib refractory chronic myeloid leukemia patients from South India. *Tumour Biol.* 2014;35(7):7187–7193.
28. Vaidya S, Vundinti BR, Shanmukhaiah C, Chakrabarti P, Ghosh K. Evolution of BCR/ABL gene mutation in CML is time dependent and dependent on the pressure exerted by tyrosine kinase inhibitor. *PLoS One.* 2015;10(1):e0114828.
29. Branford S, Rudzki Z, Parkinson I, et al. Real-time quantitative PCR analysis can be used as a primary screen to identify patients with CML treated with imatinib who have BCR-ABL kinase domain mutations. *Blood.* 2004;104(9):2926–2932.
30. Sherbenou DW, Wong MJ, Humayun A, et al. Mutations of the BCR-ABL-kinase domain occur in a minority of patients with stable complete cytogenetic response to imatinib. *Leukemia.* 2007;21(3):489–493.
31. Pagnano KB, Bendit I, Boquimpani C, et al.; Latin American Leukemia Net (LALNET). BCR-ABL mutations in chronic myeloid leukemia treated with tyrosine kinase inhibitors and impact on survival. *Cancer Invest.* 2015;33(9):451–458.
32. Marcé S, Zamora L, Cabezón M, et al.; Grupo ICO de estudio de mutaciones de ABL en pacientes afectos de LMC. Frequency of ABL gene mutations in chronic myeloid leukemia patients resistant to imatinib and results of treatment switch to second-generation tyrosine kinase inhibitors. *Med Clin (Barc).* 2013;141(3):95–99.
33. Elias MH, Baba AA, Azlan H, et al. BCR-ABL kinase domain mutations, including 2 novel mutations in imatinib resistant Malaysian chronic myeloid leukemia patients—frequency and clinical outcome. *Leuk Res.* 2014;38(4):454–459.
34. Lewandowski K, Warzocha K, Hellmann A, et al. Frequency of BCR-ABL gene mutations in Polish patients with chronic myeloid leukemia treated with imatinib. *Polskie Archiwum Medycyny Wewnętrznej.* 2009;119(12):789–794.
35. Chahardouli B, Zaker F, Mousavi SA, et al. Evaluation of T315I mutation frequency in chronic myeloid leukemia patients after imatinib resistance. *Hematology.* 2013;18(3):158–162.
36. Nicolini F, Corm S, Le Q, et al. Mutation status and clinical outcome of 89 imatinib mesylate-resistant chronic myelogenous leukemia patients: a retrospective analysis from the French intergroup of CML (Fi (φ)-LMC GROUP). *Leukemia.* 2006;6(20):1061.
37. Hochhaus A, Saglio G, Larson RA, et al. Nilotinib is associated with a reduced incidence of BCR-ABL mutations vs imatinib in patients with newly diagnosed chronic myeloid leukemia in chronic phase. *Blood.* 2013;121(18):3703–3708.
38. Kimura S, Ando T, Kojima K. BCR-ABL point mutations and TKI treatment in CML patients. *J Hematol Transf.* 2014;2(3):1022–1033.
39. Baccarani M, Castagnetti F, Gugliotta G, Rosti G. A review of the European LeukemiaNet recommendations for the management of CML. *Ann Hematol.* 2015;94(Suppl 2):S141–S147.
40. Bradeen HA, Eide CA, O'Hare T, et al. Comparison of imatinib mesylate, dasatinib (BMS-354825), and nilotinib (AMN107) in an N-ethyl-N-

nitrosourea (ENU)-based mutagenesis screen: high efficacy of drug combinations. *Blood.* 2006;108(7):2332–2338.

41. Cortes J, Jabbour E, Kantarjian H, et al. Dynamics of BCR-ABL kinase domain mutations in chronic myeloid leukemia after sequential treatment with multiple tyrosine kinase inhibitors. *Blood.* 2007;110(12):4005–4011.
42. Hughes TP, Saglio G, Quintás-Cardama A, et al. BCR-ABL1 mutation development during first-line treatment with dasatinib or imatinib for chronic myeloid leukemia in chronic phase. *Leukemia.* 2015;29(9):1832–1838.
43. Alderborn A, Kristofferson A, Hammerling U. Determination of single-nucleotide polymorphisms by real-time pyrophosphate DNA sequencing. *Genome Res.* 2000;10(8):1249–1258.
44. Ernst T, Erben P, Müller MC, et al. Dynamics of BCR-ABL mutated clones prior to hematologic or cytogenetic resistance to imatinib. *Haematologica.* 2008;93(2):186–192.
45. Lau A, Seiter K. Second-line therapy for patients with chronic myeloid leukemia resistant to first-line imatinib. *Clin Lymphoma Myeloma Leuk.* 2014;14(3):186–196.

DOI: 10.1093/labmed/lmaa052

Reporting Sysmex XN Absolute Neutrophil Count in Samples with Leukocyte Analyzer Flagging

Anna-Maria Linko-Parvinen, MD, PhD,[1*] *Heidi Turkia, PhD*[1]

Laboratory Medicine 2021;52:168-173

DOI: 10.1093/labmed/lmaa058

ABSTRACT

Objective: To provide faster laboratory data reporting, we evaluated the accuracy of Sysmex XN (Sysmex Inc, Kobe, Japan) absolute neutrophil count (ANC) in the presence of analyzer flagging.

Methods: Sysmex XN and manual microscopy ANC were compared with 80 autovalidated control specimens and with 280 study specimens with analyzer flagging regarding immature granulocytes (IG) >3% or other leukocyte abnormalities. Specimens with ambiguous neutrophil clusters were excluded.

Results: A slight positive overall method bias was seen for Sysmex XN compared to manual microscopy (n = 280), 0.025 (95% confidence interval [CI], –0.023 to 0.069) × 109/L. With IG > 10% (n = 123) the bias was larger, but not clinically significant, 0.17 (95% CI, 0.060–0.25) × 109/L. No clinically significant difference was seen in neutropenic (ANC < 1.5 × 109/L) specimens (n = 91), 0.070 (95% CI, –0.013 to 0.14) × 109/L.

Conclusion: These data indicate that Sysmex XN ANC can be reported in the presence of certain analyzer flagging to improve patient care.

Keywords: absolute neutrophil count, Sysmex XN, method comparison, hematology, immature granulocytes, analyzer flagging

Neutrophils, in addition to lymphocytes, constitute the majority of the total white blood cell count (WBC) in healthy adults and older children. Neutrophils are also the major type of granulocytes. They are formed from bone marrow stem cells by maturation via precursor cells. Normally only mature neutrophils—segmented and band cells—are found in peripheral blood.[1] Body stress reactions, such as infection, inflammation, pregnancy, and compensatory production, can cause the appearance of immature granulocytes (IG), usually metamyelocytes and myelocytes, but sometimes more immature promyelocytes or occasionally even blasts, in the circulation. Mature neutrophils are relatively short-lived and mobile with an ability to enter tissues. Neutrophils are crucial in the defense against microbes by chemotaxis, phagocytosis, and degranulation. In neutropenia the risk of infection is correlated with the severity of the neutropenia, the risk significantly increasing when the absolute neutrophil count (ANC) is less than 0.5 × 10^9/L.[2-5]

Abbreviations:

ANC, absolute neutrophil count; IG, immature granulocytes; CI, confidence interval; WBC, total white blood cell count; WNR, white cell nucleated channel; WDF, WBC differential channel; WPC, white progenitor cell channel; TAT, turnaround time; IQR, interquartile range; MGG, May-Grünwald-Giemsa dye; Q4, fourth quartile.

[1]Laboratory of Haematology, Tykslab, Laboratory Division, Turku University Hospital, Turku, Finland

*To whom correspondence should be addressed.
anna.linko-parvinen@tyks.fi

The Sysmex XN-10 and XN-20 (Sysmex Inc, Kobe, Japan) automated hematology analyzers use a flow cytometry method with cell lysing and fluorescent staining to enumerate blood cells and to perform WBC differential. Three different light detection channels enable the differential depending on the size, the structure, and the nucleic acid content of the cells. The WBC is received from white cell nucleated (WNR) and WBC subpopulations from WBC differential (WDF) channels. In case of abnormal lymphocyte or blast cell flagging, white progenitor cell (WPC) channels may be used for reflex testing, if available.

The mature neutrophil cluster and the absolute neutrophil count (ANC) include segmented neutrophils and band cells in Sysmex XN analyzers. The IG, including metamyelocytes, myelocytes, and promyelocytes, create a cluster above the mature neutrophil cluster in the side-fluorescence light vs side-scattered light gram in the WDF channel. The detection of IG is based on the granularity and nucleic acid content of the cells together with the cell size.[6]

The presence of abnormal cells, IG, or blasts or an increased amount of band cells can cause analyzer flagging based on Sysmex XN algorithms, and specimens are recommended to be reviewed by manual microscopy. The flagging may be based on qualitative characteristics of the leukocytes or quantitative changes in the leukocyte subsets. In some studies an automated hematology analyzer (Sysmex XE-2100) has been more precise in the enumeration of IG than manual counting,[7] and other studies have shown that a high IG percentage causes a systematic positive error compared with IG in manual microscopy.[8] An IG of 3% is widely used as the limit for IG flagging and microscopic review of specimens.[8] International guidelines also recommend slide review with neutropenic specimens,[9] although improvement of hematology analyzers, such as the Sysmex XN-series, has brought this need into question.[6,10]

Manual microscopy, despite being the gold standard, is generally considered to have low reproducibility and to be prone to human error. It is time consuming and labor demanding, causing delays in patient care.[11] The need for the ANC in patient care may be imminent for risk evaluation, the state of infection, or timing of certain medications.

We evaluated the performance of the Sysmex XN analyzer compared with manual microscopy in ANC enumeration in the presence of analyzer flagging, either as flagging from the WDF channel or as a reflex test from the WPC channel (only in the Sysmex XN-20 model). To improve specimen flow and turnaround time (TAT), we determined whether analyzer ANC could be reported in these specimens. In addition, we evaluated neutropenic specimens separately. We compared these data with autovalidated ANC results from control specimens without analyzer flagging.

Materials and Methods

Specimens

All specimens were anonymized routine analysis whole-blood specimens with a request for ANC from adult female and male patients, collected in K^2EDTA tubes and stored at room temperature at the Tykslab, Turku University Hospital, Turku, Finland. The Sysmex XN analysis or blood film preparation was performed within 8 hours after specimen collection. The study specimens were collected from 12,404 patients from September 1, 2017 to November 30, 2017. A total of 280 specimens, including 132 (47%) from women and an overall median age of 62 years (interquartile range [IQR] with 25th–75th percentile, ages 48–67 years), were included in the study. All the specimens had a request, based on clinical need, for ANC and had analyzer flagging regarding WBC differential or neutrophils. For those specimens with a request for ANC only, no WBC differential or IG percentage is reported. The autovalidated control specimens were routine analysis specimens with a request for ANC, based on clinical need, with no analyzer flagging from 80 adult patients, 34 (43%) from women, with an overall median age of 59 years (IQR = ages 37–71 years). They were collected, as part of the laboratory's quality control protocol, from a total of 18,196 specimens with a request for ANC from September 1, 2018 to December 31, 2018. For this kind of study, no informed consent or ethics committee evaluation is required in our institution. The Turku Clinical Research Center approved the study.

Laboratory Tests

The specimens were analyzed with the Sysmex XN-10 or Sysmex XN-20 (Sysmex Inc, Kobe, Japan), referred to as Sysmex XN in this study, or analyzers using the WNR, WDF, or WPC channels. The analyzer total leukocyte count (from the WNR channel), neutrophil percentage, ANC, and IG percentage (from the WDF channel) were recorded. The quantitative analyzer flagging reported for the study specimens showed a low WBC ($<1 * 10^9$/L), left shift, and immature granulocytes (with a limit of 3%); the qualitative analyzer flagging showed atypical/abnormal lymphocytes/blasts and an abnormal WBC scattergram. The flagging thresholds were set according to the instrument recommendations, except for the low WBC threshold. Specimens with ambiguous neutrophil clusters (ie, grey cell clusters or neutrophil clusters fused to another cell group), where the analyzer could not separate neutrophils from other leukocytes and thereafter provide a reliable ANC, were excluded from the study. The Sysmex XN ANC precision was 1.8% for intra-assay and 3.5% for interassay analysis, the reportable range was 0–440 $\times 10^9$/L for WBC, and the ANC adult reference range was 1.5–6.7 $\times 10^9$/L.

The blood films for manual microscopy were made with the Sysmex XP10 (Sysmex Inc, Kobe, Japan) and dyed with May-Grünwald-Giemsa dye (MGG; RAL Diagnostics, Martillac, France) or prepared manually and dyed with MGG

DOI: 10.1093/labmed/lmaa058

(Reagena, Toivala, Finland). In manual microscopy, 200 WBC were evaluated,[12] and segmented and band-form neutrophils were included in the mature neutrophil percentage. This percentage together with the analyzer WBC was used to determine the manual microscopy ANC, which is the usual procedure to report microscopy-reviewed ANC in our institution. The inter-reviewer imprecision for manual microscopy ANC has generally been 5% to 6% in our laboratory. The reportable range and reference range were the same as with the Sysmex XN.

The effect of reporting the ANC primarily from the Sysmex XN was evaluated later by using the TAT from specimen collection to result reporting. We compared the fourth quartiles (Q4) in 2018 (n = 13,959), when the ANC specimens were reviewed by microscopy in the presence of the analyzer flagging described above, and 2019 (n = 11,358), when only the specimens with ambiguous neutrophil clusters were reviewed. In addition, the TAT for the ANC specimens with microscopy review (n = 21) in Q4 in 2019 was assessed.

Statistical Analysis

To determine the effect of IG percentage, the study specimens were divided into 3 categories with IG <3%, and manual microscopy performed with flagging other than IG (n = 58): IG 3% to 4.9% (n = 20), 5% to 9.9% (n = 79), and ≥10% (n = 123). Neutropenia was defined as ANC < 1.5×10^9/L with manual microscopy in the study specimens and as ANC < 1.5×10^9/L with the Sysmex XN in the autovalidated control specimens. Neutropenic study specimens (n = 91) were evaluated overall and based on IG percentage as above and compared with autovalidated neutropenic specimens (n = 14). In all autovalidated control specimens the IG was <3%.

IBM SPSS Statistics 25 and MedCalc 19.1.5 with the Wilcoxon signed-rank test, Spearman's rho, and the Passing-Bablok model with the CUSUM linearity test were used for the statistical analysis.

Results

The Passing-Bablok analysis showed excellent correlation with no significant deviation from linearity for the ANC measured with the Sysmex XN and with manual microscopy in all the study specimens, including the IG percentage–based subgroups, and in the autovalidated control specimens (Figure 1). When the neutropenic specimens were examined separately, a good correlation between the analysis methods with no significant deviation from linearity was seen (Figure 2).

There was a statistically significant difference in the Sysmex XN ANC in the autovalidated control specimens (n = 80) with a slight systematic negative error compared with manual microscopy. In addition, an overall statistically significant difference with a systematic positive error was seen in the study specimens (n = 280) compared with manual microscopy. The method bias in the ANC between the Sysmex XN and manual microscopy was slightly higher with an IG >5% and more pronounced with an IG >10% compared with specimens with a lower IG percentage or specimens with flagging other than IG (**Table 1**).

There was no statistically significant difference in the neutropenic autovalidated control specimens (n = 14), but a slight systematic positive error in the neutropenic study

Table 1. Median ANC Analyzed with the Sysmex XN and Manual Slide Review, Method Bias of the Sysmex XN Compared with Manual Microscopy, Median IG Percentage, and WBC

Specimen Group (n)	ANC Sysmex XN ($\times 10^9$/L)[a]	ANC Microscopy ($\times 10^9$/L)[a]	Method Bias[b]	*P* Value	IG (%)[a]	WBC ($\times 10^9$/L)[a]
Control specimens (80)	3.6 (2.2–5.1)	3.7 (2.3–5.3)	–0.018 (– 0.075 to 0.048)	<.001	0.45 (0.30–0.80)	6.4 (4.6–8.3)
IG <3 (58)	2.0 (1.0–3.6)	1.9 (1.0–3.1)	0.049 (0.0071 to 0.099)	.793	0.97 (0.21–1.9)	3.7 (2.0–6.2)
IG 3–4.9 (20)	1.6 (1.1–12)	1.5 (1.1–12)	0.020 (–0.056 to 0.067)	.456	4.0 (3.4–4.3)	5.8 (3.1–21)
IG 5–9.9 (79)	2.2 (1.1–6.0)	2.0 (1.2–5.0)	0.085 (0.019 to 0.14)	<.001	7.8 (6.6–8.7)	4.5 (2.8–10)
IG ≥10 (123)	6.1 (2.5–13)	4.6 (1.7–11)	0.17 (0.060 to 0.25)	<.001	16 (13–21)	9.4 (3.7–18)
All study specimens (280)	3.2 (1.3–9.4)	2.8 (1.2–8.1)	0.025 (–0.023 to 0.069)	<.001	8.9 (4.2–15)	5.5 (2.8–13)

ANC, absolute neutrophil count; CI, confidence interval; IG, immature granulocytes; IQR, interquartile range; WBC, total white blood cell count.
[a]*The numbers in parentheses denote IQR (25th and 75th percentiles).*
[b]*The numbers in parentheses denote 95% CI.*

specimens (n = 91) with IG >5% or 10% (**Table 2**). Of the neutropenic study specimens, 18 were severely neutropenic (ANC < 0.5 × 10^9/L with manual microscopy). In these specimens, the ANC median (IQR) with manual microscopy was 0.19 (0–0.49) × 10^9/L and with the Sysmex XN it was 0.3 (0.090–0.82) × 10^9/L (*P* <.001).

The TAT for the ANC was slightly shorter when ANC results were primarily reported from the Sysmex XN in presence of analyzer flagging in Q4/2019 vs Q4/2018, when the ANC specimens with analyzer flagging were invariably reviewed by manual microscopy (**Table 3**). A clear delay in the TAT of the ANC was seen in those specimens still requiring microscopy review in Q4/2019 (n = 21; 0.15% of all the ANC requests). Previously, the microscopy review was performed on approximately 2% to 3% of the ANC requests (data not shown).

Discussion

The data for the ANC in the autovalidated control specimens show how well manual microscopy of 200 leukocytes correlates to the Sysmex XN result when there are no detected leukocyte abnormalities or analyzer flagging regarding the leukocytes. Interestingly, manual microscopy gave a slightly higher ANC than did the Sysmex XN. The difference was statistically significant but too small to have clinical significance. Similar deviations have been seen previously, but with IG percentage.[8] One explanation for the difference may be the lower amount of cells, usually 200, reviewed using manual microscopy. A higher cell count could reduce the effect of the random distribution of cells on the film.[13] Hematology analyzers count thousands of cells, and it is generally accepted that they are more precise and have higher repeatability compared with manual microscopy.

The majority of the specimens in this study had flagging regarding IG. The specimens with IG <3% (58/280 specimens) were reviewed by microscopy because of other analyzer flagging, mainly showing an abnormal WBC scattergram. In these specimens, the ANC measured with the Sysmex XN was slightly higher compared with manual microscopy, contrary to the results with the control specimens. The difference was statistically nonsignificant and did not have any clinical effect. The analyzer flagging primarily concerned leukocyte subpopulations other than neutrophils, mainly abnormal or atypical lymphocytes. It is possible that the leukocyte distribution on the microscopy slide in these specimens differed from that on the specimens without any analyzer flagging, explaining the opposite deviation trend compared with that in the autovalidated control specimens. This result could be because of physiological and morphological changes, such as altered adhesion properties of activated lymphocytes. It is known, for example, that monocytes may cluster on the feathered edge of the blood film.[14]

A similar, slightly positive error in the ANC was seen in the specimens with analyzer flagging for IG. The positive error increased with a higher IG percentage and was statistically significant with an IG >5%. However, up to IG = 10% the difference was minimal and had no true clinical significance. In the specimens with IG >10%, the median ANC with the Sysmex XN was 6.1 × 10^9/L compared with a median ANC of 4.6 × 10^9/L with manual microscopy. The

Table 2. Median ANC Analyzed with the Sysmex XN and Manual Slide Review, Method Bias of the Sysmex XN Compared with Manual Microscopy, Median IG Percentage, and WBC in Neutropenic (<1.5 × 10^9/L) Specimens

Specimen Group (n)	ANC Sysmex XN (× 10^9/L)[a]	ANC Microscopy (× 10^9/L)[a]	Method Bias (× 10^9/L)[b]	*P* Value	IG (%)[a]	WBC (× 10^9/L)[a]
Control specimens (14)	0.83 (0.61–1.4)	0.98 (0.82–1.3)	–0.097 (–0.28 to 0.063)	.506	0.80 (0.28–1.3)	2.6 (2.3–3.3)
IG <3 (23)	0.85 (0.32–1.2)	0.82 (0.40–1.2)	0.081 (–0.0049 to 0.14)	.088	0.93 (0–1.34)	1.7 (1.2–2.8)
IG 3–4.9 (10)	1.2 (0.95–1.4)	1.1 (0.97–1.3)	0.044 (–3.6 to 0.23)	.760	3.9 (3.4–4.3)	3.8 (2.8–5.2)
IG 5–9.9 (32)	1.1 (0.83–1.4)	1.0 (0.68–1.2)	0.11 (–0.12 to 0.31)	.005	7.3 (6.7–8.2)	2.6 (1.8–3.1)
IG ≥10 (26)	1.1 (0.92–1.3)	0.9 (0.6–1.3)	0.18 (0.0044 to 0.29)	<.001	14 (13–19)	2.1 (1.6–3.0)
All study specimens (91)	1.1 (0.81–1.3)	1.0 (0.65–1.2)	0.070 (–0.013 to 0.14)	<.001	7.8 (2.2–11)	2.3 (1.6–3.1)

ANC, absolute neutrophil count; CI, confidence interval; IG, immature granulocyte; IQR, interquartile range; WBC, total white blood cell count.
[a]*The numbers in parentheses denote IQR (25th and 75th percentiles).*
[b]*The numbers in parentheses denote 95% CI.*

DOI: 10.1093/labmed/lmaa058

Table 3. TAT with 30%, 50%, and 90% of Specimens Reported for Q4/2018 and Q4/2019.

Specimen Group	Quartile	n	TAT 30% (h)	TAT 50% (h)	TAT 90% (h)
ANC including specimens requiring microscopy review	Q4/2018	13,959	1.1	1.6	4.4
ANC not requiring microscopy review	Q4/2019	11,358	0.9	1.5	4.3
ANC requiring microscopy review	Q4/2019	21	5.2	6.4	23.4

ANC, absolute neutrophil count; TAT, turnaround time.
TAT represents time from specimen collection to result reporting. In 2018, all ANC specimens with analyser flagging were reviewed by manual microscopy; in 2019, only specimens with ambiguous cell clusters (n = 21) were reviewed.

clinical significance of this error for ANC interpretation was minimal because the most important function of the ANC is to evaluate the risk of infection and the possible recovery of a bone marrow production arrest. In the presence of large proportion of IG, compensatory bone marrow production is ongoing and possible neutropenia is decreasing. For further evaluation, we examined the neutropenic specimens (ANC < 1.5×10^9/L with manual microscopy in the study specimens or with the Sysmex XN in the autovalidated control specimens). In the neutropenic specimens, the same slightly negative error in the autovalidated specimens and the slightly positive error in the study specimen were seen as in all the ANC results. Again, the difference between the Sysmex XN and manual microscopy was statistically significant in specimens with IG >5%. However, even in the neutropenic specimens with the highest IG percentage, the method bias was 0.18×10^9/L (95% confidence interval, 0.0044–0.29), and again the clinical significance of the deviation was zero.

In severely neutropenic (ANC < 0.5×10^9/L with manual microscopy, n = 18) study specimens, a slight positive error for Sysmex XN was seen. The severely neutropenic specimens for which the Sysmex XN ANC deviated from manual microscopy ANC had IG >5%. These specimens are challenging to be reviewed by manual microscopy because they contain different neutrophil maturation stages with concurrent neutropenia; this characteristic can cause large subjective variation. In neutropenia, a methodological error with falsely high ANC combined with missing compensatory bone marrow production could be of high clinical importance. No such cases were seen in these data.

The challenges in microscopy review of cytopenic specimens can be seen in the correlation of the 2 methods. There was 1 possible outlier (ANC 3.5×10^9/L with the Sysmex XN vs 1.4×10^9/L with manual microscopy; IG 26%). This outlier was not removed from the data analysis because the ANC derived from manual microscopy was reported for the patient. It is possible that the large IG percentage caused an incorrect classification of neutrophils and subjective underestimation of granulocyte maturation of neutrophils in microscopy review. In other specimens with similar IG percentages, no clear or consistent deviations were seen in neutropenic or normocytic specimens. These considerations are of great importance when the benefits of analyzer result reporting are considered because hematology analyzers count thousands of cells, even with cytopenia, increasing the need for precision.[6,7,10]

The reliability of the analyzer result in neutropenic specimens has been debated previously.[10] According to the data presented here, the Sysmex XN was reliable in reporting the ANC in the presence of analyzer flagging and IG. The analyzer-derived ANC was reliable in neutropenic specimens even with high IG percentages. The Sysmex XN may be able to sufficiently differentiate mature neutrophil clusters from IG clusters if the amount of neutrophils is low, but a slight positive error occurred in specimens with higher ANC and higher IG compared with manual microscopy. This result may be explained by partial fusion of the cell clusters. A high proportion of IG can cause poorer repeatability and precision in manual microscopy as well. Note that neutrophils are short lived and several variables, eg, inflammation status, timing of medication, and time of day, affect the ANC.[15] Thereafter, the trend of the ANC together with a full WBC differential is usually needed to further evaluate the course of neutropenia instead of a single ANC measurement. In this context, the minor differences between the analyzer report and manual microscopy are not clinically relevant, because the analyzer report is usually readily available at any time of day and the interindividual variation in manual microscopy is considered.[2,16-18]

The TAT comparison showed a slightly faster total ANC reporting in Q4/2019, when the data from this study were applied and only a minuscule portion (0.15%) of the ANC specimens was reviewed by manual microscopy. Those specimens still requiring microscopy review, virtually all with ambiguous cell clusters, had a clearly longer TAT. This result reflects the previous TAT for the ANC specimens requiring microscopy review, ie, approximately 2% to 3% of the ANC requests in Q4/2018, indicating that ignoring analyzer flagging with ANC requests deliberately provides faster yet reliable ANC result reporting.

In our laboratory, the WBC differential or IG percentage is not reported with an ANC request, so the method comparison for these parameters was not evaluated in this study. Another weakness of this study is a rather low number of neutropenic specimens, although the total number of the study specimens is adequate.

Conclusion

This is the first study to examine the reporting of ANC in the presence of analyzer flagging in a clinical setting. In conclusion, the ANC can be reported from the Sysmex XN in the presence of analyzer flagging, regardless of IG percentage, if the neutrophil cluster is adequately identified by the analyzer. Sysmex XN analyzers can also be regarded to be as reliable as manual microscopy to report ANC in neutropenic specimens with analyzer flagging. However, clinicians should be informed of the possible uncertainty included in reporting the ANC with analyzer flagging. Each laboratory reporting clinical data should consider laboratory-specific rules to determine which analyzer flagging may be ignored and when ANC specimens should be evaluated by microscopy. **LM**

Acknowledgments

We thank the staff of Turku University Hospital laboratory for the invaluable help in analyzing the specimens.

Author Contributions

Anna-Maria Linko-Parvinen conducted the study, analyzed the data, and wrote the manuscript. Heidi Turkia participated in specimen collection and analyzing the data. Both authors read and approved the final manuscript.

Funding

This work was supported by the Finnish Society of Clinical Chemistry (23/2019, to Dr. Linko-Parvinen).

References

1. Mare TA, Treacher DF, Shankar-Hari M, et al. The diagnostic and prognostic significance of monitoring blood levels of immature neutrophils in patients with systemic inflammation. *Crit Care.* 2015;19(1):57.
2. Berliner N, Gibson C. How we evaluate and treat neutropenia in adults. *Blood.* 2014;124(8):1251–1258.
3. Serhan CN, Savill J. Resolution of inflammation: the beginning programs the end. *Nat Immunol.* 2005;6(12):1191–1197.
4. Malech HL, Deleo FR, Quinn MT. The role of neutrophils in the immune system: an overview. In: MT Quinn,FR Deleo, eds. *Neutrophil Methods and Protocols.* 2nd ed. Totowa, NJ: Humana Press 2014:3–10.
5. Amulic B, Cazalet C, Hayes GL, Metzler KD, Zychlinsky A. Neutrophil function: from mechanisms to disease. *Annu Rev Immunol.* 2012;30(1):459–489.
6. Briggs C, Longair I, Kumar P, Singh D, Machin SJ. Performance evaluation of the Sysmex haematology XN modular system. *J Clin Pathol.* 2012;65(11):1024–1030.
7. Fernandes B, Hamaguchi Y. Automated enumeration of immature granulocytes. *Am J Clin Pathol.* 2007;128(3):454–463.
8. Maenhout TM, Marcelis L. Immature granulocyte count in peripheral blood by the Sysmex haematology XN series compared to microscopic differentiation. *J Clin Pathol.* 2014;67(7):648–650.
9. Barnes PW, McFadden SL, Machin SJ, Simson E; International Consensus Group for Hematology. The International Consensus Group for Hematology review: suggested criteria for action following automated CBC and WBC differential analysis. *Lab Hematol.* 2005;11(2):83–90.
10. Ronez E, Geara C, Coito S, et al. Usefulness of thresholds for smear review of neutropenic samples analyzed with a Sysmex XN-10 analyzer. *Scand J Clin Lab Invest.* 2017;77(6):406–409.
11. Rümke CL, Bezemer PD, Kuik DJ. Normal values and least significant differences for differential leukocyte counts. *J Chronic Dis.* 1975;28(11–12):661–668.
12. Palmer L, Briggs C, McFadden S, et al. ICSH recommendations for the standardization of nomenclature and grading of peripheral blood cell morphological features. *Int J Lab Hematol.* 2015;37(3):287–303.
13. Briggs C, Bain BJ. Basic haematological techniques. In: Bain BJ, Bates I, Laffan MA, Lewis SM, eds. *Dacie and Lewis Practical Haematology.* 11th ed. London, UK: Churchill Livingstone Elsevier; 2012:23–56.
14. Bain BJ, Lewis MS. Preparation and staining methods for blood and bone marrow films. In: Bain BJ, Bates I, Laffan MA, Lewis SM, eds. *Dacie and Lewis Practical Haematology.* 11th ed. London, UK: Churchill Livingstone Elsevier; 2012:57–68.
15. Newburger PE, Dale DC. Evaluation and management of patients with isolated neutropenia. *Semin Hematol.* 2013;50(3):198–206.
16. Georges Q, Azoulay E, Mokart D, et al. Influence of neutropenia on mortality of critically ill cancer patients: results of a meta-analysis on individual data. *Crit Care.* 2018;22(1):326.
17. Walkovich K, Boxer LA. How to approach neutropenia in childhood. *Pediatr Rev.* 2013;34(4):173–184.
18. Palmblad J, Dufour C, Papadaki HA. How we diagnose neutropenia in the adult and elderly patient. *Haematologica.* 2014;99(7):1130–1133.

DOI: 10.1093/labmed/lmaa058

Effect of Addition of WZB117 as an Inhibitor of Glucose Transporter 1 for Venous Blood Glucose Determination

Lei Zhang, MS,[1] *Yaqiong Ran, BS,*[1] *Yan Zhu, MS,*[1] *Qianna Zhen, MS*[2*]

Laboratory Medicine 2021;52:197-201

DOI: 10.1093/labmed/lmaa051

ABSTRACT

Objective: Sodium fluoride (NaF) has been applied to inhibit glycolysis in venous specimens for decades. However, it has had little effect on the rate of glycolysis in the first 1 to 2 hours, resulting in a decrease of glucose, so a more efficient method is needed. Recently, we discovered that WZB117, a specific Glut1 inhibitor, restricts glycolysis by inhibiting the passive sugar transport of human red blood cells and cancer cells. The purpose of this study was to evaluate the results of intravenous blood glucose determination after the addition of WZB117.

Methods: Venous specimens from 40 pairs of healthy volunteers were collected for several days and placed in tubes containing NaF plus EDTA-disodium (Na2) without WZB117 (the A group); citric acid, trisodium citrate, and EDTA-Na2 without WZB117 (B group); and NaF plus EDTA-Na2 with WZB117 (C group). The glucose concentration was measured after venipuncture and compared with test tubes treated for 1 hour, 2 hours, and 3 hours before centrifugation. Glucose level was determined by the hexokinase method. The paired *t*-test was used to examine differences in glucose values at baseline and at different time points. The number of misdiagnoses and the misdiagnosis rate were calculated at 2 diagnostic stages: high risk of diabetes (glucose level of 6.1 mmol/L) and diagnosis of diabetes (glucose level of 7.0 mmol/L).

Results: Glucose levels decreased by 1.0% at 1 hour and by 2.1% at 3 hours in the C group tubes and simultaneously decreased by 1.7% at 1 hour and by 2.5% at 3 hours in the B group tubes. In contrast, glucose levels decreased by 4.1% at 1 hour and by 6.3% at 3 hours in the A group tubes. There was a statistically significant difference in glucose levels measured in the A group tubes and B group tubes at 1 hour, 2 hours, and 3 hours. The misdiagnosis rate of clinical diagnosis in diabetes was highest in the A group tubes (7.0‰ at 1 hour, 0.1‰ at 3 hours at 7.0 mmol/L point; 14.6‰ at 1 hour, 0.4‰ at 3 hours at 6.1 mmol/L point) and lowest in the C group tubes (2.95‰ at 1 hour, 0‰ at 3 hours at 7.0 mmol/L point; 4.8‰ at 1 hour, 0.1‰ at 3 hours at 6.1 mmol/L point).

Conclusion: The tube addition of WZB117 is more suitable for minimizing glycolysis and has no effect on glucose levels even if specimens are left uncentrifuged for up to 3 hours.

Keywords: glucose concentration, WZB117, glycolysis, NaF, Glucose Transporter 1, misdiagnosis rate

Blood glucose concentrations are essential in defining diabetes mellitus. The most recent guidelines for laboratory analysis in the diagnosis and management of diabetes mellitus recommend that glucose concentrations be measured in plasma specimens separated from cells within 60 minutes. If that cannot be achieved, a tube containing a rapidly effective inhibitor such as sodium fluoride (NaF) is used.[1] However, NaF is not an effective agent to prevent glycolysis. The glycolytic enzyme (enolase) targeted by fluoride is located far downstream in the glycolytic pathway, but enzymes upstream of enolase remain active and continue to metabolize glucose until substrates are exhausted.[2] Thus, the antiglycolytic action of fluoride is delayed for up to 4 hours.[3] Therefore, tubes with only enolase inhibitors, such as NaF, should not be relied on to prevent glycolysis.[4] A recent study reported that acidification inhibits hexokinase and phosphofructokinase, enzymes that act early in the glycolytic pathway.[5] It had been marketed in Europe as the Venosafe Glycemia tube but is not currently available in China.[2]

In reviewing the entire glycolytic pathway, we found that the first step in glycolysis is the uptake of glucose by red blood cells. However, red blood cells cannot uptake

Abbreviations:

NaF, sodium fluoride; Na2, disodium.

[1]Clinical Laboratory, the First Affiliated Hospital of Chongqing Medical University, Chongqing, China
[2]Department of Endocrinology, the First Affiliated Hospital of Chongqing Medical University, Chongqing, China

*To whom correspondence should be addressed.
leizi198315@163.com

glucose from the blood freely and need a glucose transporter, Glut1, which is the only glucose transporter isoform in red blood cells.[6]

WZB117 is a novel inhibitor of glucose transport.[7] As a potential anticancer agent, WZB117 can inhibit glucose transport in human red blood cells.[8] The purpose of this study was to prepare WZB117 buffer tubes and compare the plasma glucose results between these buffer tubes and NaF buffer tubes.

Materials and Methods

A total of 40 healthy adult participants were recruited with consent, which was approved by the First Affiliated Hospital of Chongqing Medical University ethics committee. The participants were informed about the subject and objective of the study; there were 20 men and 20 women, aged 20 years to 36 years (average 28 years). Specimens were collected in the following glass tubes: A group tubes with NaF plus EDTA-disodium (Na2) provided by Chongqing Kaiqi Medical Technology Co, Ltd (batch number: 1206267); B group tubes with citric acid, trisodium citrate, and EDTA-Na2 with WZB117; and C group tubes with NaF and EDTA-Na2 in the presence of 44.2 micrograms of WZB117.

Twenty four mL of venous specimens were collected daily according to standard procedures and each divided into the A, B, and C tubes. Blood glucose levels were measured at baseline, 1 hour, 2 hours, and 3 hours after venipuncture, respectively. The first tube was labeled "0 h," was centrifuged within 3 minutes, and glucose analysis was completed within 30 minutes. The remaining specimens, marked "1 h," "2 h," and "3 h," were stored at room temperature. They were centrifuged after their respective waiting periods, and glucose levels were analyzed.

Glucose was determined by the anhexokinase method using the Hitachi 7600-020 automatic biochemical analyzer. The agent was the original set (batch number: 68159801), the calibration product was the CFAS calibration product (batch number: 17215601), and the indoor quality control products were provided by Bio-Rad (batch numbers: 473704, 473804).

All data were normally distributed and expressed as mean ± standard deviation. The paired *t*-test was used to detect differences in baseline blood glucose (at 0 hours) and blood glucose concentrations at 1 hour, 2 hours, and 3 hours after intravenous administration in each group. A P value <.05 was considered statistically significant.

Results

The mean glucose concentrations at 0 hours, 1 hour, 2 hours, and 3 hours after venipuncture in groups A, B, and C are shown in **Table 1**. There was a significant reduction in the glucose level 1 hour, 2 hours, and 3 hours from venipuncture compared with baseline blood glucose concentration (P <.001) in groups A and B. However, there was no significant difference baseline and 1 hour in the C group (P = .116); the significant difference occurred 2 hours and 3 hours after centrifugation in the C group.

Mean biases from the respective baseline glucose measurements for all groups processed at 1 hour, 2 hours, and 3 hours are calculated in **Table 2**. The baseline glucose concentration in all 3 groups showed no significant difference.

Table 1. Mean Glucose Concentrations Measured in A, B, and C Groups Processed at Different Time Points

Tube Type	Glucose Concentration(mmol/L)				*P* Value		
	0 h	1 h	2 h	3 h	0 h vs 1 h	0 h vs 2 h	0 h vs 3 h
A	5.89 ± 1.44	5.65 ± 1.39	5.59 ± 1.43	5.53 ± 1.41	<.001	<.001	<.001
B	5.93 ± 1.44	5.86 ± 1.42	5.83 ± 1.41	5.78 ± 1.40	<.001	<.001	<.001
C	5.84 ± 1.48	5.81 ± 1.11	5.75 ± 1.46	5.72 ± 1.45	.116	<.001	<.001

NaF, sodium fluoride; Na2, disodium.
Glucose concentrations are presented as mean ± standard deviation. The 0 hour measurement means baseline glucose concentrations; 1 hour, 2 hours, and 3 hours mean glucose concentrations in specimens left uncentrifuged for 1 hours, 2 hours, and 3 hours after venipuncture, respectively. We considered P *<.05 as statistically significant. The A group represents NaF plus EDTA-Na2 without WZB117; the B group represents citric acid, trisodium citrate, and EDTA-Na2 without WZB117; and the C group represents NaF plus EDTA-Na2 with WZB117.*

Table 2. Mean Biases from Respective Baseline Glucose Measurements for All Tubes at Different Time Points

Tube Type (n = 40)	Means of Differences (%)	95% CI	*P* Value
$A_{0\,h}$–$A_{1\,h}$	–4.1	–3.4 to –4.8	<.001
$A_{0\,h}$–$A_{2\,h}$	–5.3	–4.1 to –6.5	<.001
$A_{0\,h}$–$A_{3\,h}$	–6.3	–5.3 to –7.2	<.001
$B_{0\,h}$–$B_{1\,h}$	–1.2	–1.0 to –1.3	.021
$B_{0\,h}$–$B_{2\,h}$	–1.7	–1.6 to –1.7	.012
$B_{0\,h}$–$B_{3\,h}$	–2.5	–2.3 to –2.5	.009
$C_{0\,h}$–$C_{1\,h}$	–1.0	0.8 to –1.2	.116
$C_{0\,h}$–$C_{2\,h}$	–1.5	–1.4 to –1.6	<.001
$C_{0\,h}$–$C_{3\,h}$	–2.1	–1.9 to –2.2	<.001
$A_{0\,h}$–$B_{0\,h}$	0.8	–0.5 to 2.1	.073
$A_{0\,h}$–$C_{0\,h}$	–0.9	–0.1 to –1.8	.267

Glucose bias relative to the baseline value was highest in the A tubes and lowest in the C tubes. The bias from the baseline glucose concentration was clinically significant (>2.2%) at all time points for the A group; in the C group the observed bias did not exceeded half of the recommended criteria even with a delay of 3 hours.

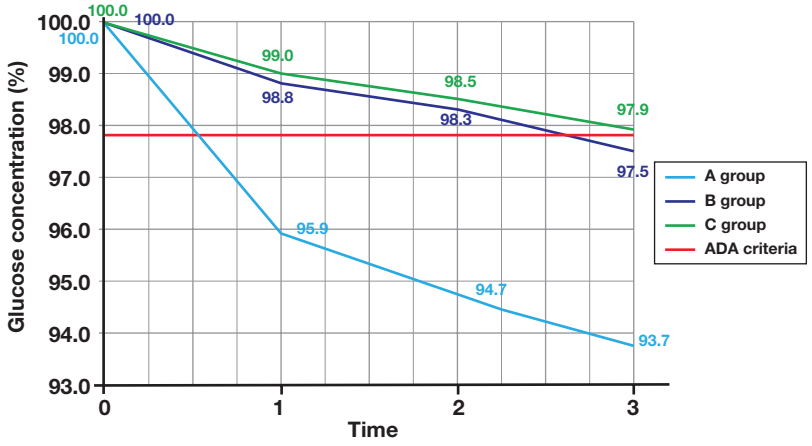

Figure 1

Decrease of glucose concentrations with time in A, B, and C groups

However, glucose levels were significantly decreased in both the A and B groups at 1 hour, 2 hours, and 3 hours, whereas the mean glucose concentration in the C group tubes decreased by only 1.0% (*P* = .116) at 1 hour. The glucose bias relative to the baseline was highest in the A group and lowest in the C group at all time points. The bias from the baseline glucose concentration was clinically significant (>2.2%) at the 3 hour time point for the A and B groups; in the C group the observed bias did not exceed half of the recommended criteria even with a delay of 3 hours (shown in **Figure 1**).

Because glucose tests have preanalytic variability, it is possible that an abnormal result (ie, above the diagnostic threshold) will produce a value below the diagnostic cutpoint, especially if the glucose specimens are collected at room temperature and not centrifuged promptly. Guidelines and recommendations for laboratory analysis in the diagnosis and management of diabetes mellitus.[10] We collected 22,630 specimens from patients whose fasting plasma glucose results were near the above 2 diagnostic thresholds from January 2018 to June 2018. There were 5669 specimens that sat for more than 1 hour after collection before acceptance by the clinical laboratory, accounting for 25% of all inpatient clinical specimens. Specifically, 5024 specimens were measured with a delay of 1 hour to 2 hours (22% of all specimens), 450 specimens were measured with a delay of 2 hours to 3 hours (2% of all specimens), and 195 specimens were measured with a delay of more than 3 hours (0.9% of all specimens). According to **Figure 1** decrease rate

DOI: 10.1093/labmed/lmaa051

Table 3. Number of Possible Misdiagnoses and Misdiagnosis Rate at 2 Diagnostic Thresholds of 7.0 mmol/L and 6.1 mmol/L at Different Time Points

Tube	7.0 mmol/L			6.1 mmol/L		
	Number/(%)			Number/(%)		
	1 h–2 h	2 h–3 h	>3 h	1 h–2 h	2 h–3 h	>3 h
A	163/7.0	9/0.4	2/0.1	398/17.6	30/1.3	9/0.4
B	69/3.0	2/0.9	1/0.05	238/10.5	19/0.8	6/0.3
C	68/2.95	2/0.9	0/0	109/4.8	10/0.4	3/0.1

The A group represents NaF plus EDTA-Na2 without WZB117; the B group represents citric acid, trisodium citrate, and EDTA-Na2 without WZB117; the C group represents NaF plus EDTA-Na2 with WZB117.

of blood glucose in the A group and C group in 1 hour to 3 hours, the number of possible misdiagnoses and the misdiagnosis rate for diabetes are calculated for the 2 diagnostic stages in **Table 3**. As shown in the table, the number of possible misdiagnoses and the misdiagnosis rate was highest in the A group and lowest in the C group at the 2 clinical diagnosis points at different time points.

Discussion

Many studies have reported lower results for plasma glucose obtained in NaF tubes. These results indicate a delayed and inefficient inhibition of glycolysis by NaF, leading to falsely low plasma glucose concentrations and, potentially, a failure to diagnose diabetes. Citric acid as an immediate inhibitor of glycolysis has been confirmed to reduce errors in glucose level measurement and diagnoses of diabetes.[9,11]

In the glycolytic pathway, fluoride inhibits enolase, which is far downstream in the pathway. Enzymes upstream of enolase remain active and continue to metabolize glucose until substrates are exhausted. A citrate buffer inhibits hexokinase and phosphofructokinase, enzymes that act early in the glycolytic pathway. However, one new problem that drew our attention is that human red blood cells cannot freely uptake glucose from the blood. They need the glucose transporter Glut1, which is the only glucose transporter isoform in red blood cells. We studied WZB117, which inhibits passive glucose transport in human red blood cells and cancer cell lines and limits glycolysis,[5] to determine whether it could be applied to inhibit glycolysis.

Our study aimed to assess the ability of tubes containing WZB117 to prevent glycolysis after delayed specimen centrifugation and to compare it with glucose stability in tubes containing citric acid, trisodium citrate, and EDTA-Na2, and tubes containing NaF plus EDTA-Na2. We observed a significant inhibition of glycolysis by WZB117 and an inability of NaF to prevent glucose loss even after a 1-hour delay from venipuncture to centrifugation.

Consequently, through this study we can confirm the ineffectiveness of NaF as a glycolysis inhibitor in the first 3 hours after venipuncture. This study also showed that glycolysis was stopped immediately with a citrate buffer and that glucose concentrations were entirely stable uncentrifuged for 3 hour, showing a 2.5% decrease. The glucose concentrations decreased only 1.0% at 1 hour, 1.5% at 2 hours, and 2.1% at 3 hours after venipuncture when WZB117 was added into the whole blood specimens. Based on the U.S. diabetes guidelines from 2015,[10] there was a significant difference in blood glucose measurements between baseline and 2 hours and 3 hours after centrifugation, and the observed bias did not exceed half of the recommended criteria even with a delay of 3 hours. A more rapid glycolysis inhibition was achieved.

There are 2 possible limitations in our study. First, a gradient experiment of WZB117 in glycolysis inhibition was not conducted because of insufficient time. Second, the effect of the addition of WZB117 to serum tubes should be measured comparing the plasma glucose results in citrate buffer tubes and NaF tubes. Further studies should be conducted to investigate the effectiveness of the above concerns and obtain more accurate and effective data.

In summary, replacement of NaF with a better and more effective glycolysis inhibitor is certainly overdue. Our study

highlights and provides the new thought that there may be some significant inhibition of glycolysis with inhibitors of glucose transporters.

Conclusion

There is a need to change preanalytical conditions to prevent the loss of glucose in whole blood for glucose estimation. As an inhibitor of glucose transport, WZB117 can significantly inhibit glycolysis. **LM**

References

1. Sacks DB, Arnold M, Bakris GL, et al. Guidelines and recommendations for laboratory analysis in the diagnosis and management of diabetes mellitus. *Clin Chem.* 2011;57(6):e1–e47.
2. Mikesh LM, Bruns DE. Stabilization of glucose in blood specimens: mechanism of delay in fluoride inhibition of glycolysis. *Clin Chem.* 2008;54(5):930–932.
3. Chan AY, Swaminathan R, Cockram CS. Effectiveness of sodium fluoride as a preservative of glucose in blood. *Clin Chem.* 1989;35(2):315–317.
4. Stahl M, Jørgensen LG, Hyltoft Petersen P, Brandslund I, de Fine Olivarius N, Borch-Johnsen K. Optimization of preanalytical conditions and analysis of plasma glucose. Impact of the new WHO and ADA recommendations on diagnosis of diabetes mellitus. *Scan J Clin Lab Invest* 2001;61:169–180.
5. del Pino IG, Constanso I, Mourín LV, Safont CB, Vázquez PR. Citric/citrate buffer: an effective antiglycolytic agent. *Clin Chem Lab Med.* 2013;51(10):1943–1949.
6. Mueckler M. Facilitative glucose transporters. *Eur J Biochem.* 1994;219(3):713–725.
7. Zhang W, Liu Y, Chen X, Bergmeier SC. Novel inhibitors of basal glucose transport as potential anticancer agents. *Bioorg Med Chem Lett.* 2010;20(7):2191–2194.
8. Liu Y, Cao Y, Zhang W, et al. A small-molecule inhibitor of glucose transporter 1 downregulates glycolysis, induces cell-cycle arrest, and inhibits cancer cell growth in vitro and in vivo. *Mol Cancer Ther.* 2012;11(8):1672–1682.
9. Juricic G, Kopcinovic LM, Saracevic A, Bakliza A, Simundic AM. Liquid citrate acidification introduces significant glucose bias and leads to misclassification of patients with diabetes. *Clin Chem Lab Med.* 2016;54(2):363–371.
10. Sacks DB, Bruns DE, Goldstein DE, Maclaren NK, McDonald JM, Parrott M. Professional practice committee for the standards of medical care in diabetes—2015. *Diabetes Care*. 2015;38(Supplement_1):S88–S89.
11. Gambino R, Piscitelli J, Ackattupathil TA, et al. Acidification of blood is superior to sodium fluoride alone as an inhibitor of glycolysis. *Clin Chem.* 2009;55(5):1019–1021.

DOI: 10.1093/labmed/lmaa051